Ruthenium Olefin Metathesis Catalysts: Tuning of the Ligand Environment

Ruthenium olefine metathese katalysatoren: Optimalisatie van de ligandsfeer

Nele Ledoux

Promotor: Prof. Dr. F. Verpoort

Proefschrift ingediend tot het behalen van de graad van
Doctor in de Wetenschappen: Scheikunde

Vakgroep Anorganische en Fysische Chemie
Vakgroepvoorzitter: Prof. Dr. S. Hoste
Faculteit Wetenschappen
2007

UNIVERSITEIT
GENT

Members of the Dissertation Committee:
Prof. Dr. F. Verpoort
Prof. Dr. Ir. C. Stevens
Dr. V. Dragutan
Dr. R. Drozdzak
Dr. R. Winde
Prof. Dr. Ir. D. Devos
Prof. Dr. J. Van der Eycken
Prof. Dr. P. Van Der Voort
Prof. Dr. K. Strubbe

This research was funded by the Fund for Scientific Research - Flanders (F.W.O.-Vlaanderen).

Acknowledgments

This dissertation is the final product of an educative and fascinating journey, which involved many contributors.
First of all, I wish to express my gratitude to the people with whom I learned how to do research. There is my promotor Prof. Dr. Francis Verpoort who gave me the opportunity to join his 'Catalysis group' and ensured the necessary funding. I'm especially grateful for his confidence and indulgence. In addition, I have been extremely lucky to work with several nice colleagues. Thank you, Thank you (= double thank you ♡) to Bart who helped me conquer many small and big difficulties, and by doing so, contributed a lot to the results reported here. Special thanks to Hans for many funny moments and support over the years. Of course, my acknowledgments also go to the other boys: Carl, Stijn, David, Jeroen, Prof. Dr. Pascal Van Der Voort and not to forget Siegfried, Steven, and Mike for the pleasant working atmosphere and supportive chats. I owe thanks to Dr. Renata Drozdzak for the introduction of Schlenk equipment, helping us to make blue THF, and for friendly words. I'd like to thank Fu and Oana for their friendship, and never-ending kindness. I've enjoyed the presence of many thesis students and foreign visitors in our group and I will remember them with pleasure. Many more S3 members deserve to be mentioned here, which is not only for good-humored coffee breaks and innocent gossip.
I'm indebted to Dr. Anthony Linden of Institute of Organic Chemistry, University of Zürich, for several single crystal analyses, and a very pleasant cooperation. More thanks go out to Jacques Pécaut of CEA-Grenoble for crystal structure analysis, and to Olivier Grenelle and Dr. Marc Proot of Chevron Technology, Ghent, for elemental analyses.
I would like to thank the members of the dissertation committee for their valuable feedback.
My parents, brother, sister, family, and friends are gratefully acknowledged for providing unconditional, warm-hearted support.

Preface

The basic subject of interest throughout this thesis is the olefin metathesis transformation. The formation of carbon-carbon double bonds is one of the most fundamental chemical processes. In this context, metathesis makes a significant contribution, since this transition metal catalyzed reaction is a C-C bond breaking and bond making process in which an overall exchange of groups around the double bonds results in several outcomes.

As were many catalytic reactions, olefin metathesis was discovered by accident. Researchers at DuPont were trying to expand the scope of the addition polymerization reactions but obtained a highly unsaturated polymer.[1] In those early days olefin metathesis was rather cumbersome, but it has been upgraded to a very practical, efficient and flexible synthetic methodology. The amount of synthetic transformations that can be accomplished is staggering, since the same catalytic systems can promote different types of metathesis reactions, depending on the substrates and reaction conditions employed. Olefin metathesis now allows cleaner, more efficient, and less expensive industrial production of polymers, fine chemicals, pesticides, and pharmaceutical intermediates. The recent Nobel Prize awarding of Y. Chauvin for groundbreaking contributions to the discovery of the olefin metathesis mechanism, and to R. R. Schrock and R. H. Grubbs, who introduced a large number of catalytic metathesis initiators, has put emphasis on this increasing industrial interest.[2–4]

Despite the recent advances, the search for commercially relevant catalyst systems remains challenging. When thinking of commercial applications, even a small increase in catalyst efficiency becomes of major importance. Today's catalysts are well defined and the mechanisms well understood. This allows for further growth of this fascinating field of research by the design of new catalysts or the improvement of existing catalytic systems, as the work presented in the next chapters will hopefully help to demonstrate.

Since specifically designed ligands are key in optimizing the efficiency of olefin metathesis mediators, we mainly focused on the effects of ligand modification. A first type of ligand which caught our attention, is a bidentate Schiff base. Schiff bases are known to strongly enhance the thermal and moisture stability of the corresponding complexes. These features were employed in the development of latent catalysts, which are chemically activated upon the addition of acids. A

second type of ligands playing an important role in the carried out research, are *N*-heterocyclic carbenes (NHCs). NHC ligands have recently gained popularity due to a large number of attractive properties. Through distinct variations in the amino side groups of the NHC ligands, we aimed at catalyst fine tuning. A range of different catalysts was synthesized, fully characterized and subjected to representative test reactions, which allowed comparison with benchmark olefin metathesis catalysts.

Outline

Chapters 3, 4, 5, and 6 have been published as peer review articles. Chapter 3 is adapted from references[5,6], chapter 4 from[7,8], chapter 5 from[9,10], and chapter 6 from[11]. All chapters contain their own abstract introducing the subject matter.

Chapter 1 was devoted to a general introduction on the olefin metathesis reactions, mechanism, catalysts, and applications.

Chapter 2 comprises a second introductory part. Since the catalyts developed during this project all contain an *N*-heterocyclic carbene (NHC) ligand, some general properties of these ligands in organometallic complexes were described. Furthermore, the beneficial properties of NHC ligands in ruthenium based olefin metathesis catalysts were explained through profound consideration of the reaction mechanism.

Chapter 3 addresses the synthesis and catalytic performance of a ruthenium benzylidene catalyst bearing a Schiff base ligand. The bidentate Schiff base ligand exerts, due to its "dangling" character, a pronounced effect on both the activity and stability of the resulting complex. This complex shows negligible metathesis activity at room temperature, while the addition of an acid was found to induce a substantial activity enhancement. The catalyst latency is of particular interest for industrial applications such as reaction injection molding (RIM) processes, since catalyst and monomer can be stored without concomitant polymerization.

Chapter 4 deals with the search for alternative synthetic pathways. When aiming at the development of new catalysts, one should not only focus on catalyst activity or stability, as highly sophisticated and well-defined initiators are sometimes too expensive for applications on an industrial scale. Other important aspects deserving consideration are the cost to make the catalyst, availability of the starting materials, and the complexity of the preparative routes. In addition, it is often relevant to search for patent-free synthetic strategies.
In this context, chapter 4 encloses a contribution to the search for new synthetic routes, which lead to alternatives for the classic ruthenium benzylidene complexes. The air and moisture stable, easy to synthesize, Ru dimer $[(p\text{-cymene})RuCl_2]_2$ was chosen as a catalyst precursor.

Chapter 5 examines the effect of new *N*-heterocyclic carbenes in Grubbs catalysts. Various symmetrical and asymmetrical NHCs bearing aliphatic amino side groups were synthesized. In our attempts to isolate the corresponding Grubbs 2nd generation catalysts, we were unsuccessful for the symmetrical aliphatic NHCs. For the asymmetrical ligands bearing an aliphatic moiety

on one side and an aromatic mesityl group on the other side, substitution of a phosphine ligand was achieved. Replacement of the NHC mesityl ring with a 2,6-diisopropylphenyl moiety was found to have a substantial effect. Facile *bis*-coordination of the NHC ligands was observed, which was assigned to an enhanced phosphine dissociation rate of the corresponding mono(NHC) complexes.

Chapter 6 describes how new NHC ligands were successfully coordinated to the Hoveyda-Grubbs catalyst. In various olefin metathesis test reactions, subtle steric differences in the NHC amino side groups were found to exert a critical influence on the activity of the corresponding catalysts.

Chapter 7 briefly summarizes the conclusions made throughout the thesis, and a short future outlook is given.

Chapter 8 summarizes this thesis in Dutch.

Table of Contents

Chapter 1

Olefin Metathesis

The history of olefin metathesis is very intriguing, beginning with its accidental discovery half a century ago, going to the design of the latest catalyst systems and applications. As it would be impossible to cover all aspects of this very versatile reaction type, we limited ourselves to a concise overview of the metathesis transformations and a brief outline of the mechanistic pathway. Furthermore, this chapter highlights some selected examples of catalyst systems and commercial applications.

1.1 Metathesis transformations

The complete family of metathesis chemistry includes olefin metathesis[12–15], alkyne metathesis[16–21], and enyne metathesis[22–32]. While in enyne metathesis the bond reorganization of an alkene and an alkyne produces a 1,3-diene, alkyne metathesis involves the redistribution of two alkyne chemical bonds. Both of these reaction types are closely related to the olefin metathesis transformations shown in figure 1.1:

- Transfer of groups between acyclic olefins: cross metathesis (CM)[33,34]
- Ring closure of acyclic dienes: ring-closing metathesis (RCM)[35]
- Formation of dienes from cyclic olefins: ring-opening metathesis (ROM)[36]
- Polymerization of cyclic olefins: ring-opening metathesis polymerization (ROMP)[37,38]
- Acyclic diene metathesis polymerization (ADMET)[39]

1.2 Mechanism

About fifty years ago, N. Calderon at Goodyear Tire & Rubber, USA, figured out that some unexpected products observed in several petrochemical companies

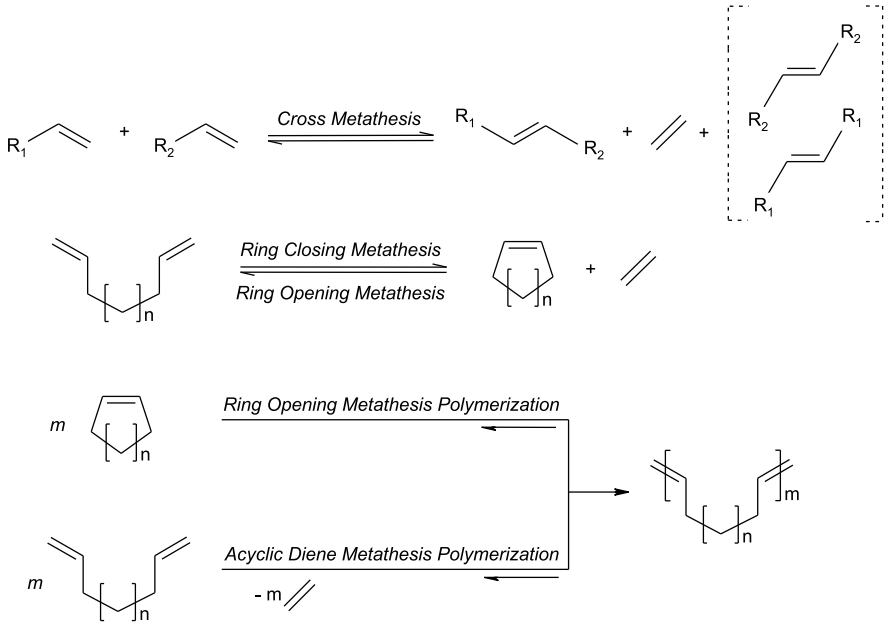

Figure 1.1: Olefin metathesis transformations.

at the time, resulted from cleavage and reformation of C-C double bonds. The elucidation of the exact mechanistic pathway has been the culmination of almost two decades of profound research and the subject of lively debate in the literature during that period.[40–45] In 1971, Y. Chauvin and J.-L. Hérisson of the French Petroleum Institute, suggested that olefin metathesis is initiated by a metal carbene. The metal carbene reacts with an olefin ([2+2]-cycloaddition) to form a metallacyclobutane intermediate, which breaks up to form a new olefin and a new metal carbene ([2+2]-cycloreversions) (Figure 1.2).[46]

After the Chauvin paper was published, consensus regarding the involvement of metal carbenes was not immediately reached. In a few important publications supporting the Chauvin-Hérisson mechanism, Katz et al. described the olefin metathesis kinetics.[47–49] The question was asked whether the reaction of a cyclic with an acyclic olefin should give three products or just one. Various experiments showed that reactions of cycloalkenes with acyclic internal olefins give two additional products, while reaction between cycloalkenes and terminal olefins do not give the additional products. Initially, these observations could not be reconciled with the Chauvin mechanism. What Chauvin did not recognize was that, when a metal carbene reacts with an olefin, two metal carbenes can be formed. If the groups around the double bond of the acyclic olefin are sufficiently different, one metal carbene product will be favored over the other. In other words, which

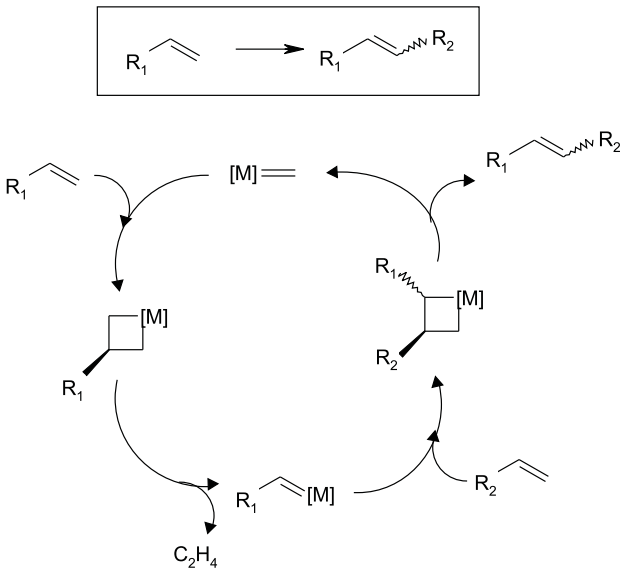

Figure 1.2: Chauvin-Hérisson mechanism.

products are formed depends on the substituents of the acyclic olefin (Figure 1.3).

The paper of Katz in 1975 was the first to give full evidence for the metal carbene mechanism[47], which was later experimentally supported by Grubbs[44], and Schrock[50–52]. The understanding of how the catalyst functions in the metathesis reaction provided a basis for scientists to construct new efficient catalysts, since it was shown that these should be found among isolable metal-carbene complexes.

1.3 Catalyst systems

A large number of catalyst systems capable of olefin metathesis initiation have been introduced. The early catalytic systems were either early transition metals supported on oxide supports (e.g. WO_3/SiO_2) or consisted of mixtures of various components (early transition metal halides and reducing/alkylating agents; e.g. alkyl aluminums). These are ill-defined in their chemical composition and inefficient due to a low amount of active species. Since these systems are very Lewis acidic and thus readily deactivated by common Lewis basic functional groups, they are only useful for reactions involving unfunctionalized hydrocarbons. Such tungsten and molybdenum based systems have served as catalysts in reaction injection molding (RIM) processes for the polymerization of dicyclopentadiene (DCPD), in the SHOP process and the Tri Olefin Process (Section 1.4).

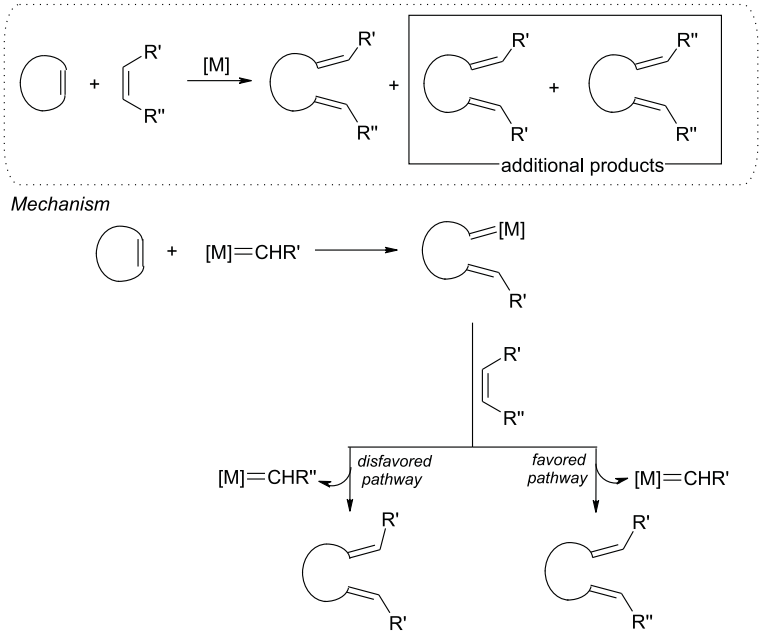

Figure 1.3: Possibility of two metal carbenes.

Once the Chauvin mechanism had been established, the road was open for the development of well-defined catalysts. In this context, the expression "well-defined" refers to isolable catalytic systems characterized by a stoichiometric composition and for which the actual propagating species is well known. Of the different metals, Mo, W and Ru have emerged as the key elements to achieve highly active and selective catalysts. They can be classified in two different families: Mo- and W-based systems are typically high oxidation state d^0 alkylidene complexes having a set of ligands aiming at an increase of the electrophilicity of the metal center. Ru-based systems are d^4 metal complexes with basic ligands, which assist in the dissociation of one ligand to generate the active species. The chemists most responsible for developing these catalysts are Richard R. Schrock at Massachusetts Institute of Technology (MIT) and Robert H. Grubbs at California Institute of Technology (Caltech). The so-called Schrock and Grubbs catalysts were developed through intensive research going back to the 1970s.[37,53–57]

The molybdenum catalyst that became widely known as the 'Schrock catalyst' was published in 1990 (Figure 1.4).[58] Despite the somewhat higher stability compared to W-based systems, this Mo-catalyst suffers from decomposition upon storage, is sensitive to ambient air and moisture and intolerant towards protic compounds such as alcohols and aldehydes. These drawbacks are caused by the

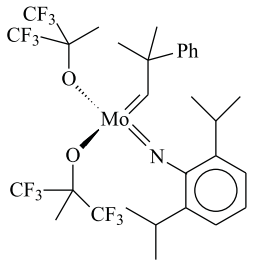

Figure 1.4: Schrock catalyst.

high oxophilicity of the early transition metal center.

Tolerance to functional groups was found to improve with increasing group number of the incorporated metal. Ruthenium displays a preference for soft Lewis bases such as olefins over hard bases such as oxygen-based compounds. While other late transition metals also allow the formation of metal-carbon double bonds, ruthenium seems to be the optimal metal. Fe-, Co- and Rh-based alkylidene complexes predominantly lead to cyclopropanation. Os- and Ir- based systems are generally metathesis active but since these systems are much more expensive and less active than their Ru-based analogues, they have not been the subject of many research projects.[37]

The ruthenium carbene complexes developed by Grubbs et al. demonstrate good chemoselectivity for carbon-carbon double bonds over seemingly more reactive sites, such as alcohols, amides, aldehydes, and carboxylic acids. In comparison to Schrock's molybdenum catalysts, Grubbs' catalysts do not require strict conditions, which makes them easier to handle. They can be used by organic chemists in ordinary laboratories; vacuum lines and dry boxes are not always necessary.[37,59–61]

The first Grubbs type ruthenium catalyst $[Cl_2Ru(=CH-CH=CPh_2)(PPh_3)_2]$ was prepared in 1992.[62] It showed good functional group tolerance but limited activity. Further refinements led to the catalyst $[Cl_2Ru(=CHPh)(PCy_3)_2]$ **1**, which is now known as the Grubbs 1st generation catalyst (Figure 1.5).[63] This is a five-coordinate, 16-electron, Ru complex exhibiting a distorted square pyramidal geometry with an alkylidene moiety in the apical site. Exchange of one phosphine ligand with a bulky *N*-heterocyclic carbene (NHC) ligand was found to allow enhanced activity and selectivity in several olefin metathesis reactions. Catalysts derived from both unsaturated and saturated NHC ligands were investigated.[64–66] The H_2IMes (1,3-dimesityl-4,5-dihydroimidazol-2-ylidene) bearing complex is also known as the Grubbs 2nd generation catalyst **2** (Figure 1.5).[67]

The slow initiation step of the Grubbs 2nd generation catalyst has been improved by replacement of the phosphine with weakly bound heterocyclic ligands such as pyridine. One synthetically simple transformation from **2** results in

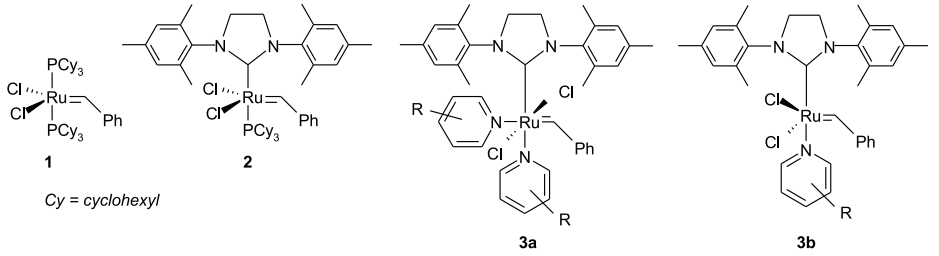

Figure 1.5: Grubbs catalysts **1**, **2** and **3a-b**.

$(H_2IMes)(py)_2(Cl)_2Ru{=}CHPh$ **3a**. This 18-electron bis-pyridine adduct possesses a very high initiation rate, and is often referred to as the Grubbs 3rd generation catalyst. Under vacuum one pyridine ligand decoordinates, with formation of the mono-pyridine complex **3b** (Figure 1.5, R = H, Br, Ph, NO_2).[68–70]

The discovery of the Grubbs complexes triggered the search for other ruthenium based metathesis active catalysts. Over the years a myriad systems were described in literature, making it impossible to describe all of them.[71–85] One intriguing example is the Hoveyda catalyst **4**, which was accidentally discovered at Boston College in 1999 during mechanistic studies of Ru-catalyzed styrenyl ether to chromene transformations (Figure 1.6).[86–88] This aryl-ether chelate complex offers the advantage that the same active species is formed as with **1**, while the catalyst is exceptionally robust and recyclable: it is recovered in high yield after a reaction by air-driven silica gel chromatography. The convenience of possible recovery after reaction, should be assigned to a release/return mechanism. The isopropoxystyrene, which decoordinates during metathesis, can react again with a Ru-intermediate to regenerate the original catalyst.[89] The 2nd generation analogue -complex **5**- is a more active catalyst which shows efficiencies similar to those of the Grubbs catalyst **2**, but provides selectivity levels for CM and RCM that are not available by the latter.[90,91]

With the aim of enantioselective metathesis reactions, catalyst **6** was prepared by Blechert et al.[92] This BINOL-derived catalyst demonstrated significantly higher catalytic activity than complex **4**, but no asymmetric induction was found. Further studies indicated that the presence of steric bulk adjacent to the chelating unit is critical. This was confirmed by the synthesis of complex **7**, which was shown to be a very active catalyst for RCM.[93,94] The increase in steric bulk improves the leaving group ability of the ligand and thus facilitates formation of the active 14-electron species (dissociative mechanism), while reassociation to the metal center is suppressed.

Electronic effects in the isopropoxystyrene ligand sphere were investigated by Grela et al.[95–98] The introduction of a strong electron-withdrawing group leads to complex **8**, which is equally stable but spectacularly more reactive than complex

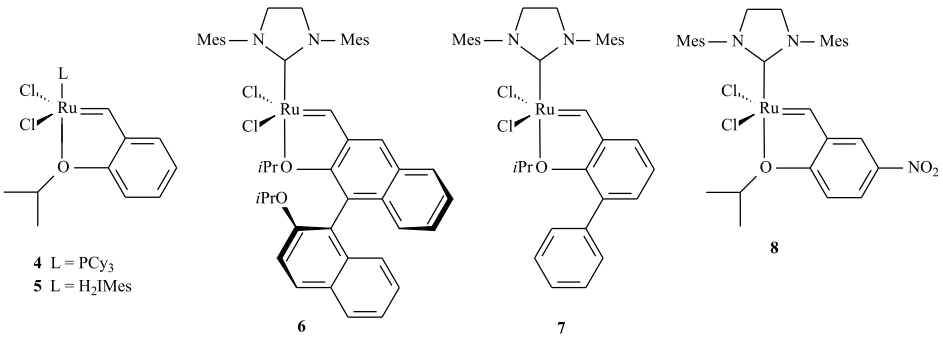

Figure 1.6: Hoveyda type catalysts.

5.[95] A decrease in electron density of the isopropoxy oxygen atom is expected to reduce its chelating ability, thereby facilitating formation of the 14-electron catalytically active species, while suppressing reassociation to the Ru center. These findings clearly demonstrate that small variations in ligand structure can result in a considerably different catalytic activity.[99]

Over the last decade, a constant improvement in the Grubbs, Schrock and Hoveyda class of catalysts, allowed the widespread use of olefin metathesis in organic synthesis as it could replace many of the traditional synthetic tools.[100] Today, several well-defined metathesis catalysts are commercially available and as a result, new perspectives are opening up in the industrial production of specific molecules. This will be briefly discussed in the next section.

1.4 Industrial applications

In general, the olefin metathesis reaction has opened up new routes in three important fields of industrial chemistry:[101]

1.4.1 Production of petrochemicals

Heterogeneously catalyzed cross metathesis has numerous industrial applications in the production of petrochemicals. The metathesis reaction is a key step in the Shell Higher Olefin Process (SHOP), in which Shell Chemicals produces up to 1.2 million tons of linear higher olefins per year from ethylene. From 1966 to 1972, Phillips Petroleum produced ethylene and *2*-butene from propylene, a process known as the Phillips triolefin process. Later on, a high global demand for propylene prompted petrochemical companies to convert ethylene and *2*-butene from naphtha crackers to propylene. This reversed Phillips triolefin process is known as the Olefins Conversion Technology (OCT). Also *1*-Hexene is one

of the olefins industrially produced by cross metathesis. Metathesis of butene yields *3*-hexene, which is then isomerized into *1*-hexene (*co*-monomer used in the production of polyethylene).

1.4.2 Polymer synthesis

Most olefin metathesis derived polymers are manufactured using homogeneous catalytic systems.[102] Polynorbornene, the first commercially available metathesis polymer, was marketed in 1976 by CdF Chimie under the trade name Norsorex®. A process using a $RuCl_3$/HCl catalyst produces an elastomer which proved useful for oil spill recovery and as a sound or vibration barrier. The ROMP of cyclooctene is performed by Degussa-Hüls AG using a tungsten based catalyst and leads to polyoctenamer with trade name Vestenamer®. Vestenamer® is mainly used as a processing aid in the rubber industry to manufacture tires, profiles, tubes, all kinds of molded rubber articles, and roller coatings.
Most recent interest has been shown in the ROMP of *endo*-dicyclopentadiene (DCPD). DCPD is an inexpensive, readily available byproduct of the petrochemical industry. When only the highly strained norbornene moiety is ring opened, a linear polymer is formed. Under certain conditions it is also possible to metathesize the double bond in the cyclopentene ring, which then gives rise to crosslinking (Figure 1.7). The crosslinked polymer is industrially processed through Reaction Injection Molding (RIM) in the production of large objects such as bathroom modules, lawn and garden equipment, construction machinery, body panels for trucks, ... and through Resin Transfer Molding (RTM) in the production of poly-DCPD incorporating fiberglass reinforcements and coring materials.
Liquid resins for the production of thermoset (= remains rigid when set, and does not soften with heating) poly-DCPD were put on the market under the trade names Telene® and Metton®. In the Telene® process, a molybdenum based precatalyst is activated by a mixture of Et_2AlCl, alcohol and $SiCl_4$. The Metton® process utilizes a WCl_6 + $WOCl_4$ precursor, which is initiated by the addition of $EtAlCl_2$.
Since ruthenium systems are more tolerant to moisture, oxygen, pigments and fillers, they are interesting alternatives for these Mo and W systems. Ruthenium based metathesis initiators were first investigated for *poly*-DCPD technology by Ciba Specialty Chemicals. Their Cl_2Ru(*p*-cymene)PCy_3 shows good latency in the neat monomer at ambient temperature while the polymerization is triggered by raising the temperature to 80 °C.[103] Some acetylenic impurities in the used DCPD are believed to enhance the polymerization rate.
Homogeneous, well-defined catalysts such as the Grubbs and Schrock type catalysts do not yet play a major role in these industrial scenarios. However, for *poly*-DCPD production, the Grubbs ruthenium technology has been made available by Materia, a company founded in 1997. Materia's *poly*-DCPD resin can be used in conjunction with glass and thermoplastic microspheres to produce high quality

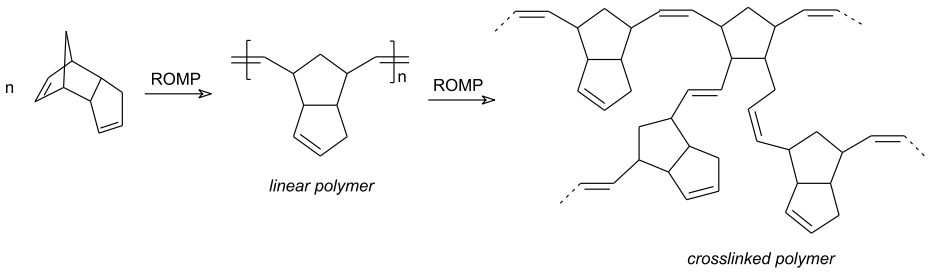

Figure 1.7: *poly*-DCPD.

foam products. A Japanese compagny, Hitachi Chemical, brought Metathene® on the market. This is a polymer produced by ruthenium technology which is used for various applications including bathroom devices. Also Cymetech uses Materia technology for polymer under the trade name Prometa®.
It is very likely that such well-defined catalysts will play a more important role in the future since they allow high efficiency of a relatively small catalyst loading. A chemically activated latent catalyst system showing promising properties for poly-DCPD RIM technology is described in chapter 3. Its potential has been further explored by the Ghent University spin-off company Viacatt in collaboration with Noveon (Telene).

1.4.3 Fine chemistry

Broad usage of ring-closing metathesis and cross metathesis in the synthesis of complex organic molecules was initially hampered by the sensitivity of early metathesis catalysts toward functional groups. More recently, the development of a number of well-defined and functional-group tolerant catalysts induced a substantial boost in this particular research area.[14,104–109] A good illustration is found in the history of the name of the Materia company. Materia was originally called Advanced Sports Materials, to reflect the development of polymers for commercial applications in sporting goods. The company's name was changed in 1998 to indicate wider commercial opportunities, such as the synthesis of fine chemicals.
Materia's technology includes the metathesis catalysts of Grubbs, Schrock, and Hoveyda. These Mo and Ru based complexes have already shown remarkable utility in the production of fine chemicals on an industrial scale. Some very important contributions were made to the pharmaceutical industry and a number of highly functional pharmaceuticals are now moving through the qualification process. A few examples of pharmaceuticals which include ring-closing metathesis as one of their synthetic steps, are Mevinolin (drug used to lower cholesterol rates), Ambruticin (anti-fungal antibiotic), and Nonenolide (anti-malarial)[110].

Metathesis can also be used to improve the synthesis of insect pheromones, which are more ecological alternatives to chemical pesticides, and in intermediate reactions to produce flavor and fragrance chemicals. The number of steps, and thus the amount of intermediate wastes that are created, are greatly reduced. More research is in process on the development of pharmaceuticals for diseases such as HIV/AIDS, hepatitis C, cancer, Alzheimer's disease, Down's Syndrome, osteoporosis, arthritis, fibrosis, migraine,... in which this reaction type will hopefully become a powerful synthetic tool.

Next to the Materia catalysts, a growing number of other ruthenium based metathesis initiators became commercially available at industrial relevant scale during the last couple of years (Figure 1.8).

In 2000 van der Schaaf et al. of Ciba Specialty Chemicals (Basel, Switzerland) described a (phenylthio)methylene Ru complex. It was commercialized after the synthesis was optimalized in 2003 by Ozawa et al.[74,111,112] Later on, also its 2nd generation analogue was distributed by Ciba.

The Chinese company Zannan (Shanghai) introduced the Hoveyda-derived air stable *Zhan*®-catalysts, which perform well in ring-closing metathesis reactions.[113]

Umicore AG&CO.KG (Hanau-Wolfgang, Germany) produces the world wide patent-free catalyst *Neolyst® M1*, an air-stable complex which was first described by Fürstner et al.[79]

In 2006, Degussa Homogeneous Catalysts (DHC) (Degussa-Hüls AG, Düsseldorf, Germany), launched *CatMETium® IMesPCy*, which is offered for pharmaceutical applications only. To market this catalyst, DHC has obtained technology licenses under patents generated by Herrmann et al. and field of use licences under patents generated by Nolan et al.[114,115] *CatMETium®* performs well in cross metathesis and in ring-closing, ring-opening, and ene-yne metathesis reactions, all of which are important in pharmaceutical syntheses.

Also in 2006, Umicore AG&CO.KG took licences under patents of Nolan et al. to enable marketing of *Neolyst® M2* for the use outside polymerization reactions. This catalyst is expected to be more reactive than *CatMETium®* due to the saturated nature of its NHC ligand.[116,117]

The most recent member of the Umicore metathesis catalysts is *Neolyst® M3*, a ruthenium indenylidene complex with two phobane ligands, which was licensed from Sasol Technology (UK). This catalyst would exhibit improved air, moisture, and heat resistance, thus giving it a prolonged reaction life time.

Umicore has more Neolyst catalysts in its pipeline. A new type of Schiff base substituted indenylidene complexes has been developed by Viacatt, a spin-off company of Ghent University, and Umicore signed an exclusive licensing and cooperation agreement in order to commercialize them.

Furthermore, Boehringer Ingelheim has licensed Grela's nitro catalyst **8** and anticipates commercializing it this year. This catalyst has been used with much success already[96], and caught the company's interest in view of its own process chemistry to produce macrocyclic drug candidates.[118]

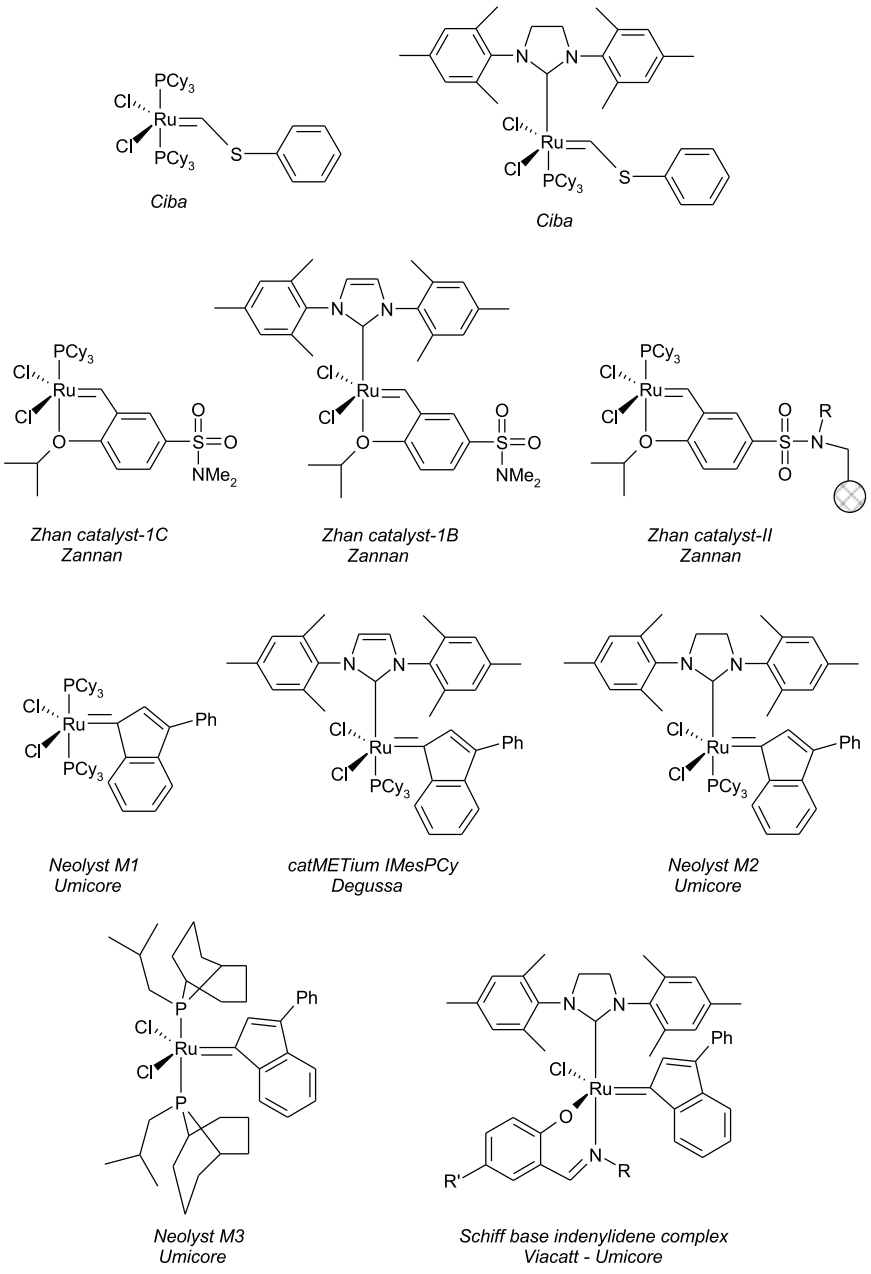

Figure 1.8: Commercial olefin metathesis catalysts.

Chapter 2

N-Heterocyclic Carbenes

The emphasis of this dissertation project lays on ruthenium alkylidene complexes coordinated with an *N*-heterocyclic carbene ligand. NHC ligands were introduced into organometallic chemistry as phosphine mimics, but have outperformed the latter in many respects. In this chapter we depict some of their interesting features such as their versatility, high electron donating ability, and applicability in a broad range of transition metal mediated reactions. Clearly, understanding of the relationship between the nature of the NHC ligand and the activity of the corresponding complexes is crucial in all efforts to design new attractive olefin metathesis initiators. Therefore, a brief overview of well-established, as well as more recent insights into the mechanism of metathesis initiated by 1st and 2nd generation ruthenium catalysts is also presented.

2.1 General properties

Over the past two decades, great achievements were made in catalysis using NHCs as ligands. Carbene complexes of late transition metals have been applied in many types of homogeneous catalytic reactions[119], including olefin polymerization and metathesis by Ru-based catalysts (section 1.3), hydrosilylation by Rh or Pt carbene complexes[120], Ir catalyzed hydrogenation and hydrogen transfer[121–123], Pd catalyzed carbon-carbon coupling reactions[124–126] and an increasing number of enantioselective reactions[127–131]. These types of reactions were traditionally carried out using phosphine based systems but NHC complexes exhibit some desirable properties not possessed by the former. Incorporation of NHC ligands improves the air and thermal stability of the complexes and makes them more resistant to oxidation. NHCs generally provide stronger bonding than the corresponding phosphines and unlike the latter remain bound to the metal center throughout catalytic cycles. For several metals the exchange of phosphines with NHC ligands proceeds readily and doesn't require the NHC to be present in excess.

This can be considered experimental evidence for the higher donor capacity of NHC ligands, which is supported by several calorimetric measurements and spectroscopic studies.[66,132–135]

2.2 Stability of *N*-heterocyclic carbenes

NHCs are singlet carbenes. This means that they possess a divalent carbon atom with six electrons in their valence shell and the nonbonding electrons paired in the same orbital. There are several reasons for the stability of these diaminocarbenes.[136–138] First, the large electronegativity of the *N*-atoms stabilizes the lone pair on the carbon atom through an inductive σ-effect. Additionally, the empty carbon orbital is stabilized by mesomeric interaction with the nitrogen lone pairs. This results in a four-electron three-center π-system, where the C-N bonds have some double bond character (Figure 2.1). For unsaturated NHCs a further stabilization is associated with a 4n+2 aromatic Hückel configuration.[139] Steric protection from the *N*-substituents may enhance carbene stability but is not a decisive factor since sterically less demanding substituents also afford isolable carbenes.[140]

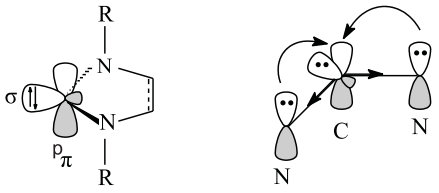

Figure 2.1: Singlet carbenes with *N*-substituents = π-donors, σ-attractors.

Initially the stability of NHCs was thought to be limited to cyclic diaminocarbenes with enough steric bulk to prevent dimerization and with a high aromatic character. Such carbenes are the imidazolin-2-ylidenes, as well as the 1,2,4-triazolin-5-ylidenes and benzimidazolylidenes (Figure 2.2).[141,142] For this family of carbenes, many different examples have been described in literature.[129,143–149] Later, also imidazolidin-2-ylidenes (or imidazolinylidenes), the saturated version of the imidazolin-2-ylidenes (or imidazolylidenes), were isolated. These were traditionally considered as more σ-donating than their unsaturated analogues. However, this assumption was overthrown by more recent studies showing that the basicity of NHC ligands has little to do with the saturated or unsaturated nature of the imidazole backbone.[134,150] In contrast to imidazolin-2-ylidenes, which dimerize only under special circumstances[151], the steric demand of the *N*-substituents in the 'C-C saturated' carbene determines whether it exists as the monomeric carbene or as the enetetramine dimer (*Wanzlick equilibrium*). The

free carbene is stable only for groups attached to the *N*-atoms that are *t*Bu or larger.[152–156] For smaller groups dimerization to the enetetramines inhibits their isolation (Figure 2.2).

A large variety of NHC ligands have since been reported which vary in ring size, substitution pattern and in their backbone elements.[157] Molecules derived from five-membered rings represent the most common class of NHC ligands, but also four-[158,159] and six-membered[160–167] heterocycles have been described. Seven-membered NHC ligands were prepared *in situ*; this is without isolation of the free carbene.[168,169]

The synthesis of the stable bis(diisopropylamino)carbene by Alder et al. demonstrated for the first time that neither aromatic stabilization nor the constraints resulting from the ring geometry are necessary to isolate diaminocarbenes.[170] Such acyclic ligands were shown to be even stronger electron donors than their

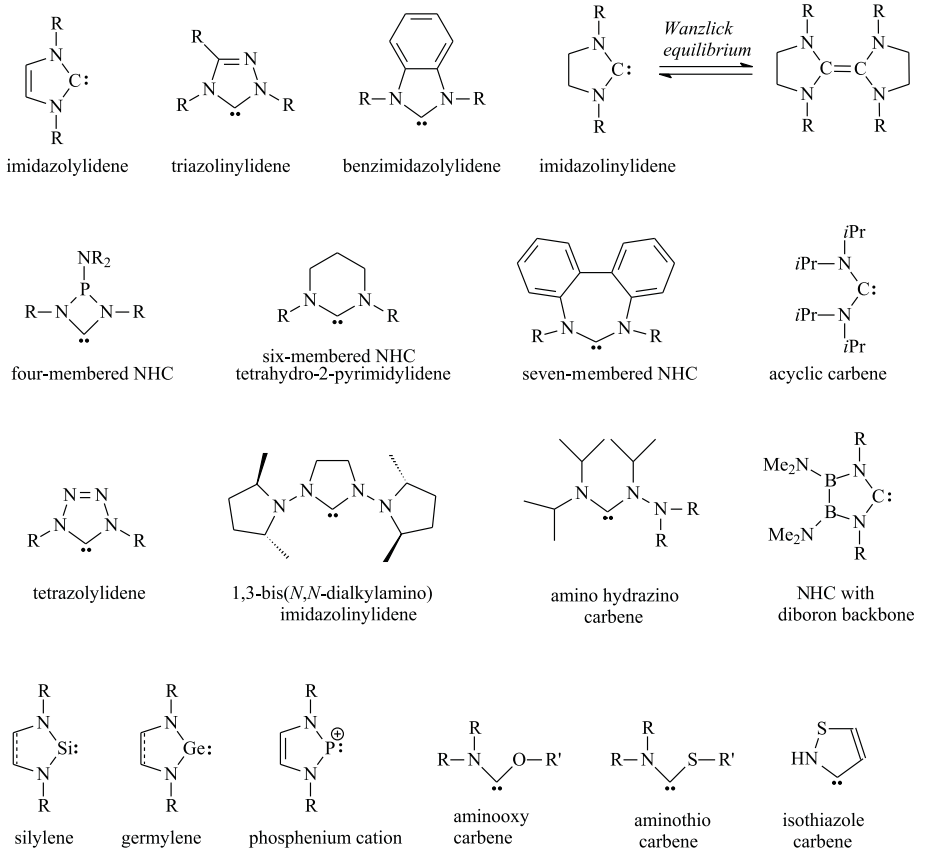

Figure 2.2: Amino carbene frameworks.

cyclic counterparts.[171,172] On the other hand, free acyclic carbenes are more fragile then cyclic carbenes, and the ensuing complexes are less robust.
Herrmann et al. recently described the synthesis of a CO-substituted Rh-complex bearing a tetrazolylidene ligand. A comparative study on CO-stretching frequencies allowed a good estimation of the relative NHC σ-donor/π-acceptor properties and revealed that the tetrazolylidene ligand is a weak σ-basic NHC (Figure 2.2).[173]
Lassaletta et al. described that the introduction of exocyclic *N*,*N*-dialkylamino groups to form 1,3-bis(*N*,*N*-dialkylamino)imidazolinylidenes maintains many of the properties of classic imidazolinylidenes and even gives rise to a slightly improved σ-donating capacity.[174] Acyclic amino hydrazino carbenes were isolated by Bertrand et al. at -30 °C. However, upon warming, an intramolecular rearrangement was found to limit the lifetime of these carbenes.[175,176]
Another interesting example of variation in the NHC framework is an *N*-heterocycle with a diborone backbone.[177] In addition, the isoelectronic carbene analogues silylenes[178–184] germylenes[185], and phosphenium cations[186,187] were reported in literature.

Stable carbenes with adjacent heteroatoms other than nitrogen are the aminooxy and aminothio carbenes developed by the groups of Warkentin[188] and Alder[189], isothiazole carbenes developed by Schulze et al.[190], as well as an impressive range of monoamino carbenes synthesized by Bertrand et al. The synthesis and isolation of aminoaryl carbenes[191], aminoalkyl carbenes[192], and cyclic alkyl amino carbenes[193,194] were described (Figure 2.3). Despite the presence of only one amino group, these carbenes are strong σ-donor / weak π-acceptor ligands, making them promising alternatives for diamino carbenes.
Another fascinating type of Bertrand carbenes are aminophosphino carbenes. These carbenes act as 4-electron donors with a strong σ-donating carbene next to a relatively labile phosphine.[195–198] Among this family, aminoaryl carbenes are the most stable, followed by aminoalkyl carbenes and aminophosphino carbenes.[199]
A last member of the series of carbenes synthesized by the Bertrand group is a *P*-heterocyclic carbene.[200,201] A computational study evidenced that the smaller singlet-triplet energy separation of PHCs compared with NHCs is of advantage to the 14 electron 'active' species in the olefin metathesis cycle.[202] This investigation indicates that the *P*-heterocyclic carbene might be an interesting candidate to

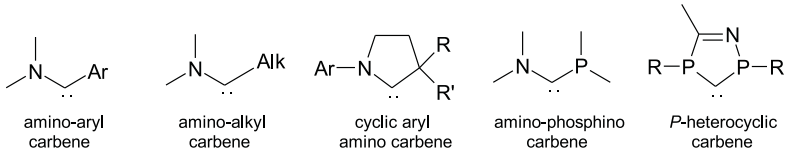

Figure 2.3: Bertrand carbenes.

alter the catalytic performance of olefin metathesis catalysts. On the other hand, a more recent report by Jensen et al. predicts a lower inherent olefin metathesis activity for ruthenium complexes incorporating PHC ligands. The lower productivity would partly be due to a larger Ru $d_\pi \rightarrow L_\pi$ backdonation, which destabilizes the metallacyclobutane intermediate in the olefin metathesis reaction.[203] This demonstrates that interesting future developments are to be expected in this particular area of research. All given examples constitute strong proof for the already existing wide ranging carbene chemistry, waiting to be further explored in catalyst development.

2.3 NHCs in organometallic complexes

2.3.1 Nature of the NHC-metal bond

NHC ligands have been coordinated to a wide range of transition metals and their complexes embody a third family of carbene complexes (Arduengo carbenes) in addition to the generally recognized Schrock and Fischer carbenes. Understanding of the nature of the NHC-metal bond constitutes a topic of ongoing research activity and is key to rational catalyst design.

NHC ligands were first believed to bind to transition metals through strong σ-bonding, while it was a common assumption that π-backbonding is negligible.[136] These binding properties were thought to result from strong π-donation by the *N*-atoms, causing a highly filled p_π orbital at the carbene carbon atom, and thus reducing the tendency towards metal to NHC π-backbonding.[204,205] Recently however, the widespread idea that NHC ligands are simple σ-donors is being replaced by the idea that π-interactions also contribute to the NHC-metal bond (Figures 2.4-2.6).[206] Meyer et al. evidenced with DFT (Density Functional Theory) calculations that NHCs can accept non-negligible electron density from electron rich metals through $d \rightarrow \pi^*$ backdonation.[207,208] Similar conclusions were made from EDA (Energy Decomposition Analysis) calculations on NHC-containing group 11 metal complexes.[209] Nolan et al. observed a remarkable $\pi \rightarrow d$ electron donation from NHC to metal for a NHC substituted Ir-complex.[210] In line with these papers, Cavallo et al. calculated that for systems with a low d electron

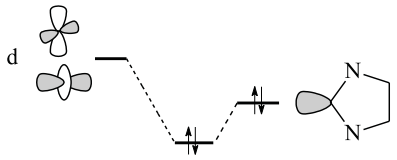

Figure 2.4: Metal-NHC $d \leftarrow \sigma$ donation.

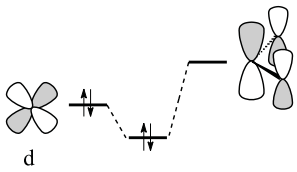

Figure 2.5: Metal-NHC d→π* back donation.

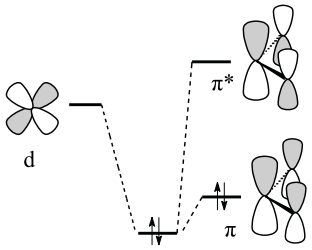

Figure 2.6: Metal-NHC d←πdonation.

count, both π-donation and π-backdonation are of importance while for systems with a high d electron count, backdonation gives the major contribution to the π-interaction.[211] This allows for the statement that NHC ligands can display an ambivalent π-bonding character, and might thus function as π-bases and as π-acids. Several recent experimental (crystallographic) and theoretical studies on the electronic structure of these transition metal complexes confirm the idea that an NHC ligand is not an entirely 'pure' σ-donor.[203,212–222] It is also clear that the donor power and π-bonding character depend not just on the ligand but also on the metal fragment and its coordination environment.

2.3.2 Synthetic routes

The synthesis of a wide range of NHC precursors is relatively straightforward, and many are now commercially available. However, the subsequent deprotonation and coordination to the metal center is often more challenging and as a result several different strategies have been elaborated and described in literature.[119,223,224]

A very popular procedure relies on simple ligand exchange and therefore hinges upon the ability to prepare the free NHCs (Figure 2.7 **(a)**).[140,141] The latter is often a limitation since the free carbenes often show high air and moisture sensitivity. Their sensitivity is caused by hydrolysis: It has been reported that the free carbene of imidazolidin-2-ylidenes hydrolyzes instantaneously while the unsaturated analogues (imidazolin-2-ylidenes) are more robust because of aromatic stabilization.[139] The general trend is that only imidazolin-2-ylidenes are isolated

prior to reaction with a metal precursor.[136] Another frequently used method is the thermal cleavage of enetetramines (= carbene dimer) in the presence of the metal species (Figure 2.7 **(b)**).[225–227] In cases where the free carbene or the '*Wanzlick dimer*' can not be synthesized, the complex formation has to be accomplished *in situ* from the ligand precursor (= imidazolium salt).
Among the numerous synthetic methods, simple *in situ* deprotonation and directly trapping of the free carbene, occupies a prominent place (Figure 2.7 **(c)**). It was first observed by Arduengo that 1,3-bis(2,4,6-trimethylphenyl)imidazolidin-2-ylidene (H_2IMes) undergoes a C-H insertion when reacted with a compound containing acidic C-H bonds to form a stable NHC adduct.[228] Given this knowledge, Lappert[229] and Grubbs[230] synthesized chloroform adducts by treatment of the azolium salts with base and chloroform, and utilized them to generate carbene complexes. An alternative synthetic strategy to make chloroform adducts uses diamines to react with chloral (Cl_3CCHO) in acetic acid.[231] Lappert and Grubbs implied that when the adduct and the metal precursor are reacted, free carbenes are generated *in situ* (Figure 2.7 **(d)**).
Enders carried out similar investigations on the triazol-methanol adduct Ph_3Tri(H)(OMe) where thermolysis liberates the corresponding free carbene (Figure 2.7 **(e)**). This free carbene was the first one to become commercially available.[142,232]
Another interesting approach to thermally generated free carbenes involves the synthesis of NHC adducts by condensation of diamines with appropriately substituted benzaldehydes. A major advantage of this method is that the free carbene does not have to be generated before it is protected. So formed pentafluorobenzene based adducts are more readily prepared than the chloroform adducts described above (Figure 2.7 **(f)**).[233,234]
Imidazolin-2-ylidenes are frequently generated by simple, direct deprotonation of the corresponding imidazolium salts with KO*t*Bu or potassium *tert*-amylate.[235] The reaction is likely driven by precipitation of the halide salts. When imidazolium salts with saturated C-C backbones are reacted with KO*t*Bu, a *tert*-butanol adduct is formed. Thermal decomposition of the NHC-alcohol adduct then allows *in situ* generation of the corresponding free carbene (Figure 2.7 **(g)**).[230]
Imidazol(in)ium-2-carboxylates are prepared from the corresponding NHCs by reaction with carbon dioxide. These CO_2 adducts are air and moisture stable species, which can transfer carbenes to a variety of metals with release of CO_2 (Figure 2.7 **(h)**).[236–238]
In 1993, Kuhn et al. found an alternative approach to alkyl-substituted NHCs relying on the reduction of imidazolthiones with potassium in boiling THF (Figure 2.7 **(i)**).[239] This strategy was further explored by Hahn et al.[240,241]
Furthermore, silver(I)-NHC complexes have shown to be convenient carbene transfer agents which usually circumvent the need for free NHC isolation. As a consequence, this method has recently gained interest in the NHC complex synthesis (Figure 2.7 **(j)**).[242–249] The driving force for this reaction is the formation of insoluble silver salts. Ag transfer agents can be particularly useful when the

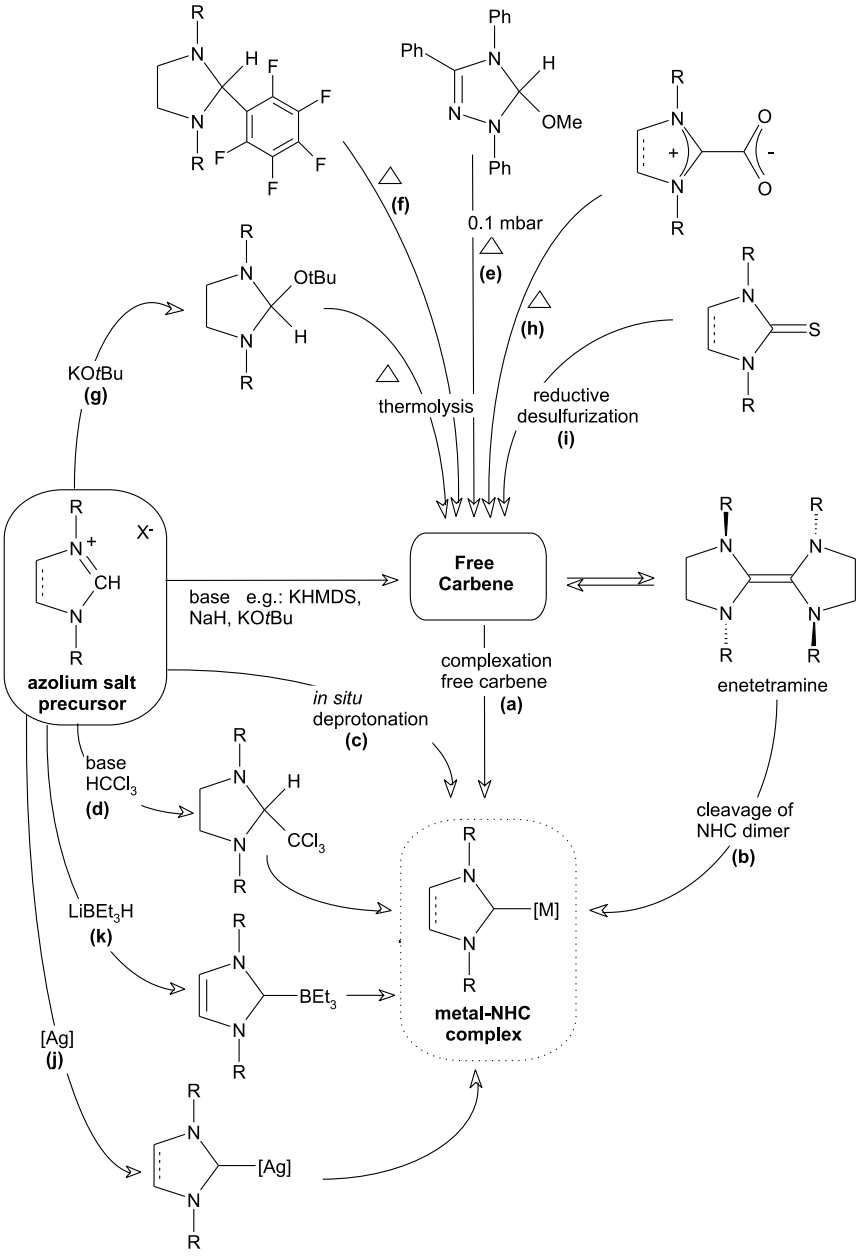

Figure 2.7: Preparation of metal-NHC complexes.

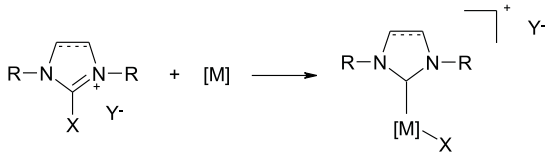

Figure 2.8: Oxidative addition of imidazolium salts.

NHC precursor has protons of comparable acidity to the imidazolium C-H (this is NC*H*N), and treatment with base is because of that not productive. Using an Ag transfer agent, Grubbs et al. were able to coordinate an unstable carbene to ruthenium while the more traditional deprotonation of NHC precursor in presence of ruthenium source was not successful.[250]
Another report describes the reaction of an imidazolium salt with $LiBEt_3H$, which affords a triethyl borane adduct serving as a carbene precursor in the synthesis of a transition metal complex (Figure 2.7 **(k)**).[251,252]
In addition, it is possible to attach NHCs to Pt[253,254], Pd[255,256] or Ni[257] through the oxidative addition of imidazolium salts (Figure 2.8).

2.3.3 Questioning the inertness of NHC ligands

There is no doubt that NHCs are significantly less reactive than Schrock carbenes and Fischer carbenes, but in the meantime a number of recent reports indicate that NHC ligands are not as inert as generally believed and occasionally participate in unanticipated side reactions.[258,259] Selected examples follow.

Considering that the NHC-metal bond has a length similar to that of a simple carbon-metal bond, reductive elimination of the NHC and associated ligands is not unlikely. Since 1998, Cavell et al. described a number of cases in which reductive elimination readily occurs between NHCs and *cis* ligands (Figure 2.9).[260–262]
A second important decomposition mechanism is C-H or C-C bond activation of a proton or methyl group on the NHC ligand (Figure 2.10).[263,264] C-H and

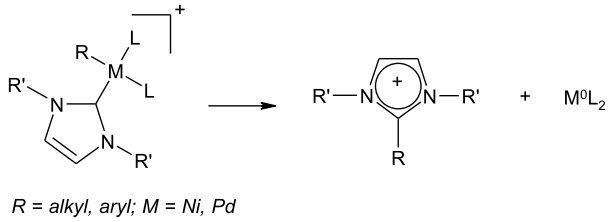

Figure 2.9: Reductive elimination.

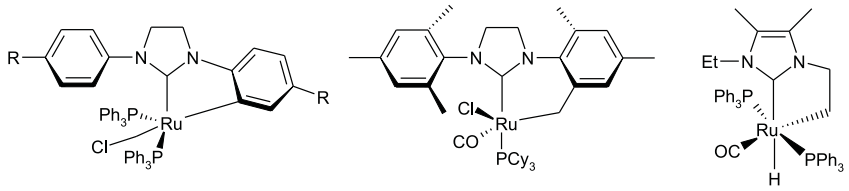

Figure 2.10: C-H and C-C bond activation.

C-C bonds are often forced into close contact with the metal center, which promotes this kind of bond activation reaction. Spontaneous metalation was already observed by Lappert et al. in 1979, for a 1,3-diphenyl-4,5-dihydroimidazol-2-ylidene ligand complexed with $RuCl_2(PPh_3)_3$.[265] Later, Grubbs et al. found that traces of air promoted metalation in the Grubbs 2nd generation catalyst **2**.[230] Also Nolan, Caddick, Whittlesey, Cabeza and Yamaguchi et al. observed analogous activation processses for their NHC substituted rhodium, ruthenium, nickel and iridium complexes.[266–273]

As decomposition reactions are detrimental to catalyst function, understanding them is of key importance to catalyst design. Therefore Grubbs et al. studied the double C-H bond activation of the *N*,*N*'-diphenylbenzimidazol-2-ylidene (biph) ligand that led to decomposition of the corresponding olefin metathesis catalyst.[274] Two decomposition products were formed (Figure 2.11). In the first product, the benzylidene inserted into an *ortho* C-H bond of one of the *N*-phenyl rings of the biph ligand with concomitant η^6 coordination to the ruthenium atom and loss of the phosphine ligand. In the second product, the Ru center has further inserted into an *ortho* C-H bond of the other *N*-phenyl ring with formation of a metallacycle.

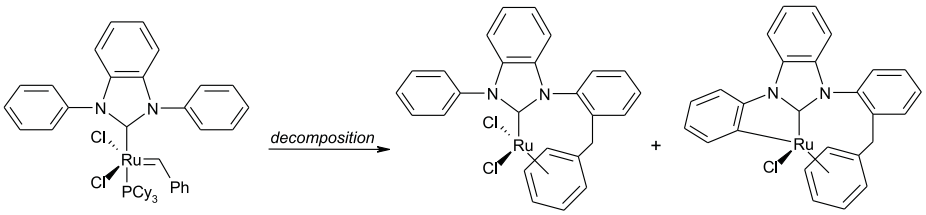

Figure 2.11: Thermal decomposition of Grubbs' *biph* catalyst.

Displacement of the NHC by a competing ligand is a third possible decomposition pathway (Figure 2.12).[275,276] Grubbs et al. synthesized the triazol complex $[(Ph_3Tri)(PCy_3)(Cl)_2Ru{=}CHPh]$, which appeared unstable in solution. Among the decomposition products were the $[Ph_3Tri(H)]^+$ salt and $[(PCy_3)_2(Cl)_2Ru{=}CHPh]$, which suggests that the triazolium ligand dissociated from the metal center

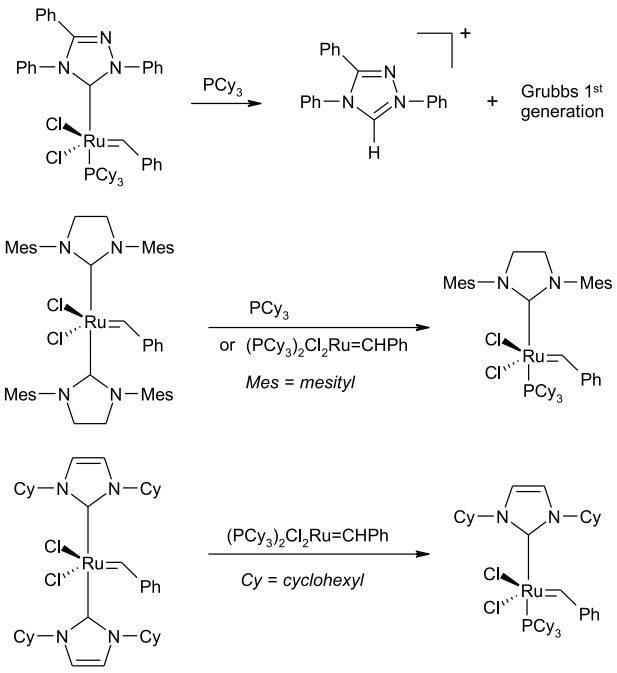

Figure 2.12: Ligand displacement.

and the phosphine reassociated to afford the more stable bisphosphine complex.[230] Another example supporting the idea of possible NHC dissociation, is the observation that when the bis(NHC) complex $[(H_2IMes)_2Cl_2Ru{=}CHPh]$ is heated in presence of an excess of PCy_3, significant quantities of $[(H_2IMes)(PCy_3)Cl_2Ru{=}CHPh]$ are generated. Even the reaction of bis(NHC) complex with **1** was found to create some of the mono(NHC) complex (Figure 2.12).[230] Similary, Herrmann et al. reported that reaction of $[(ICy)_2Cl_2Ru{=}CHPh]$ with complex **1** provided some $[(ICy)(PCy_3)Cl_2Ru{=}CHPh]$, which was attributed to a bimolecular NHC transfer rather than to a mechanism involving a free, dissociated carbene (Figure 2.12, ICy = 1,3-dicyclohexyl-imidazolin-2-ylidene).[277]

Recently, also illustrations of NHC ligands interfering in less common ways appeared in literature. These include migratory insertion of an NHC into a Ru-C double bond[278], migration of a methyl group to a coordinated NHC ligand[279], elimination of acylimidazolium salts[280], η^6-binding of a Ru center to one of the mesityl rings in the NHC[281], NHC rearrangement involving N-C bond cleavage[282], and benzylidene insertion into the mesityl group in Grubbs catalyst **2**[283].
Wagener et al. reported on the role of an NHC ligand in olefin isomerization, which is a known side reaction of ruthenium initiated olefin metathesis.[284,285]

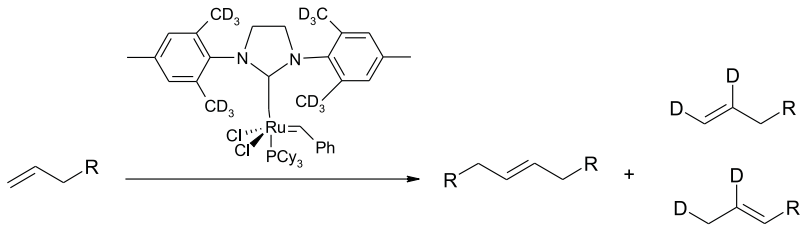

Figure 2.13: NHC ligand interfering in olefin isomerization.

The behavior of a deuterated version of complex **2** under metathesis conditions was monitored by NMR. This study revealed the incorporation of deuterium at various positions on the olefin backbone, indicating the formation of a ruthenium deuteride and the involvement of the NHC ligand during the isomerization process (Figure 2.13).[286,287]

Despite the generally strong bonding of NHC ligands to metal centers, some of the above mentioned examples exhibit NHC dissociation and NHC transfer. This questions the common belief that NHC ligands are noninterfering spectator ligands and it demonstrates that in some cases, there is the possibility of an equilibrium between NHC ligand and phosphine coordination.[288,289] NHC modifications during the reaction sequence are rare enough to be considered as exceptions, but these examples emphasize that they should not be overlooked.

2.4 NHCs in olefin metathesis catalyst design

The vast majority of NHC-metal complexes in catalysis have been applied in olefin metathesis. The 2nd generation Grubbs catalyst **2** and the Hoveyda-Grubbs catalyst **5** both contain NHCs and are the corner stones of today's extensive use of olefin metathesis in organic and polymer chemistry. These complexes outperform their phosphine analogues in many characteristics. Their NHC ligands are endowed with sterically hindered substituents on the *N*-atoms, which stabilize the catalytic intermediates against uni- and bimolecular decomposition pathways. Furthermore, systematic variations of the amino side groups and backbone substituents allow a fine tuning of their catalytic reactivity pattern, as it was demonstrated by several recent reports.[9,71,83,250,290–292]

2.4.1 Grubbs Catalysts

Olefin metathesis mechanism

To provide an understanding of the difference in catalytic behavior between 1st and 2nd generation Grubbs complexes, it is crucial to obtain a good insight

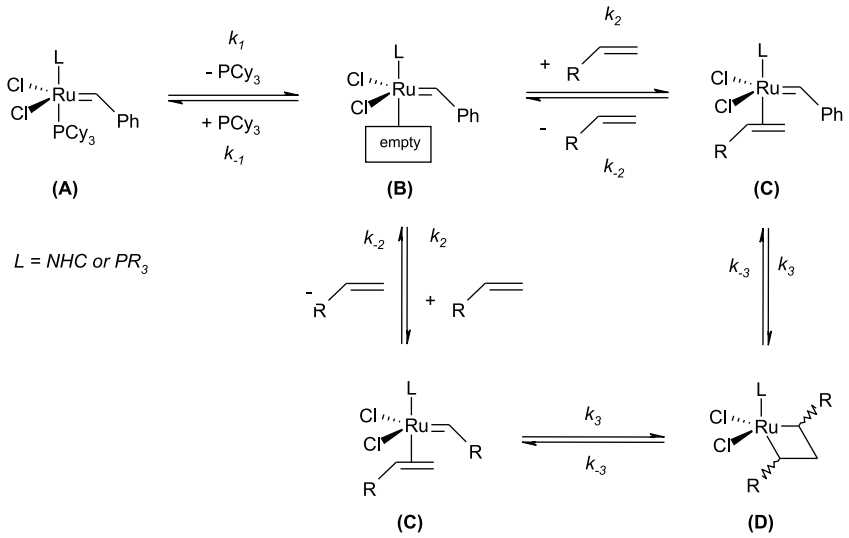

Figure 2.14: Dissociative mechanism for Grubbs catalysts.

into their mechanism for the olefin metathesis reaction. This mechanism has been thoroughly studied and was shown to proceed by initial dissociation of a phosphine ligand to form a 14-electron intermediate (Figure 2.14).[293] In the following step, the olefinic substrate coordinates to the ruthenium to give a 16-electron complex. A metallacyclobutane ring is then formed through coupling of the olefin and the alkylidene moiety within the ruthenium coordination sphere. The Ru(IV) metallacycle breaks down in a productive way to form a new olefin and a new alkylidene complex, or in an unproductive way to regenerate the starting compounds.

This dissociative pathway found strong support by computational[294–301] and experimental investigations[293,302–306] such as kinetic measurements. Ultimate proof was the recently described direct observation of a ruthenacyclobutane species **(D)** by Piers et al.[307] while Chen et al. confirmed through the identification of 14-electron active species **(B)** using gas-phase mass spectrometry.[308]

Not only have many mechanistic studies focused on catalyst initiation; there has also been a long-standing debate regarding the site of olefin coordination and metallacyclobutane formation. There is experimental evidence supporting olefin binding either *cis* (side-bound mechanism)[309,310] or *trans* (bottom-bound mechanism)[311,312] to the L-ligand (Figure 2.15). In a recent report on the issue by Piers et al., persuasive evidence is provided for the formation of a 14-electron ruthenium species in which the metallocycle lies *trans* to the NHC.[307] Several computational[294,295,298,300,313] and experimental[314] studies support this *trans* to the NHC olefin binding. Still, recent calculations by Cavallo et al. indicate that

the preferred reaction pathway is a delicate balance between electronic, steric, and even solvent effects.[315] Each of the three effects seems to be so strong that it would be a hazard to generalize any conclusions. Polar solvents push toward the side-bound reaction pathway and can overturn an electronic preference for the bottom-bound pathway.[316] So in absence of steric effects, the side-bound reaction pathway is favored. When however steric effects due to e.g. interaction of an NHC ligand and a substrate overcome other effects, the reaction mechanism is pushed toward the bottom-bound pathway.

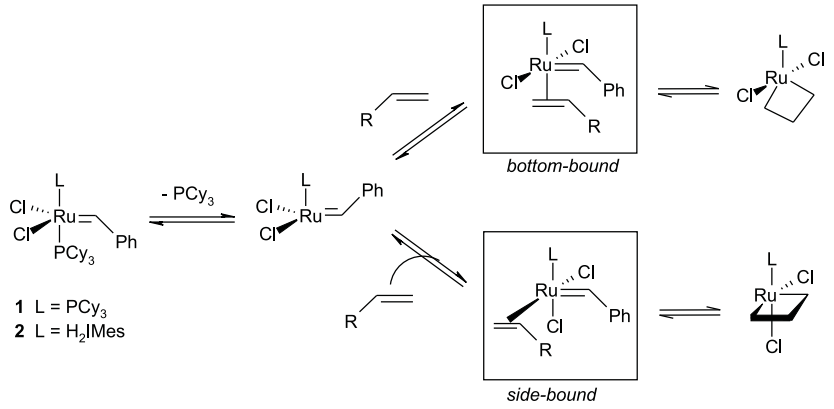

Figure 2.15: Olefin binding geometry.

For the traditional Grubbs catalysts **1** and **2**, a dissociative model with *trans* olefin coordination has emerged as the most reliable mechanism. The relative energies of the species on this pathway (**(B)**, **(C)**, and **(D)**) can be tuned by ligand variation. One notable ligand variation is the exchange of PCy_3 in catalyst **1** for the NHC ligand in catalyst **2**. As described in the next section, much effort is currently being done by various research groups to elucidate how exactly the NHC ligand influences the different intermediates formed in the metathesis reaction.

Grubbs 1st versus 2nd generation

H_2IMes (**2**) in substitution for PCy_3 (**1**) improves the activity of the corresponding Grubbs complexes in both RCM and ROMP by 10^2 to 10^3 times. This activity enhancement was initially attributed to a *trans* effect. NHC ligands are more electron donating than their phosphine analogues and were therefore believed to facilitate the dissociation of the *trans* phosphine ligand.[136] More favored phosphine dissociation would then result in higher concentrations of the catalytically active 14-electron species **(B)**. However, profound study of the reaction kinetics indicated that phosphine dissociation is considerably slower for **2** than for **1**.

The higher reactivity of **2** should thereupon not be attributed to a smoother phosphine dissociation, but to an enhanced preference for olefin coordination relative to phosphine coordination.[303,304,317] It is thus important to recognize that the activity of a catalyst is not only related to the phosphine dissociation rate k_1 but also to the ratio k_{-1} to k_2 which determines whether the catalyst binds the olefin or returns to its resting state (Figure 2.14).

The fact that the high activity of **2** is not simply a function of ligand basicity, but results from combined electronic and steric effects, was confirmed by several recent computational and gas-phase experimental studies.[298,318–321] The variation of the ligand L tunes the relative energies of *all* intermediate species in the catalytic cycle.
In a theoretical study on the model system $[(PH_3)(L)Cl_2Ru{=}CH_2]$, the intermediate **(C)** was found to be more stable than the metallacycle **(D)** for the phosphine complex (L = PH_3) and less stable for the NHC complex (L = $C_3N_2H_4$).[294] With DFT (Density Functional Theory) calculations on the 'real' catalysts $[(PCy_3)(L)Cl_2Ru{=}CHPh]$ with L = PCy_3 or H_2IMes, also Harvey et al. distinguished a more stabilized ruthenacycle intermediate for the 2nd generation catalyst. This was attributed to the greater electron-donating strength of the NHC ligand.[322]
Cavallo et al. attributed the catalytic behavior of complex **2** to a strong steric pressure exerted by the bulky mesidine substituents on the alkylidene moiety, which destabilizes the 14-electron species **(B)**. As a consequence, phosphine dissociation (initiation) is slowed down. On the other hand, the NHC was found to promote olefin coordination, lower the olefin metathesis reaction barrier and stabilize the metallacycle intermediate, which explains an overall reaction acceleration.[300] Jensen et al. confirmed that the higher catalytic activity seen for ruthenium 2nd generation catalysts can to a large extent be explained by steric effects.[203] Bulky *N*-substituents on the NHC ligand ensure an orientation of the ligand parallel to the alkylidene bond and thus very specifically put steric pressure on this Ru=C bond.
Early computational results by Chen et al. showed that during the catalytic cycle of the olefin metathesis reaction, an unfavorable rotation of the C_3-symmetric phosphine ligand has to occur whereas the C_2-symmetric NHC ligand in complex **2** does not have to rotate.[318] More recent gas-phase studies allowed Chen et al. to directly observe 14 electron active species **(B)**, and measure their intrinsic rates in the olefin metathesis reaction by means of electrospray-ionization mass spectrometry.[319] The higher reactivity of NHC ruthenium complexes was then explained twofold. A more favorable metallacyclobutane intermediate was seen experimentally and from computations.[298] Secondly a more favorable equilibrium for the π-complexation was found to be consistent with the smaller k_{-1} to k_2 value determined by Grubbs.[303]
It was described by Straub et al. that for complex **2** the conformation necessary for an immediate rearrangement into the ruthenacyclobutane ring is favored, as

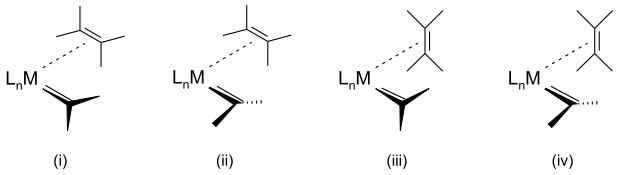

Figure 2.16: Possible conformations of olefin with respect to the carbene.

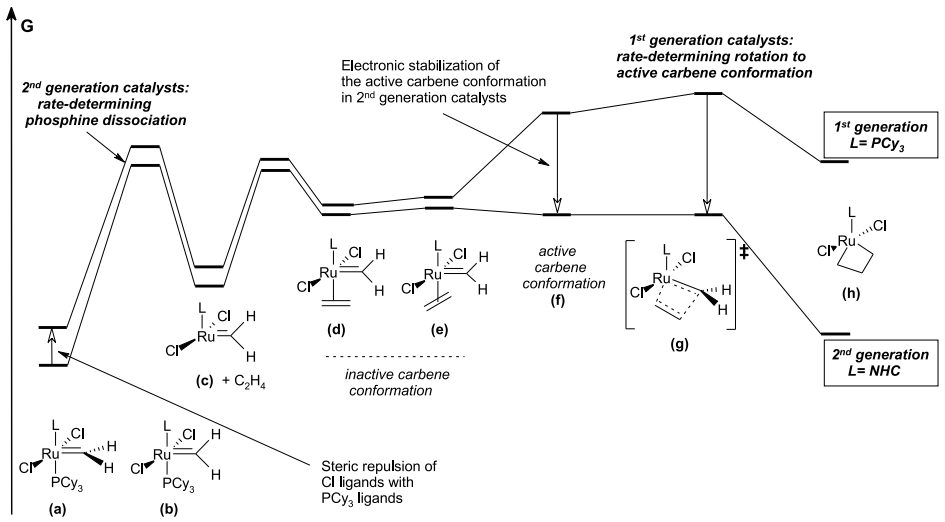

Figure 2.17: Gibbs free energy diagram of mechanistic pathways for 1st and 2nd generation Grubbs catalysts.

a result of a better electronic and steric stabilization.[323] This attainment of the proper conformation of the olefin with respect to the carbene ligand is crucial for catalytic activity. Four possible conformations are shown in figure 2.16, but only conformation (i) is productive in metathesis.[324,325] The different behavior of NHC and phosphine ligands is shown in more detail in figure 2.17. NHC ligands stabilize the active carbene conformation **(f)** and the transition state **(g)**. This makes the rotation from the inactive carbene conformers **(d)** and **(e)** electronically degenerate. On the other hand, the inactive carbene orientation is preferred in phosphine complexes, and an additional barrier for the rearrangement to an active carbene conformer exists. The rate-limiting step in 1st generation Grubbs catalysts is the cycloaddition step, the rate-limiting step in 2nd generation Grubbs catalysts is the phosphine dissociation.[326]

Unsaturated versus saturated NHC ligands

With no supporting evidence, the higher olefin metathesis activity of [(H_2IMes)-(PCy_3)Cl_2Ru=CHPh] **2** over [(IMes)(PCy_3)Cl_2Ru=CHPh] used to be attributed to an increased basicity, and thus greater electron donation of H_2IMes (1,3-dimesityl-4,5-dihydroimidazol-2-ylidene) compared with IMes (1,3-dimesityl-imidazol-2-ylidene). More recently, calorimetric studies revealed that differences in bond dissociation energies between H_2IMes and IMes are of only 1 kcal/mol.[327] An alternative experimental approach is based on the study of CO stretching frequencies in NHC-containing carbonyl transition metal complexes.[134,147,276,328] It is shown that NHCs are more σ-donating than phosphines, but none of these studies points to a pronounced difference in basicity between saturated and unsaturated NHC ligands. Results by Nolan et al. even suggest that saturated NHCs would be slightly less electron-donating than their unsaturated counterparts.[134] While small differences in donor capacities might cause a significantly different catalytic behavior, it is plausible that subtle steric differences play a more determining role.[329] Several computational studies allowing for a classification of a number of NHCs according to their basicity indicate that the most influential factors would be substitution on the NHC backbone and the NCN bond angle.[150] A recently described quantitative structure-activity relationship (QSAR) model establishes a direct connection between activity and chemically meaningful ligand properties.[203] Ligands that most efficiently promote metathesis activity are those that stabilize the metallacyclobutane intermediate relative to the other intermediates in the reaction pathway. Ligand-to-metal σ-donation stabilizes the metallacyclobutane, while metal-to-ligand π-backbonding destabilizes it. A bulky dative ligand then drives the reaction toward the less sterically congested metallacyclobutane species and contributes to catalytic activity. A relative stabilization of the metallacyclobutane intermediate, originating to a large extent from steric effects, was found upon going from IMes to H_2IMes. Some of these steric effects are caused by the shorter Ru-NHC bond obtained for the saturated ligand. In other words, the steric effects in part originate from electronic differences between the saturated and unsaturated NHC. The better σ-donating and π-accepting abilities of the saturated H_2IMes ensure a stronger Ru-NHC bond, which, in turn, causes closer contact and higher steric repulsion between the NHC and alkylidene moiety. This interplay of electronic and steric effects explains the higher metathesis activity observed for the Grubbs catalyst bearing H_2IMes, compared with the one bearing IMes, although H_2IMes is only a marginally better σ-donor and does not appear to be much bulkier than IMes.

2.4.2 Hoveyda-Grubbs Catalysts

The Hoveyda-Grubbs catalyst **5** shows efficiencies similar to those of Grubbs catalyst **2**, but with a different substrate specificity. This recyclable catalyst is unique in catalyzing RCM, ROMP, and CM reactions with highly electron-

deficient substrates.[330]
There are no detailed mechanistic studies on catalyst **4** and its phosphine-free analogue **5** yet, but it is clear that the absence of released phosphine, which can intercept the Ru active species, causes a somewhat different reactivity profile. After loss of the styrenyl ether ligand (dissociative mechanism), complex **5** will generate the same active 14-electron species as complex **2**, but the styrenyl ether ligand is a weaker ligand than phosphine and is therefore expected to compete less productively with olefin coordination. Nevertheless, when the phosphine ligand in the Hoveyda-Grubbs 1st generation catalyst **4** is replaced by the NHC ligand H_2IMes in the Hoveyda-Grubbs 2nd generation catalyst **5**, an activity enhancement similar to the one observed for the Grubbs complexes is found.

2.4.3 'New' NHC ligands

When aiming at a successful design of NHC ligands for olefin metathesis catalysts, it is important to consider both electronic and steric effects. These two effects can often not be separated, as any modification in the NHC framework alters both properties to a certain extent. While an NHC ligand with bulky *tert*-butyl substituents on the *N*-atoms is theoretically predicted to give high catalytic activity,[203] the large steric bulk of the amino side groups inhibits a strong NHC-metal bond (chapter 5).[9] Steric effects can thus be so strong to alter completely the stability of complexes.[206] Furthermore, there is no such thing as an ideal catalyst for every olefin metathesis transformation. A given catalyst can be efficient in one type of metathesis reaction and inefficient in another. The search for the ideal NHC framework is thus always substrate specific. To aim at a good combination of the electronic and steric factors, it is sometimes found necessary to synthesize a range of different ligands. These aspects are illustrated in Chapters 5 and 6 where we describe the introduction of several new NHC ligands in Grubbs and Hoveyda-Grubbs complexes respectively.

The NHC ligands described in this thesis all incorporate a saturated backbone. NHCs with unsaturated backbones have a longer history; ruthenium carbene complexes with NHCs bearing *N*-cyclohexyl groups were even amongst the first 2nd generation catalysts to be described in the literature.[331] In addition, Grubbs-type metathesis catalysts with 'unsaturated' NHCs bearing an *N*-alkyl- as well as an *N*-aryl group have thoroughly been reported in literature by Fürstner et al.[332–334] and Grubbs et al.[335,336] It was shown that substantial structural variations can be accommodated at the NHC ligand and eventually lead to designer catalysts with tailor-made properties. However, as 'saturated' NHC's generally afford more active metathesis initiators than 'unsaturated' ones,[337] recent research mainly focuses on the former.

Literature examples of Grubbs or Hoveyda-Grubbs complexes with modified 'saturated' NHC ligands mostly involve the introduction of altered *N*-aryl groups.

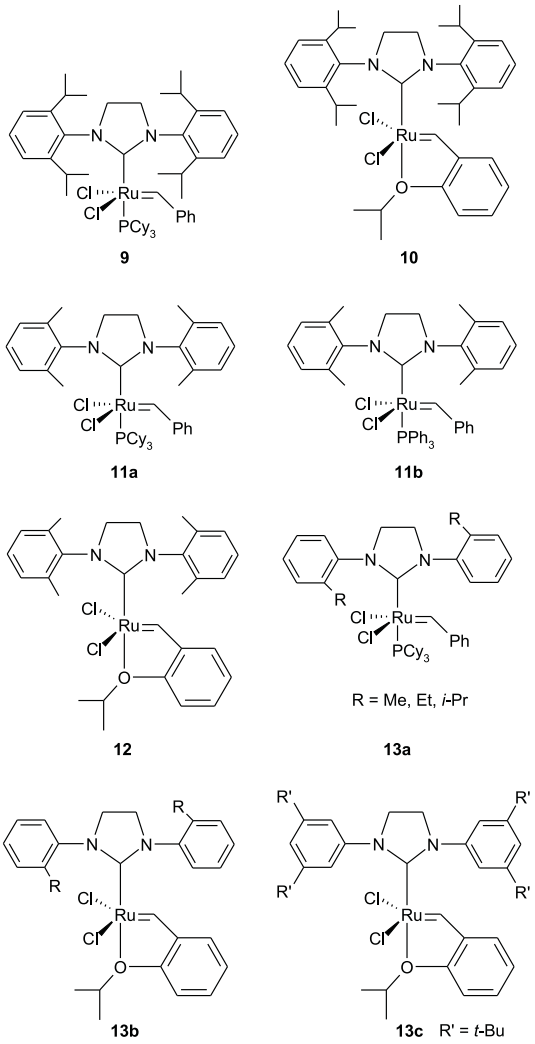

One of the first successful modifications to the Grubbs 2nd generation catalyst was described by Mol et al. in 2002. The catalyst **9**, bearing a bulky 1,3-bis(2,6-diisopropylphenyl)-4,5-dihydroimidazol-2-ylidene ligand, gave higher initial turnover frequencies relative to **2**, which was assigned to a sterically induced faster initiation rate.[291] The corresponding Hoveyda-Grubbs catalyst **10** was synthesized by Wagener et al. and used in ADMET reactions.[338] Again, at all temperatures, the steric hindrance brought about by the NHC was found to result in faster initial rates. Fürstner et al. observed some catalyst decomposition during their synthesis of complex **9**, and isolated a Ru hydride as a major

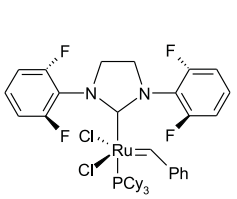

14

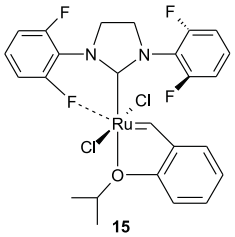

15

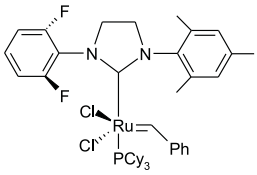

16

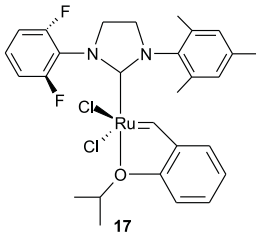

17

byproduct.[332] Similarly, Hoveyda et al. found complex **11** to be surprisingly unstable which rendered its isolation difficult. Also the triphenyl phosphine complex **11b**, prepared by He et al., was found to exhibit a low thermal stability, which led to low conversions in RCM reactions at elevated temperature.[339] These two complexes and their more stable phosphine free analogue **12** are structurally altered from complexes **2** and **5** in the lack of *para* substitution at the two aryl groups on the NHC nitrogens.[89] The increased instability of complexes **9** and **11a** relative to complex **2**, demonstrates how the absence of a methyl group, even when distant from the metal center, still greatly influences catalyst properties.
Complexes **13a**, **13b**, and **13c** were recently synthesized and the scope of their utility investigated by Grubbs and co-workers.[340,341] **13a** and **13b** proved to be the most efficient catalysts up to date in the RCM of the hindered olefin diethyl dimethallylmalonate. Also complex **13c** demonstrated considerable activity in the RCM of this tetrasubstituted cycloalkene. While a scale up of the preparation of **13c** was found to be relatively difficult, complexes **13a-b** are now commercially available.

A recent report by Grubbs et al. discloses a substantial rate enhancement in olefin metathesis reactions initiated by complex **14**, bearing *o*-fluorinated aryl groups on its NHC ligand.[250] The phosphine-free analogue **15** did not show this feature. Crystallographic analysis was able to bring some insight into the dissimilar catalytic behavior of both complexes. Complex **14** was found to display a distorted square pyramidal structure similar to the one observed for the classic Grubbs complex **2**. Complex **15**, however, shows a rotation of one of the two fluorinated aryl groups, positioning one of the fluorine atoms in close proximity to the Ru center, and resulting in an uncommon fluorine-ruthenium

interaction. The absence of this interaction in complex **14** was explained by the steric congestion of the NHC amino side groups with the bulky PCy_3 ligand upon fluorine coordination. However, when the phosphine dissociates in the initiation step of the olefin metathesis cycle, and the phosphine-free 14-elektron species **(B)** (Figure 2.14) is obtained, a fluorine-ruthenium interaction was found possible. This interaction was held responsible for an acceleration of the catalyst initiation and thus for the increased catalyst efficiency of **14**.
Based on these results, Grubbs et al. also described the metathesis catalysts **16** and **17** each bearing an unsymmetrical NHC ligand.[342] The NHC of complex **17** rotates fast around the Ru-C_{NHC} bond on the NMR time scale in solution. On the other hand, complex **16** exists as a mixture of two conformational isomers, with the mesityl ring located above the benzylidene group in the major rotational isomer. A small rate enhancement was observed in ring-closing metathesis reactions for complex **16**, which might be due to a fluorine-ruthenium interaction as found earlier for complex **14**. On the contrary, complex **17** was found less efficient than the benchmark Hoveyda-Grubbs catalyst **5** for RCM. This seems to be caused by a longer induction period, i.e. slower catalyst initiation. In CM and ROMP model reactions, both catalysts show similar or lower activity than the commercial catalysts **2** and **5**.

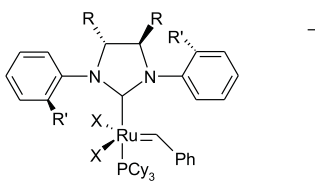

R = -$(CH_2)_4$- or Ph
R' = CH_3, $CH(CH_3)_2$

18

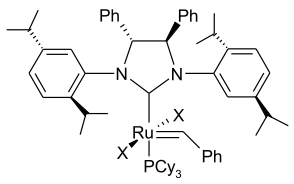

19a

X = Cl, I

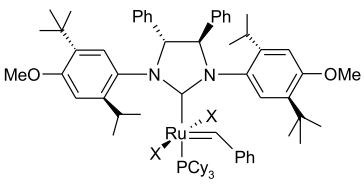

19b

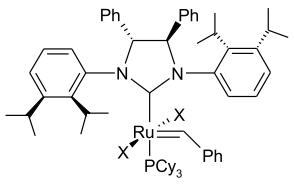

20

As NHC ligands generally do not dissociate from the Ru center during metathesis, the desymmetrization of the NHC ligand affords a chiral catalyst. Several enantioselective ruthenium olefin metathesis initiators were developed by Grubbs et al. The NHC ligands in complexes **18** have backbone stereogenicity, and the core asymmetry is amplified via preferred conformations of the *N*-substituents. These complexes have the same air and moisture stability as their parent complex

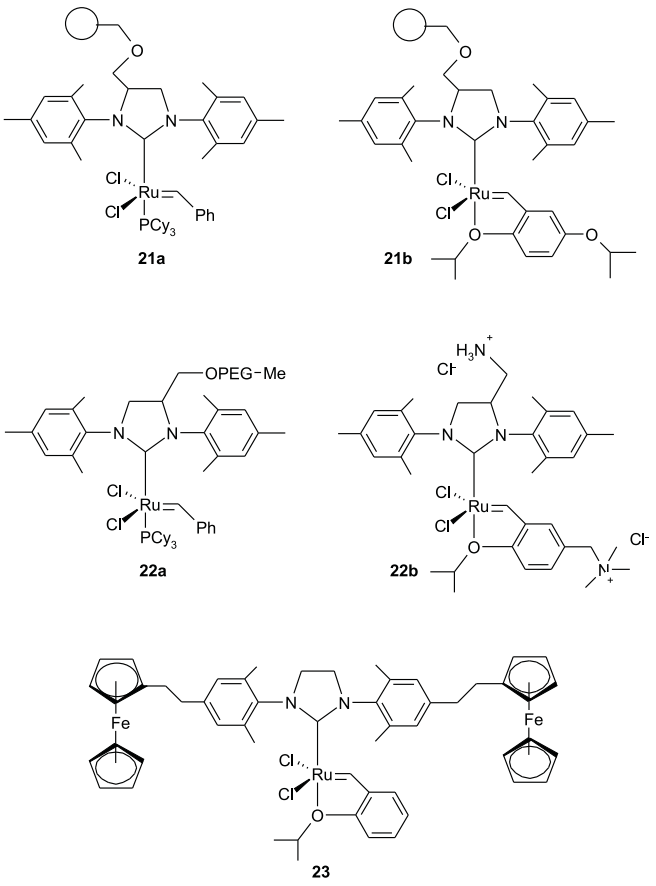

1, as well as a similar level of reactivity. Satisfactory enantiomeric excesses were measured in the RCM of achiral trienes.[71] On the basis of this initial discovery, further modifications were introduced. Catalysts **19a-b** containing substitution on the aryl ring *para* to an *o*-ispopropyl group show enantioselectivities very similar to the initial chiral catalysts **18**. On the other hand, substitution on the same side of the ring as the *o*-ispopropyl group (**20**) induced a significant increase in enantioselectivity, and allowed for high conversions with low catalyst loadings.[83,312]

An additional advantage of the strong bonding of NHC ligands to the catalyst metal center, is that immobilization of catalysts can be achieved by the use of anchored NHCs. Blechert et al. attached the NHC to a Merrifield resin via an ether linkage, affording the Grubbs type catalyst **21a**[343] and the Hoveyda-Grubbs catalyst **21b**[344] respectively. Both complexes show relatively good metathesis

activity and their recoverability makes them economically attractive alternatives for their homogeneous counterparts.
Appending poly(ethylene glycol) (PEG) to the nondissociating NHC ligand renders catalyst **22a** soluble in organic solvents as well as in water, while maintaining the stability and activity of complex **2**.[345] Complex **22b**, incorporating an NHC ligand substituted with an ionic group, is a highly competent ROMP catalyst.[346] A reasonable activity was found for the RCM of α,ω-dienes, which is a more challenging transformation in water than the ROMP reaction. With these complexes, Grubbs et al. aimed for olefin metathesis in aqueous media, which has important economic, and environmental benefits. Furthermore, an efficient removal of ruthenium byproducts from olefin metathesis products by simple aqueous extraction was found possible.[347]
Another successful strategy, next to catalyst immobilization, for the separation of homogeneous catalysts from the reaction products, is based on redox-switchable phase tags, which mutate from neutral into charged tags and vice versa. The ferrocenyl-tagged Hoveyda-Grubbs catalyst **23** was prepared by Plenio et al. in 2005.[348] After the olefin metathesis reaction, an oxidizing reagent is added. Thereupon a di-cation $\mathbf{23}^{2+}$ is formed, which precipitates within a few seconds. The catalyst is then easily reactivated by addition of a reducing agent.

Two unusual NHC novelties are found in complexes **24** and **25**. To further investigate the role of subtle changes in the steric environment around the Ru metathesis catalysts, Grubbs et al. introduced the six-membered NHC 1,3-dimesityl-1,4,5,6-tetrahydropyrimidin-2-ylidene on complex **1**. The resulting complex **24** demonstrates only moderate reactivity in RCM and ROMP reactions.[162] This was assigned to a larger steric environment around the metal atom, which may disfavor olefin binding or metallacyclobutane formation. Complex **25** is the first Ru complex bearing a four-membered NHC ligand. Catalytic tests reveal that also **25** is slower than complexes **2** and **5** in CM, RCM and ROMP reactions.[159]
Complex **26** incorporates an NHC ligand with an annelated cyclohexene moiety.[349] The presence of a double bond in the NHC framework, which is inert even at elevated temperature and offers options for further functionalization of the ligand backbone, is quite remarkable. The catalytic activity of **26** was found to be only slightly inferior to the activity of its parent complex **5** in the RCM of diallyl tosylamine.
Complexes **27** and **28** were very recently prepared by Grubbs et al. using 2-(pentafluorophenyl)imidazolidines as NHC precursors.[350] Complex **28** could not be synthesized using other methods due to an apparent instability of the complex. Both complexes bear methoxy groups on their aromatic NHC amino side groups, which can be expected to exert some influence on their olefin metathesis activity. However, catalytic data were not reported yet, but are likely to appear in the near future.
Complexes **29a-d** each incorporate a cyclic (alkyl)(amino)carbene.[351] This type of Bertrand carbenes was reported to be more electron donating than classic NHC

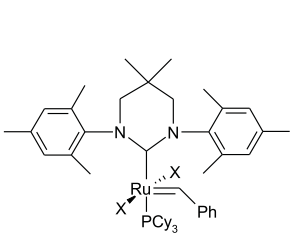

24

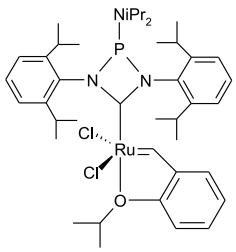

25

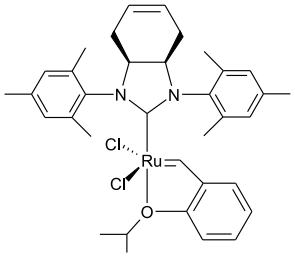

26

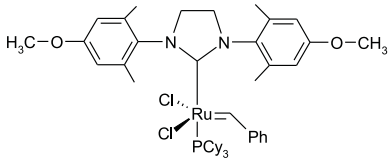

27

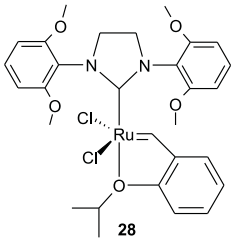

28

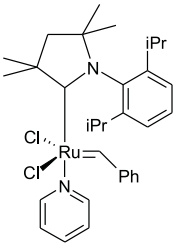

29a

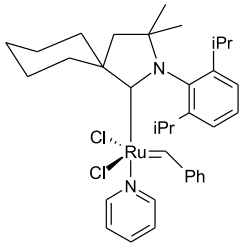

29b

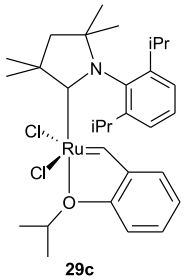

29c

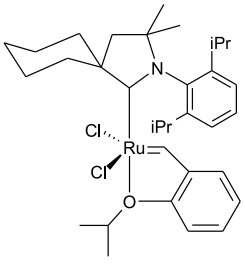

29d

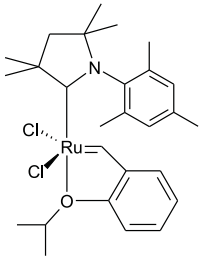

29e

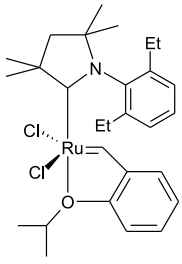

29f

ligands as a result of the greater σ-donor ability of carbon versus nitrogen.[352] In addition, the exchange of an sp^2-hybridized nitrogen for an sp^3-hybridized carbon considerably alters the steric environment relative to NHCs. The air-sensitive complexes **29a** and **29b** were isolated in modest yields and showed

rather low activity in the RCM of diethyl diallylmalonate. The more stable Hoveyda analogues **29c-d** were isolated in good yields. Also these two catalysts exhibited lower RCM activity relative to **2** and **5**. As sterics were expected to be responsible for the lower activity, a decrease of the steric bulk of the *N*-aryl ring was targeted. Complex **29e**, bearing an *N*-mesityl moeity, could not be synthesized, while complex **29f** was isolated as an air-stable solid (yield = 18%). **29f** showed a substantially higher RCM activity compared with **29c-d**, which was attributed to a more favored catalyst initiation. Catalyst initiation requires dissociation of the ether group and rotation of the benzylidene moiety into a plane parallel to the *N*-aryl group to open up a coordination site for olefinic substrate. This process may be unfavorable for complexes with more sterically demanding *N*-aryl groups as found in **29c-d**.

Undoubtedly the most impressive example of a 2nd generation Grubbs catalyst endowed with a non-symmetrical NHC, is the chiral complex **30** developed by Hoveyda et al.[353,354] This complex is less active than the achiral parent system **5** due to the replacement of a Cl with a less electronegative phenoxide and the increased steric bulk of the NHC ligand. On the other hand, several examples of asymmetric ring-opening/cross metathesis reactions (AROM/CM) indicate that complex **30** is an effective chiral Ru catalyst for enantioselective metathesis. Enantiomeric excesses up to 98% were measured.
A second type of chiral NHC complex developed by Hoveyda et al., is complex **31**.[355] The NHC ligand bears a chiral diamine backbone and an achiral biphenol group. Chirality is transferred by the stereogenic centers in the backbone, which in turn induce the achiral biphenyl amino alcohol moiety to coordinate to the metal center to form a single atropisomer. Preparation of the ligand does not require the availability of an optically pure binaphtyl-base amino alcohol, the synthesis of which requires long routes. A rather low stability was found for complex **31a**, contrasting with the high robustness of complex **30**. Reactions promoted by **31a** deliver similar or higher enantioselectivity as compared with the **30** analogue. Furthermore the reactions are typically completed within a

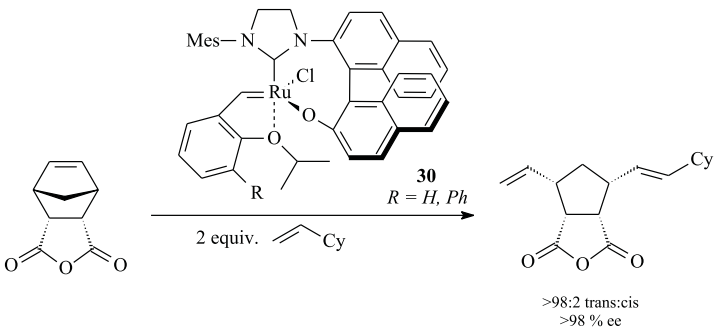

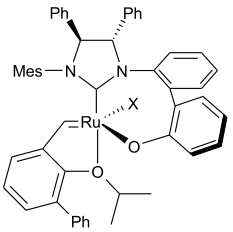

31a *X = Cl*
31b *X = I*

shorter period of time. Substitution of the chloride ligand for a iodide ligand, enhances the stability of the resulting complex, while retaining a high reactivity and enantioselectivity. Unlike chloride complex **31a**, complex **31b** is stable to silica gel chromatography in air.

The above described complexes all bear NHCs with aromatic amino side groups. In chapters 5 and 6 of this dissertation, however, we introduce three types of NHC ligands which bear at least one *N*-alkyl group: *N*,*N*'-dialkyl, *N*-alkyl-*N*'-mesityl, and *N*-alkyl-*N*'-(2,6-diisopropylphenyl) heterocyclic carbenes (Figure 2.18). For each of these three NHC types, the steric bulk of the aliphatic amino side groups was varied and the effect of these ligand modifications on catalyst activity was studied in olefin metathesis test reactions. Generally, the metathesis activity was found to be highest for the least steric amino side group (a methyl group).
This observation inspired Collins et al. to synthesize the highly active chiral Ru catalyst **32**.[356] *t*-Bu groups along the NHC backbone were expected to increase the enantioinduction in comparison to the Grubbs complexes **18**-**20**. Fearing that a too bulky NHC ligand would hinder the preparation of the catalyst, one of the *N*-aryl groups was replaced with a methyl group. NOE experiments and X-ray crystal analysis demonstrated that the resulting complex **32** has the methyl group located directly over the carbene unit. This is in direct contrast to our and Blecherts[290] observation that Grubbs or Hoveyda-Grubbs catalysts bearing *N*-alkyl-*N*'-mesityl heterocyclic carbenes coordinate in such a way that the aromatic mesityl group is oriented towards the benzylidene moiety (chapters 5 - 6). This

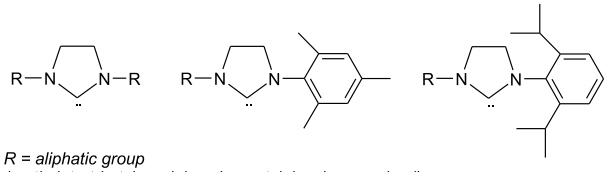

R = aliphatic group
(methyl, tert-butyl, cyclohexyl, n-octyl, isopinocampheyl)

Figure 2.18: Modified *N*-heterocyclic carbenes.

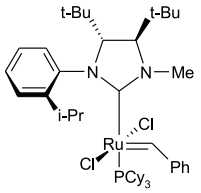

32

Figure 2.19: Highly active chiral Ru catalyst.

reversal in NHC geometry might be assigned to the di-*tert*-butyl backbone of the NHC, which puts a high steric pressure on the *N*-aryl group. The catalyst **32** was evaluated in several desymmetrization of trienes reactions, where substantial enantiomeric excesses were measured. Furthermore, an increased reactivity in comparison to Grubbs' chiral Ru catalysts bearing a C_2 symmetric NHC (**18**-**20**) was found.

Chapter 3

Acid Activation of a Ruthenium Schiff Base Complex

Commercial polymerization technology often requires a latent catalyst, which is able to catalyze the olefin metathesis under determined conditions. The ideal latent catalyst is completely inactive at room temperature, and is converted to its active form by heating, light or chemical activation. Catalysts such as Grubbs complexes **1** and **2** are competent at room temperature and are thereupon not well suited for applications where catalyst latency is beneficial.

The objective of the in this chapter described research was twofold. A primary goal was to test Ru complexes that have the potential of enhancing the catalyst pot life. Secondly, various additives which chemically activate the latent catalyst were explored. Doing this, we were able to develop a new latent catalyst system, which allows for excellent control of activity.

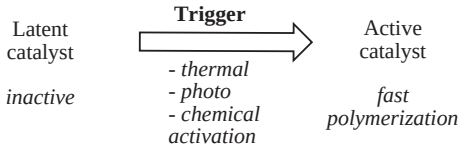

Figure 3.1: Ideal latent catalyst.

3.1 Introduction

When searching for new catalysts to use in ROMP technology, so-called *latent* catalysts are of particular interest. These catalysts display a low initiation rate, which allows for long handling of monomer/catalyst mixtures before the polymerization is started (Figure 3.1). One possible approach to develop a latent catalyst is the coordination of a *dangling* ligand, giving access to robust and stable catalysts. *Dangling* ligands are bidentate ligands stabilizing the resting state of the catalyst at room temperature while one coordination site is liberated at elevated temperature. Several examples were described in literature.[74,77,85,97,357–360] A few of them are shown in Figure 3.2: Grubbs et al. described a catalytic system substituted with an *O*,*N*-chelating Schiff base ligand[361], Slugovc et al. described *C*,*N*-chelating Schiff base ligands[362], while Herrmann et al. synthesized metathesis initiators bearing a pyridinylalcoholate unit[363]. *O*,*N*-chelating Schiff base substituted ruthenium complexes were further investigated by the Verpoort group.[6,364–370] Their main advantages are that they are very stable, that they can be used in protic media, and that the readily accessible salicylaldimine ligands lend themselves to catalyst tuning.[6,371,372] These catalysts generally turned out to be unreactive in olefin metathesis reactions at room temperature. Increas-

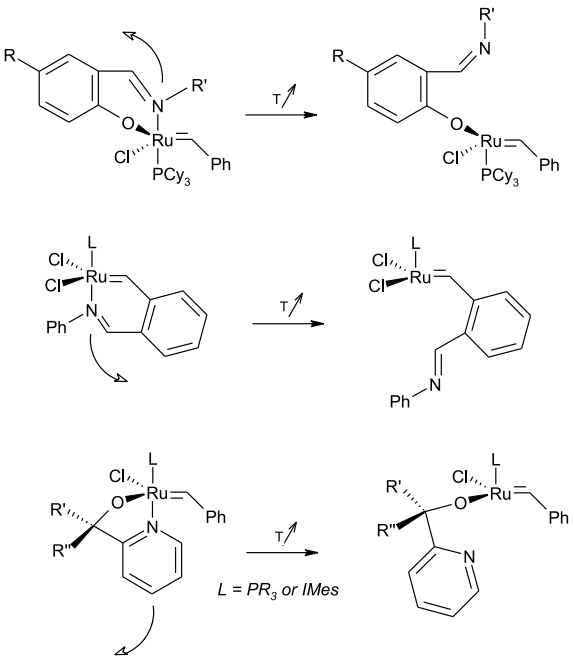

Figure 3.2: Dangling ligands.

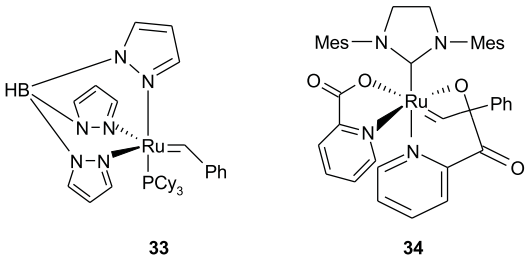

Figure 3.3: Ru-complexes requiring acid activation.

ing the temperature improved catalytic activity, but activity comparable to the corresponding complexes without Schiff bases could not be reached.
At first glance, this inactivity might be interpret as a huge disadvantage but catalyst activation by the addition of small amounts of acid was found possible. A HCl activation strategy was previously used by Grubbs et al. for Schiff base substituted Grubbs 1st generation complexes.[373] Moreover, several cocatalysts, including phosphine scavengers, Brönsted acids, and Lewis acids are known to assist in the dissociation of a ligand to generate a coordinatively unsaturated species and thus improve metathesis activity.[374–378] One example is the coordinatively saturated complex **33**, which requires ligand dissociation by activation with cocatalysts such as HCl, CuCl or $AlCl_3$ to achieve olefin metathesis activity.[379] A second example is the halide free complex **34** which becomes active in RCM once the addition of HCl led to protonation of a pyridine-2-carboxylato ligand (Figure 3.3).[358]
The new latent catalyst **36** we wish to describe here is a ruthenium complex bearing a bulky Schiff base unit together with a bulky *N*-heterocyclic carbene ligand (Figure 3.4). The catalytic activity of **36** was compared with the activity of its phosphine analogue **35** in representative non-activated and acid-activated test reactions. Various Lewis acids were able to boost catalyst **36** for olefin metathesis. The best results were obtained with trichlorosilane ($HSiCl_3$) as a cocatalyst. In

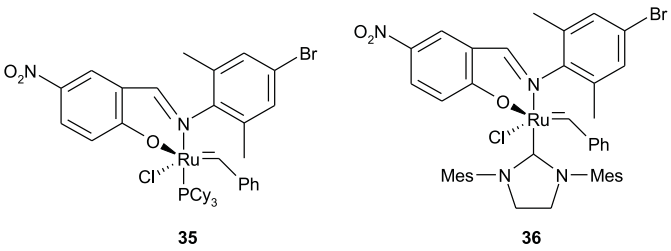

Figure 3.4: Schiff base Ru-complexes.

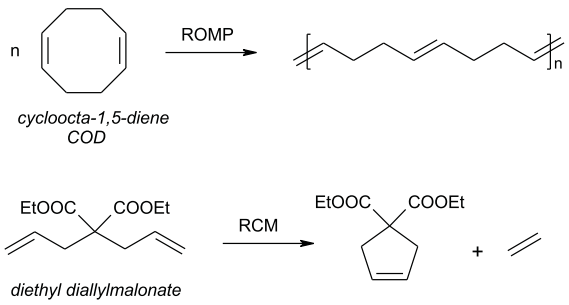

Figure 3.5: ROMP and RCM test reactions.

addition, this Lewis acid was found to improve the metathesis activity of the Grubbs 2nd generation catalyst **2** in the ROMP of cycloocta-1,5-diene and the RCM of diethyl diallylmalonate (Figure 3.5).
While complexes **2** and **35** display a certain metathesis activity at room temperature, catalyst **36** remains roughly inactive towards the ROMP of various monomers during a time range of several weeks/months. This latency allows for interesting applications such as acid-initiated reaction injection molding (RIM). RIM is a processing technique for the formation of polymer parts by direct polymerization in the mold through a mixing activated system. Two monomeric liquids are mixed together and injected into a mold where polymerization takes place. In our case, one of the monomer feeds would contain the acid, while the second monomer feed contains the inactive catalyst **36**. After mixing of the two feeds, an active catalyst is generated *in situ*, allowing polymerization of the introduced monomer (Figure 3.6). Important is that monomer and catalyst initiator can be mixed and stored without concomitant polymerization. Latent catalysts are particularly useful for the ROMP of DCPD (dicyclopentadiene), since for active catalysts such as **1** and **2**, the metathesis reaction proceeds very quickly, leading to microencapsulation of the catalyst and incomplete polymerization.
Elaboration of a RIM process was beyond the concept of this thesis, but the results presented herein do demonstrate some impressive possibilities of *in situ* acid activation.[5,380] Studies aimed at applying these *in situ* activated catalysts to industrially relevant applications were carried out by the spin-off company ViaCatt N.V. in collaboration with Noveon/Telene. Telene markets high purity DCPD resins and proprietary catalyst systems to the reaction injection molding industry.

3.2 Complex Synthesis

The Schiff base ligand of our choice is a quite steric unit bearing two aromatic rings. This ligand, illustrated in figure 3.7, provides a very stable ruthenium

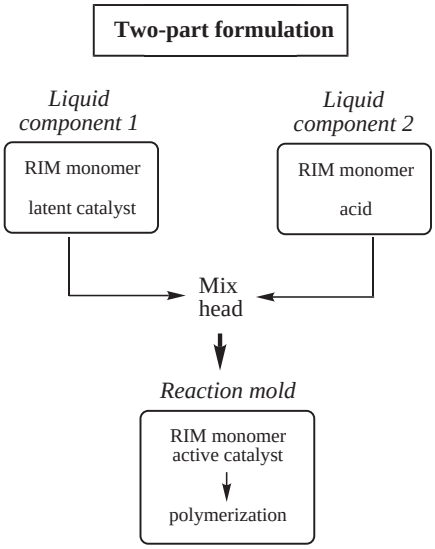

Figure 3.6: RIM process.

complex,[6] and allows for straightforward precipitation of the corresponding Tl-salt and ruthenium catalysts, which greatly simplifies purification processes during synthesis.
Schiff base ligand **37** was easily accessible through a one-step procedure via virtually quantitative condensation of primary amine (4-bromo-2,6-dimethylaniline) and aldehyde (5-nitrosalicylaldehyde). Coordination of the Schiff base to the ruthenium center was achieved using a method outlined by Grubbs et al., and involves the thallium salt of the Schiff base.[361] Thallium salt **38** was obtained as a yellow precipitate upon reaction of **37** with thallium ethoxide in THF (Figure 3.8). The salt was filtered off, dried and stored under inert atmosphere. It would be possible to avoid the toxic thallium ethoxide by synthesis of the sodium or lithium salt of the Schiff base.[361,363] However, the isolation of pure Na or Li salts is more difficult, while subsequent reaction with the Ru precursor proceeds less efficient. Furthermore it is less demanding to remove TlCl as the reaction's side

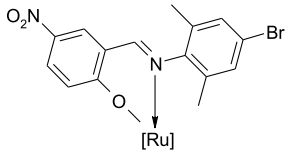

Figure 3.7: Schiff base ligand **37**.

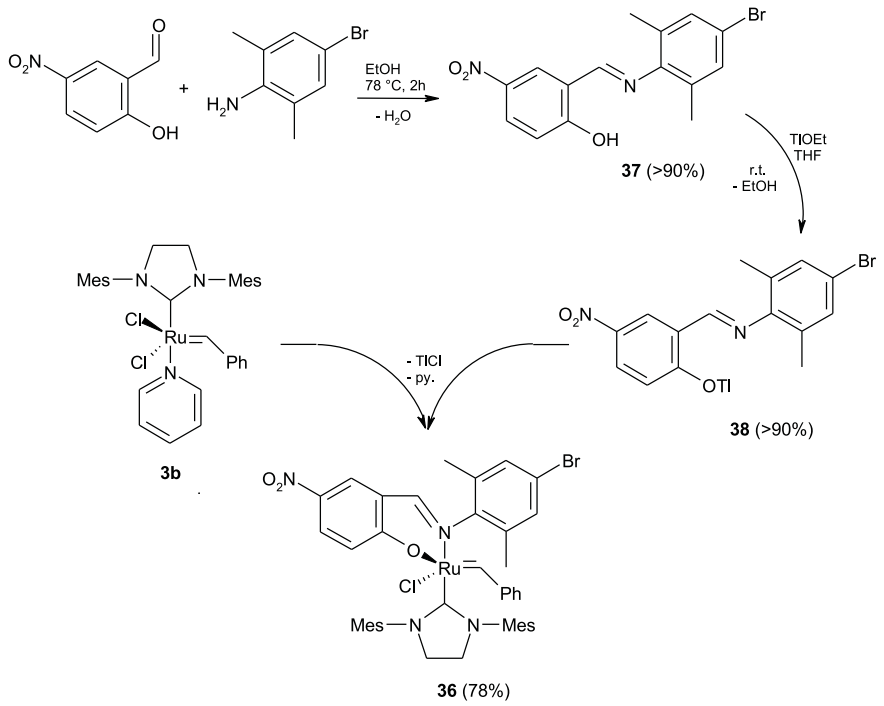

Figure 3.8: Synthetic procedure for Schiff base complex **36**.

product since it can easily be removed by filtration, while the removal of NaCl or LiCl would require decantation or extraction.
Our Schiff base complex **36** bears an *N*-heterocyclic carbene ligand. Synthesis of this complex was initially described by De Clercq and Verpoort to proceed via reaction of **35** with *in situ* formed free carbene from the imidazolium salt.[381] Attempts to reproduce this synthetic strategy were, however, found to result in decomposition of the starting material. A different and more successful approach was introduced, first by Allaert and Verpoort, and later on also by Raines et al. (Figure 3.8)[6,372] Faced with discrepancies in the synthesis reported by De Clercq and Verpoort, an alternative pathway was sought in the introduction of the Schiff base ligand to a complex already bearing the NHC ligand. It was found possible to add the Schiff base thallium salt to the Grubbs 2nd generation catalyst **2** but substitution is much faster and more efficient starting from pyridine complex **3b**.[6] This complex is characterized by a smooth detachment of its pyridine ligand, which makes it a suitable precursor for ligand exchange.[68] Reaction between **38** and **3b** goes to completion within 2 hours of reaction time at room temperature.

3.3 Catalytic Performance

To examine the scope of complex **36**, we primarily focused on its performance in the ROMP of the low strain cyclic olefin *cis*,*cis*-cycloocta-1,5-diene (COD). For comparison, also the Schiff base phosphine catalyst **35**, and the well-known Grubbs complexes **1**, **2**, and **3b** were tested (Figures 3.9-3.10).
Grubbs catalysts **1**, **2** and **3b** show expected ROMP activities (Figure 3.10): Grubbs 2nd generation **2** is typified by a slower initiation compared with **1** but shows a higher overall activity. Complex **3b** is very active and reaches full conversion within the first measurement. This demonstrates that in general, replacement of one phosphine ligand with an NHC ligand substantially improves metathesis activity. Therefore it is noteworthy that insertion of H_2IMes in our Schiff base complex did not give rise to a more active catalyst. Even at 80 °C and with high catalyst loading, NHC-substituted complex **36** was less ROMP active for the polymerization of COD than complex **35** (Figure 3.9). The low catalytic activity is likely due to a slow initiation step which requires dissociation of the *N*-arm of the Schiff base. This process is expected to be unfavorable because of chelate effects. A low rate of ligand dissociation results in a small concentration of catalytically active species and much of the ruthenium complex does not enter the catalytic cycle. Insertion of an NHC ligand could clearly not improve the initiation rate and hence not improve catalytic activity. Although NHC ligands generally improve the metathesis propagation, they tend to slow down the metathesis initiation (section 2.4.1). Likewise, the exchange of PCy_3 for an NHC decreases the intitiation rate of the Schiff base complex, and as a

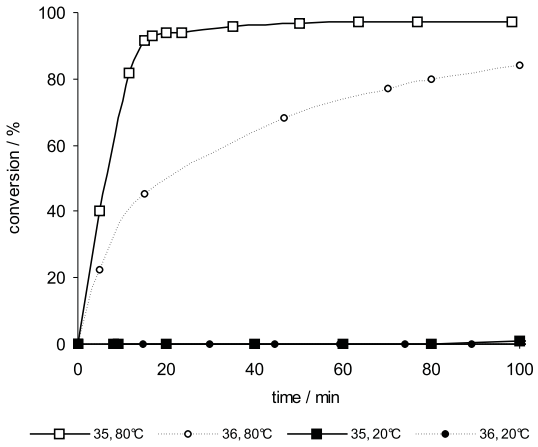

Figure 3.9: ROMP of COD. Conversions determined using ^{1}H NMR spectroscopy. Solvent = C_6D_6, COD/cat.: 100, cat. conc.: 13.56 mM.

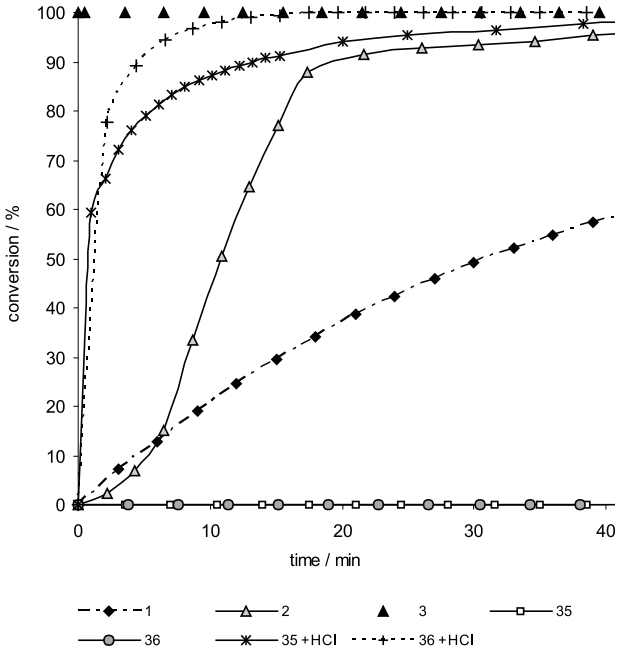

Figure 3.10: Monitoring ROMP of COD via ^{1}H NMR ($CDCl_3$, 20 °C) - COD/cat.: 300, cat. conc.: 4.52 mM. Acid addition: 0.05 mL, 1N HCl in Et_2O.

result the catalyst remains mainly dormant.
It should be noted that, in a later publication, Raines et al. also found 2nd generation Schiff base complexes (such as **36**) to be less active than their 1st generation analogues (such as **35**) for ring-closing metathesis reactions in non-polar solvents.[372] Their results were however found to contrast with previous reports by Verpoort et al.[367]

As shown in table 3.1, catalyst **36** was subjected to selected latency and stability tests to gain some idea on its pot life. Entry 1 illustrates the high stability of the Schiff base complex. During a time period of 6 weeks, only a minor degree of decomposition was observed. Entries 2-7 show the catalytic activity towards different ROMP monomers. The highly strained norbornene was found to completely polymerize within 1 h of reaction time. A molecular weight[1] of 5015 * 10^3 was measured, which is indicative for a very low initiation efficiency (0.9 %)[2] of the catalyst at room temperature. The less strained cycloocta-1,5-diene

[1] M_n: Measured by GPC ($CHCl_3$) analysis. Results are relative to polystyrene standards. A correction factor of 0.5*M_n was applied.[382]

[2] $f_i = M_{n(theor.)}/M_{n(exp.)}$ with $M_{n(theor.)} = ([monomer]_0/[cat.]_0)*MW_{monomer}$*conversion

	Time							
	1 hour	1 day	2 days	1 week	2 weeks	3 weeks	6 weeks	12 weeks
	Reaction							
1	→	→	→	→	→	[b]	2%[c]	5%[c]
2	100%							
3	[a]	14%	15%	23%	33%	39%	49%	66%
4	[a]	17%	19%	41%	72%	88%	100%	100%
5	[a]	'viscous'	'viscous'	'solid'	'solid'	'solid'	'solid'	'solid'
6	→	→	→	→	→	→	→	[a]
7	→	→	→	→	→	→	→	[a]

Table 3.1: Latency of catalyst **36** in various ROMP monomers (18 °C).
Entry 1: **36** in C_6D_6, cat. conc. = 4.5 mM.
Entry 2: norbornene/**36** = 500, 0.35 g norbornene in 10 mL of toluene.
Entry 3: COD/**36** = 100, reaction in NMR tube (C_6D_6), cat. conc. = 4.5 mM.
Entry 4: CO/**36** = 100, reaction in NMR tube (C_6D_6), cat. conc. = 4.5 mM.
Entry 5: DCPD/**36** = 500, 0.40 g DCPD in 10 mL of toluene.
Entry 6: RIM monomer (DCPD)/**36** = 30 000, no solvent.
Entry 7: RIM monomer (DCPD)/**36** = 300 000, no solvent.
[a] No reaction (viscosity increase) observed.
[b] No decomposition of the catalyst observed.
[c] percent decomposition.

and cyclooctene only slowly polymerized inspite of a very low monomer/catalyst ratio. Using a monomer/catalyst ratio of 500, which is low for highly strained monomers, also DCPD was found to polymerize at a slow rate. After 1 day the reaction mixture became more and more viscous until an insoluble solid polymer network was obtained.
More commercially relevant is the pot life of the catalyst in neat *RIM monomer*, which is a liquid formulation of DCPD and additives as industrially used in RIM processes. Using appropriate monomer/catalyst ratios, a satisfactory pot life of at least 12 weeks was found (Table 3.1, entries 6-7). This indicates that the Schiff base catalyst can be stored in the neat DCPD monomer for 6 weeks without any significant viscosity increase. After this time period, the catalyst does not suffer from consequential decomposition, and is still adequately activated upon mixture with a second DCPD formulation containing an acidic cocatalyst.

3.4 Acid Activation

While complexes **35** and **36** both show low activity in the ROMP of COD, complex **2** displays a significant initiation period, illustrating its low phosphine dissociation rate.[298,303,304] Catalyst initiation of these three complexes was found

to be triggered by the addition of appropriate Brönsted or Lewis acidic cocatalysts.

To observe the effect of a Brönsted acid on the activity of Schiff base complexes **35** and **36**, an excess of HCl (0.05 mL of an 1N HCl solution in Et_2O, approx. 20 equiv) was injected into an NMR tube charged with catalyst, COD monomer and deuterated solvent. Very high ROMP activity was observed immediately upon HCl addition (Figure 3.10). For comparison, also complex **2** was treated with HCl. HCl converts phosphine to its phosphonium salt and hence acts as a phosphine scavenger.[376] This property allows rate enhancement of olefin metathesis reactions when dissociation of a phosphine moiety is required to form the active species. It is likely that HCl protonates the phosphine moiety of the Grubbs 2nd generation catalyst **2** in a similar way.[383] However, the addition of an excess of HCl only induced decomposition of the catalyst system (Table 3.2, entry 3 and 4). We assume that the high amount of acid caused immediate and complete reaction of the phosphine yielding the 14-electron catalytically active species, which has a more exposed metal center and thus decomposes rapidly. For this particular complex, it would be necessary to find an optimal acid/catalyst ratio since too much acid clearly kills the catalyst system. Entry 8 in table 3.2 shows that HCl-

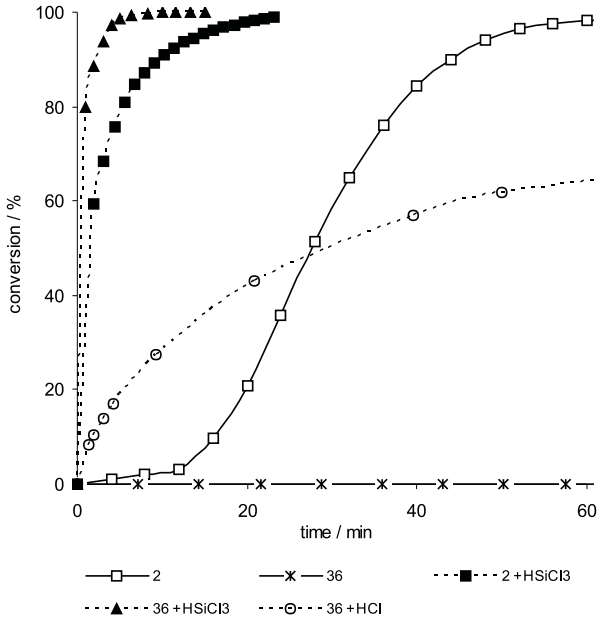

Figure 3.11: Monitoring ROMP of COD via ^{1}H NMR ($CDCl_3$, 20 °C) - cat./COD/acid(diluted in COD prior to addition): 1/3000/70, cat.conc.: 0.452 mM.

	Cat.	Acid	cat./COD/acid	t [min]	Conversion [%][a]	*cis*- [%][b]	M_n[c]	PDI [c]
1	**2**	-	1/3000/0	30	100	13	55800	1.7
2	**2**	-	1/30 000/0	[e]	31	51	80400	1.7
3	**2**	HCl[d]	1/30 000/10	[e]	0[f]			
4	**2**	HCl[d]	1/30 000/70	[e]	0[f]			
5	**2**	$HSiCl_3$	1/30 000/70	30	46			
				60	100	25	134000	1.8
6	**2**	$HSiCl_3$	1/300 000/300	60	12			
				[e]	[f]	70	161700	1.7
7	**36**	-	1/300/0	60	0			
8	**36**	HCl[d]	1/30 000/70	30	100	75	175800	1.6
9	**36**	HCl[b]	1/300 000/300	60	0			
10	**36**	$HSiCl_3$	1/30 000/70	30	93			
				60	100	14	114700	1.9
11	**36**	$HSiCl_3$	1/300 000/300	30	78			
				60	85			
				[e]	100	46	269000	1.7
12	**36**	$HSiCl_3$	1/3 000 000	30	21			
			/1000	[e]	[f]	64	363000	1.7

Table 3.2: ROMP of COD, room temperature, solvent: toluene.
[a] Determined by ^{1}H NMR.
[b] Percent olefin with *cis*-configuration in the polymer backbone - ratio based on ^{13}C NMR spectra (δ 32.9: allylic carbon *trans* - 27.6: allylic carbon *cis*).
[c] Determined by GPC ($CHCl_3$) analysis. Results are relative to polystyrene standards.
[d] 1N HCl sol. in Et_2O.
[e] Overnight.
[f] Decomposition of catalyst, conversion not further increased.

activation of complex **36** was possible despite of a high acid/catalyst ratio. Since no phosphine is present, HCl is expected to react with the Schiff base moiety in such a way that decoordination of the *N*-arm takes place, resulting in a higher concentration of active species. We found that instead of HCl, trichlorosilane ($HSiCl_3$) can be used to activate **2** and that high acid loadings are possible without the former problems due to fast catalyst decomposition (Table 3.2, entries 5 - 6). Hitherto, no effective phosphine scavengers were reported in literature for Grubbs' complex **2**.[383] The potential of $HSiCl_3$ as activating agent was thus found to be quite appealing. As witnessed by figure 3.11, $HSiCl_3$ also activates the Schiff base complex **36** in a very satisfying manner.

Similar activity enhancements were obtained in the RCM of diethyl diallylmalonate (Figure 3.12).

When thinking of commercial applications, low catalyst loadings are critical.

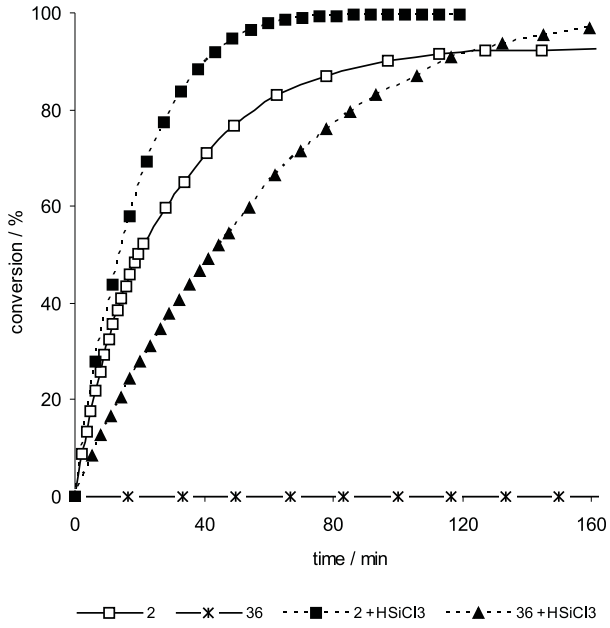

Figure 3.12: Monitoring RCM of diethyl diallylmalonate via ^{1}H NMR (CD_2Cl_2, 25 °C) cat./substrate/$HSiCl_3$(diluted in substrate): 1/200/25, cat.conc.: 4.52 mM.

Entries 10-12 in Table 3.2 demonstrate that when $HSiCl_3$ was used as activator, remarkably high turn over numbers were achieved, resulting in nice colourless polymers. These polymers were analyzed by GPC to determine their molecular weight and polydispersity, and by ^{13}C NMR to obtain the *cis*-fraction of the double bonds. Secundary chain transfer causes a higher *trans*-olefin content and shorter polymer chains. Intrigued by these results more experiments were carried out applying different cocatalysts. All tested silane compounds dichloromethylsilane ($HSiMeCl_2$), chlorodimethylsilane ($HSiMe_2Cl$), dichlorodimethylsilane ($SiMe_2Cl_2$) and tetrachlorosilane ($SiCl_4$) were found to activate complex **36** (Table 3.3, entries 1-4). Furthermore, polymerization was accelerated by the strong Lewis acids BF_3 and $AlCl_3$ (Table 3.3, entries 5-7).

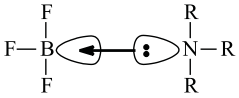

Figure 3.13: Lewis acid-base complex.

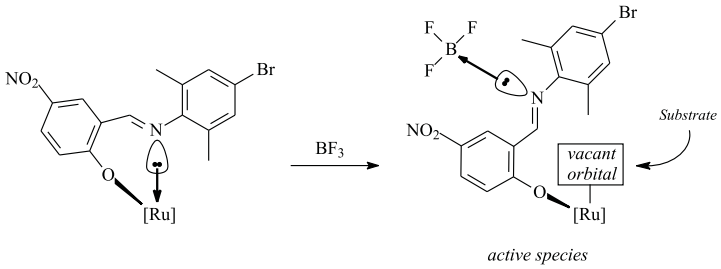

Figure 3.14: Reaction of the Schiff base with Lewis acid.

A Lewis acid like BF_3 is a species that can accept a pair of electrons and form a coordinate covalent bond. The boron atom is sp^2 hybridized, which leaves an empty $2p_z$ orbital. This empty $2p_z$ orbital picks up a pair of nonbonding electrons from a Lewis base to form a Lewis acid-base complex (Figure 3.13). Analogously, the Lewis acid cocatalysts can be expected to abstract a pair of electrons from the imine nitrogen atom of the Schiff base. This inhibits coordination of the *N*-arm of the Schiff base unit and results in a catalytically active 14-electron species (Figure 3.14). It should however be taken into consideration that Lewis acids could also react with the Schiff base catalyst in other ways, e.g. trough reaction with the Ru center.[378,384,385]

Entry 6 (Table 3.3) shows that 1 equivalent of a strong Lewis acid is sufficient for a fast reactivity enhancement of the Schiff base catalyst. The addition of more equivalents results in a fast activation, but also promotes decomposition. This likely explains the lower conversions found for BF_3 and $AlCl_3$ in comparison to $HSiCl_3$.
Also CuCl, a known phosphine scavenger, was used as an activating species (Table 3.3, entries 8-9). The activation was little effective, which we assign to slow reaction between the undissolved CuCl and the ruthenium complex. CuCl is known to activate Grubbs complexes by the formation of insoluble phosphine-copper adducts, but was not reported before to activate a phosphine free olefin metathesis initiator.[293,386,387]

NMR-scale experiments were carried out to gain some understanding on the activation mechanism. Figure 3.15 shows parts of the ^1H spectra of complex **36** in reaction with diverse acids. The spectrum resulting from reaction with ethereal HCl was included for comparison. ^1H signals at δ 10.03 (s, Ar-C(=O)H), δ 8.58 (singlet, O_2NC-CH of nitrosalicyl aldehyde moiety) and δ 8.42 (d, O_2NC-CH-CH of nitrosalicyl aldehyde moiety) indicate decondensation of the imine bond into the corresponding aldehyde and amine (Figure 3.15 (ii)). This does necessitate the presence of some water in the reaction medium. Reaction of **36** with a large

	Acid	cat./COD/acid	t [min]	Conversion [%][a]	*cis*- [%][b]	M_n[c]	PDI [c]
1	$HSiMeCl_2$	1/30 000/70	30	91			
			60	100	36	169400	1.7
2	$HSiMe_2Cl$	1/30 000/70	30	50			
			60	55			
			[d]	[e]	61	118200	1.7
3	$SiMe_2Cl_2$	1/30 000/70	120	6			
			[d]	7	79	74700	1.7
4	$SiCl_4$	1/30 000/70	30	77			
			60	89			
			[d]	93	64	181800	1.7
5	BF_3[f]	1/30 000/70	30	13			
			120	[e]	72	78100	1.7
6	$AlCl_3$[g]	1/3 000/1	30	100	17	54100	1.8
7	$AlCl_3$[g]	1/30 000/70	60	7			
			[d]	15	74	82900	1.7
8	CuCl	1/3 000/100[h]	60	41			
			120	63			
			[d]	100	38	72900	1.8
9	CuCl	1/30 000/70[h]	120	2	-	-	-

Table 3.3: ROMP of COD using catalyst **36**. room temp., solvent = toluene.
[a] Determined by ^{1}H NMR.
[b] Percent olefin with *cis*-configuration in the polymer backbone - ratio based on ^{13}C NMR spectra (δ 32.9: allylic carbon *trans* - 27.6: allylic carbon *cis*).
[c] Determined by GPC ($CHCl_3$) analysis. Results are relative to polystyrene standards.
[d] Overnight.
[e] Decomposition of catalyst, conversion not further increased.
[f] 1N BF_3 sol. in Et_2O.
[g] 0.5N $AlCl_3$ sol. in THF.
[h] CuCl = undissolved

excess (70 equiv) of dry $HSiCl_3$ afforded a ^{1}H spectrum showing only signals of the starting complex and of $HSiCl_3$; no shifts of catalyst protons were observed (Figure 3.15 (iii)). This took us by surprise since this mixture polymerized COD without any initiation period, indicating a fast reaction between catalyst and silane. Moreover, the residue upon evaporation of a toluene solution of **36** and $HSiCl_3$ was analyzed as pure complex **36** displaying no metathesis activity at room temperature. Addition of a new small portion of $HSiCl_3$ resulted again in quick activation allowing immediate ROMP reaction. We therefore assume that the trichlorosilane forms an adduct with the two electrons on the nitrogen of the Schiff base and this in a reversible way. Such a hypothesis finds support in recent research from Nakash et al. describing the reversible reaction between silanes and

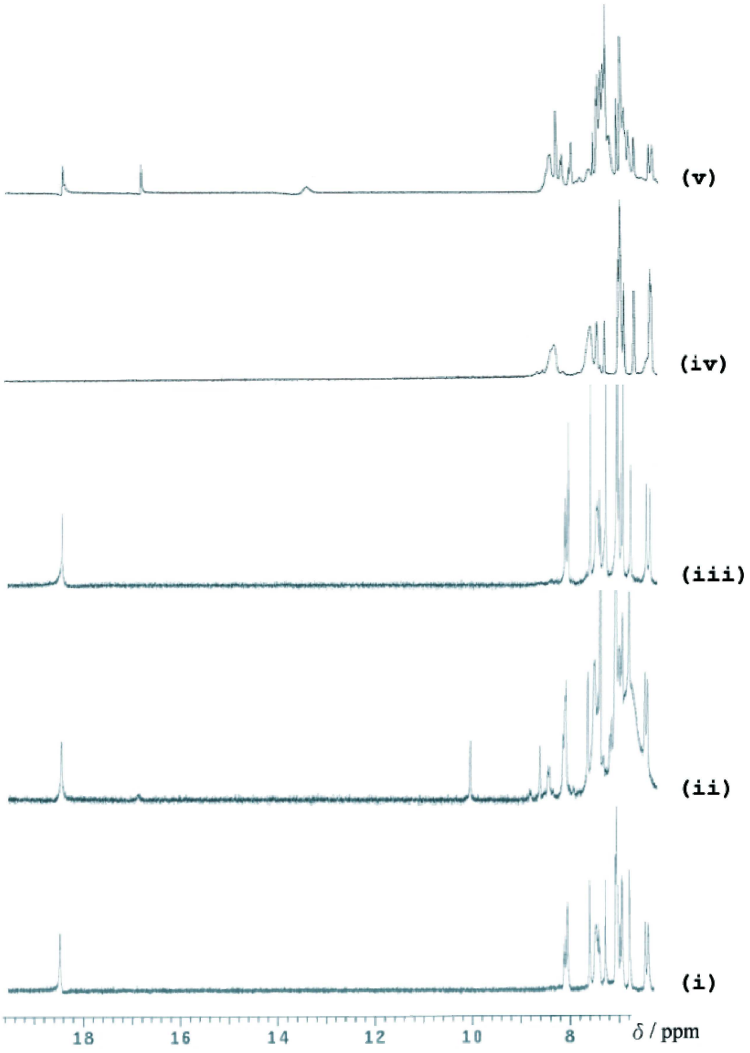

Figure 3.15: ^{1}H NMR spectra in $CDCl_3$. For clarity, only part of the spectra are shown.
(i) **36**
(ii) **36** + 5 equiv HCl sol. in Et_2O. (15 min)
(iii) **36** + 70 equiv $HSiCl_3$. (after 5 min, unchanged after 2h, 4h)
(iv) **36** + 1 equiv $AlCl_3$ sol. in THF. (15 min)
(v) **36** + 1 equiv $AlCl_3$ sol. in THF. (3 h)

pyridine. A fast equilibrium between free pyridine and a silane-amine complex with a non-covalent intermolecular Si-N interaction was evidenced through ^{29}Si NMR.[388,389] The formation of a similar silane-amine complex between $HSiCl_3$ and the Schiff base imine moiety in **36** would imply that electron donation from the basic nitrogen towards the ruthenium center is prevented. A 14-electron active species is formed which enables olefin coordination and fast metathesis reaction. On the other hand, lack of an observable reaction between $HSiCl_3$ and **36** might be due to the fact that only an undetectable small amount of catalyst initiates and hence catalyzes the reaction. However, it is plausible that the use of over 70 equiv of acid would be sufficient to activate the Schiff base catalyst to an ^{1}H NMR detectable extent. Furthermore, the large difference in spectra for HCl and $HSiCl_3$ activation indicates that the chlorosilane activation is not simply a consequence of *in situ* HCl generation.

The addition of a small excess of BF_3 to complex **36**, led to quick loss of the alkylidene moiety. Reaction of 1 equiv $AlCl_3$ with the Schiff base complex proceeded somewhat slower and allowed the observation of a small ^{1}H signal at 16.75 ppm. After 15 min of reaction time this broad signal had almost faded away, and virtually no resonance of an α-benzylidene proton was left (Figure 3.15 (iv)). Nevertheless, this solution still exhibited very good ROMP activity when added to COD. Therefore monitoring of the reaction was continued and after more than 2 h, ^{1}H resonances appeared at δ 18.51 and δ 16.91 (Figure 3.15 (v)). While the most downfield signal likely corresponds to the starting complex, the δ 16.91 signal should be assigned to the α-benzylidene proton of a new *in situ* generated catalyst. A resonance with approximately the same chemical shift was found for the HCl activation. A broad signal at δ 8.49 was ascribed to protonation of the Schiff base *N*-atom, while the one at δ 13.52 results from a protonated phenoxide moiety of the Schiff base. These are convincing arguments for the *in situ* generation of HCl caused by reaction of the initially added $AlCl_3$ or of the deuterochloroform. However, since the catalyst was found to be initiated immediately upon acid addition and the HCl generation was retarded as much as possible by using moisture free conditions, simple protonation of the Schiff base *N* is expected to be of minor importance in the actual polymerization process.

We conclude that activation doesn't require hydrolysis of the imine bond, and that it is sufficient to stimulate decoordination of the *N*-arm of the Schiff base. At no point in this investigation, direct reaction between the Lewis acids and the Ru center was evidenced.
All of these observations clearly do not allow us to propose one unambiguous mechanism for the acid activation. Moreover, it should be noted that for the Grubbs catalyst **2**, the acid activation will proceed in a different way since no Schiff base is present. However, it can be assumed that the electron pair of the phosphine and the electron pair on the nitrogen of the Schiff base react with acids in a rather analogous way.

3.5 Conclusion

Schiff base substituted ruthenium complexes were synthesized and catalytic performances compared. The strongly chelating Schiff base entity that dissociates reluctantly from the Ru center, enhances the thermal stability but drastically lowers the catalytic performance of the corresponding complexes. The chelate stabilization slows the rate of ligand dissociation which causes small concentrations of active species in the reaction mixture. Attempts to create a larger concentration of active species with acidic cocatalysts, resulted in greatly enhanced catalytic activity. The cocatalysts, which include HCl and Lewis acids, assist in the dissociation of the Schiff base imine-*N*. A trichlorosilane activated catalyst system was found to polymerize cycloocta-1,5-diene at very high rates and its high activity enabled the use of very low catalyst loadings. Compared with the other tested acids, the trichlorosilane system retained satisfying stability, allowing also high activity in the ring-closing metathesis of diethyl diallylmalonate.

3.6 Experimental Section

3.6.1 General remarks

Synthetic manipulations were performed under an oxygen free argon atmosphere using standard Schlenk techniques. Reactions were carried out in dried, distilled and degassed solvents. COD and chlorosilanes were dried over calcium hydride, distilled and degassed by standard freeze-pump-thaw cycles. $CDCl_3$ and CD_2Cl_2 were dried on P_2O_5, C_6D_6 on molecular sieves and degassed prior to use. $CDCl_3$ was stored on silver(I) oxide to avoid formation of HCl in the solvent. HCl was purchased from Acros as an 1N solution in Et_2O. Other chemicals were purchased from Aldrich, -BF_3 as a 1N solution in Et_2O and $AlCl_3$ as a 0.5M soluton in THF- and used as received. NMR spectra were recorded with a Varian Unity-300 spectrometer. Complex **35**[361], Schiff base ligand **37**[361], Tl-salt of the Schiff base **38**[361], and $[H_2IMes(H)][Cl]$[230,390] were prepared according to literature procedures.

3.6.2 Complex synthesis

Grubbs 2nd generation $[(\mathbf{H_2IMes})(\mathbf{PCy_3})(\mathbf{Cl})_2\mathbf{Ru{=}CHPh}]$ 2

The introduction of the NHC is possible through the well established *in situ* generation of free carbene using KO*t*Bu.[67] However, we found it more convenient to employ the more steric base potassium hexamethyldisilazide (KHMDS). This base does not react with **1** during the applied reaction time, which allowed us to mix the imidazolium salt, catalyst precursor **1** and KHMDS all together. Such a *one-pot* procedure would not be possible when using KO*t*Bu, since this base is known to react with **1** to form $(t\mathrm{BuO})_2(\mathrm{PCy_3})\mathrm{Ru{=}CHPh}$.[375] Another important

advantage of the KHMDS base compared with KO*t*Bu or K*t*amylate[235] is that heating of the reaction mixture is not required.
A flame-dried Schlenk flask was charged with complex **1** (1.32 g, 1.6 mmol), [H_2IMes(H)][Cl] (0.658 g, 19.2 mmol, 1.2 equiv), toluene (5 mL), and 3.84 mL of a 0.5 M sol. KHMDS in toluene. The initially purple, turbid reaction mixture was stirred for 45 min. at room temperature, during which time the solution turned dark red. After evaporation of solvent the residue was purified by sonification in methanol and subsequent filtration, affording clean pinkish complex **2** in good yield. (93% = higher than when KO*t*Bu is used)
^{1}H NMR ($CDCl_3$): δ 19.13 (s, 1H, Ru=C*H*Ph), 9.00 (br s, 1H, *o*-C_6H_5), 7.38 (t, 1H, *p*-C_6H_5), 7.10 (m, 2H, *m*-C_6H_5), 7.02 (s, 2H, $C_6H_2Me_3$), 6.75 (br s, 1H, *o*-C_6H_5), 5.83 (br s, 2H, $C_6H_2Me_3$), 3.96 (s, 4H, NCH_2CH_2N), 2.71-1.04 (m, 51H). ^{31}P NMR ($CDCl_3$): δ 30.05. ^{13}C NMR ($CDCl_3$): δ 294.1 (Ru=*C*H), 220.1 (d, N*C*N), 151.1 (*i*-C_6H_5), 138.9-127.7 (several peaks), 52.3 (N*C*H_2CH_2N), 51.6 (NCH_2*C*H_2N), 32.0-26.3 (several peaks), 21.3, 20.2, 18.8.

Grubbs bis(pyridine)complex [(**H_2IMes**)(**py**)$_2$(**Cl**)$_2$**Ru=CHPh**] **3a** / mono(pyridine) complex [(**H_2IMes**)(**py**)(**Cl**)$_2$**Ru=CHPh**] **3b**[68–70]

A dry Schlenk flask was charged with **2** and an excess of pyridine (approx. 10 equiv) was added while stirring. The solution immediately changed from dark red to green in color. Simple addition of hexane (= approx. 3 times the volume of added pyridine) led to precipitation of the desired complex as a bright green solid. The complex was isolated in good yield by filtration. High and prolongued vacuum affords solely the mono(pyridine) complex [(H_2IMes)(py)(Cl)$_2$Ru=CHPh] due to loss of pyridine under vacuum.
^{1}H NMR ($CDCl_3$): δ 19.18 (s, 1H, Ru=C*H*Ph), 8.63 (br s, 2H, py), 7.83 (s, 1H, py), 7.64 (s, 1H), 7.61 (s, 1H), 7.48 (s, 1H), 7.07 (m, 2H), 6.97 (m, 1H), 6.76 (s, 1H), 4.17 (m, 2H, NCH_2CH_2N), 4.06 (m, 2H, NCH_2CH_2N), 2.65 (s, 6H, CH_3), 2.33 (s, 3H, CH_3), 2.30 (s, 3H, CH_3), 2.24 (s, 6H, CH_3).

Schiff base complex 36

Thallium salt **38** (0.196 g, 0.355 mmol, 1.1 equiv) was weighed into an oven-dried flask together with complex **3b** (0.209 g, 0.322 mmol). Dry THF was added, while the resulting solution immediately turned bright orange. After stirring for 2 hours at room temperature the solvent was removed in vacuo. The residue was redissolved in a small amount of toluene (5 mL) and filtered to remove TlCl. The solution was concentrated to approx. 1 mL, followed by addition of hexane (15 mL) to precipitate the desired complex as an orange-brown solid. Yield: 78%.
^{1}H NMR ($CDCl_3$): δ 18.50 (s, 1H, Ru=C*H*Ph), 8.08 (d, 1H), 8.04 (s, 1H), 7.58 (s, 1H), 7.43-7.37 (m, 2H), 7.05 (s, 2H), 7.02 (s, 2H), 6.95 (s, 1H), 6.91 (s, 2H), 6.75 (s, 1H), 6.43 (1H), 6.36 (1H), 4.12 - 4.01 (m, 4H, CH_2CH_2), 2.57 (s, 3H, CH_3), 2.40 (s, 3H, CH_3), 2.29 (s, 3H, CH_3), 2.26 (s, 3H, CH_3), 2.13 (s, 3H, CH_3),

2.01 (s, 3H, CH_3), 1.48 (s, 3H, CH_3), 1.03 (s, 3H, CH_3). ^{13}C NMR ($CDCl_3$): δ 301.7 (Ru=C), 219.3 (NCN), 174.7 (C-O), 167.4 (C=N), 151.9, 150.1, 140.3-128.3 (several peaks), 124.0, 118.8, 118.0, 51.7 (CH$_2$CH$_2$), 51.1 (CH$_2$$CH_2$), 21.2-17.8 (several peaks).
Anal. Calcd. for $C_{43}H_{44}N_4O_3ClBrRu$: C 58.61, H 5.03, N 6.36. Found C 58.81, H 5.87, N 6.38.

3.6.3 Catalytic reactions

Monitoring ROMP of COD (Figures 3.9, 3.10, 3.11)

After charging an NMR tube with the appropriate amount of catalyst dissolved in deuterated solvent, COD or a COD/acid mixture was added. The polymerization reaction was monitored as a function of time at 20 °C by integrating olefinic ^{1}H signals of the formed polymer (5.38 - 4.44 ppm) and the consumed monomer (5.58 ppm).

Monitoring RCM of diethyl diallylmalonate (Figure 3.12)

An NMR tube was charged with 0.6 mL of a catalyst solution in CD_2Cl_2 (4.52 mM or 2.712 μmol catalyst per experiment). Next 200 equiv or 0.13 mL of diethyl diallylmalonate was added and the NMR tube was closed. $HSiCl_3$ was diluted in diethyl diallylmalonate prior to addition in such a way that the catalyst/substrate/$HSiCl_3$ ratio was 1/200/25. The progress of the ring-closing reaction was monitored at 25 °C by integration of ^{1}H signals of allylic protons of the ring closed product (2.25 ppm) and of the substrate (2.64 ppm).

Representative procedure for ROMP tests (Tables 3.2, 3.3)

Prior to the polymerization experiments various COD/acid solutions were prepared in Schlenk tubes, which made it possible to add monomer and acid to the reaction vials in the mentioned ratios. Small oven-dried glass vials with septum were charged with a stir bar and the appropriate amounts of catalyst taken from a CH_2Cl_2 stock solution. The dichloromethane was subsequently evaporated, and the glass vials with solid catalyst were kept under an argon atmosphere. To start the ROMP test, 200 μL of toluene was added in order to dissolve the catalyst. The appropriate amount of COD/acid mixture was then transferred to the vial containing the catalyst via syringe, under vigorous stirring at room temperature. After a certain time span, a small quantity of the reaction mixture, which had become viscous, was taken out of the vial and dissolved in $CDCl_3$. The conversion was then easily determined by ^{1}H NMR spectroscopy. Prior to GPC analysis, a solution of 2,6-di-*tert*-butyl-4-methylphenol and ethylvinylether in $CHCl_3$ was added to quench the polymerization reaction. The polymer was then precipitated in MeOH, and dried under vacuum.

Remarks:

- The acid/catalyst ratios vary from 1 up to 1000, which can be considered rather high. This is due to the low catalyst loadings and to the fact that acids like trichlorosilane are difficult to add in small excess when doing reproducable small scale reactions even though the acid is diluted in the monomer before addition. As a consequence of the big acid excesses, the required reaction times are often very low and the reaction mixture becomes viscous in only seconds of time. We presume that smaller excesses of acid would be sufficient to activate the catalyst in a satisfying manner, which would be possible when using bigger batches of monomer.
- All solvents were thoroughly dried in order to avoid reaction of the metal halogenides with water leading to the *in situ* formation of HCl.

Chapter 4

The Exploration of New Synthetic Strategies

Up to now, most synthetic pathways toward the Grubbs 2nd generation class of complexes proceed through bisphosphine benzylidene systems. A more direct pathway using moderate reaction conditions and readily available starting materials is quite desirable. This also involves the need for alternative means to introduce the alkylidene moiety, which avoid the quite cumbersome preparative routes via diazo compounds. In this context, the Ru dimer [(*p*-cymene)$RuCl_2$]$_2$ is an air and moisture stable, easy to handle precursor, that is an ideal starting material for the synthesis of allenylidene or vinylidene metathesis catalysts. In order to find a resembling alternative for the classic Grubbs catalyst **2**, it would be necessary to coordinate H_2IMes to Ru dimer. While several groups claim to have synthesized [(*p*-cymene)(H_2IMes)$RuCl_2$] *in situ*, it was never isolated, nor fully characterized. Driven by the fascinating challenge to find new synthetic strategies, we herein describe the endeavor we undertook to contribute to this quest.

4.1 Introduction

Since the late 90's a lot of research was aimed at finding new routes to equipotent Grubbs analogues which circumvent the rather inconvenient synthesis of the benzylidene complex (Figure 4.1). Ru dimer **39** has already shown great utility as a catalyst precursor in the synthesis of Ru allenylidene, Ru vinylidene, and even Ru indenylidene complexes.[391–397]

An attractive feature of ruthenium allenylidene complexes is the relatively easy formation of the Ru=C double bond. As a result, a variety of neutral allenylidene

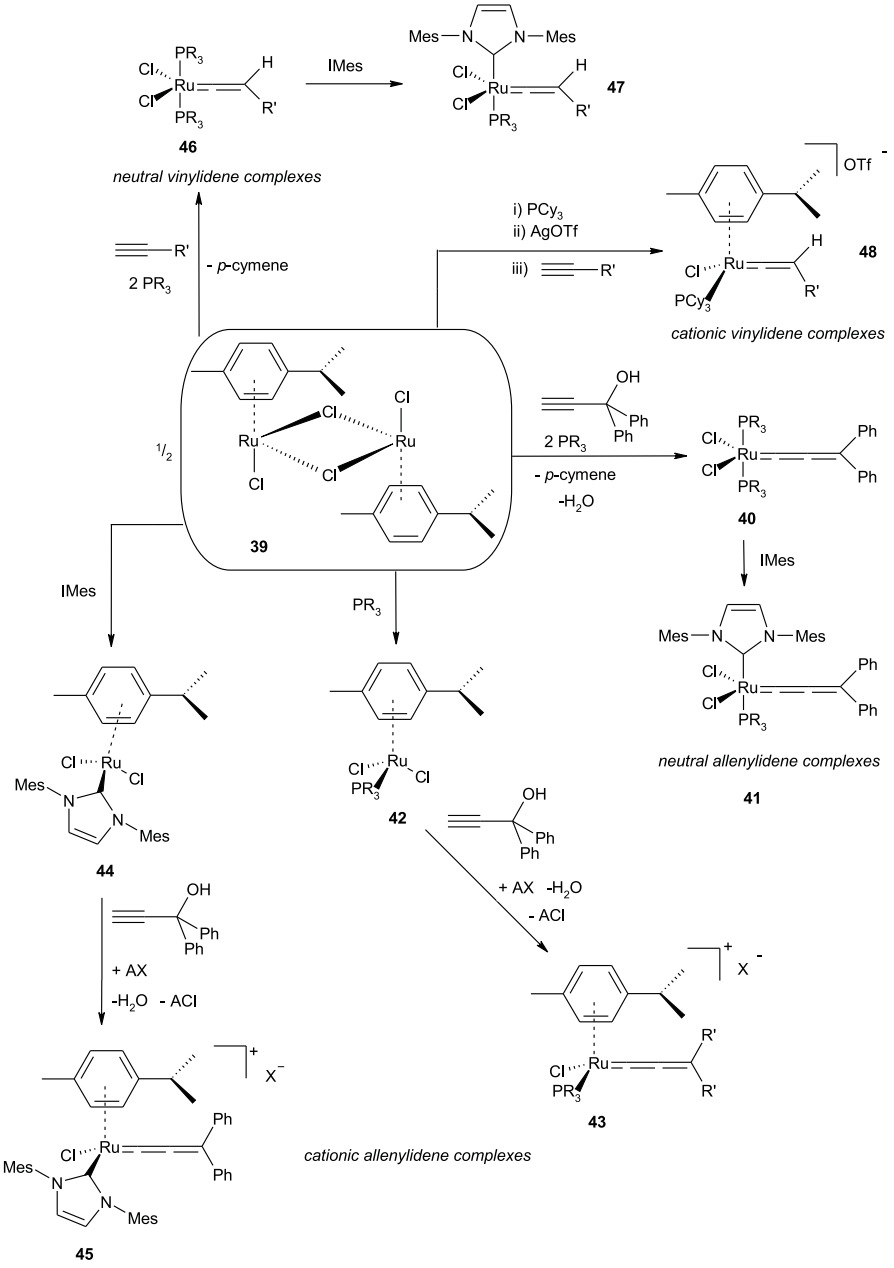

Figure 4.1: Ru dimer as a catalyst precursor.

complexes have been reported in literature. One example is the bisphosphine complex **40**, which is the allenylidene counterpart of the Grubbs 1st generation catalyst. This complex is obtained from the reaction of Ru dimer with 1,1-diphenyl-2-propyn-1-ol and phosphine ligand, and performs poorer in metathesis reactions than **1**. Remarkable is that introduction of an imidazolylidene ligand (IMes) does not improve the catalytic activity.[398]
Cationic, coordinatively saturated 18-electron ruthenium allenylidene complexes contain an η^6-arene ligand associated with chloride ligands and an additional phosphine or NHC ligand, in conjunction with a "non-coordinating" counterion. They can be synthesized by treatment of Ru dimer with 1 equiv of phosphine, leading to formation of the monomeric species [(*p*-cymene)(PR_3)$RuCl_2$] **42**. This compound reacts with 1,1-diphenyl-2-propyn-1-ol in the presence of an alkali metal salt (e.g.: $NaPF_6$, $NaBF_4$) to form the corresponding allenylidene complex **43**.[392,393,396] Replacement of the alkali metal salts by AgX (X = OTf^-, $PF_6{}^-$, $BF_4{}^-$) results in an even more practical preparation since this method allows the isolation of an intermediate cationic 16-electron species [(*p*-cymene)(PR_3)RuCl]X, which can be stored under inert atmosphere, and later on reacted with propargyl alcohol. To study the effect of replacing a phosphine with an NHC ligand, Ru dimer was treated with IMes to form [(*p*-cymene)$RuCl_2$(IMes)] **44**. This complex does not bear any alkylidene moiety but does show some RCM activity. In contrast to complexes of the type **42**, which only become RCM active upon UV-irradiation[103], the RCM reactions catalyzed by **44** were not photoinduced as no change in outcome was observed when reactions were carried out in the dark.[399] Reaction of **44** with HCCC(OH)Ph_2, in the presence of an alkali metal salt, then affords the corresponding cationic allenylidene complex **45**. This catalyst was found to be more active for the RCM of diethyl diallylmallonate than the phosphine substituted complexes.[399,400]

The preparation of neutral 16-electron ruthenium vinylidene complexes **46** from terminal alkynes and ruthenium dimer was first described by Katayama and Ozawa.[401–403] These vinylidene complexes show only moderate metathesis activity, but exchange of one of the phosphine ligands by an NHC ligand (IMes) allows for a substantial activity improvement.[404] The observed reaction rates are however still considerably lower than for the corresponding Grubbs benzylidene catalysts. Dixneuf et al. attempted to synthesize cationic vinylidene complexes **48** with phenyl acetylene and benzyl acetylene as carbene precursors. These complexes were found to be unstable at room temperature, but full characterization was possible at −30 °C.[405]

In 2003 Dixneuf et al. reported on the *in situ* generation of a ruthenium arene indenylidene complex **49** from a ruthenium arene allenylidene complex upon treatment with strong acids (HOTf, HBF_4). Low temperature NMR studies at −40 °C gave evidence of the formation of a dicationic alkenylcarbyne ruthenium species, which, upon heating at −20 °C, readily converted to the indenylidene

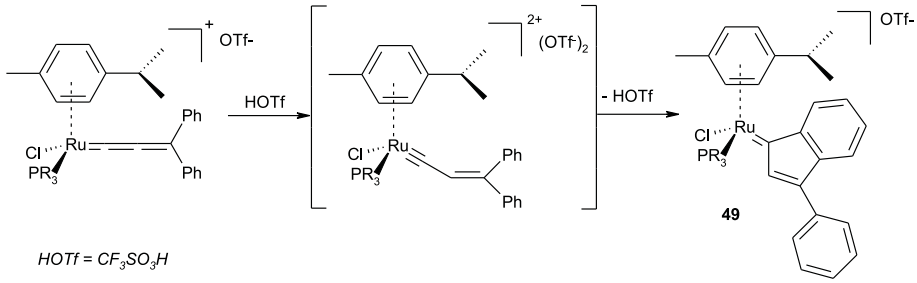

Figure 4.2: *In situ* generation of a Ru indenylidene.

complex (Figure 4.2). This catalyst exhibits high activity in ADMET, RCM, enyne metathesis and ROMP reactions.[406] Attempts to generate the related IMes-indenylidene complex failed.[407]

The above given small overview illustrates that ruthenium complexes generated from Ru dimer could constitute a valid alternative for the more popular Ru benzylidene complexes. However, for these catalyst architectures to adequately compete with the Grubbs catalysts, there is still one important challenge to meet. The coordination of the saturated NHC ligand H_2IMes in these complexes was never accurately reported in literature, while its beneficial properties have abundantly been described for other Ru-based olefin metathesis catalysts (*vide supra*).

4.2 Results and Discussion

4.2.1 NHC-arene complexes

In situ generated [(*p*-cymene)$RuCl_2$(H_2IMes)] has been the subject of several catalytic test reactions but hitherto no one succeeded in it's isolation or characterization.[408,409] While the coordination of IMes (1,3-dimesityl-imidazol-2-ylidene) to Ru dimer proceeds readily via standard synthetic strategies[399], analogous binding of H_2IMes was found to be more problematic. Regardless of the reaction conditions applied, a mixture of Ru complexes was obtained (Figure 4.3). Only when the chloroformadduct H_2IMes(H)(CCl_3) was used as a carbene precursor, a small rate of NHC coordination could be evidenced through ^{13}C NMR spectroscopy. A ^{13}C NMR resonance was found at δ 202.5 ppm, which is characteristic for the carbene carbon atom coordinated to the metal center. However, ^{1}H NMR analysis of the reaction products revealed that the desired complex **50**, was only formed

as a minor product together with undefined hydridic species.[1]
Since the failure in our efforts to isolate **50** was assigned to a lack of stability of the

[1] NMR resonances were found at δ -3.64, -3.98, -5.09 and -5.62 ppm.

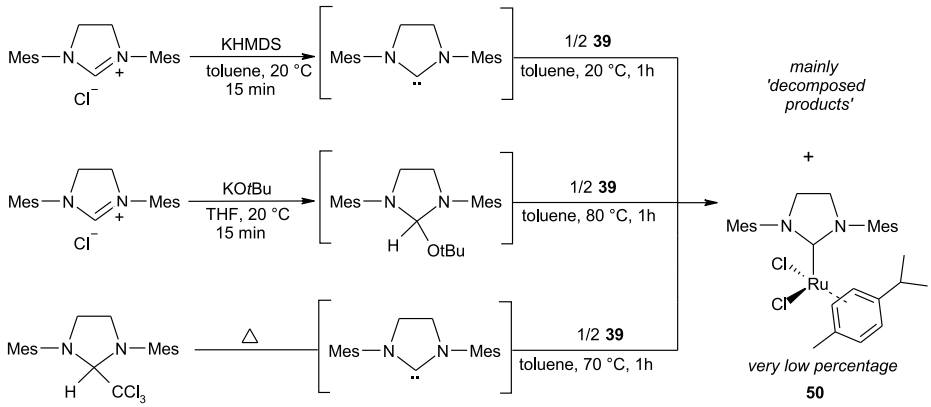

Figure 4.3: Synthesis of [(*p*-cymene)$RuCl_2$(H_2IMes)].

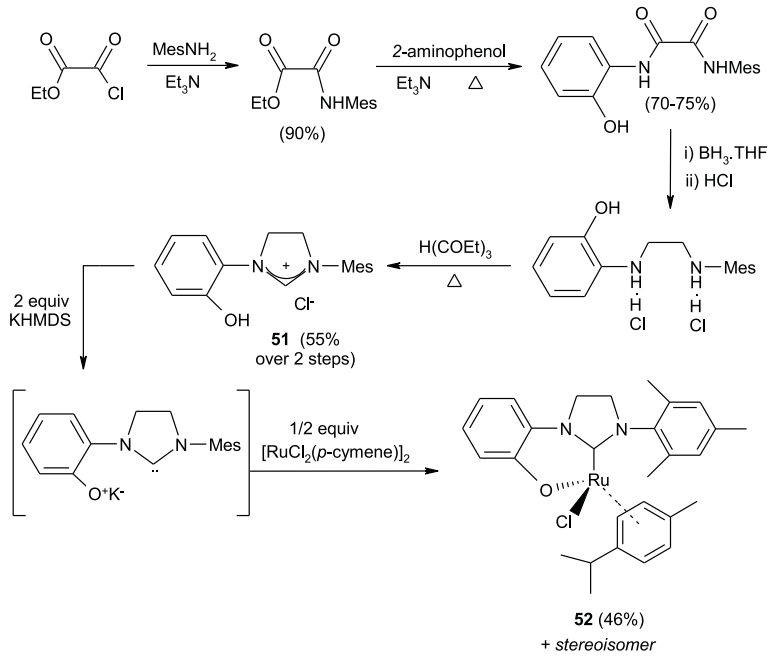

Figure 4.4: Synthesis of NHC arene complex **52**.

complex, a bidentate analogue of the NHC ligand was synthesized. The chelating properties of a bidentate NHC were expected to ameliorate the complex stability through a 'chelate effect'. The synthesis of 1-mesityl-3-(2-hydroxyphenyl)-4,5-dihydroimidazolium chloride salt **51** was straightforward following a synthetic procedure described by Grubbs et al.[410] Treatment of ethylchlorooxoacetate with 2,4,6-trimethylaniline in the presence of triethylamine provides an *N*-(mesityl)-oxanilic acid ethyl ester. Subsequent reaction with 2-aminophenol results in the desired bis-amide. Reduction with borane then affords the diamine, which is reacted with triethyl orthoformate to give the corresponding imidazolinium chloride salt (Figure 4.4).

In order to effectuate ligand coordination, the NHC precursor was treated with 2 equiv of base; this is, 1 equiv to liberate the free carbene and 1 equiv to deprotonate the phenolic group. After 15 min of reaction time, Ru dimer **39** (0.5 equiv) was added to the reaction mixture.[2] As expected, the ligand bound to the metal center in a chelating manner. The new complex **52** shows high stability and can be handled in air without any sign of decomposition. Due to the pseudo-tetrahedral arrangement of the ligands, a stereogenic center was created at the Ru center, leading to the existence of two stereoisomers. These enantiomers are necessarily present in an exact 1:1 ratio.

Dark red crystals suitable for X-ray structure analysis were grown by slow evaporation of a toluene/CH_2Cl_2 solution. As seen in figure 4.5, the molecular species consists of a *p*-cymene ligand showing η^6-bonding, an anionic chloride ligand, and a bidentate (C,O) chelating *N*-heterocyclic carbene ligand. The isopropylgroup on the arene ligand is a little distorted away from the metal center as a result of

[2] A one-pot procedure, as described in chapters 3 and 5, could here not be used since the KHMDS base was found to immediately react with the Ru dimer instead of with the ligand salt.

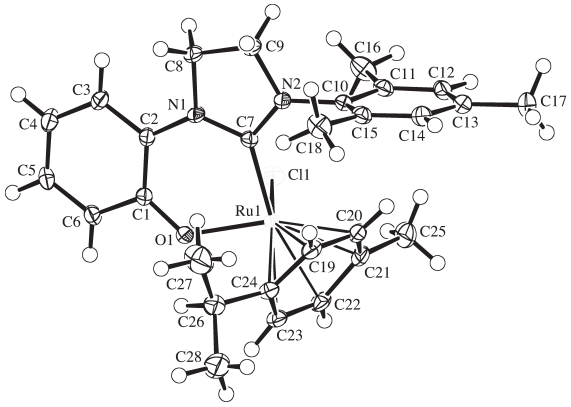

Figure 4.5: The molecular structure of **52**, showing 50% probability ellipsoids. The compound in the crystal was racemic.

Bond Lengths		**Bond Angles**	
Ru-C7	2.060(2)	O-Ru-Cl	86.13(5)
Ru-O	2.046(2)	O-Ru-C7	86.88(7)
Ru-Cl	2.4185(6)	C7-Ru-Cl	84.83(6))
Ru-C19	2.171(2)	N2-C7-N1	107.1(2)
Ru-C20	2.213(2)	C7-N2-C10	129.0(2)
Ru-C21	2.208(2)	C7-N1-C2	128.6(2)
Ru-C22	2.271(2)		
Ru-C23	2.249(2)		
Ru-C24	2.169(2)		

Table 4.1: Selected Bond Lengths [Å] and Angles [°] for complex **52**.

steric factors.

The catalytic activity of **52** was evaluated in the ROMP of the highly strained monomer norbornene, and compared with the activity of Ru dimer **39**, complex **42** and **44** (Table 4.2). Our results reveal that **52** displays very poor metathesis activity; only 20% of the norbornene polymerized during a reaction time of 3 hours at 85 °C (Entry 4). It has been described in literature that for this catalyst type, decomplexation of the arene ligand is the prior requirement for the generation of catalytic activity.[103,411–413] The complex must be coordinatively unsaturated for a substrate to enter the coordination sphere of the metal. In other words, for the catalyst to become active, a ligand has to decoordinate and generate a vacant site. However, the high thermal stability of complex **52** indicates that arene ligand decoordination is greatly restrained.

Aiming at the *in situ* generation of a vinylidene moiety, an excess (20 equiv) of phenylacetylene was added to the catalyst (Table 4.2, entry 5). Only a minor activity enhancement was observed. Also the addition of trimethylsilyl diazomethane (TMSD), which is known to activate [(*p*-cymene)(PCy_3)$RuCl_2$] **42** with the *in situ* formation of [$RuCl_2$(=$CHSiMe_3$)(PCy_3)][411,414], did not significantly enhance catalytic activity (Entry 6). Using $K^+PF_6^-$ and 1,1-diphenyl-2-propyn-1-ol, we aimed for the generation of an allenylidene moiety (Figure 4.6). Despite the use of high temperatures, the starting complex **52** was found to be very unreactive. Only when long reaction times (24 h) were used, the formation of a new ruthenium species was observed. Decomposition products also formed, and the desired allenylidene complex could not be isolated.
In a dissociative ligand substitution pathway, dissociation of the *p*-cymene is a prerequisite for the generation of an empty coordination site, where the alkylidene moiety can be introduced. Due to the exceptional stability of the complex **52**[3],

[3]The catalyst is air and moisture stable and can be kept in solution for 1 month without any sign of decomposition.

Entry	Catalyst	Conversion (%)	cis-(%)[a]	M_n[b]	PDI[b]
1	**39**	84	45	198	2.1
2	**42**	≈100	16	85	2.9
3	**44**	≈100	49	339	2.8
4	**52**	20	57	108	3.8
5	**52**+phenylacetylene	33	52	228	3.0
6	**52**+TMSD	21	75	588	3.0
7	**53**	17	81	1954	2.0
8	**53**+AgOTf = **54**	16	78	1112	2.6
9	**55**	4	-	-	-
10	**55**+phenylacetylene	7	42	32	3.1
11	**55**+TMSD	10	65	65	4.5
12	**56**	14	61	932	2.1

Table 4.2: ROMP of 2-norbornene.
Temperature = 85 °C, 3 h reaction time, catalyst/norbornene = 1/2500, cat. conc. = 0.41 mM, solvent: 0.5 mL CH_2Cl_2 + 10 mL toluene.
[a] Percent olefin with *cis*-configuration in the polymer backbone - ratio based on ^{1}H NMR spectra (δ 5.36 CH=CH *trans*, 5.22 CH=CH *cis*).
[b] Determined by GPC ($CHCl_3$) analysis. Results are relative to polystyrene standards. A correction factor of 0.5*M_n was applied.[382]

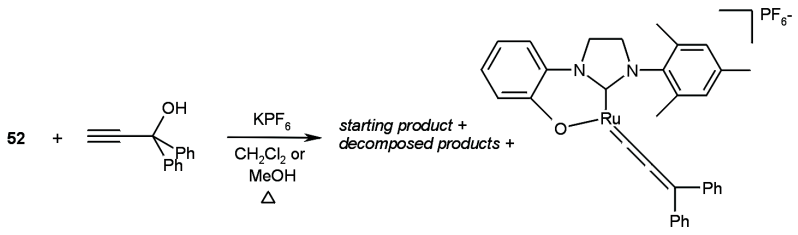

Figure 4.6: Reaction of **52** with propargyl alcohol.

which accompagnies a low dissociation tendency of the *p*-cymene ligand, the addition of a terminal alkyne or a diazo compound was found to have only minor effect.

The addition of an excess of ethereal HCl to **52** caused protonation of the phenolic oxygen, therefrom affording complex **53** as a bright orange solid. Through breaking of the chelate, the complex was expected to lose part of its extreme stability and become more reactive. Entry 7 in table 4.2 shows that a loss of catalytic activity was observed instead! Also the cationic counterpart **54** exhibited poor ROMP activity (Entry 8).
1,1-diphenyl-2-propyn-1-ol was not able to react with **54** in a favourable manner

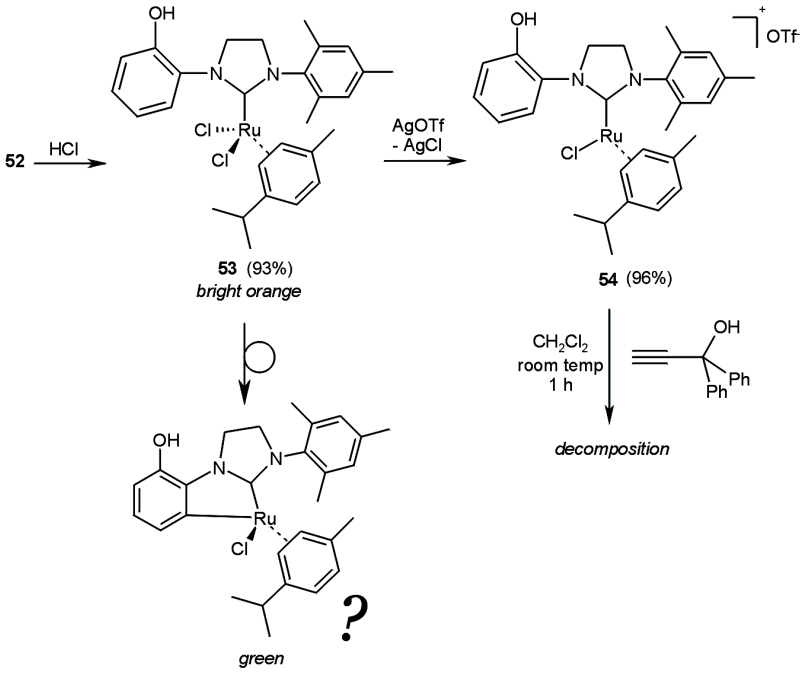

Figure 4.7: Losing the chelate effect.

to generate an allenylidene unit. Propargyl alcohol (1.2 equiv) and **54** were stirred in dry CH_2Cl_2 at room temperature. After 1 h of reaction, only decomposition of the starting complex was observed (Figure 4.7).

As expected, losing the chelate effect induced a significantly decreased stability of complex **53**. The complex was found to decompose rapidly in solution. Even as a solid stored under inert atmosphere the complex was unstable, and slowly changed color from orange to green (time course of two weeks). NMR analysis of the decomposition product indicated that both NHC and *p*-cymene ligand were still coordinated to the Ru center. Therefore, we suggest that **53** suffers from a tendency to *ortho*-metalation with the 2-hydroxy-phenyl amino side group (Figure 4.7).

Anticipating that this *ortho*-metalation might be avoided by a small modification in the NHC framework, a methyl unit was introduced at the carbon in *ortho* position of the 2-hydroxyphenyl group. Coordination of the new bidentate NHC afforded the air and moisture stable complex **55**. Also this complex is a poor metathesis initiator and the addition of a terminal alkyne or TMSD only slightly increases the polymer yield (Table 4.2, entries 9-11). Again, HCl was added to 'break' the chelate, affording complex **56**. Thereupon the catalytic activity in the

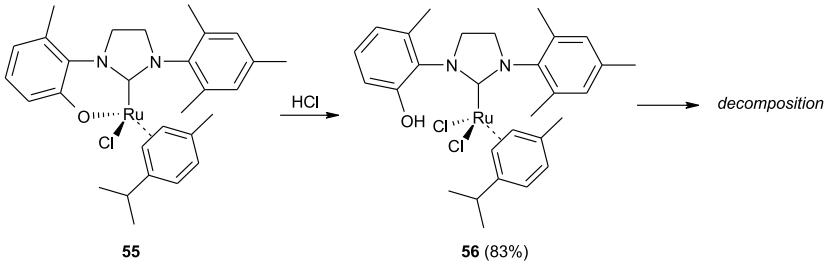

Figure 4.8: Modified complexes **55** and **56**.

ROMP of 2-norbornene was slightly enhanced (Table 4.2, entry 12). In spite of the small ligand modification (*ortho* methylation), also this complex was found to slowly decompose. A solution of **56** in CH_2Cl_2 changed color from orange to dark green during a time course of 1 hour. Unfortunately, a complex mixture of products was obtained, and we were not able to identify the decomposition products (Figure 4.8).

From these results, it is clear that complexes of the type [(*p*-cymene)(L)$RuCl_2$] (with L = H_2IMes or resembling NHC) are not very reactive and too unstable for practical use. Likely due to stability problems, we were unable to isolate complex [(*p*-cymene)(H_2IMes)$RuCl_2$] **50**. The similar complexes **53** and **56** were succesfully isolated, but only when an uncommon synthetic strategy was followed. The NHCs were first introduced as bidentate ligands which greatly enhanced complex stability through the chelate effect. Subsequent treatment with hydrochloric acid caused a breaking of the chelate O-Ru bond, with formation of complexes [(*p*-cymene)(NHC)$RuCl_2$] bearing monodentate NHCs. Upon loss of the chelate effect, a dramatic decrease in complex stability was observed and as a result, complexes **53** and **56** could not be kept for more than a few days even when stored as a solid under inert atmosphere. In solution both complexes decomposed very rapidly, which drastically restricted their catalytic value.

To adequately compete with the Grubbs catalysts, it is unquestionable that better activity and stability levels have to be reached. Therefore, our attention was drawn to other synthetic methods which first introduce an alkylidene moiety and then, in a second reaction step, realize the coordination of an NHC ligand.

4.2.2 NHC-phosphine complexes

Vinylidene complexes

The reaction of Ru dimer **39** with phenylacetylene and two equivalents of PCy_3 afforded the bis(phosphine) vinylidene complex **46**.[401–403] In a subsequent reaction

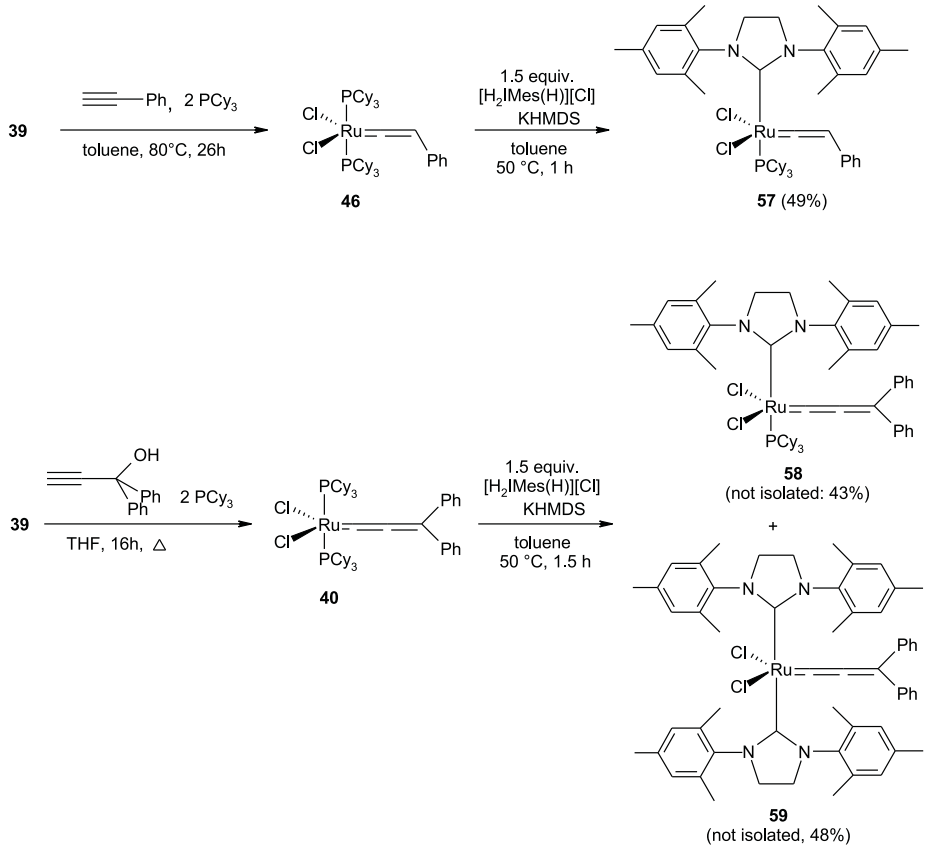

Figure 4.9: Synthesis of vinylidene **57**, and allenylidenes **58** - **59**.

with imidazolinium salt and base, coordination of the NHC was accomplished, with formation of the 2nd generation vinylidene complex **57** (Figure 4.9).
When tested in the ROMP of cyclooctadiene (COD) and the RCM of diethyl diallylmalonate, both the 1st and 2nd generation vinylidenes **46** and **57** were found to display poor metathesis activity (Figures 4.12 - 4.13). Even at 60 °C, complex **57** remained distinctly inferior to the activity level of the Grubbs catalysts. It is thus undeniable that vinylidenes are not convincing competitors for the benzylidene catalysts **1** and **2**.

Allenylidene complexes

Upon reaction of H_2IMes (1.5 equiv) with Ru allenylidene **40** at 50 °C, both the mono(NHC) complex **58** and the bis(NHC) complex **59** were formed (Figure

4.9). A temperature of 50 °C was used, since full ligand substitution could not be effectuated at room temperature. This was assigned to the low dissociation tendency of the phosphine ligands in the allenylidene precursor, which slows down the NHC substitution.
After a reaction time of 45 min, the reaction mixture consisted of ≈39% of **40**, 56% of **58**, and 5% **59**. Increasing the reaction time to 90 min afforded 9% of **40**, 43% of **58**, and 48% of **59**. A rather high percentage of bis(NHC) complex was thus formed, while some of the starting product (complex **40**) remained unreacted (Figure 4.10). This shows that complexes **40** and **58** have a quite similar tendency to exchange a phosphine ligand for NHC (affording **58** and **59** respectively). Aiming at improved reaction conditions, a H_2IMes/**40** ratio of 1.3 was found to be optimal, allowing a 61% isolated yield in **58** (see experimental section for further details). Furthermore, the observation was made that when the bis(NHC) complex **59** was heated in the presence of 3 equiv PCy_3 at 75 °C, the mono(NHC) complex **58** was formed exclusively after 90 min of reaction time. Figure 4.10 (*bottom spectrum*) shows the NHC diamine backbone ^{1}H NMR resonances (NCH_2CH_2N) in a mixture of the complexes **58** and **59**. While the NHC backbone protons show a multiplet in complex **58**, a broad singlet is found for the backbone protons of the two NHC ligands in **59**. We therefore suggest that, in complex **59**, rotation of the NHC ligands is fast on the NMR time scale. On the other hand, the NHC ligand in **58** has a higher rotational barrier, and as a consequence no coalescence of the protons is observed. The hindered rotation of the NHC in **58** is likely caused by steric interactions between the aromatic NHC amino side group and the phosphine ligand, which are absent in **59**. It can be seen in the ORTEP plot of **58** that one of the phosphine cyclohexyl groups is in close proximity to the NHC mesityl group, which is illustrative for the prominent steric interactions between both groups (Figure 4.11).[4]

Crystals of **58** suitable for X-ray structure analysis were grown from CH_2Cl_2. The complex shows a molecular structure where the Ru-atom has a slightly distorted square pyramidal coordination with the Cl-atoms trans to one another and the apical position occupied by the Ru=C bond (Figure 4.11). A structural comparison of complexes **40**, **41**, and **58** is shown in table 4.3. In all three complexes, the Ru=C_α bond distances are similar with a length of ≈1.79 Å, which is shorter than the Ru=C_α bond distance in the Grubbs benzylidene complex **2** (1.835(2) Å). This indicates a better overlap of the π-orbitals on the Ru center and C_α. Comparing the Ru-P bond length in complexes **41** and **58**, we see that the Ru-P bond is weaker in the latter. This can be assigned to the higher donating ability of H_2IMes compared with IMes, causing a higher *trans* influence. However, since only a minor difference in Ru-CNN bond exists between both complexes, it is

[4]The ORTEP plot in figure 4.11 shows the *solid* state structure of **58**, while the ^{1}H NMR spectrum in figure 4.10 was measured in the *liquid* phase (solution of the complex in $CDCl_3$). The ORTEP plot is thus only illustrative for the steric interactions between the phosphine and amino side group, which hinder rotation of the NHC in the NMR solvent.

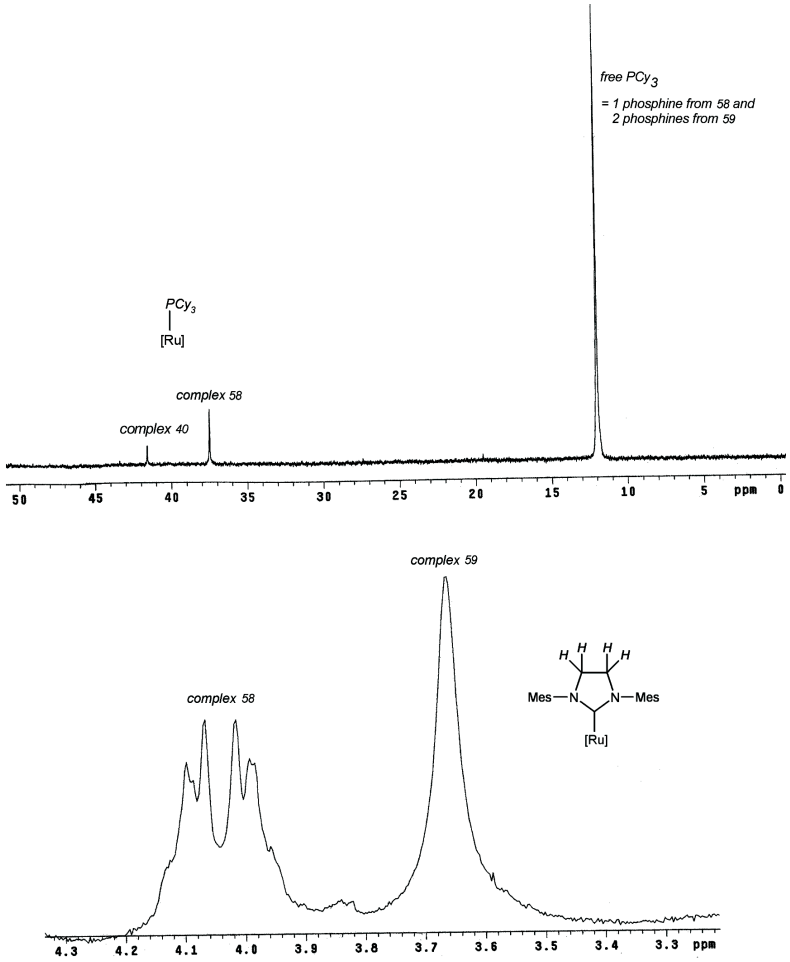

Figure 4.10: The reaction of **40** and H_2IMes (1.5 equiv), 90 min, 50 °C. *Top*: ^{31}P NMR spectrum. *Bottom*: Part of the ^{1}H NMR spectrum.

plausible that steric effects play a more determining role (see also section 2.4.1). The higher steric encumbrance of H_2IMes compared with IMes would then be at the origin of the longer Ru-P bond in **58**. Furthermore, the Ru-C_α-C_β and C_α-C_β-C_γ angle values reveal that the allenylidene chain is less bent in the 2nd generation complexes **41** and **58** than in the 1st generation complex.

In contrast to the arene complexes **52-56**, which show no reactivity in the ROMP of cycloocta-1,5-diene (COD), the allenylidene complexes are sufficiently active to allow for the polymerization of this low-strain monomer (Figure 4.12). The

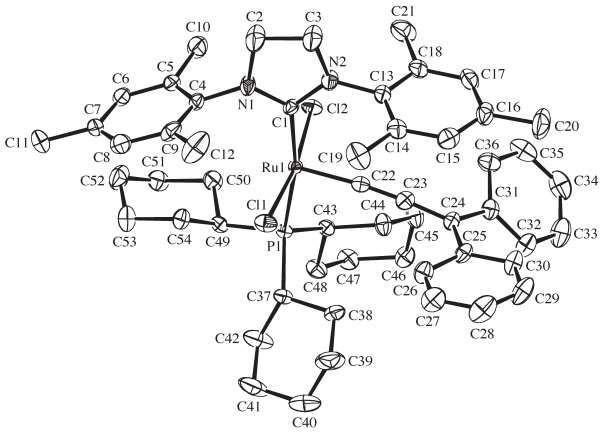

Figure 4.11: The molecular structure of **58**, showing 50% probability ellipsoids.

	40[a]	**41**[a]	**58**[b]
Ru=C_α	1.794(11)	1.7932(13)	1.796(3)
Ru-CNN		2.0893(14)	2.085(3)
Ru-P	2.358(5)	2.4107(4)	2.4240(7)
	2.413(5)		
Ru-Cl(1)	2.371(5)	2.3640(4)	2.3644(7)
Ru-Cl(2)	2.382(5)	2.3916(4)	2.3922(7)
C_α=C_β	1.273(12)	1.2605(17)	1.255(4)
C_β=C_γ	1.346(12)	1.3447(17)	1.342(4)
P-Ru=C_α	91.4(4)	92.19(4)	91.92(8)
	101.4(5)		
N_2C-Ru-C_α		98.89(5)	98.9(1)
C_α=Ru-Cl(1)	91.6(5)	93.13(4)	92.99(9)
C_α=Ru-Cl(2)	96.2(5)	95.89(4)	95.70(9)
Ru=C_α=C_β	169.20(12)	175.36(11)	175.2(3)
C_α=C_β=C_γ	167.20(18)	175.29(13)	175.1(3)

Table 4.3: Selected Bond Lengths [Å] and Angles [°].
Structural comparison of **40**, **41** and **58**. [a] [398] [b]This work.

bis(NHC) complex **59** is inactive at 40 °C, and active at 80 °C. A higher temperature is necessary to induce catalyst initiation (NHC decoordination[5]) due to the increased bond strength of Ru-NHC compared with Ru-PCy_3. At a temperature of 40 °C, both complex **40** and complex **58** show a substantial ROMP and RCM activity, but do not reach the catalytic activity of the Grubbs catalysts (Figures

[5] A dissociative pathway is then taken for granted.

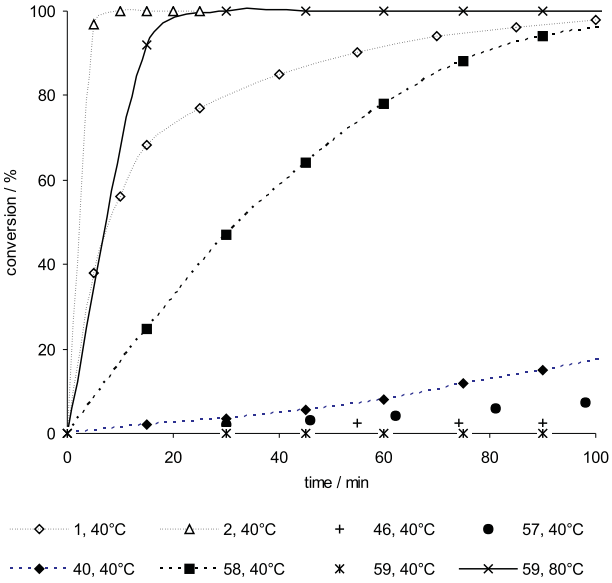

Figure 4.12: ROMP of COD, COD/cat. = 1000. See experimental section for further reaction details.

4.12 - 4.13). Nevertheless, their lower synthetic cost and more practical synthesis partly compensate for a lower inherent activity.

A further improved catalytic performance was aimed for with the synthesis of the 3rd generation allenylidene complex **60**. The addition of an excess of pyridine to **58**, resulted in a rapid color change from orange-brown to blood red. The complex precipitated as the 18-electron bis(pyridine) complex **60** upon addition of hexane (Figure 4.17). While the Grubbs complex **3a** readily loses one pyridine ligand, complex **60** did not liberate a pyridine even under prolonged vacuum.
As can be deducted from figures 4.14 and 4.15, bis(pyridine) complex **60** is significantly more active in the ROMP of COD than its 1st (**40**) and 2nd (**58**) generation allenylidene analogues, but somewhat less active than the mono(pyridine) Grubbs complex **3b**. Complex **60** shows slow reaction in the RCM of diethyl diallylmalonate, and performs peculiarly poorly in comparison to complexes **40** and **58** (Figure 4.16). This low reaction rate should not be assigned to decomposition of the starting catalyst, as undecomposed complex was still present in the reaction mixture after 20 hours of reaction time. Grubbs complex **3b** is considerably less stable and rapidly carries the RCM to 27% conversion before catalyst decomposition inhibits further reaction. The structural difference between complex **60** and **3b** is twofold; there is a rigid allenylidene unit versus a more reactive

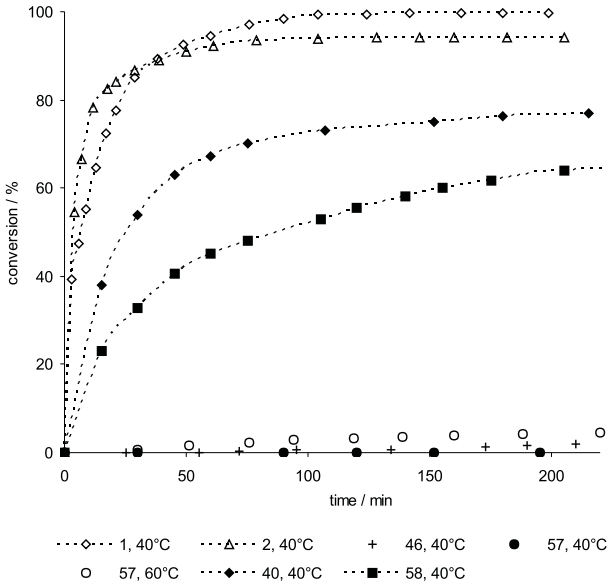

Figure 4.13: RCM of diethyl diallylmalonate, 1 mol% cat, C_6D_6.

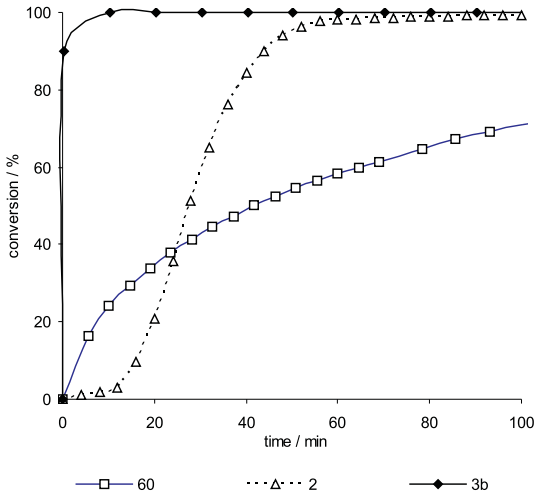

Figure 4.14: Monitoring ROMP of COD via ^{1}H NMR spectroscopy. COD/cat. = 3000, cat. conc. = 0.452 mM, 20 °C, solvent = $CDCl_3$.

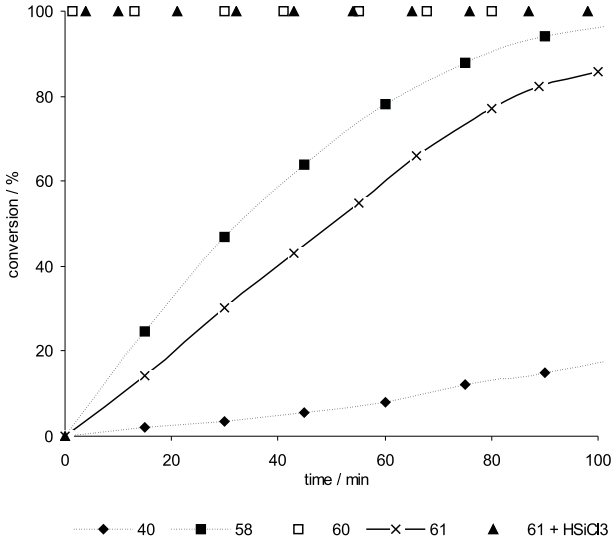

Figure 4.15: Monitoring ROMP of COD. COD/cat. = 1000, 40 °C, acid/**61** = 30. See experimental section for further reaction details.

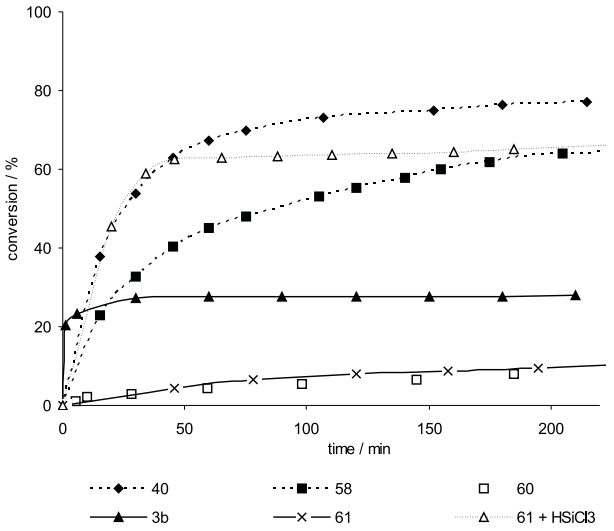

Figure 4.16: Monitoring RCM of diethyl diallylmalonate via ^{1}H NMR. substrate/cat. = 100, 40 °C, cat. conc. = 7.08 mM, solvent = C_6D_6, acid/**61** = 25.

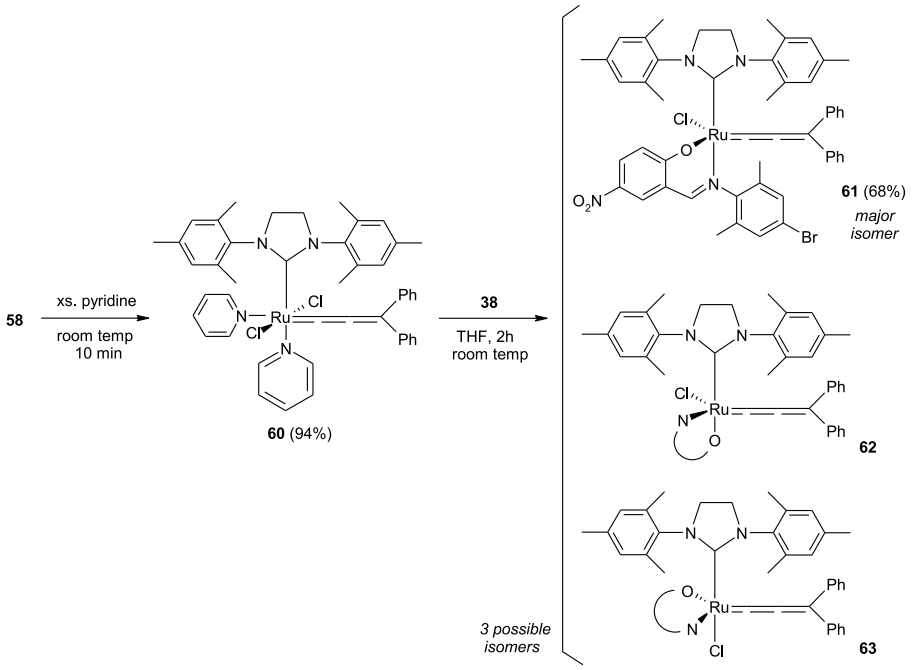

Figure 4.17: Synthesis of allenylidene complexes **60-63**.

benzylidene unit, and the coordination of two pyridine ligands versus only one pyridine. Complex **60** has to decoordinate 2 pyridine ligands to form a 14-electron metathesis active species, which is a requisite step for olefin metathesis in a dissociative reaction mechanism. As a result, it is to be expected that initiation is slow for **60**. A slow initiation would be in full agreement with the high complex stability (particularly in comparison with **3b**) and slow ring-closing metathesis reaction, but then it remains noteworthy that this effect is less pronounced in the ROMP reaction.

4.2.3 Phosphine free Schiff base allenylidene complex

As the Schiff base benzylidene catalyst **36** was shown to have a high industrial applicability (chapter 3), it is of considerable interest to develop an allenylidene counterpart of this particular complex. This would avoid synthetic pathways which necessitate the purchase of expensive Grubbs precursor **1**, and would circumvent Grubbs' patents on NHC benzylidene complexes.

The addition of the Schiff base Tl-salt **38** to bis(pyridine) complex **60** induced coordination of the Schiff base ligand (Figure 4.17). Analysis of the reaction product

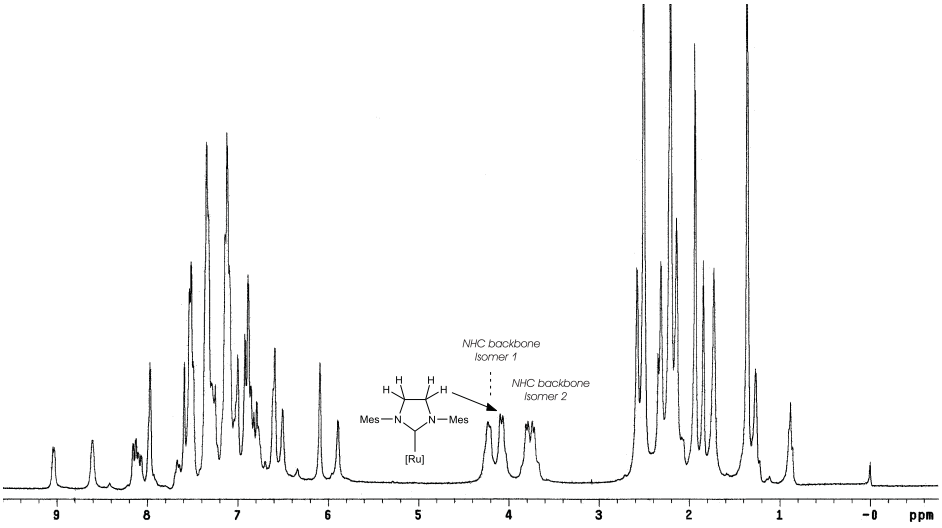

Figure 4.18: ^{1}H NMR spectrum showing two Schiff base allenylidene isomers.

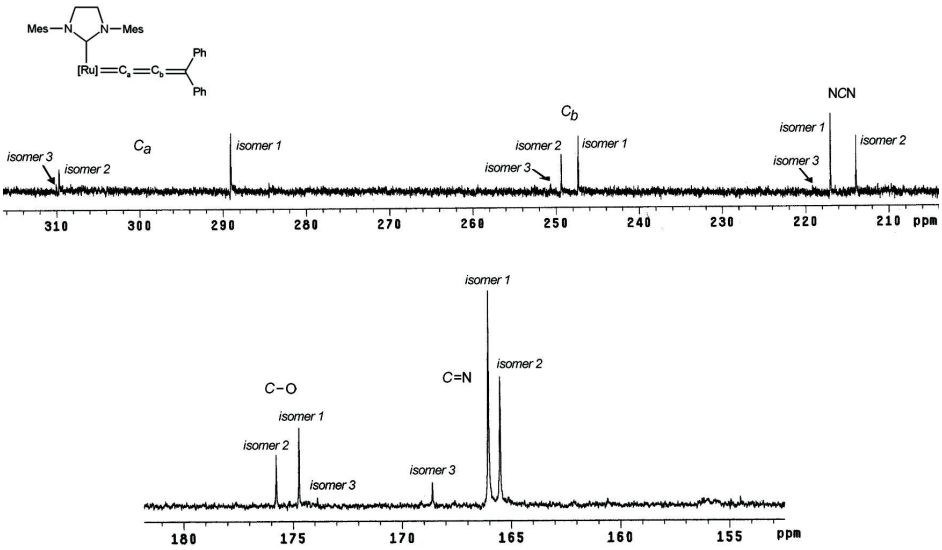

Figure 4.19: Parts of the ^{13}C NMR spectrum showing three Schiff base allenylidene isomers.

with NMR spectroscopy revealed that three different isomers were formed (Figures 4.18 - 4.19). ^{13}C NMR signals of the *C*=N and *C*-O carbons evidence that the Schiff base is bound to the Ru center via the oxygen as well as the nitrogen, and

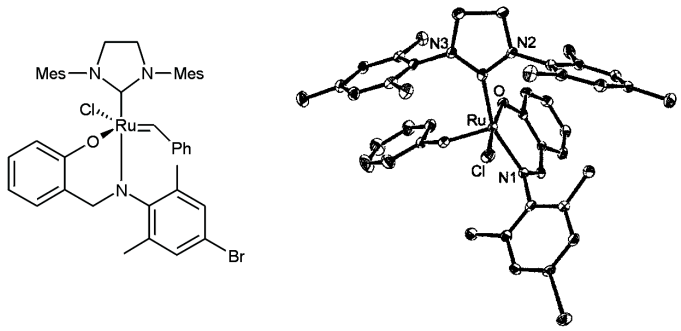

Figure 4.20: Solid-state molecular structure of Schiff base benzylidene complex **64**. From: Raines et al., *Adv. Synth. Catal.* **2007**.[372]

this in all three isomers. Also Ru=*C*, Ru=C=*C* and N*C*N resonances were found for the three isomers. When the coordination of the Schiff base was carried out at a temperature of 15 °C, almost 50% of isomers 1 and 2 were formed. The third isomer was only formed in a low ratio. When the reaction temperature equaled 20 °C, more of isomer 1 was formed (≈ 86%). Using column chromatographic separation, the major isomer was successfully separated from the other isomers, isolated and characterized with NMR spectroscopy.
The formation of more than one isomer contrasts with the single isomer found earlier for benzylidene complex **36**. Literature single crystal X-ray analyses of Schiff base benzylidene complexes point to an arrangement where the anionic moieties are *trans* oriented.[6] An illustrative example is shown in figure 4.20. This ORTEP plot was taken from a recently published article by Raines et al., and shows the molecular structure of a Schiff base benzylidene complex **64**, which is only discrepant from complex **36** in the absence of the nitro-group.[372]

A handful of Grubbs-like ruthenium complexes with an uncommon *cis*-arrangement of the anionic moieties were recently described in the literature. Fürstner et al. described two complexes rearranging from a *trans*-dichloro to a *cis*-dichloro disposition upon treatment of the starting materials with silica gel.[334] Slugovc et al. reported several 2nd generation metathesis catalysts bearing a chelating carbene ligand. For chelating carbene ligands derived from 2-vinylbenzaldehyde or 2-vinylbenzoic acid ester, a *cis*-dichloro arrangement with the chelating carbene oriented parallel to the mesityl group of the NHC ligand was found (Figure 4.21, complex **65**).[77] For chelating carbene ligands with imine functionalities, a *trans*-stereochemistry of the halide ligands was found (Figure 4.21, complex **66**).[362] Grubbs et al. published on complex **67**, which slowly converts to its isomer **68** when heated.[359] Likewise, Grela et al. observed that their metathesis catalysts of type **69**, possessing five-membered chelate rings, slowly isomerized from a common *trans*-dichloro geometry to the corresponding *cis*-dichloro isomers (Figure 4.21).[85]

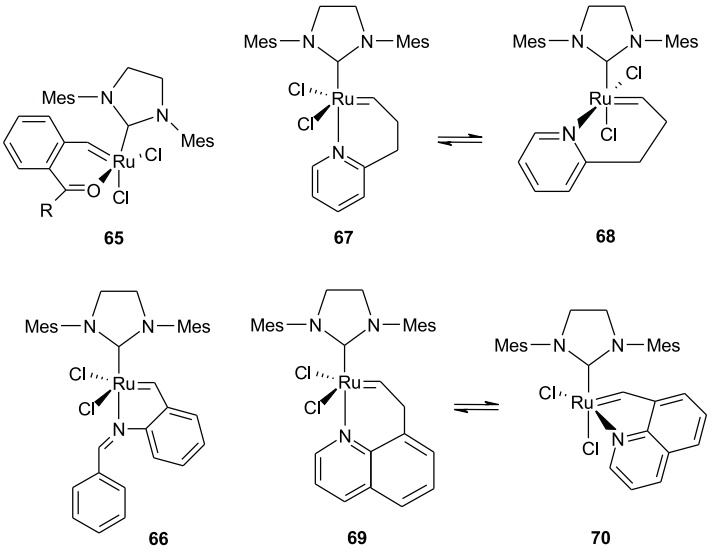

Figure 4.21: Literature examples of complexes with a *cis*-dichloro arrangement (**65**, **68**, **70**).

Bearing these literature examples in mind, we propose three possible structures for our allenylidene Schiff base complex: **61** with the anionic units in a *trans* position, and complexes **62** and **63** with the anionic units in a *cis* position (Figure 4.17). Unfortunately, NMR analysis could not unambiguously determine the relative position of the ligands. However, in analogy with Schiff base benzylidene complexes (e.g. complex **64**), it is plausible that the major isomer has its anionic units in the *trans* position. In what follows, this complex has been named **61** but one should bear in mind that its geometrical arrangement is only an assumption.

The catalytic performance of the allenylidene imine complex **61** was investigated in olefin metathesis test reactions. Complex **61** showed an inferior latency compared with complex **36**, as a certain metathesis activity was observed in the ROMP of COD at room temperature (Table 4.4, entries 1-2). At 40 °C, complex **61** almost reached the catalytic activity of its PCy_3 substituted 2nd generation analogue **58** (Figure 4.15). In the RCM of diethyl diallylmalonate, only low activity was measured (Figure 4.16). The addition of a Brönsted acid (HCl) improved the ROMP activity, and a turnover number of ≈3000 was obtained (Table 4.4, entry 3). In a much shorter reaction time, a turnover number of 3000 was attained with $HSiCl_3$ as the activating agent (entry 5). A few data with benzylidene Schiff base catalyst **36** were included for comparison. It is clear that

	cat.	acid	cat/COD/ acid	t [h]	Conv. [%][a]	*cis*- [%][b]	M_n[c] *10^3	PDI [c]	TON
1	**61**	-	1/300/-	1	1	-	-	-	-
				16	78	76	79	1.4	228
2	**36**	-	1/300/-	4	0	-	-	-	0
3	**61**	HCl[d]	1/3000/10	1	2	-	-	-	-
				16	93	66	68	1.6	2790
4	**36**	HCl[d]	1/30 000/70	0.5	100	75	176	1.6	$3*10^4$
5	**61**	$HSiCl_3$	1/3000/10	0.25	100	27	43	1.7	$3*10^3$
6	**61**	$HSiCl_3$	1/30 000/70	16	≈0[e]	-	-	-	0
7	**36**	$HSiCl_3$	1/30 000/70	1	100	25	134	1.8	$3*10^4$
8	**36**	$HSiCl_3$	1/300 000/300	0.5	78				
				1	85				
				16	100	46	269	1.7	$3*10^5$
9	**61**	$PhSiCl_3$	1/3000/1	4	15	-	-	-	450
				16	16	49	21	1.8	480
10	**61**	$PhSiCl_3$	1/3000/10	0.1	100	58	70	1.7	$3*10^3$
11	**61**	$PhSiCl_3$	1/30 000/70	0.25	100	29	84	1.7	$3*10^4$
12	**61**	$PhSiCl_3$	1/100 000/100	16	6	-	-	-	$6*10^3$
13	**61**	HOTf	1/3000/2	16	0[e]	-	-	-	0

Table 4.4: ROMP of COD, room temperature, solvent: toluene.
[a] Determined by ^{1}H NMR.
[b] Percent olefin with *cis*-configuration in the polymer backbone - ratio based on ^{13}C NMR spectra (δ 32.9: allylic carbon *trans* - 27.6: allylic carbon *cis*).
[c] Determined by GPC ($CHCl_3$) analysis. Results are relative to polystyrene standards.
[d] 1 N HCl sol. in Et_2O.
[e] Decomposition of catalyst, conversion not further increased.

the allenylidene complex **61** failed to meet the turnover numbers attained by **36** (Entry 4).

As the complex **61** quickly changes color from orange-red to yellow when acid (HCl or $HSiCl_3$) is added, a fast reaction between both components can be expected. This contrasts with our results obtained earlier for complex **36** (chapter 3), where no significant color change was seen and where NMR analysis excluded an irreversible reaction between $HSiCl_3$ and the Schiff base complex. To further elucidate our observations, the reaction of **61** and HCl was followed using ^{1}H NMR spectroscopy (Figure 4.25). Immediately upon acid addition, a change in the spectrum was observed, and after 5 min of reaction time the mixture had turned completely yellow. All NHC amino backbone protons now gave one common broad singlet, while less signals of the methyl groups in the NHC and the Schiff base were observed. This likely indicates a fast rotation of the NHC ligand around the Ru-CN_2 axis (on the NMR time scale). Possibly, there is also a less hampered rotation of the 4-bromo-2,6-dimethylphenyl group, due to decoordination of the imine-*N*. At this point, decoordination or decondensation of

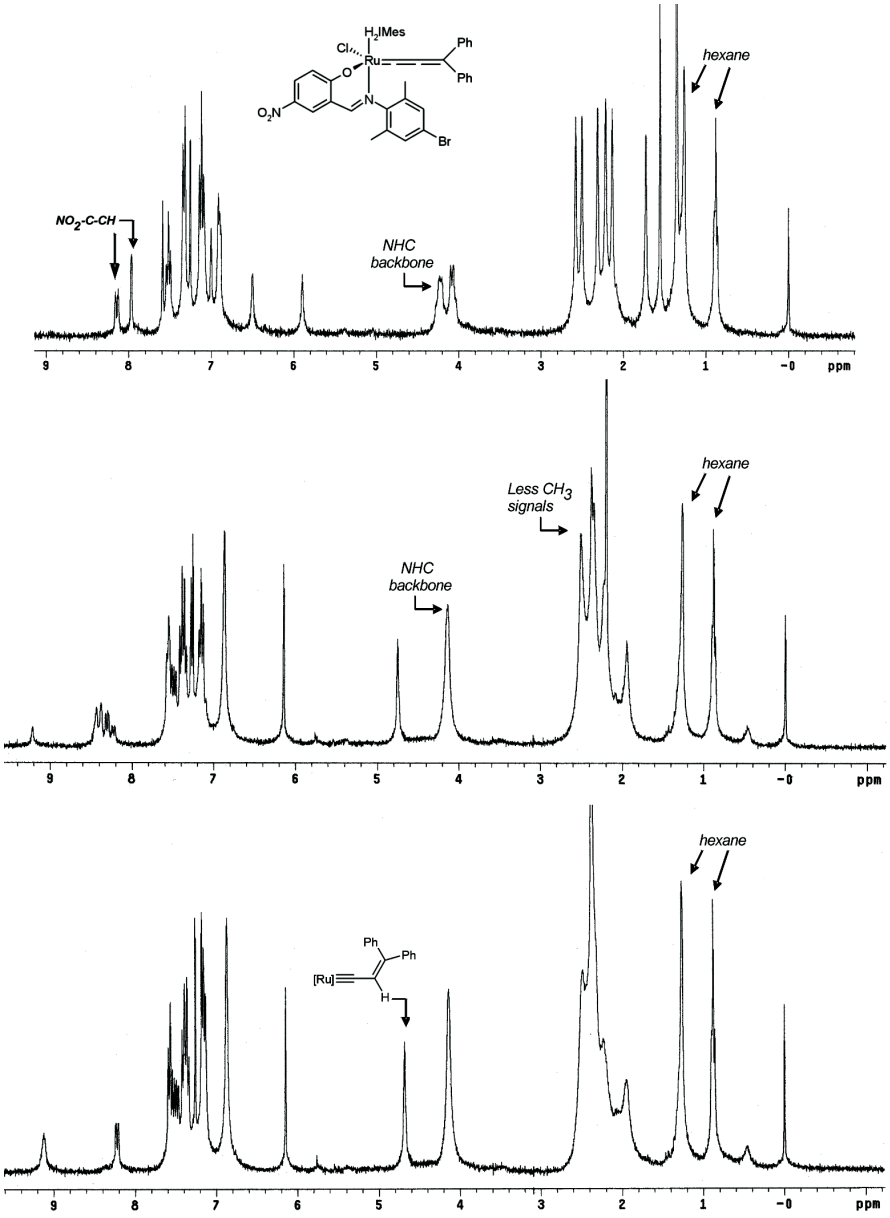

Figure 4.22: ^{1}H NMR spectra of the major allenylidene Schiff base isomer **61** (*top spectrum*), and the reaction intermediates in the reaction of **61** with an excess of HCl. $CDCl_3$, 20 °C, reaction time: *middle* 1 min, *bottom* 5 min.

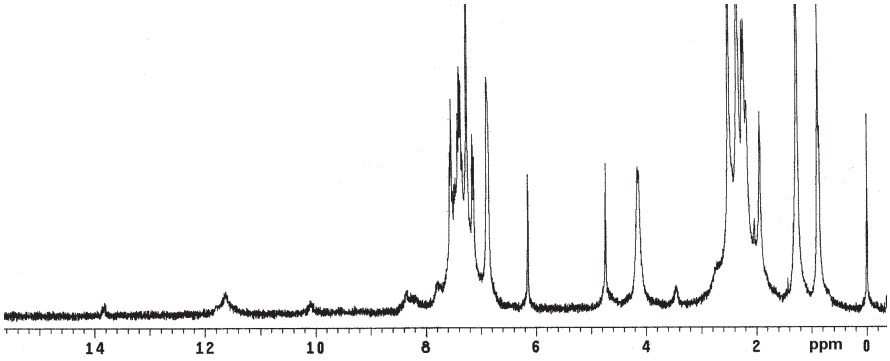

Figure 4.23: ^{1}H NMR spectrum after reaction of **61** with xs. HCl (1 hour). The decoordination + decondensation of the Schiff base ligand with formation of complex **71** is shown.

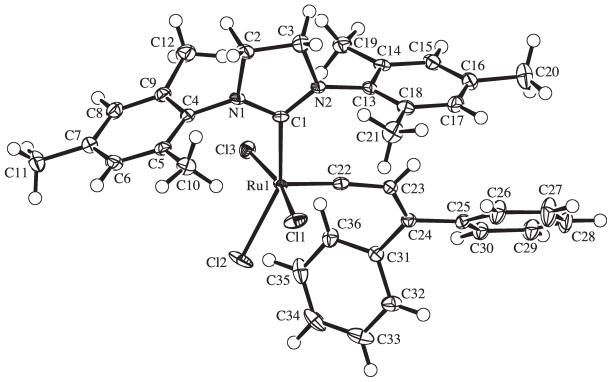

Figure 4.24: The molecular structure of **71**, showing 50% probability ellipsoids. Crystals were grown from $CDCl_3$.

Bond Lengths		**Bond Angles**	
Ru-C22	1.688(3)	C22-Ru-C1	97.5(1)
Ru-C1	2.036(3)	C22-Ru-Cl2	111.2(1)
Ru-Cl1	2.3563(8)	C1-Ru-Cl2	151.26(8)
Ru-Cl2	2.3439(8)	C1-Ru-Cl3	92.55(8)
Ru-Cl3	2.3470(8)	C1-Ru-Cl1	87.22(8)
C22-C23	1.396(4)		
C23-C24	1.372(4)		

Table 4.5: Selected Bond Lengths [Å] and Angles [°] for complex **71**.

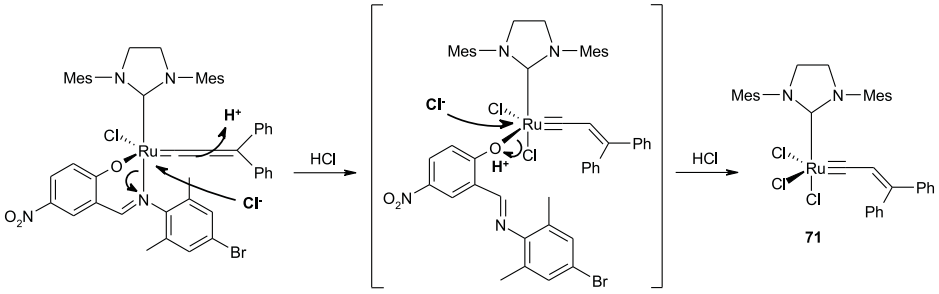

Figure 4.25: The formation of **71** from **61** and HCl.

the Schiff base ligand was not confirmed. After 1 h however, ^{1}H NMR resonances at δ 13.82 ppm (Ar-O*H* of Schiff base) and δ 11.63 ppm (Ar-O*H* of nitrosalicyl aldehyde, = decondensated Schiff base) showed that the Ru-O bond was cleaved, while a resonance at δ 10.03 ppm (Ar-C(=O)*H*) revealed that some of the Schiff base imine decondensated with formation of nitrosalicyl aldehyde (Figure 4.23).

A single crystal of the reaction product **71** was grown successfully. Its molecular structure presented in figure 4.24 evidences protonation of the allenylidene C_β and loss of the Schiff base ligand. A neutral Ru carbyne complex coordinated with 3 chloride ligands was thus formed. The Ru atom has a slightly distorted square pyramidal coordination with the apical position occupied by the Ru-C triple bond. From our observations, it seems reasonable to assume that the acid quickly attacks the allenylidene unit with formation of a carbyne, while cleavage of the Ru-O bond proceeds more slowly (Figure 4.25). Simple protonation of the imine-*N* is likely, but was not evidenced.

Figures 4.15 - 4.16 demonstrate that the acid $HSiCl_3$ more successfully activates **61** in comparison with HCl. In the ROMP of COD as well as in the RCM of diethyl diallylmalonate, there is a pronounced activity enhancement upon $HSiCl_3$ addition. Entry 5 in table 4.4, however, shows that the *in situ* generated system has only limited stability, which restricts the monomer/catalyst ratio that can be reached.
Figure 4.26 shows the ^{1}H spectrum of the product of reaction between **61** and an excess of $HSiCl_3$ ($\approx$ 100 equiv). The reaction was carried out in dry toluene under an inert atmosphere[6] at room temperature. After 15 min, the solvent was removed under reduced pressure and the yellow-orange reaction product was precipitated in hexane. No decoordination or decondensation of the Schiff base ligand was observed, but a new ^{1}H signal was found at δ 5.11 ppm. A singlet with approx. the same chemical shift was found for the Ru carbyne complex

[6]Rigorously dry reaction conditions were used to avoid the formation of HCl.

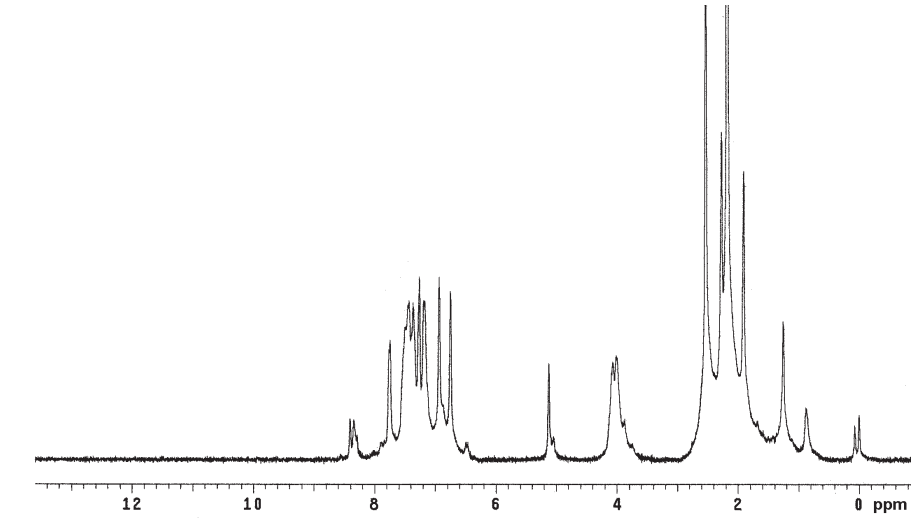

Figure 4.26: ^{1}H NMR spectrum after reaction of **61** with an excess of $HSiCl_3$.

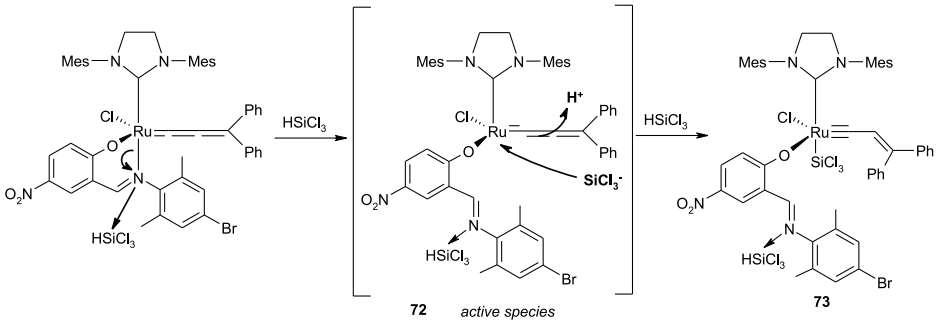

Figure 4.27: Proposed structure of the complexes resulting from the reaction of **61** and $HSiCl_3$.

71, and most likely had to be assigned to the RuCC*H* proton. Therefore, a reaction product with structure **73** is proposed (Figure 4.27). Possibly the activity enhancement induced by the addition of $HSiCl_3$ can be explained by the formation of an intermediate active species **72**.

As both HCl and $HSiCl_3$ are expected to induce the formation of a Ru carbyne, it is normal that poorer activity enhancements were reached in the ROMP of COD when the allenylidene Schiff base complex **61** was used instead of its benzylidene counterpart **36** (Table 4.4). In theory, there are two possibilities for carbyne complexes **71** and **73** to generate catalytic activity, both of them being unlikely.

In a dissociative metathesis mechanism, the complexes would have to decoordinate the neutral NHC ligand or an anionic chloride in order to liberate a coordination place for an olefinic substrate. In view of the strong NHC-Ru bond, NHC decoordination is very unlikely to happen at room temperature. Decoordination of Cl^-, which would lead to the formation of a cationic complex, is also not expected to take place readily. An alternative would be an associative mechanism, but then the Ru-C triple bond would imply a reaction mechanism which is different from the general associative mechanism of Ru alkylidene complexes.

To avoid the formation of a carbyne species, the acid $HSiCl_3$ was replaced by $PhSiCl_3$. The latter does not possess a hydrogen which can react with the allenylidene unit of the Schiff base complex **61**, and allows for an activation of the catalyst as observed earlier for **36**. Using $PhSiCl_3$ instead of HCl or $HSiCl_3$, we were able to use higher monomer/catalyst ratios, and turnover numbers of 30 000 were reached (Table 4.4, entries 9-12). This acid does necessitate rigorously dry reaction conditions, since it can react with water to form HCl, which eventually leads to the generation of a Ru carbyne.

The formation of an alkenylcarbyne Ru complex upon treatment of an allenylidene species with a suitable acid (HOTf = CF_3SO_3H), was also observed by Dixneuf et al. Their Ru carbynes were reported to be key intermediates for metal-indenylidene complex formation (Figure 4.2).[406,407] Based on these results, HOTf was added in a small excess (2 equiv) to our ROMP reaction mixture (Table 4.4, entry 13). No catalytic activity was found at all, and since further NMR analysis did not point to the *in situ* generation of an indenylidene, we did not further investigate the effects of this particular acid on our catalytic system.

4.3 Conclusion

In order to develop new synthetic strategies which afford alternatives for the classic Grubbs benzylidene catalysts, the air and moisture stable Ru dimer [(*p*-cymene)$RuCl_2$]$_2$ was chosen as a catalyst precursor. Given our experience with the coordination of saturated NHC ligands, and the knowledge that these ligands provide advantageous metathesis initiators, we attempted to fill a gap in the olefin metathesis catalyst design. Up to know, the coordination of the extensively used H_2IMes ligand to Ru dimer or therefrom derived complexes was not adequately reported in literature.

In a first part of our research was aimed for the synthesis of an NHC bearing Ru arene complex. The strong sigma donation of a saturated NHC was expected to facilitate decoordination of the *p*-cymene ligand in [(*p*-cymene)$RuCl_2$(NHC)] complexes, which would lead to an enhanced catalytic activity. Since the desired [(*p*-cymene)$RuCl_2$(H_2IMes)] could not be isolated, presumably due to a low

stability of the complex, a chelating NHC ligand was introduced instead. An extremely stable complex was formed, which showed very poor olefin metathesis activity. Treatment of the complex with HCl resulted in an unstable [(*p*-cymene)$RuCl_2$(NHC)] complex, which -due to its instability- only afforded low polymer yield. We conclude that there was no benefit in the stronger sigma donation of saturated NHCs compared with unsaturated NHCs. While [(*p*-cymene)$RuCl_2$(IMes)] is a fairly stable complex, [(*p*-cymene)$RuCl_2$(H_2IMes)] and analogous complexes were found to be too unstable for utile olefin metathesis reactions.

To circumvent this stability problem, the synthetic sequence was reversed: an alkylidene unit was introduced before the coordination of an NHC ligand. Accordingly, NHC bearing vinylidene and allenylidene complexes were synthesized and tested in representative metathesis reactions. Since both the 1st and 2nd generation vinylidene complexes demonstrated only modest activity, our attention was mainly focused on the allenylidene complexes. These complexes show lower activity than the corresponding Grubbs benzylidene complexes, but benefit from their lower synthetic cost and easier synthetic procedure. When the Tl-salt of a Schiff base was added to the 3rd generation allenylidene complex, the formation of three different isomers was observed. Three possible ligand arrangements were proposed; this is, one complex with the anionic units in a *trans* position, and two complexes with the anionic units in a *cis* position. The major isomer **61** was successfully isolated thanks to colum chromatography, and subjected to olefin metathesis test reactions. A low but significant activity was found in the ROMP of COD at room temperature. The addition of hydrochloric acid or trichlorosilane was found to enhance the catalytic activity, but the obtained turnover numbers did not meet the impressive results obtained for the corresponding benzylidene complex **36**. ^{1}H NMR and X-ray analysis revealed that HCl reacts directly with the allenylidene unit in **61** to form a Ru carbyne **71**. Also $HSiCl_3$ is expected to react with the allenylidene moiety to afford a carbyne complex **73**. A non-covalent intermolecular Si-N interaction with the Schiff base ligand as observed in the silane activation of complex **36**, possibly led to the formation of an intermediate active species **72**. Using $PhSiCl_3$ as the activating agent, the formation of an alkenylcarbyne ruthenium species was successfully avoided, which allowed for higher turnover numbers in shorter reaction times.

4.4 Experimental Section

4.4.1 General remarks

All reactions and manipulations involving organometallic compounds were conducted in oven-dried glassware under an argon atmosphere using standard Schlenk techniques. Solvents were dried with appropriate drying agents and distilled prior to use. Ru dimer **39**[415], H_2IMes(H)(CCl_3)[231], complex **40**[398], and complex **46**[402]

were prepared according to literature procedure. (Trimethylsilyl)diazomethane (TMSD) was purchased from Aldrich as a solution in hexane.

4.4.2 Ligand synthesis

NHC salt 1-mesityl-3-(2-hydroxyphenyl)-4,5-dihydroimidazolium chloride **51** was prepared according to literature procedure.[410] 1-mesityl-3-(2-hydroxy-6-methylphenyl)-4,5-dihydroimidazolium chloride was prepared analogously:

N-Mesityl-N'-(2-hydroxy-6-methylphenyl)-oxalamide
Yield: 83%. ^{1}H NMR ($CDCl_3$): δ 9.50 (s, 1H), 8.76 (s, 1H), 8.21 (s, 1H), 7.14 (t, 1H), 6.97 (m, 1H), 6.95 (m, 2H), 6.82 (d, 1H), 2.37 (s, 3H, CH_3), 2.30 (s, 3H, CH_3), 2.24 (s, 6H, CH_3). ^{13}C NMR ($CDCl_3$): δ 158.2 (C=O), 158.0 (C=O), 148.1, 138.9, 134.8, 129.4, 128.6, 123.0, 119.2, 118.6, 21.2 (p-CH$_3$), 18.6 (CH$_3$), 18.3 (o-CH$_3$).

1-mesityl-3-(2-hydroxy-6-methylphenyl)-4,5-dihydroimidazolium chloride
Yield: 80%. ^{1}H NMR ($CDCl_3$): δ 10.98 (s, 1H), 8.19 (s, 1H), 7.34 (d, 1H), 7.03 (t, 1H), 6.96 (s, 2H), 6.67 (d, 1H), 4.49-4.45 (m, 4H, NCH_2CH_2N), 2.37 (s, 3H, CH_3), 2.36 (s, 3H, CH_3), 2.33 (s, 6H, CH_3). ^{13}C NMR ($CDCl_3$): δ 160.8 (NCN), 153.8 (C-OH), 141.0, 135.4, 135.0, 131.1, 130.3, 121.5, 116.6, 52.1 (NCH$_2$$CH_2$N), 52.0 (N$CH_2CH_2$N), 21.3 ($p$-$CH_3$), 18.1 ($CH_3$), 18.0 ($o$-$CH_3$).

4.4.3 Complex synthesis

[(*p*-cymene)RuCl$_2$(IMes)] 44
The synthesis of complex **44** was previously reported by Nolan et al. to result from the reaction of Ru dimer with free IMes carbene.[399] We herein describe a slightly altered synthetic strategy, which avoids the isolation and handling of the air and moisture sensitive free carbene.
To a dry Schlenk flask charged with 1,3-bis(2,4,6-trimethylphenyl)imidazolium chloride (0.490 g, 1.44 mmol) and 5 mL of dry toluene was added LiHMDS (1.44 mL of a 1.0 M sol in toluene, 1 equiv). The resulting suspension was stirred at room temperature for 15 min. Ru dimer **39** (0.43 g, 0.70 mmol) was then added as a solid, and the mixture was stirred at room temperature for an additional 45 min. The solution was filtered to remove residual salts and the filtrate was concentrated under vacuum. The residue was dissolved in a small amount of CH_2Cl_2 (1 mL) and precipitated upon addition of hexane (25 mL). The orange solid was filtered off and vacuum dried. Yield: 78%.
NMR data are similar to those reported by Nolan et al.: ^{1}H NMR ($CDCl_3$): δ 6.95 (s, 4H, Mes-3,5-H), 6.90 (s, 2H, NCHCHN), 5.03 (d, J = 5.5 Hz, 2H, p-cymene aryl-H), 4.63 (d, J = 5.5 Hz, 2H, p-cymene aryl-H), 2.51 (m, 1H, p-cymene CH(CH$_3$)$_2$), 2.35 (s, 6H, mesityl p-CH_3), 2.23 (s, 6H, mesityl o-CH_3),

1.79 (s, 3H, *p*-cymene CH_3), 1.07 (d, J = 6.8 Hz, 6H, *p*-cymene CH(CH_3)$_2$). ^{13}C NMR ($CDCl_3$): δ 172.0 (NCN), 139.0, 138.9, 130.1, 128.9, 125.4, 103.1, 96.0, 87.0, 85.9, 30.4 (*p*-cymene CH(CH_3)$_2$), 22.9, 22.7, 21.4, 19.3, 18.24, 18.0.

NHC-arene complex 52

The NHC precursor 1-mesityl-3-(2-hydroxyphenyl)-4,5-dihydroimidazolium chloride (0.765 g, 2.41 mmol) was treated with 2 equiv of potassium hexamethyldisilazide (KHMDS) in toluene (9.66 mL of a 0.5 M solution in toluene, 4.83 mmol) during 15 min at room temperature. A suspension of Ru dimer **39** (0.7g, 1.14 mmol) in toluene was added and the resulting mixture was stirred for an additional 1.5 h at room temperature. The toluene solution was filtered and washed with CH_2Cl_2 (2 * 10 mL). After evaporation of the filtrate, cold acetone was added while stirring. Subsequent filtration allowed the isolation of pure red-pink catalyst, which was thoroughly dried. Yield: 46%.

^{1}H NMR ($CDCl_3$): δ 6.93-7.02 (m, 3H, aryl CH), 6.79 (t, $^3J_{HH}$ = 7.3 Hz, 1H, aryl CH), 6.71 (d, $^3J_{HH}$ = 7.9 Hz, 1H, aryl CH), 6.43 (t, $^3J_{HH}$ = 7.3 Hz, 1H, aryl CH), 5.52 (d, 1H, *p*-cymene aryl-H), 5.26 (d, 1H, *p*-cymene aryl-H), 5.09 (d, 1H, *p*-cymene aryl-H), 4.43 (pseudo q, J_{app} = ≈10.5 Hz, 1H, NCH_2CH_2N), 4.18 (pseudo q, J_{app} = ≈10.5 Hz, 1H, NCH_2CH_2N), 4.02 (pseudo q, J_{app} = ≈10.5 Hz, 1H, NCH_2CH_2N), 3.92 (pseudo q, J_{app} = ≈10.5 Hz, 1H, NCH_2CH_2N), 3.69 (d, 1H, *p*-cymene aryl-H), 2.50 (s, 3H, mesityl CH_3), 2.42 (s, 3H, mesityl CH_3), 2.41 (m, 1H, *p*-cymene CH(CH$_3$)$_2$), 2.33 (s, 3H, mesityl CH_3), 1.58 (s, 3H, *p*-cymene CH_3), 0.96 (d, $^3J_{HH}$ = 6.7 Hz, 3H, *p*-cymene CH(CH_3)$_2$), 0.83 (d, $^3J_{HH}$ = 6.7 Hz, 3H, *p*-cymene CH(CH_3)$_2$). ^{13}C NMR ($CDCl_3$): δ 202.7 (NCN), 157.4 (*C*-O), 139.7 (NHC aryl-C), 139.0 (NHC aryl-C), 138.0 (NHC aryl-C), 136.2 (NHC aryl-C), 130.9 (NHC aryl-C), 130.5 and 130.3 (NHC aryl-C), 128.9 and 128.8 (NHC aryl-C), 124.92 and 124.86 (NHC aryl-C), 121.3 and 121.2 (NHC aryl-C), 116.3 and 116.2 (NHC aryl-C), 113.9 and 113.8 (NHC aryl-C), 101.1 (*p*-cymene aryl-C), 95.2 (*p*-cymene aryl-C), 94.7 (*p*-cymene aryl-C), 93.1 (*p*-cymene aryl-C), 83.8 (*p*-cymene aryl-C), 79.4 (*p*-cymene aryl-C), 51.1 (*C*H$_2$CH$_2$), 48.7 (CH$_2$*C*H$_2$), 30.2 and 30.1 (*p*-cymene *C*H(CH$_3$)$_2$), 23.3 (*C*H$_3$), 21.3 and 21.1 (*C*H$_3$), 20.0 and 19.8 (*C*H$_3$), 18.6 and 18.5 (*C*H$_3$), 18.3 and 18.1 (*C*H$_3$).

Some carbon atoms have a double peak in the ^{13}C-spectrum, which indicates the presence of two diastereomers in roughly an equal ratio.

Anal. Calcd. (%) for $C_{28}H_{33}N_2OClRu$: C 61.14, H 6.05, N 5.09; found: C 61.39, H 6.08, N 5.12.

NHC-arene complex 53

0.125 g of complex **52** (0.227 mmol) was dissolved in 5 mL of CH_2Cl_2. An excess of HCl (1 ml of a 1 N solution in Et_2O) was added and the resulting mixture was stirred at room temperature for 5 min. Solvents were evaporated and hexane (25 mL) was added to precipitate complex **53** as a bright orange solid. Yield: 93%.

^{1}H NMR ($CDCl_3$): δ 8.02 (d, 1H, aryl CH), 7.10 (s, 1H, aryl CH), 7.03 (s, 1H, aryl CH), 6.96 (m, 1H, aryl CH), 6.89 (m, 2H, aryl CH), 5.70 (br s, 2H, *p*-cymene aryl-

H), 5.32 (br s, 2H, *p*-cymene aryl-H), 4.34 (m, 2H, NCH_2CH_2N), 4.10 (m, 1H, NCH_2CH_2N), 3.98 (m, 1H, NCH_2CH_2N), 2.86 (sept, 1H, *p*-cymene CH(CH_3)$_2$), 2.58 (s, 3H, mesityl CH_3), 2.38 (s, 3H, mesityl CH_3), 2.35 (s, 3H, mesityl CH_3), 1.75 (s, 3H, *p*-cymene CH_3), 1.02 (m, 6H, *p*-cymene CH(CH_3)$_2$). ^{13}C NMR (CDCl$_3$): δ 203.0 (NCN), 146.1 (C-OH), 139.8 (NHC aryl-C), 138.8 (NHC aryl-C), 137.4 (NHC aryl-C), 135.5 (NHC aryl-C), 130.4 (NHC aryl-C), 129.5 (NHC aryl-C), 129.2 (NHC aryl-C), 125.1 (NHC aryl-C), 121.7 (NHC aryl-C), 118.9 (NHC aryl-C), 117.7 (NHC aryl-C), 105.0 (broad, *p*-cymene aryl-C), 97.3 (broad, *p*-cymene aryl-C), 92.1 (broad, *p*-cymene aryl-C), 82.3 (broad, *p*-cymene aryl-C), 52.0 (NCH$_2$CH$_2$N), 49.7 (NCH$_2$$CH_2$N), 30.4 (*p*-cymene CH(CH$_3$)$_2$), 23.6 (CH$_3$), 21.3 (CH$_3$), 21.2 (CH$_3$), 19.8 (CH$_3$), 18.9 (CH$_3$), 18.5 (CH$_3$).
Signals of the aromatic *p*-cymene protons appear as broad signals due to internal rotation of the ligand.
Anal. Calcd. (%) for $C_{28}H_{34}N_2OCl_2Ru$ (586.57): C 57.34, H 5.84, N 4.78; found: C 56.62, H 5.79, N 4.54.

Cationic NHC-arene complex 54
Silver triflate (0.049 g, 0.19 mmol) was added to a solution of **53** (0.109 g, 0.19 mmol) in CH_2Cl_2 (5 mL). The reaction mixture was stirred for 15 min at room temperature. The solution was filtered to remove AgCl and the solvent was evaporated to almost complete dryness. The addition of hexane (10 mL) led to precipitation of the desired cationic complex as a bright orange solid, which was filtered off and dried in vacuo. Yield: 96%.
^{1}H NMR (CDCl$_3$): δ 7.51 (d, 1H, aryl CH), 7.08 (s, 1H, aryl CH), 7.02 (m, 4H), 5.75 (br s, 2H, *p*-cymene aryl-H), 5.43 (br s, 2H, *p*-cymene aryl-H), 4.53 (m, 1H, NCH_2CH_2N), 4.28 (m, 1H, NCH_2CH_2N), 4.09 (m, 2H, NCH_2CH_2N), 2.59 (s, 3H, mesityl CH_3), 2.47 (m, 1H, *p*-cymene CH(CH$_3$)$_2$), 2.36 (s, 3H, mesityl CH_3), 2.33 (s, 3H, mesityl CH_3), 1.63 (s, 3H, *p*-cymene CH_3), 0.95 (m, 6H, *p*-cymene CH(CH_3)$_2$). ^{13}C NMR (CDCl$_3$): δ 204.4 (NCN), 144.2 (C-OH), 139.9 (NHC aryl-C),138.8 (NHC aryl-C), 136.8 (NHC aryl-C), 135.5 (NHC aryl-C), 130.6 (NHC aryl-C), 129.4 (NHC aryl-C), 129.0 (NHC aryl-C), 125.7 (NHC aryl-C), 123.5 (NHC aryl-C), 118.4 (NHC aryl-C), 117.8 (NHC aryl-C), 91.8 (broad, *p*-cymene aryl-C), 83.2 (broad, *p*-cymene aryl-C), 52.1 (NCH$_2$CH$_2$N), 49.6 (NCH$_2$$CH_2$N), 30.6 (*p*-cymene CH(CH$_3$)$_2$), 23.0 (CH$_3$), 21.2 (CH$_3$), 21.1 (CH$_3$), 19.9 (CH$_3$), 18.7 (CH$_3$), 18.2 (CH$_3$).
Signals of the aromatic *p*-cymene protons/carbons appear as broad signals due to internal rotation of the ligand.

NHC-arene complex 55
In an analogous procedure as for complex **52**, 1-mesityl-3-(2-hydroxy-6-methylphenyl)-4,5-dihydroimidazolium chloride (0.284 g, 0.86 mmol), KHMDS (3.43 mL of a 0.5 M sol in toluene), and Ru dimer **39** (0.25 g, 0.41 mmol) afforded complex **55** as an orange-red solid. Yield: 32%.
^{1}H NMR (CDCl$_3$): δ 7.02 (m, 2H, aryl CH), 6.84 (t, 1H, aryl CH), 6.73 (d, 1H,

aryl CH), 6.46 (m, 1H, aryl CH), 5.56 (d, 1H, *p*-cymene aryl-H), 5.29 (br s, 1H, *p*-cymene aryl-H), 5.11 (d, 1H, *p*-cymene aryl-H), 4.43 (pseudo q, 1H, NCH_2CH_2N), 4.18 (pseudo q, 1H, NCH_2CH_2N), 4.04-3.92 (m, 2H, NCH_2CH_2N), 3.71 (br s, 1H, *p*-cymene aryl-H), 2.53 (s, 3H, mesityl CH_3), 2.45 (s, 6H, 2-hydroxy-6-methylphenyl and mesityl CH_3), 2.41 (m, 1H, *p*-cymene CH(CH_3)$_2$), 2.36 (s, 3H, mesityl CH_3), 1.61 (s, 3H, *p*-cymene CH_3), 0.98 (d, 3H, *p*-cymene CH(CH_3)$_2$), 0.85 (d, 3H, *p*-cymene CH(CH_3)$_2$). ^{13}C NMR (CDCl$_3$): δ 201.5 (NCN), 156.1 (C-OH), 138.6 (NHC aryl-C), 137.8 (NHC aryl-C), 136.8 (NHC aryl-C), 134.9 (NHC aryl-C), 129.5 (NHC aryl-C), 129.2 (NHC aryl-C), 127.5 (NHC aryl-C), 123.8 (NHC aryl-C), 120.0 (NHC aryl-C), 114.9 (NHC aryl-C), 112.6 (NHC aryl-C), 99.5 (broad, *p*-cymene aryl-C), 97.6 (*p*-cymene aryl-C), 93.9 (broad, *p*-cymene aryl-C), 91.9 (*p*-cymene aryl-C), 82.4 (broad, *p*-cymene aryl-C), 78.0 (*p*-cymene aryl-C), 49.8 (NCH$_2$CH$_2$N), 47.4 (NCH$_2$$CH_2$N), 28.9 (*p*-cymene C$H$(CH$_3$)$_2$), 22.1 ($CH_3$), 20.0 ($CH_3$), 19.8 ($CH_3$), 18.6 ($CH_3$), 17.3 ($CH_3$), 16.9 ($CH_3$).

NHC-arene complex 56

Analogous to **53**, complex **56** was obtained as an orange solid in good yield (83%). Characterization through ^{1}H NMR was troublesome since aromatic *p*-cymene protons and the backbone protons on the NHC appeared as very broad signals due to internal rotation of the ligands.

^{1}H NMR (CDCl$_3$): δ 7.19 (m, 1H, aryl CH), 7.07 (broad s, 1H, aryl CH), 7.03 (s, 1H, aryl CH), 6.88 (m, 1H, aryl CH), 6.58 (m, 2H, aryl CH), 5.49-5.36 and 5.19 (broad signals, 4H, *p*-cymene aryl-H), 4.26-3.92 (broad m, 4H, NCH_2CH_2N), 2.69-0.88 (several signals). ^{13}C NMR (CDCl$_3$): δ 202.2 (NCN), 151.2 (C-OH), 138.2 (NHC aryl-C), 136.5 (NHC aryl-C), 134.9 (NHC aryl-C), 131.1 (NHC aryl-C), 129.4 (NHC aryl-C), 128.2 (NHC aryl-C), 124.3 (NHC aryl-C), 119.4 (NHC aryl-C), 118.1 (NHC aryl-C), 116.9 (NHC aryl-C), 98.1 (broad, *p*-cymene aryl-C), 95.0 (broad, *p*-cymene aryl-C), 93.4 (broad, *p*-cymene aryl-C), 80.9 (broad, *p*-cymene aryl-C), 53.8 (broad, NCH$_2$$CH_2$N), 29.3 (*p*-cymene CH(CH$_3$)$_2$), 22.4 (CH$_3$), 21.7 (CH$_3$), 21.0 (CH$_3$), 20.4 (CH$_3$), 19.6 (CH$_3$), 19.1 (CH$_3$).

(H$_2$IMes)(PCy$_3$)Cl$_2$Ru(=C=CHPh) 57

The synthesis of complex **47** was previously reported by Verpoort et al.[370] Herein, an alternative synthetic pathway is presented. Furthermore, the ^{1}H NMR and ^{31}P NMR characterization, as described below, was found to slightly differ from that in the former literature data. [H$_2$IMes(H)][Cl] (0.196 g, 0.57 mmol), and KHMDS (1.2 mL of a 0.5 M sol. in toluene) were stirred in 8 mL of toluene at room temperature. First generation complex **46** (0.318 g, 0.38 mmol) was added and the resulting mixture was stirred at 50 °C for 1 h. The solvent was removed in vacuo and the crude reaction product was purified using column chromatography with Et$_2$O/hexane 1/9 as the eluent. The desired complex slowly precipitated in a small amount of hexane (2 mL) as a red solid. Yield: 49%.

^{1}H NMR (CDCl$_3$): δ 7.05 (d, 2H), 6.93 (m, 2H), 6.71 (m, 2H), 6.47 (t, 3H), 4.38 (m, 1H, =C=CH), 3.95 (m, 2H, NCH$_2$CH$_2$N), 3.64 (m, 1H, NCH$_2$CH$_2$N), 3.15

(m, 1H, NCH_2CH_2N), 2.40, 2.28, 2.16, 2.09, 1.69, 1.58, 1.27, 1.07, 0.88, 0.86 (all: remaining 51H). ^{31}P NMR ($CDCl_3$): δ 23.56.

(H_2IMes)(PCy_3)Cl_2Ru(=C=C=CPh_2) 58
[H_2IMes(H)][Cl] (0.188 g, 0.55 mmol, 1.3 equiv.), and KHMDS (1.1 mL of a 0.5 M sol. in toluene) were stirred in 10 mL of toluene at room temperature. Complex **40** (0.385 g, 0.42 mmol) was then added as a solid and the resulting mixture was stirred at 50 °C for 75 min. The solution was filtered, and the filtrate solvent was concentrated in vacuo. Formation of bis(NHC) complex could not be avoided, while some of the allenylidene precursor **40** remained unreacted. Thereupon, the crude product was purified by column chromatography using Et_2O/hexane 1/9 as the eluent. After evaporation of the chromatography solvent, the residue was washed with hexane to afford complex **58** as an orange-brown solid in 61% yield.
^1H NMR ($CDCl_3$): δ 7.68 (d, 4H), 7.53 (t, 2H), 7.27-7.23 (m, 4H), 7.04 (s, 2H), 6.20 (s, 2H), 4.03-3.94 (m, 4H, NCH_2CH_2N), 2.68 (s, 6H), 2.33 (s, 12H), 2.22 (m, 3H), 1.75 (s, 3H), 1.61-0.88 (27H). ^{31}P NMR ($CDCl_3$): δ 37.52. ^{13}C NMR ($CDCl_3$): δ 285.7 (d, Ru=*C*), 265.2 (Ru=C=*C*), 219.2 (d, $J_{(P,C)}$ = 85.9 Hz, N*C*N), 145.9, 139.3, 139.0, 138.0, 137.5, 137.4, 134.5, 130.3, 129.9, 129.4, 129.2, 128.7, 128.0, 52.3 (NCH_2CH_2N), 51.8 (NCH_2CH_2N), 31.8, 31.6, 29.3, 28.0, 27.9, 27.1, 26.5, 26.4, 21.4, 20.1, 19.1.
Anal. Calcd. (%) for $C_{54}H_{69}N_2Cl_2PRu$ (949.12): C 68.34, H 7.33, N 2.95; found: C 68.01, H 7.41, N 3.00.

(H_2IMes)$_2Cl_2$Ru(=C=C=CPh_2) 59
[H_2IMes(H)][Cl] (0.211 g, 0.62 mmol), and KHMDS (1.3 mL of a 0.5 M sol. in toluene) were stirred in 10 mL of toluene at room temperature. Complex **40** (0.187 g, 0.21 mmol) was added and the resulting mixture was stirred at 50 °C for 1.5 h. The solution was filtered to remove residual salts, and the filtrate solvent was concentrated in vacuo. The residue was washed with hexane (3 * 10 mL), filtered and dried to afford complex **59** as an orange solid in 73% yield.
^1H NMR ($CDCl_3$): δ 7.61 (d, 4H), 7.54 (t, 2H), 7.27-7.18 (m, 4H), 6.86 (br s, 4H), 6.03 (br s, 4H), 3.59 (br s, 8H), 2.49-2.13 (36H). ^{13}C NMR ($CDCl_3$): δ 287.7 (d, Ru=*C*), 267.8 (Ru=C=*C*), 217.6 (N*C*N), 144.6, 137.5 (broad), 136.8, 133.6, 130.7, 130.4, 130.1, 127.9, 127.3, 52.7 (broad, NCH_2CH_2N), 21.3 (CH_3), 19.1 (CH_3).
Anal. Calcd. (%) for $C_{57}H_{62}N_4Cl_2Ru$ (975.13): C 70.21, H 6.41, N 5.75; found: C 70.18, H 6.58, N 5.70.

(H_2IMes)(py)$_2Cl_2$Ru(=C=C=CPh_2) 60
An excess of pyridine (2 mL, 24.7 mmol) was added to 0.16 g (0.17 mmol) of **58** The resulting mixture was stirred for 5 min and hexane (10 mL) was added. The bis(pyridine) complex precipitated as a bright red solid, which was filtered off, washed with hexane (5 mL), and dried in vacuo. Yield: 94%.
^1H NMR ($CDCl_3$): δ 9.14 (br s, 2H), 8.01 (br s, 3H), 7.79 (d, 4H), 7.56 (m, 3H),

7.44 (m, 1H), 7.24 (m, 3H), 7.04 (br s, 1H), 6.92 (br s, 2H), 6.40 (m, 5H), 3.90 (br s, 4H, NCH_2CH_2N), 2.47 (s, 12H, CH_3), 1.94 (br s, 6H, CH_3). ^{13}C NMR ($CDCl_3$): δ 312.4 (Ru=C), 253.2 (Ru=C=C), 215.9 (NCN), 156.5, 152.4, 150.9, 146.7, 138.4, 137.7, 135.3, 135.0, 129.7, 129.3, 129.0, 128.8, 127.8, 124.2, 123.1, 122.6, 51.8 (NCH$_2$$CH_2$N), 21.2 ($CH_3$), 19.4 ($CH_3$).
Anal. Calcd. (%) for $C_{46}H_{46}N_4Cl_2Ru$ (826.88): C 66.82, H 5.61, N 6.78; found: C 65.84, H 6.11, N 6.66.

Allenylidene Schiff base complex 61 + two isomers 62 and 63
The thallium salt of the Schiff base **38** (0.109 g, 19.7 mmol) was added to the 3rd generation allenylidene complex **60** (0.136 g, 16.4 mmol). 10 mL of dry THF was added as a solvent and the resulting reaction mixture was stirred at room temperature for 2 h. The solvent was evaporated and toluene (5 mL) was added. The solution was filtered to remove TlCl. After almost full evaporation of the toluene, hexane (15 mL) was added while vigorously stirring. The precipitated red solid was filtered off, and washed with hexane (2 * 2 mL). ^{1}H and ^{13}C NMR analysis revealed the existence of three isomers in a ratio of 86%/13%/1% (20 °C reaction temperature). This ratio was found to be temperature dependent. More of the major isomer was formed with increasing temperature. Upon silica gel chromatography (Et_2O/hexane 3/7) the major isomer was isolated and characterized: Yield: 68%.
Major isomer: ^{1}H NMR ($CDCl_3$): δ 8.15 (d, 1H), 7.97 (s, 1H), 7.60 (s, 1H), 7.52 (m, 2H), 7.34 (s, 2H), 7.32 (s, 3H), 7.15-7.10 (m, 5H), 7.01 (s, 1H), 6.92-6.90 (m, 2H), 6.51 (s, 1H), 5.89 (br s, 1H), 4.23 (m, 2H, NCH_2CH$_2$N), 4.08 (m, 2H, NCH$_2$CH_2N), 2.58 (s, 3H, CH_3), 2.51 (s, 3H, CH_3), 2.32 (s, 3H, CH_3), 2.22 (s, 3H, CH_3), 2.14 (s, 3H, CH_3), 1.73 (s, 3H, CH_3), 1.56 (s, 3H, CH_3), 1.35 (s, 3H, CH_3). ^{13}C NMR ($CDCl_3$): δ 289.1 (Ru=C), 247.4 (Ru=C=C), 217.0 (NCN), 174.7 (C-O), 166.1 (C=N), 148.9, 144.6, 140.6, 139.6, 138.7, 138.4, 136.8, 136.6, 136.0, 134.5, 133.5, 132.3, 131.0, 129.4-127.5 (several peaks), 122.3, 118.0, 117.5, 97.5, 50.3 (NCH$_2$CH$_2$N), 49.8 (NCH$_2$$CH_2$N), 30.6, 21.6, 20.1, 18.9, 17.3, 16.9, 16.5, 13.1. Anal. Calcd. (%) for $C_{51}H_{48}N_4O_3ClBrRu$ (981.4): C 62.42, H 4.93, N 5.71; found: C 61.88, H 5.26, N 5.51.
The formation of a second and third isomer was evidenced through NMR spectroscopy, although full characterization was inaccessible due to the complexity of the catalyst mixture:
2nd *isomer*: ^{1}H NMR ($CDCl_3$): δ 9.04 (d, 1H), 8.6 (s, 1H), several signals, 3.77 (m, 4H, NCH_2CH_2N), several signals. ^{13}C NMR ($CDCl_3$): δ 309.7 (Ru=C), 249.4 (Ru=C=C), 213.9 (NCN), 175.8 (C-O), 165.5 (C=N), + several signals.
3rd *isomer*: ^{13}C NMR ($CDCl_3$): δ 310.0 (Ru=C), 250.8 (Ru=C=C), 218.9 (NCN), 173.9 (C-O), 168.6 (C=N) + several signals.

Note:
CCDC-652147 contains the supplementary crystallographic data for complex **52**. These data can be obtained free of charge from The Cambridge Crystallographic

Data Centre via www.ccdc.cam.ac.uk/data_request/cif.

4.4.4 Catalytic reactions

ROMP of 2-norbornene (Table 4.2)
In a typical ROMP experiment, 0.004248 mmol of catalyst in 0.5 mL of CH_2Cl_2 was transferred into a 15 mL vessel followed by the addition of 1 g of 2-norbornene (2500 equiv) and 10 mL of toluene. The reaction was then kept stirring at 85 °C for 3 h. To stop the polymerization, a 2-ethylvinylether/BHT(2,6-di-*tert*-butyl-4-methylphenol) solution in $CHCl_3$ was added. The reaction mixture was then poured into 50 mL of MeOH to precipitate the polymer. The polymer was isolated upon filtration, and analysed gravimetrically, with ^{1}H NMR spectroscopy and GPC (gel permeation chromatography).

ROMP of COD (Figures 4.12 and 4.15)
To a reaction vessel containing 0.0042 mmol of catalyst in 1 mL of toluene was added 0.52 mL of cyclooctadiene (1000 equiv). After an appropriate time span, a little amount was taken out of the reaction vial and analyzed by ^{1}H NMR spectroscopy.

ROMP of COD (Table 4.4)
Prior to the polymerization experiments, various COD/acid solutions were prepared in Schlenk tubes, which made it possible to add monomer and acid to the reaction vials in the mentioned ratios. Small oven-dried glass vials with a septum were charged with a stirrer bar and the appropriate amounts of catalyst taken from a CH_2Cl_2 stock solution. The dichloromethane was subsequently evaporated, and the glass vials with solid catalyst were kept under an argon atmosphere. To start the ROMP test, 200 μL of toluene was added as a solvent. The appropriate amount of the COD/acid mixture was then transferred to the vial containing the catalyst via syringe under vigorous stirring at room temperature. After the reaction had finished, the viscous reaction mixture was dissolved in a $CDCl_3$ solution of 2,6-di-*tert*-butyl-4-methylphenol and ethylvinylether to quench the polymerization reaction. The solution was poured in MeOH to precipitate the polymer, which was filtered off and dried under vacuum. Average molecular weights were then determined using gel permeation chromatography (GPC) calibrated with polystyrene standards.

RCM of diethyl diallylmalonate (Figures 4.13 and 4.16)
An NMR tube was charged with catalyst in C_6D_6 (concentration = 7.08 mM), and 100 equiv of diethyl diallylmalonate. The NMR tube was capped and heated to 40 °C. The reaction was then monitored via ^{1}H NMR spectroscopy by integration of the ^{1}H signals of the allylic protons of the ring closed product (2.25 ppm) and of the substrate (2.64 ppm).

Chapter 5

New NHC Ligands in Grubbs Catalysts

Ever since the discovery that well-defined ruthenium alkylidene complexes were able to catalyze olefin metathesis reactions, much effort has been devoted to the fine tuning of the Grubbs systems. The catalytic activity of these complexes varies widely depending on the ligands coordinated to the metal center. In this section, we describe *N*,*N*'-dialkyl, *N*-alkyl-*N*'-(2,4,6-trimethylphenyl), and *N*-alkyl-*N*'-(2,6-diisopropylphenyl) heterocyclic carbenes as modified NHC ligands. The introduction of aliphatic amino side groups into the NHC framework alters the metathesis activity of the corresponding Grubbs complexes through both electronic and steric effects.

5.1 Introduction

In spite of their booming success, variation of NHC ligands remained rather unexplored for Grubbs type catalysts, while it is obvious that this could have a significant influence on both catalytic activity and selectivity.[332] Up till today, symmetrical saturated NHC ligands seem to be limited to aromatic *N*-substituents (e.g. mesityl[67] and 2,6-diisopropylphenyl[291]). Also all NHC-Ru complexes previously developed in the Verpoort research group, incorporate classic, commercially available NHC ligands such as 1,3-dimesityl-4,5-dihydroimidazol-2-ylidene (H_2IMes) or 1,3,4-triphenyl-4,5-dihydro-1H-1,2,4-triazol-5-ylidene.[6,364–366,368,370,381,416–418].

Aiming at a further improvement of the application profile of Grubbs 2nd generation catalysts, we decided to pursue the coordination of dihydro NHC ligands bearing aliphatic amino groups with different steric bulk. A previous attempt towards the coordination of an aliphatic NHC ligand by Mol et al. was how-

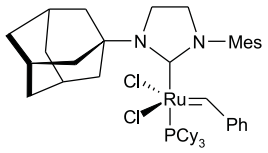

Figure 5.1: Complex **74**.

ever not promising. Synthesis of 1,3-di(1-adamantyl)-4,5-dihydroimidazolinium chloride [H_2IAd(H)][Cl] and the unsymmetrical 1-(1-adamantyl)-3-mesityl-4,5-dihydroimidazolinium chloride [H_2IAdMes(H)][Cl] was described.[292] Noteworthy is that only H_2IAdMes reacted in a favourable manner to give its 2nd generation analogue **74** (Figure 5.1). Failure of the reaction with H_2IAd was assigned to the bulkiness of the adamantyl moiety which couldn't take place directly overhead the benzylidene unit. The X-ray structure of **74** showed that the only isomer formed had the mesityl group above the benzylidene moiety. Surprisingly, complex **74** displayed only negligible metathesis activity, which was ascribed to steric blocking.

We were hoping that a reduced bulkiness of the *N*-substituents would allow easier NHC coordination and have a positive effect on the metathesis activity of the resulting catalysts. Higher electron density at the carbenic center of saturated NHCs compared to their unsaturated analogues[150,171,327], in combination with even further enhancement of this electron donation caused by alkyl *N*-substituents[419], would allow an increase in catalyst activity. However, this constitutes a subject of discussion since Nolan et al. reported unexpected weaker Pd-C(NHC) bonds for electron-donating alkyl-substituted NHCs.[420] Even more noteworthy was their study of the CO stretching frequencies in $Ni(CO)_3$(NHC) complexes.[134] Alkyl substituted NHCs were found to be only marginally more electron donating than aryl substituted ones. Furthermore, saturated NHCs turned out slightly less electron donating than their unsaturated counterparts, which is not in line with the common assumption that metal complexes bearing a saturated NHC perform better in catalytic reactions because of a higher electron donation. This demonstrates that considering only ligand basicity would be an oversimplification of the metal-NHC bonding properties.[206]

5.2 Results and Discussion

5.2.1 *N*,*N*'-dialkyl heterocyclic carbenes

The synthesized NHC precursors include 1,3-diisopinocampheyl-4,5-dihydroimidazolinium chloride **75a**, 1,3-di-*tert*-butyl-4,5-dihydroimidazolinium chloride **75b**, 1,3-dicyclohexyl-4,5-dihydroimidazolinium chloride **75c**, 1,3-di-*n*-octyl-4,5-dihydroimidazolinium chloride **75d**, and the pinane based imidazolinium chloride **75e** (Figure 5.2). Ligands **75a** and **75e** could induce some enantioselectivity,

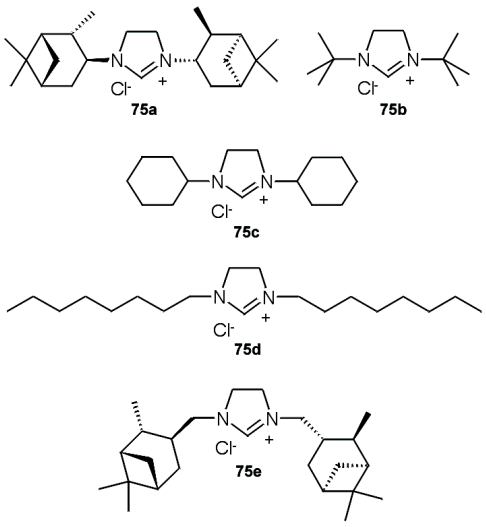

Figure 5.2: *N,N'*-dialkyl heterocyclic carbene precursors **75a-e**.

which might be driven to a higher extent by modification of the pinane derived moiety.[130] As a base to deprotonate the imidazolium chloride, we used potassium bis(trimethylsilyl)amide (KHMDS). This base liberates the free carbene at room temperature and its steric bulk is high enough to prevent fast reaction with Grubbs' catalyst **1**, thereby allowing for a *one-pot* procedure.

Reaction of one equiv of **75a** with one equiv of base and **1** in dry toluene did not allow substitution of the phosphine, even when the reaction mixture was heated or stirred for several hours. An excess of NHC ligand (1.5 equiv) led to the observation of a new benzylidene α-proton at δ=20.61 ppm with a conversion of approximately 25 %. ^{31}P NMR showed a new signal at δ 20.14 as well as a signal of free PCy_3 (Figure 5.3). This was assigned to NHC coordination. However, the downfield shift of the benzylidene signal surprised us since generally for Grubbs 2nd generation complexes this peak is situated more upfield. The addition of more than a 2-fold excess of ligand allowed full conversion but at this point difficulties to remove the ligand excess and free phosphine arose. Efforts to isolate pure compound by precipitation remained unsuccessful due to high solubility in all common organic solvents. The complex decomposed upon chromatography on silica gel.

Several attempts to exchange one phosphine with H_2I*t*Bu **75b**, applying an excess of ligand as well as prolonged reaction times, failed. Hahn et al. recently reported the synthesis of a H_2I*t*Bu substituted rhodium(I) complex, which showed low stability in solution. This was rationalized by the steric demand of the *N-tert*-butyl substituents, resulting in a weak bond between the metal and the carbene

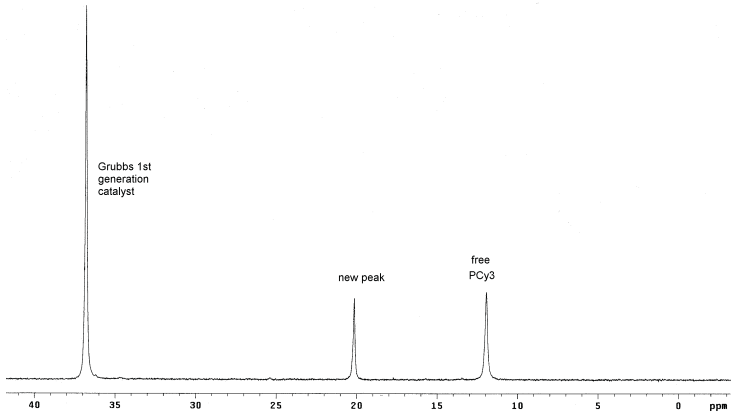

Figure 5.3: ^{31}P-spectrum showing partial reaction of **1** with ligand **75a**.

carbon atom.[421] Likewise, we assume to have encountered steric obstruction, and we decided to synthesize **75c**-**75e**, hoping that their different geometry allows coordination. Our endeavor involving ligand precursor **75c** led to the observation of a new ^{1}H benzylidene resonance at δ=20.28 ppm, and a new ^{31}P signal at δ=27.49 ppm. ^{13}C NMR of the crude mixture showed a small doublet at δ=210.2 ppm, which corresponds to the NHC-carbene carbon coordinated to ruthenium. Various attempts were undertaken to achieve isolation in order to get full characterization, but the new complex was found to be too unstable. Reaction involving **75e** gave rise to a new small ^{1}H peak at δ=20.08 ppm; this is a little downfield to the original benzylidene signal. Efforts to obtain full conversion of **1** by applying longer reaction times, led to decomposition of most of the catalytic species, which made it impossible to obtain pure product. Also ligand **75d** derived from a primary amine, did not allow the isolation of a NHC-substituted complex and induced decomposition of the catalytic system.

5.2.2 *N*-alkyl-*N*'-mesityl heterocyclic carbenes

Given the instability of Grubbs complexes coordinated with symmetrical aliphatic NHCs, we decided to synthesize the unsymmetrical analogues of our NHC salts, that is, 1-mesityl-3-isopinocampheyl-4,5-dihydroimidazolium chloride **76a**, 1-mesityl-3-*tert*-butyl-4,5-dihydroimidazolium chloride **76b**, 1-mesityl-3-cyclohexyl-4,5-dihydroimidazolium chloride **76c**, 1-mesityl-3-*n*-octyl-4,5-dihydroimidazolium chloride **76d**, and 1-mesityl-3-methyl-4,5-dihydroimidazolium chloride **76e**, and to react them with **1**. Preparation of these NHCs was straightforward following a synthetic pathway similar to the one described for the bidentate NHC ligand **51**.[410,422] Condensation of ethyl chlorooxoacetate and 2,4,6-trimethylaniline affords the desired oxanilic ethylester, which is then treated with the aliphatic amine

to provide the corresponding oxalamide. Reduction and subsequent addition of HCl results in the dihydrochloride salt, which cyclizes to the desired 4,5-dihydroimidazolium chloride in reaction with triethyl orthoformate. Exposure of the catalyst **1** to these asymmetrically substituted NHC precursors and KHMDS as a base afforded the complexes **77a-77e** under mild reaction conditions (Figure 5.4). Compared to the unsymmetrical ligands bearing one mesityl moiety, the symmetrical ligands **75a-75e** were significantly more difficult to coordinate to the Grubbs parent complex **1**. We observed coordination of ligands **75a**, **75c** and **75e** but ligand excesses were required and the so formed complexes showed limited stability which prevented their isolation. Therefore, we assume that π-interaction between the benzylidene and the amino side group might be of considerable importance. This is confirmed by the observation that the carbene derived from **76c** coordinates in such a way that the mesityl group is oriented towards the benzylidene moiety. (Single-crystal X-ray analysis of complex **77c**: Figure 5.5, Table 5.1) Both aromatic rings are nearly co-planar, allowing π-π interaction. The observation that intramolecular π-π stacking between the benzylidene carbene and the *N*-aryl substituents on the NHC residu might constitute a strong structural element

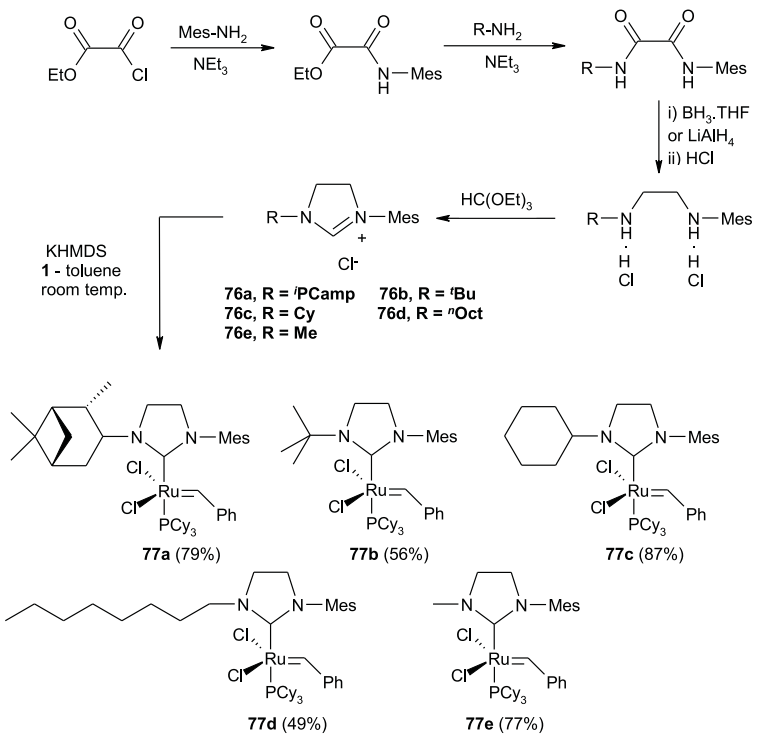

Figure 5.4: Synthesis of complexes **77a-77e**.

in 2nd generation metathesis catalysts was previously reported by Fürstner et al. for unsaturated NHC entities.[332,334]

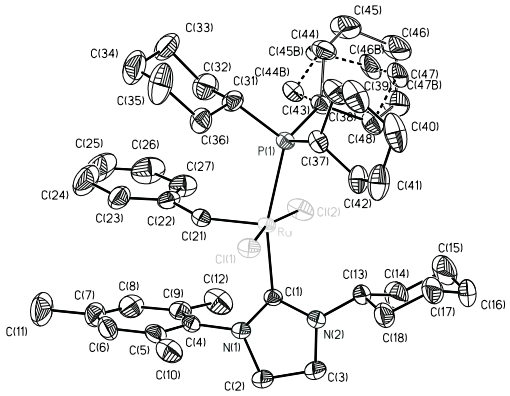

Figure 5.5: ORTEP diagram of **77c**. For clarity hydrogen atoms have been omitted.

	77c[a]	**2**[b]	**74**[c]
Ru=C	1.830(6)	1.835(2)	1.851(5)
Ru-CNN	2.060(5)	2.085(2)	2.083(5)
Ru-Cl(1)	2.419(3)	2.3988(5)	2.427(1)
Ru-Cl(2)	2.376(3)	2.3912(5)	2.398(1)
Ru-P	2.481(3)	2.4245(5)	2.521(1)
Cl-Ru-Cl	167.73(6)	167.71(2)	167.98(5)
N_2C-Ru-P	162.42(14)	163.73(6)	171.1(1)
N_2C-Ru=C	98.9(2)	100.24(8)	96.9(2)
P-Ru=C	98.63(18)	95.98(6)	91.5(2)
N_2C-Ru-Cl(1)	85.58(15)	83.26(5)	84.7(1)
N_2C-Ru-Cl(2)	89.18(16)	94.55(5)	88.1(1)
Ru=C-Ph	137.2(4)	136.98(16)	137.0(4)

Table 5.1: Selected Bond Lengths [Å] and Angles [°] - Structural comparison of **77c**, **2** and **74**. [a] This work [b][230,423] [c][292].

In contrast to Mol's complex **74**, most of our complexes showed nice olefin metathesis activities. Their catalytic performance in the ring-opening metathesis polymerization (ROMP) of cycloocta-1,5-diene (COD) was compared with the reactivity of Grubbs catalysts **1** and **2**, using different solvents and monomer/catalyst

ratios (Figures 5.6 and 5.7). Coordination of the NHC ligand led to a positive effect on the ROMP actvity for complexes **2**, **77a**, **77c**, **77d** and **77e**. In contrast, for complexes **74** and **77b**, NHC coordination induced activity loss. These last two complexes required heating and a low COD/cat. ratio in order to obtain high conversion (Figure 5.6, Table 2).
It is worth noting that the catalytic activity of complex **2** strongly depends on the solvent used, while a solvent effect is less significant for complexes **77a**-**77e**. The catalysts **77a**, **77c**, **77d** and **77e** show a slightly higher ROMP activity in $CDCl_3$ than in C_6D_6 when a monomer/catalyst ratio of 300 is used. Their activity is somewhat higher in C_6D_6 when the monomer/catalyst ratio equals 3000, which is due to an induction period and loss of activity in the $CDCl_3$ polymerization. **2** is unambiguously more active in C_6D_6. Such an increased reactivity in aromatic solvents was also observed by Fürstner et al. for $[Cl_2Ru(=CHPh)(IMes)(PCy_3)]$. This was assigned to competing interactions of the *N*-mesityl group with the solvent molecules, which reduce the intramolecular π-π interactions with the benzylidene moiety.[332] Like mentioned earlier, we expect **77a**, **77c**, **77d** and **77e** to have similar π-π interactions, but when lower COD/cat. ratios were applied, we did not observe such a *competition* effect. The increased activity of **2** in aromatic solvents might be assigned to a π-π interaction between the mesityl group that is not coplanar with the benzylidene moiety and the aromatic solvent (Figure 5.8). An alternative explanation for the different response of complex **2** on the solvent change might be that a rotation of the NHC ligand allows two populations stabilized by π-π interactions, compared to only one for catalysts **77a**-**77e**. This would also explain its longer induction period and high reactivity after the retarding π-π stacking effect is lost. It is, however, taken for granted that for **77a**-**77e**, rotation of the NHC ligand is disfavored due to the higher steric demand of the *N*-alkyl substituents.[1]
Furthermore, it is obvious that when high substrate/catalyst ratios are used, decomposition of the catalyst system is not negligible, leading to incomplete conversion as observed for catalyst **77a**.

^{13}C NMR spectroscopy allowed the determination of the *cis* fraction of the newly formed double bonds in the polymer chains (Table 5.2).[2] The *cis*/*trans* ratio can be seen as the primary microstructural characteristic, having a well established relationship with the solid state and solution properies of the ROMP polymer.[37] Grubbs 2nd generation catalyst **2** gave rise to ROMP polymer with a predominately *trans*-olefin content, while other catalyst systems generally led to a higher *cis* value. A high *trans* content for **2** was also observed by Grubbs et al. as it could be expected for an equilibrium-controlled polymerization in which secondary chain transfer occurs.[337] Entries 1-8 demonstrate that all NHC-bearing complexes

[1] Only one single isomer was formed.
[2] Differences in the NoE effect are minimal for similar carbon atoms. ^1H NMR showed different chemical shift values for the *cis* and *trans* olefinic protons but the distinct signals were not resolved enough to allow quantitative determination of the *cis*/*trans* ratio.

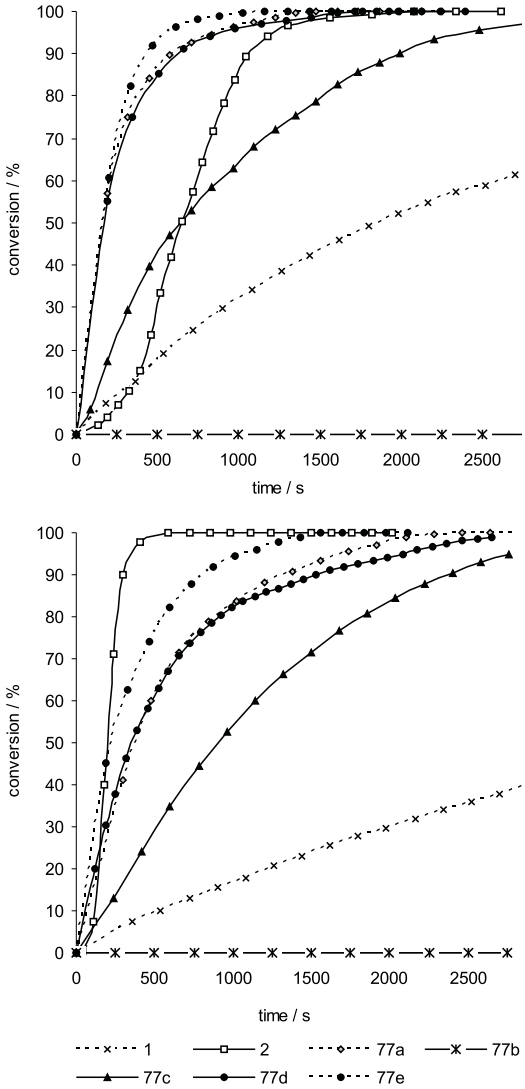

Figure 5.6: Monitoring ROMP of COD via ^{1}H NMR spectroscopy. COD/cat. = 300, cat. conc. = 4.52 mM, 20 °C, solvent = $CDCl_3$ (Top) C_6D_6 (Bottom).

show a significantly higher *trans* content than the 1st generation Grubbs complex **1**. For a higher COD/catalyst ratio (Entry 9-13) all catalysts but **2** show a predominately *cis*-olefin content, which indicates that for the former considerably less chain transfer occurred, probably caused by a quicker decomposition of the

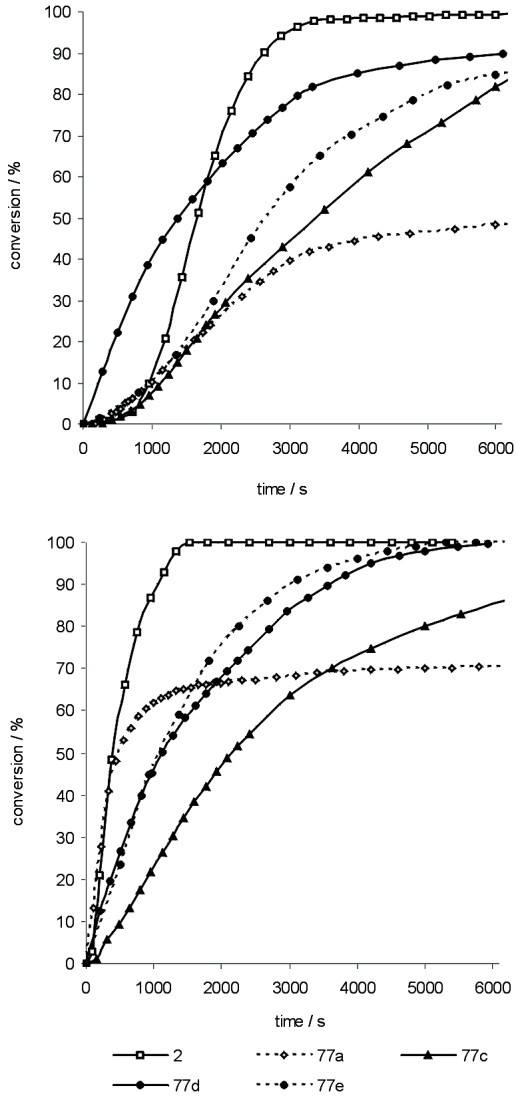

Figure 5.7: Monitoring ROMP of COD via ^{1}H NMR spectroscopy. COD/cat. = 3000, cat. conc. = 0.452 mM, 20 °C, solvent = $CDCl_3$ (Top) C_6D_6 (Bottom).

catalyst systems.

The RCM activity of the new complexes was tested on the standard RCM substrate diethyl diallylmalonate (Figure 5.9). A significant dependence of the

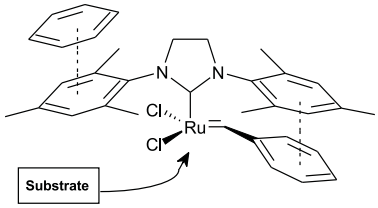

Figure 5.8: Increased activity of **2** in aromatic solvents.

Entry	Cat.	T [°C]	COD/cat.	t [min.]	Conversion [%]	*cis* [%][a]
1	**1**	RT	3 000	30	23	75
				60	55	71
2	**2**	RT	3 000	30	100	9
3	**74**	RT	3 000	30	0	-
4	**77a**	RT	3 000	30	100	17
5	**77b**	RT	3 000	30	0	-
6	**77c**	RT	3 000	30	100	37
7	**77d**	RT	3 000	30	100	51
8	**77e**	RT	3 000	30	100	46
9	**2**	RT	30 000	30	86	12
				[b]	100	13
10	**77a**	RT	30 000	30	7	-
				[b]	30	80
11	**77c**	RT	30 000	30	48	78
				[b]	71	76
12	**77d**	RT	30 000	30	74	82
				[b]	94	83
13	**77e**	RT	30 000	60	10	-
				120	26	80
				[b]	34	80
14	**74**	70	300	120	69	75
15	**77b**	70	300	120	72	77

Table 5.2: ROMP of COD.
[a] Percent olefin with *cis*-configuration in the polymer backbone; ratio based on ^{13}C NMR: allylic carbon $\delta = 32.9$ ppm *trans*; $\delta = 27.6$ ppm *cis*.
[b] Overnight.

reactivity on the bulkiness of the NHC entities was observed. The most crowded NHCs correspond to the lowest RCM activity, while activity increases considerably for complexes bearing less bulky NHCs. The most active catalyst system was found to be complex **77e**, bearing an NHC ligand with a small methyl amino moiety. This complex was substantially more active than the Grubbs complex

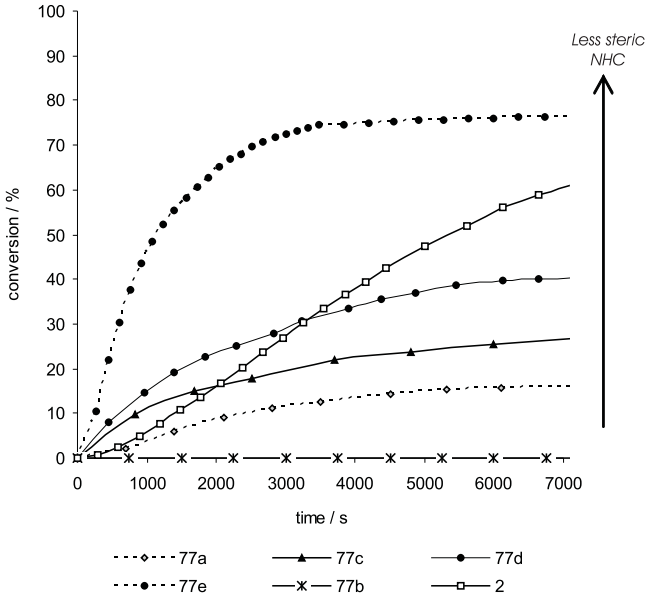

Figure 5.9: Monitoring RCM of diethyl diallylmalonate via ^{1}H NMR spectroscopy. 20 °C, substrate/catalyst = 200, cat. conc. = 4.52 mM, solvent = CD_2Cl_2.

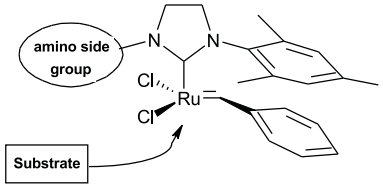

Figure 5.10: Importance of the steric bulk of the amino side groups.

2. It is therefore undeniable that the steric bulk of the amino sidegroup is of great importance (Figure 5.10). During the course of our investigation, Blechert et al. preceded us with a report on the synthesis of complex **77e**. **77e** was found to give a better diastereoselective RCM and significantly different E/Z ratios in cross metathesis.[290] This study constitutes more evidence of the interesting characteristics of these novel metathesis initiators.

It is worth pointing out that complexes **77b** and **74** are both bright green complexes, while the more active complexes **2**, **77a**, **77c**, **77d** and **77e** are all pinkish. We assume this is the result of higher steric requirements of the *tert*-

butyl and adamantyl groups. These NHCs are the only ones in the series where the first carbon atom adjacent to the amino group is bonded to three other carbons. Whereas the other NHC entities can orient their side groups perpendicularly to the imidazoline plane in order to minimize steric interactions, such an orientation cannot be obtained for the adamantyl and *tert*-butyl bearing ligands.[134] Mol et al. reported the possibility of an interaction of a β-carbon atom of the adamantyl group with the metal center.[292] Analogously **77b** might show a similar interaction resulting in the green color and reduced activity of the catalyst.

To monitor their relative rates of decomposition, the complexes **77a-e**, **1** and **2** were heated at 80 °C in C_6D_6 (Figure 5.11). The decomposition reaction was followed using ^{31}P NMR spectroscopy. Complex **77b**, which exhibits low olefin metathesis activity, shows a high thermal stability. A half life of ≈7 hours was measured. In contrast, complex **77a** has a half life of only ≈10 min. A relatively

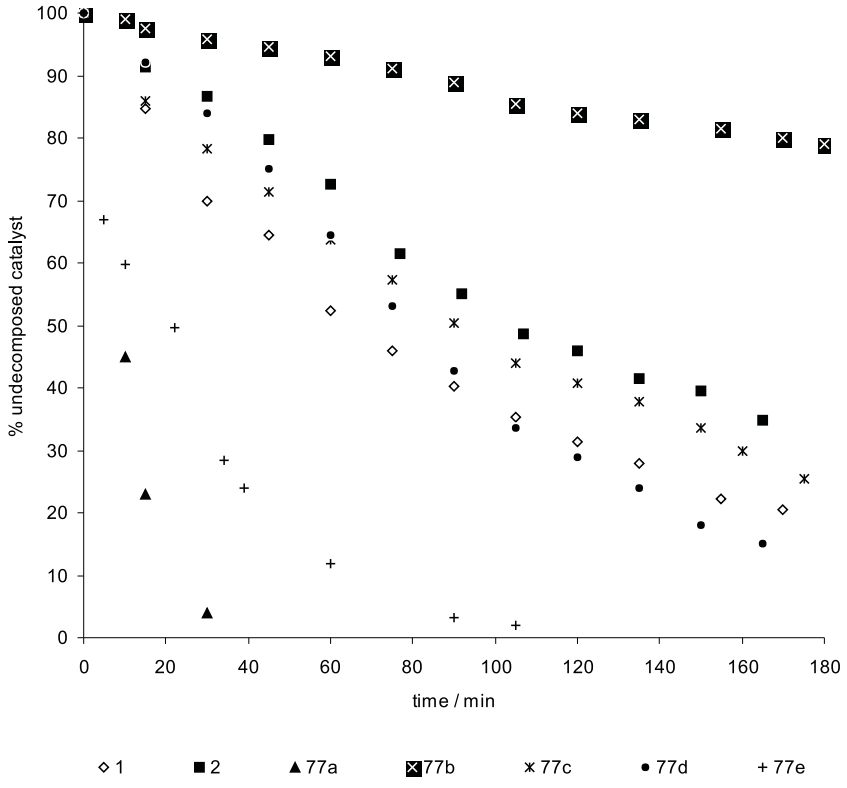

Figure 5.11: Decomposition at 80 °C.

low stability of **77a** is in line with the flattened reaction curve (incomplete polymerization) observed in the ROMP of COD when using a high monomer/catalyst ratio (Figure 5.7). This demonstrates that thermolytic decomposition limits the usefulness of the catalyst system in challenging reactions. While the rather poor thermal stability of **77e** can easily be justified by the presence of a small methyl group, which does not provide sufficient steric protection of the metal center, no suitable explanation was found for the behavior of **77a**. Complexes **77c** and **77d** display half lifes which are more in the range of the classic Grubbs complexes **1** and **2**, making them more utile in reactions at higher temperature and longer reaction times in comparison to **77a** and **77e**.

5.2.3 *N*-alkyl-*N*'-(2,6-diisopropylphenyl) heterocyclic carbenes

Complex **9**, described by Mol et al. in 2002, generally displays higher turnover numbers in comparison to complex **2**.[291] The reason for this enhanced activity is not entirely clear, but likely results from the increased steric bulk of the NHC ligand. We anticipated that replacing the NHC's mesityl group (**77a** and **77c**) with a 2,6-diisopropylphenyl group (**78a-b**) would analogously have a considerable effect on the catalytic behavior of the corresponding Grubbs complex. To our surprise, the *N*-alkyl-*N*'-(2,6-diisopropylphenyl) carbenes were found to display an exceptional tendency towards bis(NHC) coordination in their reaction with the Grubbs complex $[RuCl_2(=CHPh)(PCy_3)_2]$ **1**.[10]

Upon treatment of **1** with 1.2 equiv of 1-(2,6-diisopropylphenyl)-3-methyl-4,5-dihydroimidazolium chloride $[H_2IMePr][Cl]$ and 1.2 equiv of a base, the bis(NHC) complex **79a** was formed exclusively, while the expected mono(NHC) complex **78a** was observed only in small traces during the reaction course. In a similar attempt to synthesize the cyclohexyl bearing analogue **78b**, a mixture of three complexes

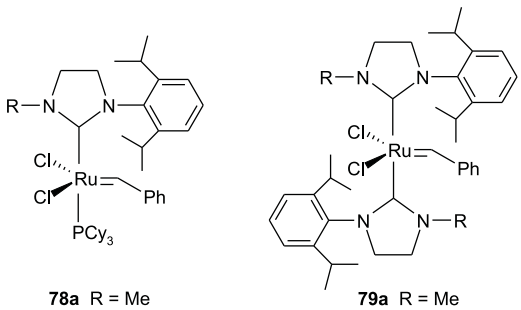

Figure 5.12: Mono(NHC) complexes **78a-b** and bis(NHC) complexes **79a - b**.

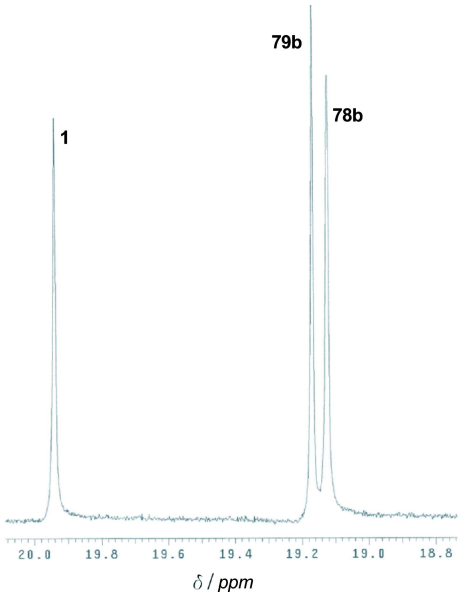

Figure 5.13: ^{1}H NMR spectrum after reaction at room temperature of **1** with 1.2 equiv of [H_2ICyPr][Cl] and 1.2 equiv of base. (Only part of the spectrum is shown.)

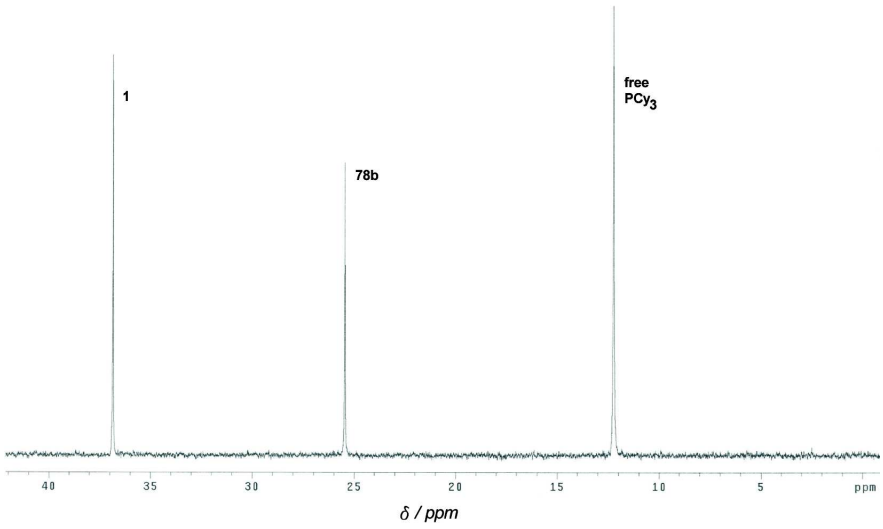

Figure 5.14: ^{31}P NMR spectrum after reaction at room temperature of **1** with 1.2 equiv of [H_2ICyPr][Cl] and 1.2 equiv of base. (Only part of the spectrum is shown.)

was obtained. After analysis of the ^{1}H and ^{31}P NMR spectra, they were identified as the starting complex **1**, mono(NHC) complex **78b** and bis(NHC) complex **79b** (Figures 5.13 and 5.14). Reaction of **1** with 2.2 equiv of the appropriate NHC ligand allowed full conversion into complexes **79a-b**.
The molecular structure of both bis(NHC) complexes was confirmed by single crystal X-ray analysis (Figures 5.15 and 5.16). In both complexes, the Ru atom has a distorted square pyramidal coordination with the Cl atoms trans to one another and the apical position occupied by the Ru=C bond (Table 5.3). To minimize steric congestion around the metal center, the NHC ligands are arranged in such a way that only one NHC has the diisopropylphenyl group orientated toward the benzylidene side of the ruthenium center. Dihedral angles of 17.0(3) ° (complex **79a**) and 29.8(2) ° (complex **79b**) show that the two NHC rings are

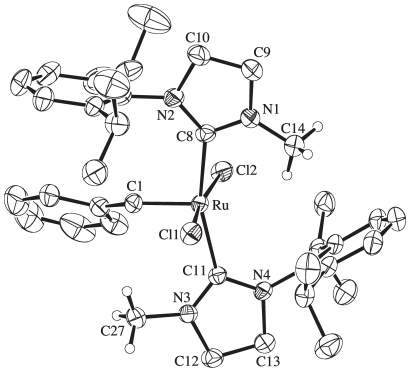

Figure 5.15: The molecular structure of **79a**. Most hydrogen atoms have been omitted for clarity. Crystals were grown from Et_2O.

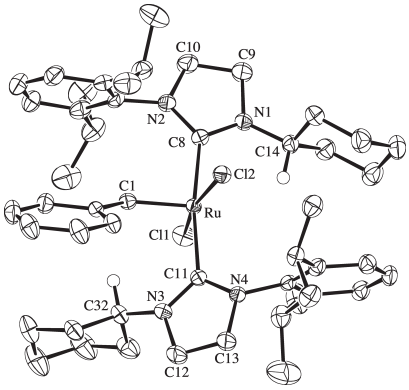

Figure 5.16: The molecular structure of **79b**. Most hydrogen atoms have been omitted for clarity. Crystals were grown from CH_2Cl_2 / THF.

	79a	**79b**	**2** [230,423]
Ru=C	1.818(4)	1.828(3)	1.835(2)
Ru-*C*NN Ru-C(8)	2.073(4)	2.086(3)	2.085(2)
Ru-*C*NN Ru-C(11)	2.121(4)	2.122(3)	-
Ru-P	-	-	2.4245(5)
Cl-Ru-Cl	170.66(4)	167.08(3)	167.71(2)
Ru=C-Ph	134.4(3)	133.7(3)	136.98(16)
N_2C-Ru-CN_2	162.0(2)	171.2(1)	-
N_2C-Ru-P	-	-	163.73(6)
N_2C-Ru=C C(8)-Ru=C(1)	95.9(2)	94.6(1)	100.24(8)
N_2C-Ru=C C(11)-Ru=C(1)	102.0(2)	94.2(1)	-
P-Ru=C	-	-	95.98(6)

Table 5.3: Selected Bond Lengths [Å] and Angles [°] - Structural comparison of **79a**, **79b** and **2**.

somewhat staggered as a result of their high steric demand. The benzylidene and diisopropylphenyl aromatic rings are not coplanar. This contrasts with our expectation of a π-π interaction between the two aromatic units as observed in section 4.2.2. The short distances between the metal center and a H atom at C(14) (H(14)-Ru: 2.53 Å) for complex **79a** and between the metal atom and the H atom at C(14) (H(14)-Ru: 2.64 Å) for complex **79b**, suggest the existence of agostic interactions. These agostic interactions were also reflected in the ^{1}H spectra of **79a** (δ = 0.07 ppm) and **79b** (δ = -0.43 ppm). Interestingly, the Ru-CNN bond length for the ligand potentially involved in the agostic interaction is slightly shorter than the other Ru-CNN bond.

To gain some insight into their catalytic performance, complexes **79a** and **79b** were tested in the ROMP of *cis*,*cis*-cycloocta-1,5-diene (COD) (Table 5.4). Both complexes display poor activity at room temperature (entry 1 and 6), while the use of an elevated temperature (80 °C) substantially improves conversions (entry 2-5 and 7-10). The NHC decoordination, which is expected to induce catalyst initiation[64,230], thus proceeds more smoothly when temperature is raised. A dissociative mechanistic model is generally accepted for Grubbs catalysts **1**-**2** and finds strong support by computational[294,295,298,300,301,424] and experimental[293,303–305] studies. However, since the lability of NHC ligands in organometallic complexes is typically quite low[119,132], particularly in comparison to phosphine ligands, further investigation was needed to obtain more support for the hypothesized NHC dissociation pathway. This was achieved through NMR monitoring of the reaction between complex **79a** or **79b** and a 10-fold excess of PCy_3 at 80 °C. For **79a**, the formation of the mono(NHC) analogue **78a** and the bis(phosphine) complex **1** was observed after 30 min (Figure 5.17). A time span of 6 hours allowed

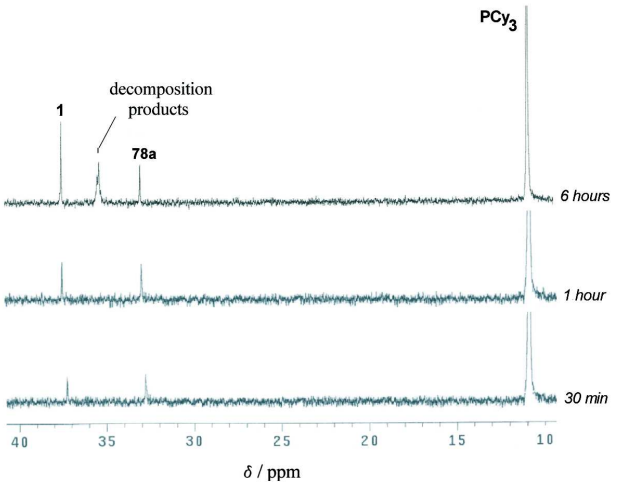

Figure 5.17: ^{31}P NMR spectra showing the reaction of **79a** with 10 equiv of PCy_3, C_6D_6, 80 °C.

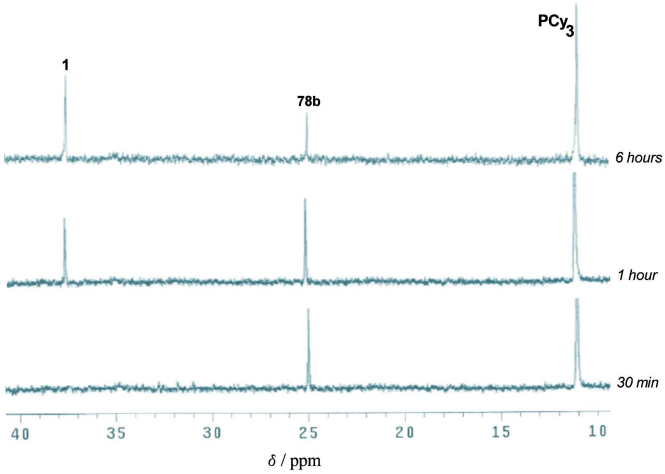

Figure 5.18: ^{31}P NMR spectra showing the reaction of **79b** with 10 equiv of PCy_3, C_6D_6, 80 °C.

full reaction of the starting complex, but at this point decomposition products were also observed. Likewise, the reaction of complex **79b** with an excess of PCy_3 resulted in NHC decoordination (Figure 5.18). A precise selection of the reaction conditions even allowed us to trap and isolate the mono(NHC) complex **78b** (see experimental section). The here observed NHC lability strengthens the

Entry	Cat.	Temp. (°C)	COD/cat.	Time (h.)	Conv. (%)[a]	cis-(%)[b]	M_n[c]	PDI[c]
1	**79a**	20	100	20	2	-	-	-
2	**79a**	80	100	1	100	43	31200	1.4
3	**79a**	80	300	1	96	73	33200	1.6
4	**79a**	80	3000	20	100	60	42800	1.7
5	**79a**	80	30 000	20	4	-	-	-
6	**79a**	20	100	20	24	91		
				40	63	80	48100	1.5
7	**79b**	80	100	0.5	100	21	33500	1.3
8	**79b**	80	300	0.5	100	31	39000	1.6
9	**79b**	80	3 000	1	98	46	44300	1.8
10	**79b**	80	30 000	20	60	81	80000	2.5
11	**78b**	20	300	1	94	76		
				1.5	100	74	49000	1.6
12	**78b**	20	3 000	1	79	76		
				1.5	85	72		
				20	100	64	69000	1.8
13	**78b**	20	30 000	20	13	85	77000	2.0

Table 5.4: ROMP of COD.
[a] Conversion, determined by ^{1}H NMR spectroscopy.
[b] Percent olefin with *cis*-configuration in the polymer backbone - ratio based on ^{13}C NMR spectra (δ = 32.9 ppm: allylic carbon *trans*; δ = 27.6 ppm: allylic carbon *cis*).
[c] Determined by GPC ($CHCl_3$) analysis. Results are relative to polystyrene standards.

idea that complexes **79a** and **79b** are metathesis active because NHC dissociation at elevated temperature provides the necessary initiation step.

In contrast to the bis(NHC) complexes **79a-b**, complex **78b** displays substantial ROMP activity at room temperature (Table 5.4: entries 11-13). Figure 5.19 illustrates a somewhat higher initiation rate for **78b** than for **77c** and **2**; however propagation appears to be slower. Also in the RCM of diethyl diallylmalonate, complex **78b** displays faster initial reaction than complexes **77c** and **2** (Figure 5.20). Even though we are not able to provide full evidence, one could presume that the higher initiation rate of **78b** goes together with a higher lability of its phosphine ligand. A dissociative mechanism in which catalyst initiation depends upon phosphine dissociation is then taken for granted. As mentioned above, such a dissociative model has emerged as the most reliable mechanism for the olefin metathesis reaction catalyzed by Grubbs complexes **1** and **2**, and more than likely also holds for complexes with modified NHC ligands (**77c**, **78a-b**).

As phosphine dissociation promotes catalyst decomposition[297,303], it is then not surprising that complex **78b** was found to decompose faster than its mesityl

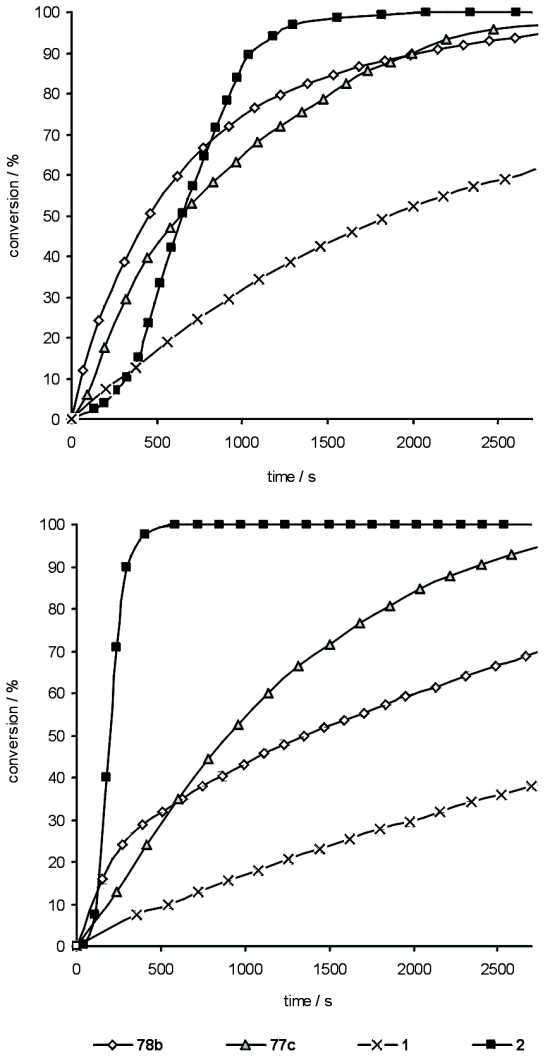

Figure 5.19: Monitoring ROMP of COD via ^{1}H NMR spectroscopy (20 °C) - Conditions: monomer/catalyst = 300, catalyst concentration = 4.52 mM, solvent = $CDCl_3$ (top), C_6D_6 (bottom).

analogue **77c**. It is plausible that an even higher initiation rate is responsible for the low stability of complex **78a**. The exclusive formation of bis(NHC) complex **79a** when an approximately equimolar quantity of H_2IMePr is reacted with **1**, suggests that the presumed intermediate **78a** is much more likely to react

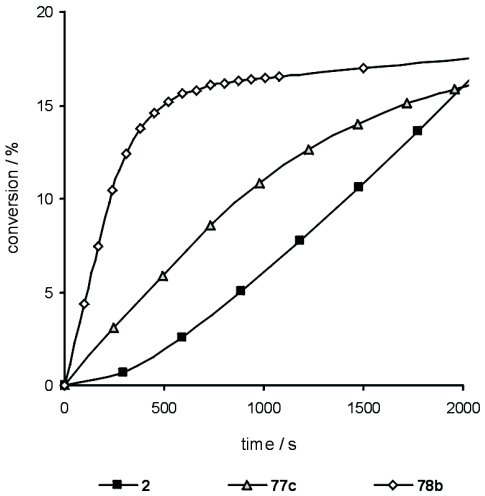

Figure 5.20: Monitoring RCM of diethyl diallylmalonate via ^{1}H NMR spectroscopy (20 °C) - Conditions: diethyl diallylmalonate/catalyst = 200, catalyst concentration = 4.52 mM, solvent = CD_2Cl_2.

with remaining NHC than its precursor **1**. We assign this to a high phosphine exchange rate, which accompanies fast NHC coordination in a dissociative ligand substitution pathway.

The heating of complexes **77c**, **77e**, or **2** in the presence of an excess of PCy_3 does not cause any NHC decoordination at all. On the other hand, the NHCs in complexes **78a-b** are capable of decoordination and therefore their NHC-metal bond is expected to be weaker. This demonstrates that the strength of the (NHC)-metal bond, which is believed to depend mainly[136], though not exclusively[206,208,209,211,215,217,219], on the σ-donating ability of the NHC, does not correlate directly with the dissociation rate of the phosphine ligand. Our observations confirm that other, more subtle effects than a *trans* effect determine the reactivity of Grubbs type complexes.[318,323,325,425] The *trans* effect which explains the dissociation energies of non steric ligands in Grubbs complexes[294,298], should be compensated by additional effects when sterically demanding ligands are used[300,315].

5.3 Conclusion

A series of NHC ligands bearing aliphatic amino sidegroups were synthesized and reacted with the Grubbs 1st generation catalyst. Reactions involving symmetrical NHCs did not allow the isolation of any pure NHC substituted complexes due to

their instability. Unsymmetrical NHCs having a planar mesityl group on one amino side reacted in a favourable manner, and the resulting complexes were stable enough to be isolated. X-ray crystallographic analysis demonstrated that the mesityl group is co-planar with the phenyl ring of the benzylidene, which indicates that a π-π interaction between the mesityl arm and the benzylidene moiety might constitute an important structural element and that this needs to be considered in future catalyst design of Grubbs 2nd generation analogues. Catalysts **77a**, **77c**, **77d** and **77e** were found to surpass the parent-complex **1** for the ROMP of cycloocta-1,5-diene. Catalyst **77b**, substituted with an NHC derived from *t*Bu-NH_2 was considerably less metathesis active than the catalysts derived from amines with primary or secondary groups on the nitrogen atom. Furthermore the observation that the least steric complex **77e** is the most active for RCM, clearly demonstrates that modification of the NHC ligand can induce substantial changes in the reactivity pattern of the corresponding catalysts. Not only catalytic activity is highly influenced by the systematic variation of the NHC *N*-substituents, also the complex stability was found to be altered considerably. The half life of the complexes ranges between ≈10 min (**77a**) and 7 hours (**77b**) at 80 °C. Depending on the substrate and the reaction conditions applied, an appropriate choice of the NHC amino groups may thus eventually allow catalyst fine tuning.

Also two new *N*-alkyl-*N*'-(2,6-diisopropylphenyl) heterocyclic carbenes were synthesized. These NHC ligands revealed a different reactivity towards Grubbs complexes than the hitherto reported imidazolinylidenes: i) facile bis(NHC) coordination was found; ii) both NHCs on the bis(NHC) complexes can be exchanged with a phosphine, thereupon regenerating the Grubbs 1st generation complex. The exchange of one NHC in **79b** for PCy_3 allowed the isolation of a new mono(NHC) complex **78b**, which displays fair olefin metathesis activity with a higher initiation rate than the benchmark catalyst **2**. On the other hand, the rather low stability of mono(NHC) complex **78a**, together with the low ratio present in the reaction mixture, prevented its isolation. These observations confirm that small changes in the *N*,*N*'-substitution pattern of NHC ligands significantly alter the catalytic activity of the corresponding metathesis catalysts.

5.4 Experimental Section

5.4.1 General remarks

All reactions and manipulations involving organometallic compounds were conducted in oven-dried glassware under argon atmosphere using standard Schlenk techniques and dried, distilled and degassed solvents. ^{1}H, ^{13}C and ^{31}P NMR measurements were performed with a Varian Unity-300 spectrometer. The crystallographic data set was collected by Jacques P*é*caut of DRFMC (D*é*partement

de Recherche Fondamentale sur la Matière Condense - Laboratoire du CEA, Grenoble). Elemental analyses (ASTM-method D5291: Standard test methods for the instrumental determination of C, H and N) were carried out at Chevron Technology, Ghent.

5.4.2 *N,N'*-dialkyl imidazolinium salts

Synthesis of [$H_2I^iPCamp(H)$][Cl] 75a

Procedure 1[390]

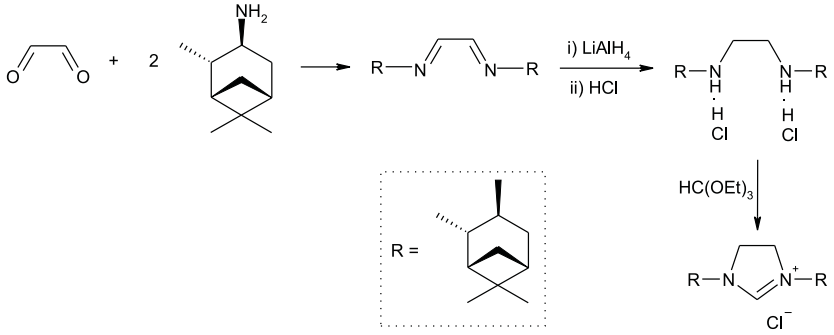

Figure 5.21: Synthesis of **75a**; procedure 1.

***N,N'*-diisopinocampheylethylenediimine [CH(=N^{i}PCamp)]$_2$**
To a flask charged with (1R,2R,3R,5S)-(-)-isopinocampheylamine (4.82 g, 95%, 29.9 mmol) in 40 mL ethanol was added 1.7 mL of aqueous glyoxal (40% wt. solution in H_2O, 14.9 mmol). The resulting reaction mixture was stirred overnight at room temperature. The next day, a white precipitate had formed and after addition of 10 mL of water more of this white compound precipitated. The product was filtered off, washed with 20 mL of pentane and dried *in vacuo*. Yield: 91%.
^{1}H NMR ($CDCl_3$): δ 7.86 (s, 2H, C*H*=N), 3.46 (m, 2H, C*H*-N), 2.41 (m, 2H), 2.28 (2H), 2.09 (2H), 1.99 (2H), 1.88 (4H), 1.25 (s, 6H, H_h), 1.18 (d, 2H), 1.05 (s, 6H, H_g), 1.02 (d, 6H, H_i). ^{13}C NMR ($CDCl_3$): δ 159.7 (*C*=N), 70.2 (C_a-N), 47.7 (C_c), 43.5 and 41.8 (C_b and C_d), 39.1(C_j), 35.9 (C_e), 34.1 (C_f), 28.2 (C_h), 23.8 (C_g), 20.0 (C_i).

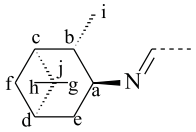

Diamine dichloride salt $[CH_2(NH^iPCamp)]_2[Cl]_2$
The diimine (2.8 g, 8.5 mmol) was dissolved in dry Et_2O (50 mL) and cooled to 0 °C. $LiAlH_4$ (0.65 g) was added in small portions. The resulting mixture was allowed to warm to room temperature and stirred overnight. Water was then slowly dropped until all bubbling ceased. The so formed solid was filtered off and washed with Et_2O. The organic filtrate was extracted with 100 mL of water; the resulting aqueous layer extracted two times more with CH_2Cl_2. All organic phases were combined and concentrated to ≈50 mL under reduced pressure. Concentrated HCl (12 M) was added to precipitate the desired white coloured dichloride salt, which was obtained in a pure form by filtration and washing with hexane. Yield: 85%.
Part of the organic phase was fully evaporated for NMR characterization of the diamine $[CH_2(NH^iPCamp)]_2$ *(yellowish oil)*: ^{1}H NMR ($CDCl_3$): δ 2.85 (m, 4H, NCH_2CH_2N), 2.85, 2.71, 2.33, 1.94, 1.78, 1.62, 1.21 (s, 6H, H_h), 1.11 (d, 6H, H_g), 0.97 (s, 6H, H_i). ^{13}C NMR ($CDCl_3$): δ 57.1 (C_a-N), 48.2 (NCH_2CH_2N), 48.0 (C_c), 45.4 and 42.0 (C_b and C_d), 38.7 (C_j), 37.2 (C_e), 34.1 (C_f), 28.1 (C_h), 23.6 (C_g), 21.9 (C_i).

***N*,*N*'- Diisopinocampheylimidazolinium chloride $[H_2I^iPCamp(H)][Cl]$**
A suspension of the dichloride salt (2.1 g) in $HC(OEt)_3$ (25 mL) was heated overnight at 120 °C. The reaction mixture was cooled to room temperature. After the formed EtOH was removed by evaporation, the imidazolinium salt precipitated as a white solid which was filtered off and washed with hexane. Yield: 74%.
^{1}H NMR ($CDCl_3$): δ 10.42 (s, 1H, NCHN), 4.68 (m, 2H, N-C_aH), 4.01 (m, 4H, NCH_2CH_2N), 2.55 (m, 2H), 2.45 (m, 2H), 2.11 (m, 2H), 2.03 (m, 2H), 1.89 (m, 2H), 1.82 (m, 2H), 1.23 (s, 6H, H_h), 1.21 (d, 6H, H_i), 1.07 (s, 6H, H_g), 0.86 (d, 2H). ^{13}C NMR ($CDCl_3$): δ 159.3 (NCN), 57.5 (C_a-N), 47.3 (NCH_2CH_2N), 43.6 and 41.4 and 40.5 (C_c, C_b and C_d), 38.7 (C_j), 35.0 (C_e), 32.4 (C_f), 28.1 (C_h), 23.8 (C_g), 20.5 (C_i).

Procedure 2
An alternative procedure was carried out by reacting oxalyl chloride with 2 equiv of (1R,2R,3R,5S)-(-)-isopinocampheylamine to form a bisamide.

***N*,*N*'-Di((-)-isopinocampheyl)oxamide**
Oxalyl chloride (0.6 mL, 6.9 mmol) was slowly dropped into a cold (0 °C) solution of (-)-isopinocampheylamine (2.5 mL, 14.2 mmol) and Et_3N (2 mL) in dry CH_2Cl_2 (15 mL). The resulting mixture was stirred for 2 h while warming to room temperature. The solution was then diluted with water (20 mL) and extracted twice with CH_2Cl_2 (2 * 20 mL). The combined organic layers were washed with water (20 mL) before being dried over $MgSO_4$, filtered and evaporated under reduced pressure. Hexane was added to the residue while vigorously stirring.

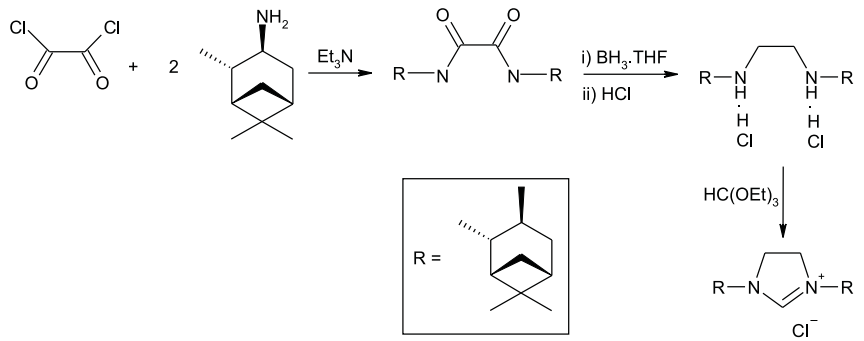

Once the white solid was finely ground, it was filtered and vacuum dried. Yield: 71%.
^{1}H NMR ($CDCl_3$): δ 7.38 (br s, 2H, NH), 4.22 (m, 2H, N-C$_a H$), 2.58 (m, 2H), 2.43 (m, 2H), 1.96 (m, 2H), 1.86 (m, 2H), 1.58 (m, 4H), 1.24 (s, 6H, H$_h$), 1.11 (d, 6H, H$_i$), 1.06 (s, 6H, H$_g$), 0.90 (2H). ^{13}C NMR ($CDCl_3$): δ 159.7 (C=O), 48.7 (C_a-N), 47.9 (C$_c$), 45.9 and 41.6 (C$_b$ and C$_d$), 38.6 (C$_j$), 36.6 (C$_e$), 35.3 (C$_f$), 28.1 (C$_h$), 23.6 (C$_g$), 21.0 (C$_i$).

N,N'-Di((-)-isopinocampheyl)ethane-1,2-diamine dihydrochloride
2.014 g of N,N'-Di((-)-isopinocampheyl)oxamide (5.6 mmol) was reacted with an excess of BH_3-THF (1 M in THF, 40 mL, 40 mmol) under reflux overnight. After cooling to room temperature, MeOH was slowly added until all bubbling ceased. Conc. HCl was added (2 mL) in order to obtain the dichloride salt. The solvent was evaporated and MeOH was again added while stirring. MeOH was again removed by evaporation. In this way boron was removed as $B(OMe)_3$. Hexane was added under vigorous stirring and the white product was filtered and dried. Subsequent ring closure with $HC(OEt)_3$ was carried out as described above. Yield: 77%.

Synthesis of [H_2ItBu(H)][Cl] 75b

N,N'- Di(*tert*-butyl)ethylenediimine[CH(=NtBu)]$_2$
To an excess of *tert*-butylamine (20 mL, 186.5 mmol) was slowly added glyoxal (40% wt. solution in H_2O, 5 mL, 43.6 mmol). The resulting mixture was stirred for 4 h at room temperature. The excess of amine was evaporated and EtOAc was added to dissolve the product. The organic phase was washed with water (2 * 50 mL) and the aqueous layers were extracted with EtOAc. The organic extracts were combined and dried over $MgSO_4$. Evaporation of the solvent then afforded the desired product as a white powder. Yield: 84 %.
^{1}H NMR ($CDCl_3$): δ 7.95 (s, 2H, CH=N), 1.27 (s, 18H, CH_3). ^{13}C NMR ($CDCl_3$): δ 158.1 (C=N), 58.4 (C-N), 29.6 (CH$_3$).

Diamine dichloride salt $[CH_2(NHtBu)]_2[Cl]_2$
6 g (35.65 mmol) of the diimine $[CH(=NtBu)]_2$ in dry Et_2O was cooled to 0 °C and an excess of $LiAlH_4$ (2 g) was slowly added. The resulting mixture was allowed to heat to room temperature and stirred overnight. It was then cooled to 0 °C and water was slowly dropped until bubbling ceased. The formed precipitate was filtered off and washed with Et_2O. The filtrate was extracted with water and the aqueous layer extracted two times more with CH_2Cl_2. The organic extracts were combined and evaporated.
Diamine [CH_2(NHtBu)]$_2$: Yield: 89%.
^{1}H NMR ($CDCl_3$): δ 2.66 (s, 4H, CH_2), 1.10 (s, 18H, CH_3). ^{13}C NMR ($CDCl_3$): δ 50.14 (*C*-N), 43.2 (*C*H$_2$-N), 29.1 (*C*H$_3$).
The diamine was dissolved in 20 mL of Et_2O. HCl gas was bubbled through the solution to precipitate the desired off-white dichloride salt, which was obtained in a pure form by filtration and washing with hexane.

***N*,*N*'-Di(*tert*-butyl)imidazolinium chloride $[H_2ItBu(H)][Cl]$**
A suspension of 3.4 g of the dichloride salt in 50 mL of $HC(OEt)_3$ was heated overnight at 120 °C. The reaction mixture was cooled to room temperature and after the formed EtOH was removed by evaporation, precipitation of the white product occured. The solid was filtered off and vacuum dried. Yield: 58%.
^{1}H NMR ($CDCl_3$): δ 8.78 (s, 1H, NC*H*N), 4.05 (s, 4H, NCH_2CH_2N), 1.55 (s, 18H, CH_3). ^{13}C NMR ($CDCl_3$): δ 153.8 (N*C*N), 57.2 ((CH$_3$)$_3$*C*-N), 45.6 (N*C*H$_2$*C*H$_2$N), 28.4 (*C*H$_3$).

Synthesis of $[H_2ICy(H)][Cl]$ 75c

***N*,*N*'-Dicyclohexylethylenediimine $[CH(=NCy)]_2$**
To a solution of cyclohexylamine (10 mL, 87.4 mmol) in ethanol (50 mL) was added aqueous glyoxal (40% wt. solution in H_2O, 5 mL, 43.6 mmol). The reaction mixture was stirred for 2 h at room temperature, while a white precipitate formed. The product was collected by filtration, washed with hexane (2 * 20 mL) and dried *in vacuo*. Yield: 94%.
^{1}H NMR ($CDCl_3$): δ 7.94 (s, 2H, C*H*=N), 3.16 (m, 2H, N-C*H*), 1.79 (m, 4H), 1.70 (m, 6H), 1.45-1.29 (m, 10H). ^{13}C NMR ($CDCl_3$): δ 160.3 (*C*=N), 69.6 (*C*1-N), 34.2 (C2-C6 of Cy), 25.7 (C4 of Cy), 24.8 (C3-C5 of Cy).

Diamine dichloride salt $[CH_2(NHCy)]_2[Cl]_2$
A solution of the diimine (4.6 g, 20.8 mmol) in dry Et_2O (100 mL) was cooled to 0 °C and $LiAlH_4$ (95%, 1.60 g, 40.0 mmol) was added in small portions. The resulting mixture was allowed to warm to room temperature and stirred overnight. Water was slowly added until bubbling stopped. This way, the grey aluminium alkoxides hydrolysed and the reaction medium turned white. The solid was filtered off and washed with CH_2Cl_2. The organic phase was extracted with 100 mL of water and the aqueous layer extracted two times more with CH_2Cl_2. The organic

extracts were combined and concentrated to ≈50 mL under reduced pressure. Concentrated HCl (12 M) was added to precipitate the desired white dichloride salt, which was obtained in a pure form by filtration and washing with hexane. Yield: 86%.

Complete evaporation of the organic phase allowed isolation of the diamine [CH_2-(NHCy)]$_2$: ^{1}H NMR ($CDCl_3$): δ 2.65 (s, 4H, NCH_2CH_2N), 2.32 (m, 2H, CH-N), 0.97-1.83 (remaining 20 protons). ^{13}C NMR ($CDCl_3$): δ 56.9 (N-C1 of Cy), 47.0 (NCH$_2$$CH_2$N), 33.7 (C2-C6 of Cy), 26.2 (C4 of Cy), 25,1 (C3-C5 of Cy).

N,N'-Dicyclohexylimidazolinium chloride [H_2ICy(H)][Cl]

A mixture of 3.20 g (10.8 mmol) of the dichloride salt and 50 mL of HC(OEt)$_3$ was heated to 120 °C, while the formed EtOH was removed by distillation. After cooling to room temperature a white solid was filtered off and washed with Et_2O. This solid was analyzed as the pure desired product. Since the yield was rather low (41%), the filtrate was evaporated until more white solid precipitated. However, this solid turned out to be a sideproduct (unreacted chloride salt and/or the product of reaction of one dichloride salt molecule with two molecules of HC(OEt)$_3$).

[H_2ICy(H)][Cl]: (Yield: 41%) ^{1}H NMR ($CDCl_3$): δ 9.89 (s, 1H, NCHN), 3.91 (s, 4H, NCH_2CH_2N), 3.49 (m, 2H, HC1-Cy), 2.06 (2H), 1.86 (2H), 1.68 (2H), 1.47 (2H), 1.21 (2H). ^{13}C NMR ($CDCl_3$): δ 155.8 (NCN), 57.1 (C1-Cy), 45.4 (NCH$_2$$CH_2$N), 30.9 (C2-C6 of Cy), 24.6 (C3-C4-C5 of Cy).

It was found possible to obtain higher yield of imidazolinium salt by the synthesis of the tetrafluoroborate salt instead of the chloride salt: After reduction of the diimine with $LiAlH_4$ no HCl was added. The bisamine was brought into a dry flask, and 1.1 equiv of $NH_4^+BF_4^-$ was added together with HC(OEt)$_3$. The resulting suspension was heated at 120 °C overnight during which time the reaction mixture turned clear. After cooling to room temperature, an off-white solid precipitated which was collected by filtration and washed with hexane. No sideproducts were observed. [H_2ICy(H)][BF_4]: Yield: 79%.

^{1}H NMR ($CDCl_3$): δ 8.05 (s, 1H, NCHN), 3.94 (s, 4H, NCH_2CH_2N), 3.59 (2H, HC1-Cy), 2.03, 1.87, 1.72-1.67, 1.58, 1.41, 1.17. ^{13}C NMR ($CDCl_3$): δ 154.3 (NCN), 57.8 (C1-Cy), 45.8 (NCH$_2$$CH_2$N), 31.0 (C2-C6 of Cy), 25.0 (C3-C4-C5 of Cy).

Synthesis of [H_2I*n*oct(H)][Cl] 75d

N,N'-Di(*n*-octyl)ethylenediimine [CH(=N*n*oct)]$_2$

2 equivalents of *n*-octylamine (14.6 mL, 88.1 mmol) were solved in *n*-propanol (150 mL) and 5 mL of glyoxal (40% wt. solution in H_2O, 43.6 mmol) was slowly added via syringe. Immediately upon addition a white solid precipitated which was collected by filtration after 10 min of reaction time. The formed diimine was very unstable and could not be kept in solvent for larger time spans. Yield: 87%.

^{1}H NMR ($CDCl_3$): δ 7.92 (s, 2H, CH=N), 3.57 (t, 4H, CH_2), 1.77 (t, 4H, CH_2),

1.70 (t, 4H, CH_2), 1.27 (br signal, 16H, CH_2), 0.88 (t, 6H, CH_3).

Diamine dichloride salt [CH_2(NH*n*oct)]$_2$[Cl]$_2$
To 2 g of the diimine was added 80 mL of dry Et_2O. The resulting suspension was cooled to 0 °C before $LiAlH_4$ was added in small portions in order to minimize heating of the reaction mixture which would cause decomposition of the imine. The resulting mixture was allowed to stir overnight, while warming to room temperature. Water was then slowly dropped until all bubbling ceased. The formed precipitate was filtered off and washed with Et_2O. The filtrate was extracted with water; the aqueous layer extracted two times more with EtOAc. The organic extracts were combined and dried over $MgSO_4$. Solvents were evaporated. *Diamine [CH_2(NH*n*oct)]$_2$*: Yield: 74%.
^{1}H NMR ($CDCl_3$): δ 2.79 - 2.57 (br m, 8H, -CH_2NCH_2CH_2NCH_2-), 2.02 (br s, 2H, NH), 1.48 (t, 4H, CH_2), 1.28 (br signal, 20H, CH_2), 0.88 (t, 6H, CH_3). ^{13}C NMR ($CDCl_3$): δ 50.24 (NCH_2CH_2N), 49.6 (CH_2-N), 32.1 (C2 of *n*-octyl), 30.3 (C3), 29.8 (C4), 29.5 (C5), 27.6 (C6), 22.9 (C7), 14.3 (C8).
The diamine was dissolved in 20 mL of Et_2O and HCl (12 M) was added to precipitate the desired white dichloride salt, which was filtered and washed with hexane.

***N*,*N*'-Di(*n*-octyl)imidazolinium chloride [H_2I*n*oct(H)][Cl]**
A suspension of 1.4 g of the dichloride salt in 25 mL of $HC(OEt)_3$ was heated overnight at 120 °C. The reaction mixture was cooled to room temperature and after evaporation of half of the solvent, precipitation of an off-white product occured. The precipitate was filtered and washed with pentane. The initially solid powder slowly became sticky but was stable. Yield: 49%.
^{1}H NMR ($CDCl_3$): δ 9.79 (s, 1H, NCHN), 3.95 (s, 4H, NCH_2CH_2N), 3.65 (t, 4H, CH_2N), 1.66 (t, 4H, CH_2), 1.31-1.27 (20H, CH_2), 0.88 (t, 6H, CH_3). ^{13}C NMR ($CDCl_3$): δ 158.7 (NCN), 48.5 and 48.4 (*C*1-N and NCH_2CH_2N), 31.9 (C2), 29.3 (C3-C4), 27.6 (C5), 26.6 (C6), 22.8 (C7), 14.3 (C8).

Synthesis of the pinane based imidazolinium chloride 75e

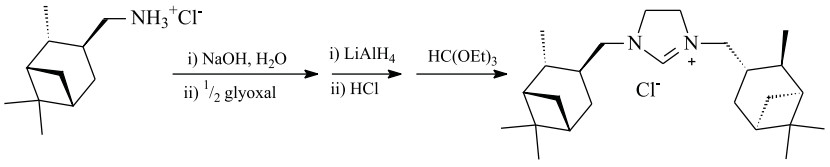

Diimine
To a solution of the chloride salt of the amino pinane derivative (3.0 g) in H_2O (15 mL) was added 1 equiv of NaOH (0.58 g). The resulting mixture was stirred at room temperature for 30 min. CH_2Cl_2 (15 mL) was added and the organic layer

was separated from the aqueous solution. The aqueous layer was extracted twice more with CH_2Cl_2 (20 mL). The combined organic phases were dried over $MgSO_4$, filtered and evaporated, leaving the free amine as a colourless liquid. To 2.4 g of the amine solved in ethanol (20 mL), was added 0.82 mL of aqueous glyoxal (40% wt. solution in H_2O, 7.2 mmol). The reaction mixture was stirred overnight at room temperature. After evaporation of solvent, a yellowish oil remained, which was purified with a small Al_2O_3 based column (hexane as eluting solvent). The diimine had limited stability and could not be stored for a long time before onset of decomposition took place. Yield: 86%.

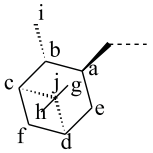

^{1}H NMR ($CDCl_3$): δ 7.87 (s, 2H, C*H*=N), 3.60 (2H, C*H*-N), 3.35 (2H, C*H*-N), 2.19 (2H), 2.04 (4H), 1.83 (2H), 1.70 (4H), 1.44 (d, 2H), 1.11 (s, 6H, H_h), 0.96 (d, 6H, H_i), 0.94 (s, 6H, H_g), 0.70 (d, 2H). ^{13}C NMR ($CDCl_3$): δ 160.9 (*C*=N), 69.4 (*C*-N), 47.0, 40.6, 40.0, 38.0 (C_j), 36.1, 32.7, 31.6, 27.0 (C_h), 21.9 (C_g), 20.6 (C_i).

Diamine dichloride salt

To a cooled (0 °C) solution of the diimine (1.8 g, 5.4 mmol) in dry Et_2O (40 mL) was slowly added 0.45 g of $LiAlH_4$. The resulting mixture was allowed to heat to room temperature and stirred overnight. Water was added dropwise till bubbling ceased. The white precipitate was filtered off and washed with Et_2O. The filtrate was extracted with water and the aqueous layer was extracted two times more with CH_2Cl_2. After combining all organic extracts the volume was reduced to ≈20 mL by evaporation. Concentrated HCl (12 M) was added while stirring to precipitate the white dichloride salt, which was collected by filtration, washed with Et_2O and dried under vacuum. The compound was used in the next step without further purification.

After complete evaporation of part of the organic phase, NMR confirmed that reduction of the diimine was complete. *Diamine (colourless oil):* ^{1}H NMR ($CDCl_3$): δ 2.67 (s, 4H, NC*H*$_2$C*H*$_2$N), 2.60 (2H), 2.38 (2H), 2.20 (2H), 2.09 (2H), 1.83 (2H), 1.69 (2H), 1.57 (2H), 1.44 (2H), 1.40 (2H), 1.12 (s, 6H, H_h), 0.99 (d, 6H, H_i), 0.94 (s, 6H, H_g), 0.67 (d, 2H). ^{13}C NMR ($CDCl_3$): δ 58.9 (*C*-N), 48.6 (N*C*H$_2$*C*H$_2$N), 47.0, 40.7, 40.4, 37.9 (C_j), 35.5, 32.7, 32.1, 27.0 (C_h), 21.9 (C_g), 21.0 (C_i).

Pinane based imidazolinium chloride

To the dichloride salt was added $HC(OEt)_3$ (30 mL) and the resulting suspension was heated at 120 °C for 4 h. The reaction mixture was cooled to room temper-

ature. At first, no precipitation was observed, but after removing the EtOH by evaporation, a white solid was formed, which was filtered and washed with Et_2O. Yield (reduction + ring closure): 64%.
^{1}H NMR ($CDCl_3$): δ 10.38 (s, 1H, NC*H*N), 3.97 (s, 4H, NCH_2CH_2N), 3.65 (m, 4H, N-CH_2), 2.35 (m, 2H), 2.04 (2H), 1.97 (2H), 1.80 (4H), 1.56 (d, 2H), 1.21 (s, 6H, H_h), 1.05 (d, 6H, H_i), 1.01 (s, 6H, H_g), 0.88 (d, 4H). ^{13}C NMR ($CDCl_3$): δ 159.5 (N*C*N), 56.7 (N-*C*), 48.5 (N*C*H_2*C*H_2N), 47.9, 41.3, 40.8, 39.0 (C_j), 33.8, 33.7, 31.9, 28.0 (C_h), 23.3 (C_g), 22.1 (C_i).

5.4.3 *N*-alkyl-*N*'-mesityl imidazolinium salts

The general reaction sequence was outlined by Grubbs et al.[410]

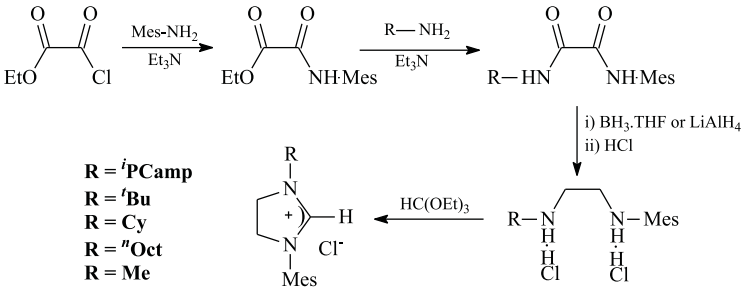

***N*-mesityl-oxanilic acid ethyl ester**
The reaction was carried out as described by Grubbs et al.[410]

***N*-mesityl-*N*'-isopinocampheyl-oxalamide**
N-mesityl-oxanilic acid ethyl ester (5.51 g, 25.7 mmol) and 1.0 equiv of (1R,2R, 3R,5S)-(-)-isopinocampheylamine (95% sol., 4.5 mL) were dissolved in toluene (60 mL). Et_3N (3.6 mL, 1.0 equiv) was added and the resulting mixture was refluxed overnight. After cooling to room temperature, the solution was washed twice with a 2 M HCl solution (2 * 60 mL). The aqueous layer was washed with EtOAc. The combined organic extracts were washed with brine before being dried over $MgSO_4$, filtered and evaporated to afford a white solid. The product was washed with hexane and filtered. Yield: 74%.
^{1}H NMR ($CDCl_3$): δ 8.83 (s, 1H, MesN*H*), 7.50 (br s, 1H, ^{i}PCampN*H*), 6.92 (s, 2H, Ar-*H*), 4.29 (m, 1H, N-C*H*), 2.61 (m, 1H), 2.43 (m, 1H), 2.29 (s, 3H, *p*-CH_3), 2.20 (s, 6H, *o*-CH_3), 1.99 - 1.65 (multiplets, 4H), 1.25 (s, 3H, H_h), 1.14 (d, 3H, H_i), 1.10 (s, 3H, H_g), 0.92 (d, 1H). ^{13}C NMR ($CDCl_3$): δ 159.5 (MesNH*C*=O), 158.7 (^{i}PCampNH*C*=O), 137.7 (Ar *i*-C), 135.0 (Ar *o*-C), 130.1 (Ar *p*-C), 129.3 (Ar *m*-C), 48.9 (C_a ^{i}PCamp), 47.9 - 45.8 - 41.7 (C_c, C_b and C_d), 38.7 (C_j), 36.6 (C_e), 35.3 (C_f), 28.2 (C_h), 23.6 (C_g), 21.2 (*p*-*C*H$_3$), 21.0 (C_i), 18.6 (*o*-*C*H$_3$).

***N*-mesityl-*N*'-(*tert*-butyl)-oxalamide**
To 3.99 g of *N*-mesityl-oxanilic acid ethyl ester (18.6 mmol) was added an excess of *tert*-butylamine (15 mL, 142.8 mmol) since 1 equiv of amine didn't lead to full conversion. Dry toluene (50 mL) and Et_3N (5.2 mL) were added and the resulting mixture was heated to 100 °C. The starting product dissolved during reaction and after one night of heating a white precipitate had formed. The suspension was cooled and EtOAc was added to dissolve all product. The solution was washed with 2 M HCl (50 mL * 2). The aqueous layer was washed with EtOAc; the combined organic layers were extracted with brine and dried over $MgSO_4$. The organic fraction was evaporated, leaving a white solid. Toluene (50 mL) was added while stirring, the precipitate was collected by filtration and washed with pentane. Yield: 74%.
^{1}H NMR ($CDCl_3$): δ 8.76 (s, 1H, MesN*H*), 7.44 (s, 1H, *t*BuNH), 6.92 (s, 2H, Ar-*H*), 2.29 (s, 3H, *p*-CH_3), 2.20 (s, 6H, *o*-CH_3), 1.45 (s, 9H, *t*Bu CH_3). ^{13}C NMR ($CDCl_3$): δ 159.3 (MesNH*C*=O), 159.1 (*t*BuNH*C*=O), 137.7 (Ar *i*-C), 135.0 (Ar *o*-C), 130.1 (Ar *p*-C), 129.3 (Ar *m*-C), 52.0 ((CH$_3$)$_3$*C*-N), 28.6 ((*C*H$_3$)$_3$C-N), 21.2 (*p*-*C*H$_3$), 18.6 (*o*-*C*H$_3$).

***N*-mesityl-*N*'-cyclohexyl-oxalamide**
In an analogous way, *N*-mesityl-oxanilic acid ethyl ester (4.12 g, 19.2 mmol), cyclohexylamine (2.2 mL, 1.9 g, 19.2 mmol) and Et_3N (2.7 mL, 1 equiv) afforded the desired *N*-(Mesityl)-*N*'-(cyclohexyl)-oxalamide as a white solid. Yield: 79%.
^{1}H NMR ($CDCl_3$): δ 8.78 (s, 1H, MesN*H*), 7.50 (br s, 1H, CyN*H*), 6.91 (s, 2H, Ar-*H*), 3.78 (m, 1H, N-C*H*), 2.28 (s, 3H, *p*-CH_3), 2.18 (s, 6H, *o*-CH_3), 1.96 (d, 2H), 1.76 (m, 2H), 1.64 (d, 2H), 1.41-1.66 (br m, 4H). ^{13}C NMR ($CDCl_3$): δ 159.1 (MesNH*C*=O), 158.7 (CyNH*C*=O), 137.6 (Ar *i*-C), 135.0 (Ar *o*-C), 130.1 (Ar *p*-C), 129.2 (Ar *m*-C), 49.3 (C1 Cy), 32.8 (C2 Cy), 25.5 (C4 Cy), 25.0 (C3 Cy), 21.2 (*p*-*C*H$_3$), 18.5 (*o*-*C*H$_3$).

***N*-mesityl-*N*'-(*n*-octyl)-oxalamide**
In an analogous way, *N*-mesityl-oxanilic acid ethyl ester (5.99 g, 27.9 mmol), *n*-octylamine (4.63 mL, 1 equiv) and Et_3N (4 mL, 1 equiv) afforded *N*-mesityl-*N*'-(*n*-octyl)-oxalamide as a white solid in 86% yield.
^{1}H NMR ($CDCl_3$): δ 8.77 (s, 1H, MesN*H*), 7.59 (s, 1H, *n*octN*H*), 6.91 (s, 2H, Ar-*H*), 3.35 (m, 2H, N-CH_2), 2.28 (s, 3H, *p*-CH_3), 2.18 (s, 6H, *o*-CH_3), 1.60 (t, 2H, CH_2), 1.31-1.28 (10H, CH_2), 0.90 (t, 3H, CH_3). ^{13}C NMR ($CDCl_3$): δ 160.0 (MesNH*C*=O), 158.6 (*n*octNH*C*=O), 137.7 (Ar *i*-C), 134.9 (Ar *o*-C), 130.0 (Ar *p*-C), 129.3 (Ar *m*-C), 40.2 (*C*H$_2$-N), 34.5 (C2 of *n*octyl), 32.0 (C3), 29.4 (C4-C5), 27.1 (C6), 22.9 (C7) 21.1 (*p*-*C*H$_3$), 18.5 (*o*-*C*H$_3$), 14.3 (C8).

***N*-mesityl-*N*'-methyl-oxalamide**
To 4.55 g of *N*-mesityl-oxanilic acid ethyl ester (21.2 mmol) was added 15 mL of a 2.0 M methylamine solution in THF (30 mmol), 3.2 mL of Et_3N and 30 mL of dry toluene. The resulting solution was heated overnight. After cooling to room

temperature, the solution was washed with 2 M HCl (100 mL * 2). The aqueous layer was washed with EtOAc and the combined organic layers were dried over $MgSO_4$. The organic fraction was evaporated, leaving a white solid. Hexane was added while stirring, allowing filtration of the desired compound as a white powder. Yield: 92%.
^{1}H NMR ($CDCl_3$): δ 8.73 (s, 1H, MesN*H*), 7.57 (s, 1H, MeN*H*), 6.91 (s, 2H, Ar-*H*), 2.96 (d, 2H, NCH_3), 2.28 (s, 3H, *p*-CH_3), 2.18 (s, 6H, *o*-CH_3). ^{13}C NMR ($CDCl_3$): δ 160.9 (MesNH*C*=O), 158.5 (MeNH*C*=O), 137.7 (Ar *i*-C), 134.9 (Ar *o*-C), 129.9 (Ar *p*-C), 129.3 (Ar *m*-C), 26.5 (N*C*H$_3$), 21.1 (*p*-*C*H$_3$), 18.5 (*o*-*C*H$_3$).

_N_-mesityl-_N_'-(1-adamantyl)-oxalamide
The synthesis of *N*-mesityl-*N*'-(1-adamantyl)-oxalamide was previously established by Mol et al. by reaction of adamantanamine with a mesidine substituted acetyl chloride.[292] The here described alternative synthetic strategy involves reaction of the adamantanamine with *N*-(mesityl)-oxanilic acid ethyl ester as was done for the other unsymmetrical substituted oxalamides. Since overnight heating of the reaction mixture was not sufficient to get full conversion, 3.0 g of the *N*-(mesityl)-oxanilic acid ethyl ester (14.0 mmol, 1 equiv), 1-adamantanamine (2.32 g, 15.4 mmol, 1.1 equiv) and 4 mL of Et_3N (excess) were dissolved in 50 mL of toluene and refluxed for 40 h. A white precipitate formed, which was dissolved by the addition of EtOAc. The resulting solution was washed with a 2 M HCl solution (2 * 100 mL). The aqueous layer was washed with EtOAc, and the combined organic layers were washed with brine and dried over $MgSO_4$. $MgSO_4$ was filtered off and the solvents evaporated. The resulting white solid was washed with 20 mL of toluene and filtered. Yield: 81%.
^{1}H NMR ($CDCl_3$): δ 8.85 (br s, 1H, MesN*H*), 7.33 (br s, 1H, AdN*H*), 6.91 (s, 2H, Ar-*H*), 2.28 (s, 3H, *p*-CH_3), 2.19 (s, 6H, *o*-CH_3), 2.12 (s, 3H, H$_a$), 2.07 (s, 6H, H$_b$), 1.71 (s, 6H, H$_c$). ^{13}C NMR ($CDCl_3$): δ 159.2 (MesNH*C*=O), 158.8 (AdNH*C*=O), 137.7 (Ar *i*-C), 134.9 (Ar *o*-C), 130.1 (Ar *p*-C), 129.3 (Ar *m*-C), 52.6 (C1 Ad), 41.2 (C2 Ad), 36.4 (C4 Ad), 29.5 (C3 Ad), 21.2 (*p*-*C*H$_3$), 21.0 (C$_i$), 18.6 (*o*-*C*H$_3$).

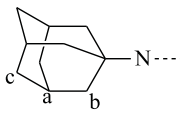

1-mesityl-3-isopinocampheyl-4,5-dihydroimidazolium salt 76a
To a flask charged with the oxalamide (2.8 g, 8.2 mmol), was added BH_3.THF (1 M in THF, 50 mL, 6 equiv). The resulting mixture was refluxed overnight while the solution turned clear. The mixture was then cooled to room temperature and MeOH was added dropwise till all bubbling ceased. Conc. HCl (12 M, 2 mL) was added and the solvent was removed by evaporation. The resulting solid

was redissolved in MeOH and the solvent was again evaporated to remove the boron as $B(OMe)_3$. MeOH was added and removed in this way twice more. The remaining white solid was washed with hexane (50 mL). The so formed suspension was rapidly stirred until a finely ground powder had formed, which was filtered and vacuum dried. The dichloride salt was transferred into a flask followed by addition of triethyl orthoformate (30 mL). The solution was heated at 120 °C overnight. After cooling to room temperature, the reaction volume was reduced to ≈10 mL. A white precipitate was collected on a coarse frit, washed with Et_2O and vacuum dried.

Note: In some batches, some unreacted startproduct and a sideproduct, which might result from the reaction of each aminegroup with a separate molecule of $HC(OEt)_3$, had to be removed from the desired product. This was possible since the startproduct remained undissolved in $HC(OEt)_3$, while the undesired sideproduct only precipitated after addition of Et_2O to a almost completely evaporated $HC(OEt)_3$ solution. [H_2I^iPCampMes(H)][Cl]: Yield: 42%.

^{1}H NMR ($CDCl_3$): δ 10.27 (s, 1H, NC*H*N), 6.91 (s, 2H, Ar-*H*), 5.31 (m, 1H, N-C$_a$*H*), 4.22 (m, 4H, NC*H*$_2$C*H*$_2$N), 2.68 (m, 1H), 2.51 (m, 1H), 2.29-2.27 (9H, *o*-C*H*$_3$ and *p*-C*H*$_3$), 2.17 (m, 1H), 2.06 (1H), 1.91 (2H), 1.24 (s, 3H, H$_h$), 1.21 (d, 3H, H$_i$), 1.13 (s, 3H, H$_g$), 8.85 (d, 1H). ^{13}C NMR ($CDCl_3$): δ 160.55 (N*C*HN), 140.26 (*i*-$C_6H_2Me_3$), 135.2 (*o*-$C_6H_2Me_3$), 131.04 (p-$C_6H_2Me_3$), 130.15 (*m*-$C_6H_2Me_3$), 57.12 (C$_a$ ^{i}PCamp), 50.87 (*C*H$_2$NMes), 47.37 (^{i}PCampN*C*H$_2$), 43.91, 41.48, 40.28 (C$_c$, C$_b$ and C$_d$), 38.72 (C$_j$), 35.38 (C$_e$), 32.12 (C$_f$), 28.25 (C$_h$), 23.76 (C$_g$), 21.25 (C$_i$), 20.31 (*p*-*C*H$_3$), 18.31 (*o*-*C*H$_3$).

1-mesityl-3-(*tert*-butyl)-4,5-dihydroimidazolium chloride 76b

To a flask charged with the oxalamide (2.6 g, 9.9 mmol), was added an excess of BH_3.THF (1 M in THF, 50 mL). Heating for 24 h was required to get full reduction. After cooling to room temperature, MeOH was added dropwise till all bubbling ceased. Conc. HCl (12 M, 2 mL) was added and the solvent was removed by evaporation. The resulting solid was redissolved in MeOH and the solvent was again evaporated to remove the boron as $B(OMe)_3$. MeOH was added and removed in this way twice more. $HC(OEt)_3$ (30 mL) was added and after heating at 120 °C overnight, the solution had turned clear. The mixture was cooled to room temperature and the volume was reduced to ≈10 mL. An off-white precipitate was collected on a coarse frit, washed with pentane and vacuum dried. Yield: 59%.

The salt became sticky when stored but remained stable.

^{1}H NMR ($CDCl_3$): δ 9.13 (s, 1H, NC*H*N), 6.93 (s, 2H, Ar-*H*), 4.34-4.29 (m, 4H, NC*H*$_2$C*H*$_2$N), 2.33 (s, 6H, *o*-C*H*$_3$), 2.28 (s, 3H, *p*-C*H*$_3$), 1.61 (s, 9, C*H*$_3$ *t*-Bu). ^{13}C NMR ($CDCl_3$): δ 157.4 (N*C*HN), 140.1 (*i*-$C_6H_2Me_3$), 135.5 (*o*-$C_6H_2Me_3$), 131.2 (*p*-$C_6H_2Me_3$), 130.0 (*m*-C_6H_2Me3), 57.8 ((CH$_3$)$_3$*C*-N), 51.3 (*C*H$_2$NMes), 46.6 (*t*BuN*C*H$_2$), 28.6 ((*C*H$_3$)$_3$C-N), 21.2 (*p*-C*H*$_3$), 18.2 (*o*-C*H*$_3$).

Notes:

(i) An alternative for the BH_3 as reducing agent is $LiAlH_4$, which also requires

heating of the reaction mixture, but this only for < 6 h.
(ii) In a second batch, the precipitate after ring closing was analyzed as a mixture of the desired product and a sideproduct resulting from reaction of the amino groups with each a separate $HC(OEt)_3$ molecule. This side product was not observed when the tetrafluoroborate salt was synthesized instead of the chloride salt.

1-mesityl-3-cyclohexyl-4,5-dihydroimidazolium chloride 76c
In an analogous way, *N*-mesityl-*N*'-cyclohexyl-oxalamide (3.0 g, 10.4 mmol), BH_3.THF (1 M in THF, 63 mL, 6 equiv), conc. HCl (12 M, 2.5 mL), and $HC(OEt)_3$ (30 mL) afforded a white solid which was collected on a coarse frit, washed with Et_2O and vacuum dried. Yield: 59%.
^{1}H NMR ($CDCl_3$): δ 9.74 (s, 1H, NC*H*N), 6.93 (s, 2H, Ar-*H*), 4.35 (m, 1H, N-C*H*), 4.21-4.18 (m, 4H, NCH_2CH_2N), 2.32 (s, 6H, *o*-CH_3), 2.28 (s, 3H, *p*-CH_3), 2.15, 1.88-1.55 and 1.21 (10 H, Cy protons). ^{13}C NMR ($CDCl_3$): δ 158.8 (NCHN), 140.1 (*i*-$C_6H_2Me_3$), 135.4 (*o*-$C_6H_2Me_3$), 131.1 (*p*-$C_6H_2Me_3$), 130.0 (m-$C_6H_2Me_3$), 57.7 (C1 Cy), 50.9 (CH_2NMes), 46.3 (CyNCH_2), 31.3 (C2-C6 of Cy), 25.0 (C4 of Cy), 24.9 (C3 - C5 of Cy), 21.2 (*p*-CH_3), 18.2 (*o*-CH_3).

1-mesityl-3-(*n*-octyl)-4,5-dihydroimidazolium chloride 76d
Reduction of the bisamide was found to proceed more slowly than with other amino side groups, and therefore the reduction step was carried out with $LiAlH_4$ as reducing agent. 5.1 g of *N*-mesityl-*N*'-(*n*-octyl)-oxalamide (16.0 mmol) was dissolved in 100 mL of dry THF and cooled to 0 °C in an ice bath. $LiAlH_4$ (1.5 g = excess) was slowly added and the resulting suspension was heated to reflux overnight. The next day, the reaction mixture was cooled to room temperature and water was slowly dropped till all bubbling ceased. The white precipitation was filtered off and washed with Et_2O (20 mL). The organic filtrate was washed with water (100 mL) and the aqueous layer was extracted with 100 mL of Et_2O. The combined organic layers were reduced to ≈20 mL. HCl (12 M) was slowly added to precipitate the chloride salt of the bisamine. The white solid was filtered and washed with 20 mL of pentane. A suspension of this *N*-mesityl-*N*'-(*n*-octyl)ethane-1,2-diamine dihydrochloride in $HC(OEt)_3$ (50 mL) was heated overnight at 120 °C. The reaction mixture was cooled to room temperature and evaporated to ≈20 mL. Et_2O (10 mL) was added to precipitate the desired imidazolium salt as off-white crystals which were filtered and washed with 5 mL of Et_2O. Yield: 72%.
The salt became sticky when stored but remained stable. When the compound was kept in a small amount of Et_2O, it was possible to filter the salt just before its use in a subsequent reaction.
^{1}H NMR ($CDCl_3$): δ 9.84 (s, 1H, NC*H*N), 6.92 (s, 2H, Ar-*H*), 4.19 (m, 4H, NCH_2CH_2N), 3.99 (t, 2H, NCH_2CH_2N-CH_2), 2.30 (s, 6H, *o*-CH_3), 2.28 (s, 3H, *p*-CH_3), 1.73 (t, 2H, CH_2), 1.34-1.21 (10H CH_2), 0.88 (t, 3H, CH_3). ^{13}C NMR ($CDCl_3$): δ 160.1 (NCHN), 140.5 (*i*-$C_6H_2Me_3$), 135.4 (*o*-$C_6H_2Me_3$), 130.8 (*p*-

$C_6H_2Me_3$), 130.2 (*m*-$C_6H_2Me_3$), 50.9 (CH_2NMes), 48.8 and 48.6 (*n*oct NCH_2 and C1 of *n*-octyl), 31.9 (C2), 29.4 (C3-C4), 27.5 (C5), 26.6 (C6), 22.8 (C7), 21.2 (*p*-CH_3), 18.1 (*o*-CH_3), 14.3 (C8).

1-mesityl-3-methyl-4,5-dihydroimidazolium chloride 76e

Following an analogous procedure to the one carried out for **76a** and **76c**, 1-mesityl-3-methyl-4,5-dihydroimidazolium chloride was obtained as an off-white powder with 83% yield.

^{1}H NMR ($CDCl_3$): δ 9.79 (s, 1H, NC*H*N), 6.93 (s, 2H, Ar-H), 4.21-4.17 (m, 4H, MeNCH_2CH_2NMes), 3.63 (s, 3H, NCH_3), 2.31 (s, 6H, *o*-CH_3), 1.86 (s, 3H, *p*-CH_3). ^{13}C NMR ($CDCl_3$): δ 160.2 (N*C*HN), 140.5 (*i*-$C_6H_2Me_3$), 135.6 (*o*-$C_6H_2Me_3$), 130.4 (*p*-$C_6H_2Me_3$), 130.2 (*m*-$C_6H_2Me_3$), 51.9 (CH_2NMes), 51.1 (CH_3NCH_2), 35.9 (CH_3N), 21.2 (*p*-CH_3), 18.2 (*o*-CH_3).

1-mesityl-3-adamantyl-4,5-dihydroimidazolium chloride[292]

Similary 1-mesityl-3-adamantyl-4,5-dihydroimidazolium chloride was isolated as a white powder with 69% yield.

^{1}H NMR ($CDCl_3$): δ 9.03 (s, 1H, NC*H*N), 6.91 (s, 2H, Ar-*H*), 4.40 (dd, 2H, AdNCH_2CH_2NMes), 4.25 (dd, 2H, AdNCH_2CH_2NMes), 2.31 (s, 6H, *o*-CH_3), 2.27 (s, 3H, *p*-CH_3), 2.12 (br s, 9H, H_a H_b Ad), 1.73 (s, 6H, H_c Ad). ^{13}C NMR ($CDCl_3$): δ 156.8 (N*C*HN), 140.1 (i-$C_6H_2Me_3$), 135.5 (o-$C_6H_2Me_3$), 131.2 (*p*-$C_6H_2Me_3$), 130.1 (*m*-$C_6H_2Me_3$), 57.5 (C1 Ad), 51.0 (CH_2NMes), 45.4 (AdNCH_2), 41.2 (C2 Ad), 35.6 (C4 Ad), 29.4 (C3 Ad), 20.7 (*p*-CH_3), 18.4 (*o*-CH_3).

5.4.4 *N*-alkyl-*N*'-(2,6-diisopropylphenyl) imidazolinium salts

***N*-(2,6-diisopropylphenyl)-oxanilic acid ethyl ester**

The reaction was carried out as described by Grubbs et al.[410]

***N*-(2,6-diisopropylphenyl)-*N*'-methyl-oxalamide**

N-(2,6-diisopropylphenyl)-oxanilic acid ethyl ester (3.584 g, 12.98 mmol) was dissolved in toluene (50 mL). Triethylamine (1.9 mL, 13.52 mmol) and methylamine (12 mL of a 2M solution in THF, 24 mmol) were added and the resulting suspension was heated overnight at 80 °C. After cooling to room temperature the solution was washed twice with a 2M HCl solution (2 * 60 mL). The aqueous layer was washed with ethyl acetate and the combined organic extracts were dried over $MgSO_4$, filtered and evaporated to afford a white solid. This solid was washed with hexane and filtered. Yield: 81%.

^{1}H NMR ($CDCl_3$): δ 8.76 (s, 1H, ArN*H*), 7.57 (s, 1H, MeN*H*), 7.33 (t, 1H, Ar-*H*), 7.20 (d, 2H, Ar-*H*), 3.04-2.96 (m, 5H, CH_3NH and C*H*$(CH_3)_2$), 1.19 (d, 12H, CH(CH_3)$_2$). ^{13}C NMR ($CDCl_3$): δ 160.7 (ArNH*C*=O), 159.6 (MeNH*C*=O), 146.1 (Ar *i*-C), 129.8 (Ar *o*-C), 129.2 (Ar *m*-C), 124.0 (Ar *p*-C), 29.1 (*C*H$(CH_3)_2$), 26.6 (NCH_3), 23.9 (CH(CH_3)$_2$).

_N_-(2,6-diisopropylphenyl)-_N'_-cyclohexyl-oxalamide
The reaction of _N_-(2,6-diisopropylphenyl)-oxanilic acid ethyl ester (1.367 g, 4.95 mmol) and cyclohexylamine (0.6 mL, 5.19 mmol) in the presence of triethylamine (0.7 mL, 5.02 mmol) was carried out in a similar way. Yield: 87%.
^{1}H NMR ($CDCl_3$): δ 8.82 (s, 1H, ArNH), 7.46 (d, 1H, CyN*H*), 7.33 (t, 1H, Ar-*H*), 7.20 (d, 2H, Ar-*H*), 3.80 (m, 1H, N-C*H*), 3.00 (sept, 2H, C*H*(CH3)2), 1.98 (d, 2H), 1.80-1.76 (m, 2H), 1.65 (br s, 2H), 1.46-1.26 (br m, 4H), 1.19 (d, 12H, CH(CH_3)$_2$). ^{13}C NMR ($CDCl_3$): δ 159.8 (ArNH*C*=O), 159.0 (CyNH*C*=O), 146.08 (Ar *i*-C), 129.9 (Ar *o*-C), 129.0 (Ar *m*-C), 123.9 (Ar *p*-C), 49.5 (C-1 Cy), 32.9 (C-2 Cy), 29.0 (*C*H(CH$_3$)$_2$), 25.5 (C-4 Cy), 25.0 (C-3 Cy), 23.9 (CH(*C*H$_3$)$_2$).

1-(2,6-diisopropylphenyl)-3-methyl-4,5-dihydroimidazolium chloride
To _N_-(2,6-diisopropylphenyl)-_N'_-methyl-oxalamide (2.221 g, 8.46 mmol) was added BH_3.THF (1 M in THF, 51 mL, 51 mmol, 6 equiv). The resulting solution was refluxed overnight. It was then cooled to room temperature and MeOH was added slowly until all effervescence ceased. Conc. HCl (12 M, 3 mL) was added and the solvent was removed by evaporation. The resulting solid was redissolved in MeOH and the solvent was again evaporated to remove the boron as B(OMe)$_3$. MeOH was added and removed in this way twice more. To the remaining white solid was added triethyl orthoformate (30 mL) and the resulting suspension was heated at 120 °C for 2 h. After cooling to room temperature, the volume was reduced to ≈10 mL. The addition of Et_2O (5 mL) led to the formation of an insoluble oil, which was separated from the rest of the solution by decantation. This oil was dissolved in 10 mL of CH_2Cl_2. Hexane (10 mL) was added and the resulting mixture was kept in the fridge. White crystals formed overnight, which were filtered and dried. These crystals melted at room temperature and had to be removed from the filter quickly. Yield: 58%.
^{1}H NMR ($CDCl_3$): δ 9.92 (s, 1H, NC*H*N), 7.43 (t, 1H, Ar-*H*), 7.24 (d, 2H, Ar-*H*), 4.27 (m, 2H, MeNCH$_2$C*H*$_2$NAr), 4.16 (m, 2H, MeNC*H*$_2$CH$_2$NAr), 3.69 (s, 3H, NC*H*$_3$), 2.91 (m, 2H, C*H*(CH$_3$)$_2$), 1.31-1.26 (m, 12H, CH(C*H*$_3$)$_2$). ^{13}C NMR ($CDCl_3$): δ 160.1 (N*C*HN), 146.8 (Ar *i*-C), 135.9 (Ar *o*-C), 131.3 (Ar *m*-C), 125.2 (Ar *p*-C), 53.5 (*C*H$_2$NMes), 51.2 (CH$_3$N*C*H$_2$), 36.1 (*C*H$_3$N), 29.0 (*C*H(CH$_3$)$_2$), 25.2 (CH(*C*H$_3$)$_2$), 24.6 (CH(*C*H$_3$)$_2$).

1-(2,6-diisopropylphenyl)-3-cyclohexyl-4,5-dihydroimidazolium chloride
BH_3.THF (1M in THF, 32 mL, 32 mmol, 8 equiv) was added to _N_-(2,6-diisopropylphenyl)-_N'_-cyclohexyl-oxalamide (1.3 g, 3.94 mmol). The resulting solution was refluxed for 24 h. It was then cooled to room temperature and MeOH was added slowly till all bubbling ceased. Conc. HCl (12 M, 1.5 mL) was added and the solvent was removed by evaporation. The resulting solid was redissolved in MeOH and the solvent was again evaporated to remove the boron as B(OMe)$_3$. MeOH was added and removed in this way twice more. To the remaining white solid

was added triethyl orthoformate (5 mL) and toluene (20 mL). The resulting suspension was heated at 120 °C for 4 hours. The reaction mixture was cooled to room temperature and after evaporation of approx. half of the solvent the desired product precipitated as a white solid. It was filtered off and washed with 10 mL of hexane. Yield: 66%.
^{1}H NMR ($CDCl_3$): δ 9.57 (s, 1H, NC*H*N), 7.43 (t, 1H, Ar-*H*), 7.23 (d, 2H, Ar-*H*), 4.52 (m, 1H, N-C*H*), 4.32 (m, 2H, CyNCH_2CH_2NAr), 4.19 (m, 2H, CyNCH_2CH_2NAr), 2.90 (sept, 2H, C*H*(CH_3)$_2$), 2.14 (2H), 1.87 (2H), 1.77 (1H), 1.72 (1H), 1.61 (2H), 1.57-1.54 (2H), 1.32-1.27 (m, 12H, CH(CH_3)$_2$), 1.19 (1H).
^{13}C NMR ($CDCl_3$): δ 158.6 (N*C*HN), 146.8 (Ar *i*-C), 135.8 (Ar *o*-C), 131.3 (Ar *m*-C), 125.2 (Ar *p*-C), 57.7 (C1 Cy), 53.2 (*C*H_2NMes), 46.3 (CyN*C*H_2), 31.6 (C2-C6 of Cy), 29.1 (CH(CH_3)$_2$), 25.2, 24.8 and 24.5 (CH(CH_3)$_2$, C4 - C3 - C5 of Cy).

5.4.5 Complex synthesis

***One-pot* synthesis of complexes 74, 77a, 77c.**
1 equiv of [$RuCl_2$(=CHPh)(PCy_3)$_2$], 1.5 equiv of NHC chloride salt and 1.5 equiv of KHMDS (0.5 M sol. in toluene) were dissolved in dry toluene and stirred at room temperature for 1 h. Toluene was evaporated under vacuum and a small amount of MeOH was added while vigorously stirring. The precipitate was filtered off, washed with MeOH and dried. The spectroscopic and analytical data of the complexes prepared by this method are compiled below.

[$RuCl_2$(=CHPh)(IAdMesH_2)(PCy_3)] 74
Bright green solid, Yield: 81%. NMR data equal those described by Mol et al.[292]

[$RuCl_2$(=CHPh)(I^{i}PCampMesH_2)(PCy_3)] 77a
Pink solid, Yield: 79%. ^{1}H NMR ($CDCl_3$): δ 19.20 (s, 1H, Ru=C*H*Ph), 8.91 (br s, 1H, *o*-C_5H_6), 7.42 (t, 1H, *p*-C_5H_6), 7.15 (m, 2H, *m*-C_5H_6), 6.64 and 5.81 (br s, 2H, *o*-C_5H_6 and $C_6H_2Me_3$), 5.19 (s, 1H, $C_6H_2Me_3$), 4.09 (m, 1H, N-C_aH), 3.76 (m, 2H, ^{i}PCampNCH_2CH_2NMes), 3.63 (m, 2H, ^{i}PCampNCH_2CH_2NMes), 2.89 (br s, 1H), 2.52-1.05 (several peaks). ^{31}P NMR ($CDCl_3$): δ 22.41. ^{13}C NMR ($CDCl_3$): δ 297.2 (Ru=*C*HPh), 217.1 (d, $J_{P,C}$ = 77.0 Hz, ^{i}PCampN*C*NMes), 151.1 (*i*-C_6H_5), 137.8, 137.3, 131.8-126.8 (several peaks), 58.6 (C_a ^{i}PCamp), 50.9 (^{i}PCampNCH_2*C*H_2NMes), 48.0 (^{i}PCampN*C*H_2CH_2NMes), 44.3, 41.9, 40.7, 38.7, 35.9, 35.1, 33.8, 32.8, 28.3-26.5 (several peaks), 24.2, 21.2 (*p*-*C*H_3), 18.6 (*o*-*C*H_3). Elemental analysis calcd (%) for $C_{47}H_{71}N_2Cl_2PRu$ (867.04): C 65.11, H 8.25, N 3.23; found: C 64.73 H 8.25 N 3.19.

[$RuCl_2$(=CHPh)(I*t*BuMesH_2)(PCy_3)] 77b
Since [I*t*BuMesH_2][Cl] was found to be a sticky compound, which dissolves only slowly in toluene, it was reacted with KHMDS before addition of **1**. A 0.5 M solution of KHMDS in toluene (1.7 mL, 0.850 mmol) was added to [I*t*BuMesH_2][Cl]

(0.231 g, 0.823 mmol) in 5 mL of dry toluene. The resulting suspension was stirred for 30 min. **1** (0.34 g, 0.414 mmol) was added and the reaction mixture was stirred for another 1.5 h to reach full conversion of the Ru precursor. The solution was filtered and evaporated. Since the desired complex dissolved in MeOH and hexane, acetone was used to precipitate the catalyst. The desired complex was filtered off as a bright green powder in 56% yield.
^{1}H NMR ($CDCl_3$): δ 19.09 (s, 1H, Ru=C*H*Ph), 9.16 (br s, 1H, *o*-C_6H_5), 7.38 (t, 1H, *p*-C_6H_5), 7.24 (m, 2H, *m*-C_6H_5), 6.95 (br s, 1H, *o*-C_6H_5), 6.71 (s, 1H, $C_6H_2Me_3$), 5.80 (s, 1H, $C_6H_2Me_3$), 3.91-3.64 (m, 4H, *t*BuNC*H*$_2$C*H*$_2$NMes), 2.42 (s, 6H, *o*-C*H*$_3$), 2.37 (s, 3H, *p*-C*H*$_3$), 2.06 (s, 9H, (C*H*$_3$)$_3$C), 2.09 - 1.94 - 1.90 - 1.70 - 1.56 - 1.27 - 1.10 (all PCy_3 protons). ^{31}P NMR ($CDCl_3$): δ 22.92. ^{13}C NMR ($CDCl_3$): δ 300.3 (Ru=*C*HPh), 217.5 (d, $J_{P,C}$ = 77.3 Hz, *t*BuN*C*NMes), 152.4 (*i*-C_6H_5), 138.2, 137.9, 137.8, 137.2, 132.7, 131.3, 129.5, 129.3, 128.8, 128.6, 127.2, 57.3 ((CH$_3$)$_3$*C*), 51.2 (*t*BuNCH$_2$*C*H$_2$NMes), 46.1 (*t*BuN*C*H$_2$CH$_2$NMes), 35.5, 33.2, 30.3, 28.9, 27.9, 27.2, 27.1, 26.7, 26.5, 21.1 (*p*-*C*H$_3$), 19.0, 18.6 (*o*-*C*H$_3$).
Elemental analysis calcd (%) for $C_{41}H_{63}N_2Cl_2PRu$ (786.91): C 62.58, H 8.07, N 3.56; found C 62.09, H 7.77, N 3.40.

[RuCl$_2$(=CHPh)(ICyMesH$_2$)(PCy3)] 77c
Pink solid, Yield: 87%. ^{1}H NMR ($CDCl_3$): δ 19.10 (s, 1H, Ru=C*H*Ph), 8.73 (br s, 1H, *o*-C_6H_5), 7.39 (t, 1H, *p*-C_6H_5), 7.12 (m, 2H, *m*-C_6H_5), 6.62 (br s, 1H, *o*-C_6H_5), 6.00 (br s, 2H, $C_6H_2Me_3$), 4.53 (m, 1H, N-C*H*), 3.89 (m, 2H, CyNCH$_2$C*H*$_2$NMes), 3.72 (m, 2H, CyNC*H*$_2$CH$_2$NMes), 3.47 (s, 1H), 2.46 (br s, 1H), 2.22, 1.89, 1.60-1.11 (several peaks). ^{31}P NMR ($CDCl_3$): δ 28.13. ^{13}C NMR ($CDCl_3$): δ 295.7 (Ru=*C*HPh), 215.5 (d, $J_{P,C}$ = 76.9 Hz, CyN*C*NMes), 151.2 (*i*-C_6H_5), 137.7, 137.6, 136.7, 130.7-128.1 (several peaks), 58.2 (C1 Cy), 50.7 (CyNCH$_2$*C*H$_2$NMes), 43.8 (CyN*C*H$_2$CH$_2$NMes), 32.3, 31.1, 30.5, 29.4-25.0 (several peaks), 21.1 (*p*-*C*H$_3$), 18.7 (*o*-*C*H$_3$).
Elemental analysis calcd (%) for $C_{43}H_{65}N_2Cl_2PRu$ (812.95): C 63.53, H 8.06, N 3.45; found C 63.20, H 7.99, N 3.40.

[RuCl$_2$(=CHPh)(I*n*octMesH$_2$)(PCy3)] 77d
Imidazolinium chloride **76d** (0.29 g, 0.861 mmol) was stirred with an equimolar quantity of KHMDS in toluene for 15 min. **1** (0.4 g, 0.487 mmol) was added and the resulting solution was allowed to stir at room temperature for 1 h, during which the mixture changed color from purple to dark red. The solution was filtered to remove salts and the solvent was evaporated. The crude mixture was loaded onto a column of silica gel and the product was eluted by flash chromatography (hexane/Et_2O: 9/1). Complex **77d** was obtained as a pure pinkish compound with 49% yield.
^{1}H NMR ($CDCl_3$): δ 18.99 (s, 1H, Ru=C*H*Ph), 7.96 (br s, 1H, *o*-C_6H_5), 7.37 (m, 1H, *p*-C_6H_5), 7.09 (m, 2H, *m*-C_6H_5), 6.88 (br s, 1H, *o*-C_6H_5), 6.86 (br s, 1H, $C_6H_2Me_3$), 6.22 (br s, 1H, $C_6H_2Me_3$), 4.17 (t, 2H, NCH$_2$CH$_2$N-C*H*$_2$), 3.89

(t, 2H, *n*octNCH$_2$C*H*$_2$NMes), 3.74 (t, 2H, *n*octNC*H*$_2$CH$_2$NMes), 2.27- 2.16 - 1.87 - 1.61 - 1.30 - 1.11 - 0.90 (57H). ^{31}P NMR ($CDCl_3$): δ 32.61. ^{13}C NMR ($CDCl_3$): δ 294.5-293.3 (broad signal, Ru=*C*HPh), 217.1 (d, $J_{P,C}$ = 75.2 Hz, *n*octN*C*NMes), 149.9 (*i*-C_6H_5), 136.5, 136.2, 135.4, 129.4 (broad), 128.4, 127.8, 127.4, 127.0, 126.8, 125.5, 49.9 and 49.7 (*n*octNCH$_2$*C*H$_2$NMes and C1-*n*octyl), 47.3 (*n*octN*C*H$_2$CH$_2$NMes), 34.8, 34.0, 30.9, 30.8, 30.5, 28.8, 28.3, 27.4, 26.8, 26.7, 26.1, 25.9, 25.5, 25.4, 25.2, 24.4, 21.7 (*p*-*C*H$_3$), 19.8, 17.4 (*o*-*C*H$_3$), 13.1 (C8-*n*octyl).
Elemental analysis calcd (%) for $C_{45}H_{71}N_2Cl_2PRu$ (843.02): C 64.11, H 8.49, N 3.32; found: C 63.27 H 8.38 N 3.28.

[RuCl$_2$(=CHPh)(IMeMesH$_2$)(PCy$_3$)] 77e
Imidazolinium chloride **76e** (0.091 g, 0.381 mmol) was stirred with an equimolar quantity of KHMDS in toluene for 30 min. Complex **1** (0.2 g, 0.24 mmol) was added and the resulting solution was allowed to stir at room temperature for 1 hour. The solution was filtered to remove salts and evaporated in vacuo. Precipitation of pure pink product was achieved by addition of hexane to a concentrated CH_2Cl_2 solution. Yield: 77%.
^{1}H NMR ($CDCl_3$): δ 18.89 (s, 1H, Ru=C*H*Ph), 7.81 (br s, 1H, *o*-C_6H_5), 7.37 (t, 1H, *p*-C_6H_5), 7.10 (m, 2H, *m*-C_6H_5), 6.90 (s, 1H, *o*-C_6H_5), 6.82 (br s, 1H, $C_6H_2Me_3$), 6.28 (br s, 1H, $C_6H_2Me_3$), 3.95 (m, 2H, MeNCH$_2$C*H*$_2$NMes), 3.82 (s, 3H, NC*H*$_3$), 3.49 (m, 2H, MeNC*H*$_2$CH$_2$NMes), 2.32, 2.17, 1.89, 1.61, 1.27, 1.12, 0.88. ^{31}P NMR ($CDCl_3$): δ 34.92. ^{13}C NMR ($CDCl_3$): δ 294.3-239.4 (broad signal, Ru=*C*HPh), 219.4 (d, $J_{P,C}$ = 74.4 Hz, MeN*C*NMes), 151.0 (*i*-C_6H_5), 137.8, 137.2, 136.5, 130.5, 130.0 (broad), 129.0, 128.3, 127.9, 52.4 (MeNCH$_2$*C*H$_2$NMes), 51.4 (MeN*C*H$_2$CH$_2$NMes), 37.6, 35.9, 35.1, 31.7, 31.5, 31.4, 30.6, 30.1, 29.6, 28.0, 27.1, 26.8, 22.8, 21.1 (*p*-*C*H$_3$), 18.4 (*o*-*C*H$_3$).
Elemental analysis calcd (%) for $C_{38}H_{57}N_2Cl_2PRu$ (744.83): C 61.28, H 7.71, N 3.76; found C 60.98, H 7.55, N 3.60.

Note:
For all of these complexes (**77a-e**) only one ^{31}P signal and one single ^{1}H α-benzylidene signal was found, suggesting that only one single isomer had been formed.

[RuCl$_2$(=CHPh)(IMePrH$_2$)$_2$] 79a
A 0.5 M solution of KHMDS in toluene (2.06 mL, 1.03 mmol) was added to [H$_2$IMePr][Cl] (0.290 g, 1.03 mmol) in 5 mL of dry toluene. The mixture was stirred for 10 min. Complex **1** (0.37 g, 0.450 mmol) was added and the reaction mixture was stirred for 2 h. The solvent was evaporated, followed by addition of 50 mL of diethyl ether. The resulting suspension was filtered to remove salts. The volume of the green filtrate was reduced to ≈10 mL and stored in the fridge overnight. The bis(NHC) complex precipitated as green crystals, which were filtered and washed with hexane (5 mL). Yield: 0.23 g, 69%.

^{1}H NMR ($CDCl_3$): δ 19.01 (s, 1H, Ru=C*H*Ph), 7.45 (m, 2H, aryl-*H*), 7.34 (m, 2H, aryl-*H*), 7.24 (m, 4H, aryl-*H*), 7.13 (m, 3H, aryl-*H*), 3.95 (m, 4H, C*H*(CH_3)$_2$), 3.66 (m, 4H, NC*H*$_2$C*H*$_2$N), 3.47 (m, 4H, NC*H*$_2$C*H*$_2$N), 3.11 (br s, 3H, NC*H*$_3$), 2.12 (br s, 2H, NC*H*$_3$), 1.60 (m, 6H, CH(C*H*$_3$)$_2$), 1.25-1.15 (several peaks, 18H, CH(C*H*$_3$)$_2$), 0.07 (app. s, 1H, H$_{agostic}$). ^{13}C NMR ($CDCl_3$): δ 309.5 (Ru=CHPh), 218.9 (s, MeN*C*NAr), 216.3 (s, MeN*C*NAr), 151.4 (*i*-C_6H_5), 148.5 (Ar-*C*), 148.4 (Ar-*C*), 138.2 (Ar-*C*), 137.3 (Ar-*C*), 129.7 (Ar-*C*), 129.2 (Ar-*C*), 128.9 (Ar-*C*), 128.0 (Ar-*C*), 124.6 (Ar-*C*), 123.6 (Ar-*C*), 54.7 (MeNCH$_2$*C*H$_2$NAr), 53.9 (MeNCH$_2$*C*H$_2$NAr), 51.9 (MeN*C*H$_2$CH$_2$NAr), 51.4 (MeN*C*H$_2$CH$_2$NAr), 37.6 (*C*H$_3$N), 29.3, 27.9, 27.6, 26.6, 23.1.
Elemental analysis calcd (%) for $C_{39}H_{54}N_4Cl_2Ru$ (750.87): C 62.39, H 7.25, N 7.46; found C 62.03, H 7.77, N 7.05.

[RuCl$_2$(=CHPh)(ICyPrH$_2$)$_2$] 79b
Analogously, [H$_2$ICyPr][Cl] (0.345 g, 0.989 mmol) was reacted during 10 min with a 0.5 M solution of KHMDS in toluene (1.98 mL, 0.989 mmol) in 5 mL of dry toluene. After addition of the Ru precursor **1** (0.35 g, 0.426 mmol), the reaction mixture was stirred for an additional 2 h. The solution was filtered to remove residual salts and evaporated to dryness. Acetone was added and the resulting suspension was stirred until a finely ground green precipitate had formed which was filtered and dried thoroughly. Yield: 0.32 g, 84%.
^{1}H NMR ($CDCl_3$): δ 19.22 (s, 1H, Ru=C*H*Ph), 8.64 (br s, 1H, *o*-C_6H_5), 7.45 (t, 2H, aryl-*H*), 7.38 (m, 2H, aryl-*H*), 6.99 (s, 2H, aryl-*H*), 6.82 (s, 2H, aryl-*H*), 6.32 (br s, 2H, aryl-*H*), 4.03 (m, 2H), 3.89 (m, 2H), 3.76 (m, 1H), 3.47 (m, 4H), 3.14 (m, 1H), 2.84 (m, 2H), 2.32 (m, 1H), 1.62 - 0.57 (several peaks, 44H), -0.43 (br m, 1H, H$_{agostic}$). ^{13}C NMR ($CDCl_3$): δ 307.5 (Ru=*C*HPh), 216.1 (CyN*C*NAr), 215.6 (CyN*C*NAr), 149.8 (*i*-C_6H_5), 148.7 (Ar-*C*), 147.4 (Ar-*C*), 146.7 (Ar-*C*), 146.0 (Ar-*C*), 139.4 (Ar-*C*), 137.4 (Ar-*C*), 131.1 (Ar-*C*), 130.0 (Ar-*C*), 128.0 (Ar-*C*), 127.4 (Ar-*C*), 126.9 (Ar-*C*), 125.9 (Ar-*C*), 123.9 (Ar-*C*), 123.4 (Ar-*C*), 57.5 (N*C*H), 56.4 (N*C*H), 53.2 (N*C*H), 53.0 (N*C*H), 43.2 (N*C*H), 42.1 (N*C*H), 32.1, 30.3, 29.6, 28.6, 27.9, 27.4, 27.0, 26.1, 25.8, 25.0, 24.5, 24.0, 23.5, 23.3, 22.7, 21.0.
Elemental analysis calcd (%) for $C_{49}H_{70}N_4Cl_2Ru$ (887.11): C 66.34, H 7.95, N 6.32; found C 66.16, H 7.96, N 6.26.

[RuCl$_2$(=CHPh)(ICyPrH$_2$)(PCy$_3$)] 78b
A solution of bis(NHC) complex **79b** (0.250 g, 0.282 mmol) and tricyclohexylphosphine (0.80 g, 2.853 mmol, 10 equiv) in toluene (10 mL) was stirred at 70 °C for 1 h, during which time it turned red-brown from green. Toluene was removed by evaporation in vacuo, and MeOH (15 mL) was added under vigorous stirring. The resulting suspension was filtered, washed with more MeOH (3 * 5 mL) and dried to give complex **78b** as a light pink powder. Yield: 0.14 g, 59%.
(The yield decreased considerably due to repeated washing with MeOH which was necessary to remove all PCy$_3$). ^{1}H NMR ($CDCl_3$): δ 19.18 (s, 1H, Ru=C*H*Ph),

7.84 (br s, 1H, *o*-C_6H_5), 7.36 (t, 1H, *p*-C_6H_5), 7.04 (m, 2H), 6.94 (br s, 1H), 6.82 (m, 1H), 6.74 (m, 2H), 4.58 (m, 1H, N-C*H*), 3.85 (app. s, 4H, NCH_2CH_2N), 3.27 (m, 2H, C*H*$(CH_3)_2$), 2.45 (d, 2H), 2.09 (m, 2H), 1.88 (m, 2H), 1.75, 1.55, 1.43, 1.23, 1.02 (remaining 49 protons). ^{31}P NMR ($CDCl_3$): δ 25.43. ^{13}C NMR ($CDCl_3$): δ 296.2 (broad signal, Ru=*C*HPh), 213.8 (d, $J_{P,C}$ = 76.0 Hz, CyN*C*NAr), 149.3, 146.5, 135.7, 130.4, 129.0, 128.0, 127.8, 127.6, 126.9, 126.6, 123.4, 122.6, 56.8 (N*C*H), 52.4 (N*C*H), 42.3 (N*C*H), 34.7, 33.9, 31.4, 31.2, 29.3, 28.1, 26.5, 26.4, 26.0-25.1 (several peaks), 24.3, 23.7, 22.2.
Elemental analysis calcd (%) for $C_{46}H_{71}N_2Cl_2PRu$ (855.04): C 64.62, H 8.37, N 3.28; found C 64.05, H 8.36, N 3.22.

Crystallographic data for the structures reported in this chapter have been deposited with the Cambridge Crystallographic Data Centre as supplementary publication no. CCDC-295190 (**77c**), CCDC-623189 (**79a**) and CCDC-623190 (**79b**). Copies of the data can be obtained free of charge on application to CCDC, 12 Union Road, Cambridge CB2 1EZ, UK [fax.: + 44 1223/336-033; e-mail: deposit@ccdc.cam.ac.uk] or via www.ccdc.cam.ac.uk/data_request/cif.

5.4.6 Catalytic reactions

Monitoring ROMP of COD (Figures 5.6, 5.7 and 5.19)

After charging an NMR tube with the appropriate amount of catalyst dissolved in dry, deuterated solvent ($CDCl_3$ or C_6D_6),*cis*-cycloocta-1,5-diene was injected into the tube. The polymerization reaction was monitored as a function of time at 20 °C by integrating olefinic ^{1}H signals of the formed polymer and the disappearing monomer.

Monitoring RCM of diethyl diallylmalonate (Figure 5.9 and 5.20)

An NMR tube was charged with 0.6 mL of a catalyst solution in CD_2Cl_2 (4.52 mM or 0.002712 mmol catalyst). 200 equiv or 0.13 mL of diethyl diallylmalonate was added and the NMR tube was closed. The ethylene generated during the reaction process was not removed so that the RCM reactions were carried out under equilibrium conditions. The progress of the ring closing reaction was monitored at 20 °C by integration of ^{1}H signals of allylic protons of the ring closed product and of the disappearing substrate.

Representative procedure for ROMP tests (Table 5.2 and 5.4)

Small oven-dried glass vials with septum were charged with a stirring bar and the appropriate amount of catalyst taken from a CH_2Cl_2 stock solution. The dichloromethane was subsequently evaporated, and the glass vials with solid catalyst were kept under argon atmosphere. To start the ROMP test, 200 μL

of toluene was added in order to dissolve the catalyst. The appropriate amount of COD monomer was transferred to the vial via syringe. After a certain time span, a small quantity of the reaction mixture, which had become viscous, was taken out of the vial and dissolved in $CDCl_3$. Conversion was then determined by ^{1}H NMR spectroscopy.

Decomposition experiment (Figure 5.11)

30 μmol of catalyst was weighed out in a dry NMR tube and 0.6 mL of C_6D_6 was added. The NMR tube was then closed and decomposition of the catalyst was followed by ^{31}P NMR at 80 °C.

Chapter 6

New NHC Ligands in Hoveyda-Grubbs Catalysts

This chapter reports the structural modification of Hoveyda-Grubbs complexes. The effect of diversified *N*-heterocyclic carbene (NHC) ligands was investigated in representative ROMP, RCM and CM reactions. A pronounced influence on both catalyst activity and selectivity was found to be exerted by the NHC amino substituents, which emphasizes that a rigorously selected steric environment is critical in olefin metathesis catalyst design.

6.1 Introduction

Next to the Grubbs catalysts **1** and **2**, the Hoveyda catalyst **4** and the Hoveyda-Grubbs catalysts **5** and **10** represent an important class of olefin metathesis mediators.[88–91] Their remarkable stability and reactivity toward electron-deficient substrates create an interesting application profile.[330,426] Furthermore, these aryl-ether chelate complexes offer the advantage of possible recovery after reaction, which should be assigned to a release/return mechanism. Steric[92–94] and electronic[95,96,427] effects in the isopropoxystyrene ligand sphere were thoroughly investigated, and were both found to exert a strong influence on catalyst activity. However, steric and electronic effects in the NHC ligand were only scarcely investigated. An intriguing example was given by Blechert et al. who described the *N*-methyl-*N'*-mesityl derived catalyst **80a**, which does not improve the catalytic activity but induces higher selectivity in diastereoselective ring-closing metathesis (RCM) and significantly alters E/Z ratios in cross metathesis (CM).[290] The results described in chapter 5 for Grubbs complexes encouraged us to further explore the effects of similar NHC modifications in Hoveyda-Grubbs catalysts.

Several *N*-alkyl-*N*'-mesityl and *N*-alkyl-*N*'-(2,6-diisopropylphenyl) heterocyclic carbenes were successfully coordinated to **4**. Next to these two types of asymmetrical NHCs, also symmetrical *N*,*N*'-dialkyl heterocyclic carbenes smoothly coordinated to the Hoveyda precursor. As described in chapter 4, the low stability of Grubbs benzylidene complexes **81** and **82** prevented their isolation. The lack of stability was attributed to steric effects resulting in a weakened NHC to metal bond. Likely, the sterically less demanding geometry of Hoveyda-Grubbs complexes explains a herein described more fruitful outcome.

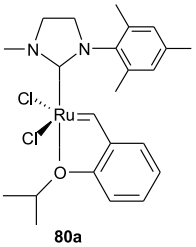

80a

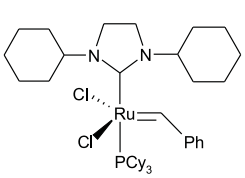

81
unstable

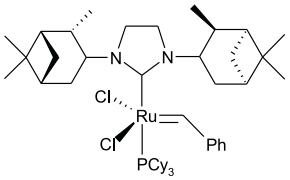

82
unstable

6.2 Results and Discussion

In contrast to complexes **5**, **10** and **80a-c**, which were prepared through an established route involving their Grubbs 2nd generation analogue and CuCl as a phosphine scavenger (Figure 6.1, route A)[90,92–96,427], complexes **84a-b** required an alternative protocol. Since the *N*-alkyl-*N*'-(2,6-diisopropylphenyl) heterocyclic carbenes induce preferential bis-coordination in their reaction with **1**, we disclose an unconventional synthetic strategy which uses the bis(NHC) complexes **79a-b** as starting material. Reaction with an excess of 2-isopropoxystyrene at elevated temperature allows for the decoordination of one NHC ligand with formation of the desired complexes in good yield (Figure 6.1, route B). In addition, a synthetic approach inspired by a procedure described by Blechert et al. proved successful.[91] Treatment of Hoveyda catalyst **4** with the appropriate NHC chloride salt and LiHMDS (lithium hexamethyldisilazane) as a base afforded the intermediates **83a-c**, which were stirred in chloroform to liberate their phosphine ligand (Figure 6.1, route C). Here, it is notheworthy that no bis(NHC) substitution was observed

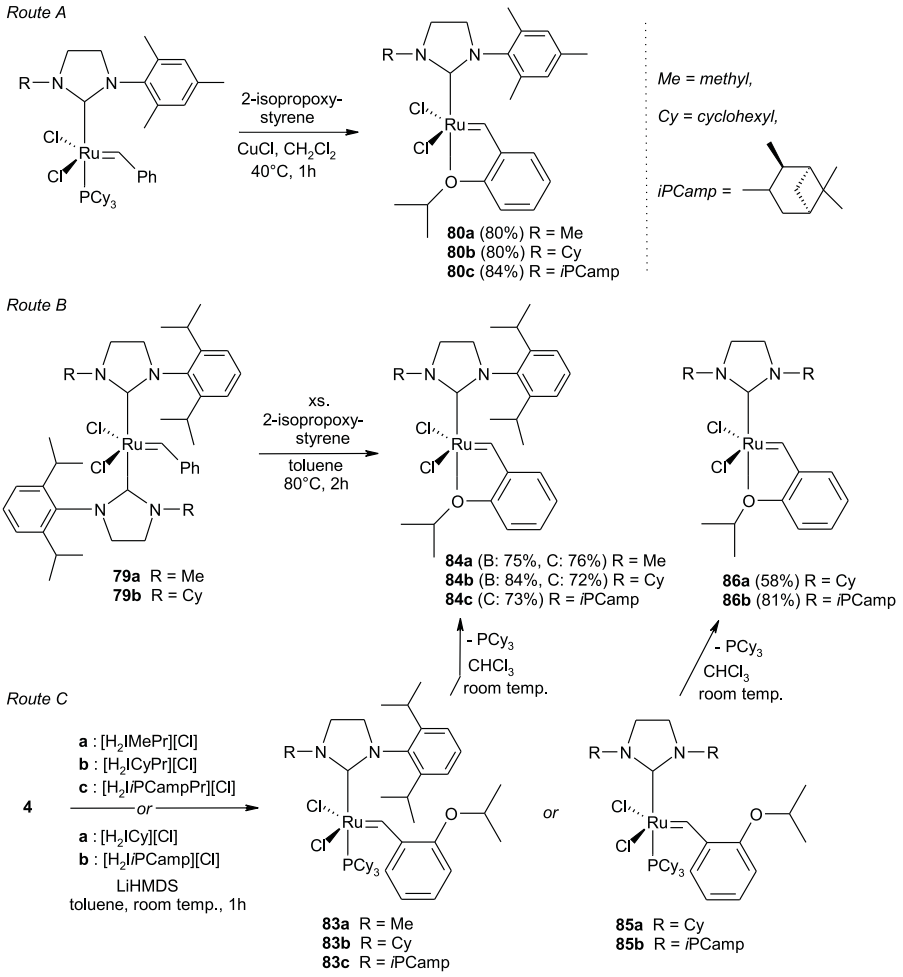

Figure 6.1: Reaction scheme.

during the course of the reaction. This strategy, which circumvents the need for Grubbs precursors **81** and **82**, was also applied to synthesize complexes **86a-b** bearing symmetrical aliphatic NHC ligands.

Single crystals suitable for X-ray crystal-structure analysis were obtained for **80b-c**, **84a-b**, and **86a**. The resulting structures shown in Figures 6.2-6.6 confirm the formation of a single isomer. Selected bond lengths and angles are provided in Table 1. All complexes display a typical distorted square pyramidal coordination with the Cl-atoms trans to one another and the apical position occupied by

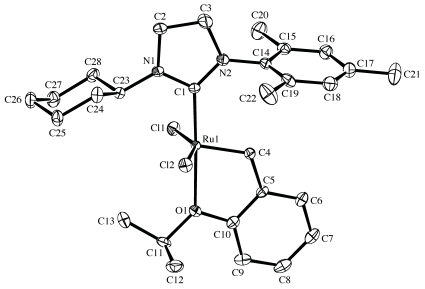

Figure 6.2: The molecular structure of **80b**, showing 50% probability ellipsoids. Hydrogen atoms have been omitted for clarity. Crystals were grown from toluene.

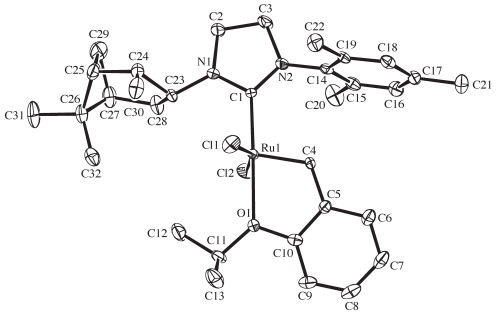

Figure 6.3: The molecular structure of **80c**, showing 50% probability ellipsoids. Crystals were grown from CH_2Cl_2/acetone.

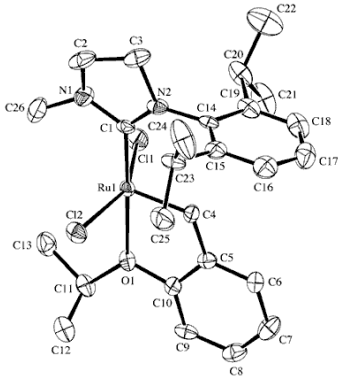

Figure 6.4: The molecular structure of **84a**, showing 50% probability ellipsoids. Crystals were grown from benzene.

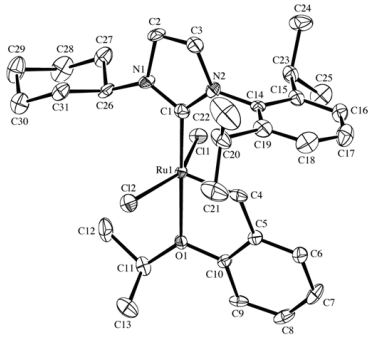

Figure 6.5: The molecular structure of **84b**, showing 50% probability ellipsoids. Crystals were grown from CH_2Cl_2/MeOH.

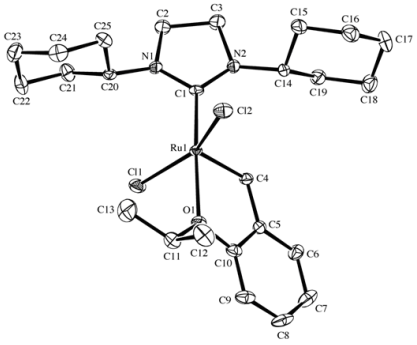

Figure 6.6: The molecular structure of **86a**, showing 50% probability ellipsoids. Crystals were grown from CH_2Cl_2/hexane.

the Ru=C bond. Compared with the standard Hoveyda-Grubbs catalyst **5**, all complexes bearing an aliphatic NHC amino side group are characterized by a slightly decreased Ru-CNN bond length. This indicates a stronger σ-donation of the NHC ligand caused by the aliphatic amino groups. While for complexes **80a-c**, the Ru-O bond remains within the same range as for **5**, a slightly longer bond length is observed for complexes **84a** and **84b**. This is probably due to steric requirements demanded by the presence of a bulkier diisopropylphenyl group.

Remarkably, complexes **80a-c** and **84a-b** all have their aromatic amino side group oriented towards the benzylidene unit. This formation of only one isomer is well precedented in the literature for Grubbs-type complexes, and was assigned to a π-π interaction between the two nearly coplanar aromatic groups.[9,290,332,334] In the here described Hoveyda-Grubbs type complexes the two aromatic groups are arranged almost perpendicularly and the observed molecular feature can thus

	5[a]	**80a**[b]	**80b**	**80c**	**84a**	**84b**	**86a**
Ru=C	1.828(5)	1.821(3)	1.836(2)	1.832(3)	1.839(5)	1.834(6)	1.824(3)
Ru-C	1.981(5)	1.978(3)	1.964(2)	1.973(3)	1.968(6)	1.980(6)	1.972(3)
Ru-O	2.261(3)	2.270(2)	2.266(2)	2.260(2)	2.281(4)	2.297(4)	2.274(2)
N1-C1	1.351(6)	1.341(4)	1.344(3)	1.360(4)	1.353(8)	1.327(8)	1.346(4)
N2-C2	1.350(6)	1.345(4)	1.353(3)	1.349(4)	1.456(9)	1.343(8)	1.348(4)
Cl-Ru-Cl	156.5(5)	153.53(4)	153.19(2)	157.41(3)	151.47(6)	152.08(6)	154.36(3)
C-Ru=C	101.5(14)	102.68(13)	102.9(10)	102.52(11)	101.5(2)	101.20(18)	96.68(13)
C-Ru-O	176.2(14)	178.16(10)	178.04(8)	174.21(11)	178.5(2)	177.8(2)	175.66(10)

Table 6.1: Selected Bond Lengths [Å] and Angles [°] with standard uncertainties in parentheses. [a][90,91], [b][290].

not be ascribed to an intramolecular π-π stacking as stated formerly for Grubbs complexes. In complexes **80a-c** and **84a-b**, the α-benzylidene proton is located directly underneath the *N*-aryl group of the NHC, however, in complex **86a** the *N*-alkyl group is distorted away from the benzylidene unit. This different arrangement reduces the NHC-benzylidene steric interactions and explains the smaller N_2C-Ru=C angle found for complex **86a**.

To explore the catalytic potential of the new complexes, they were compared with the benchmark catalysts **4**, **5** and **10** in a few model olefin metathesis reactions. (Figure 6.7) Figures 6.8 and 6.9 illustrate how the catalysts perform in the ROMP of the low strain *cis,cis*-cycloocta-1,5-diene (COD) under standard conditions. Using a COD/catalyst ratio of 300, the Hoveyda-Grubbs complexes bearing symmetric NHC ligands (**5**, **10**, and **86a-b**) reach full conversion within the first measurement. When a COD/catalyst ratio of 3000 is applied, complexes **86a-b** show an increased activity relative to the classic Hoveyda-Grubbs complexes **5** and **10**. The Hoveyda-Grubbs complexes coordinated with an *N*-alkyl-*N*'-mesityl carbene (**80a-c**) display a higher ROMP activity than the ones substituted with

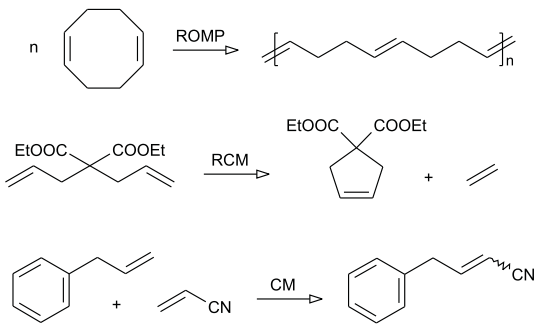

Figure 6.7: Catalytic test reactions.

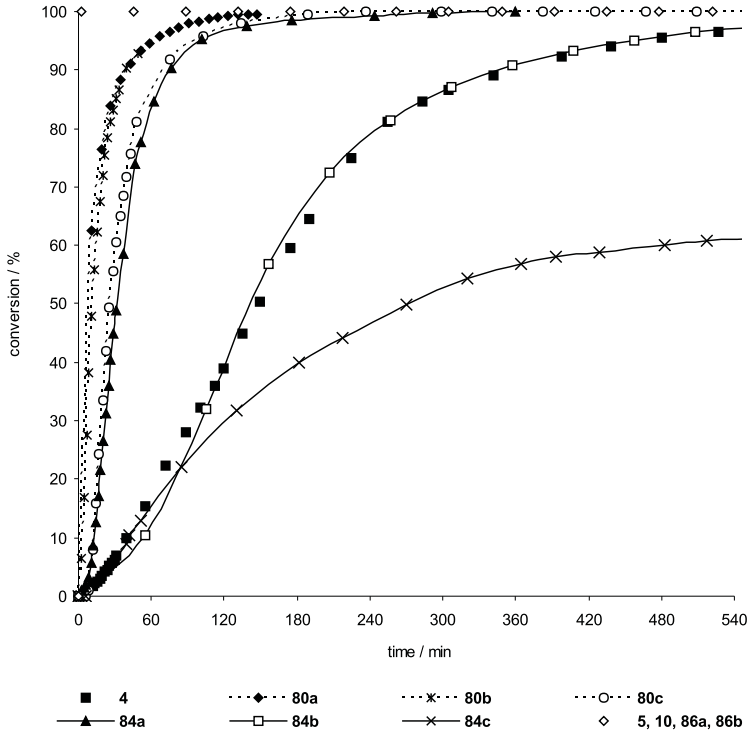

Figure 6.8: Monitoring ROMP of COD via ^{1}H NMR spectroscopy (20 °C), COD/catalyst = 300, catalyst concentration = 4.52 mM, solvent = $CDCl_3$.

N-alkyl-*N*'-(2,6-diisopropylphenyl) carbenes (**84a-c**). Furthermore, complexes **84b** and **27c** fail to reach the reactivity of their phosphine precursor **4**.

The activity trends observed in the RCM of diethyl diallylmalonate (Figure 6.10) are somewhat different from those observed in the ROMP of COD. Originally, we anticipated that changing the electronic nature of the NHC through the introduction of aliphatic groups might positively affect the catalytic activity of the corresponding complexes. However, we came to conclude that the influence of the steric bulk plays a much more compelling role in determining the RCM activity. As the steric bulk of the NHC ligand increases, a decrease in catalyst activity is found. In all three series of catalysts we observe a distinct negative steric bulk - catalytic activity relationship: **80a** > **80b** > **80c**, **84a** > **84b** > **84c**, **86a** > **86b**. It is also noteworthy that the highly ROMP-active complexes **86a-b** display rather modest RCM activity. This substrate specificity likely results from a large steric bulk around the ruthenium center, which hampers coordination of

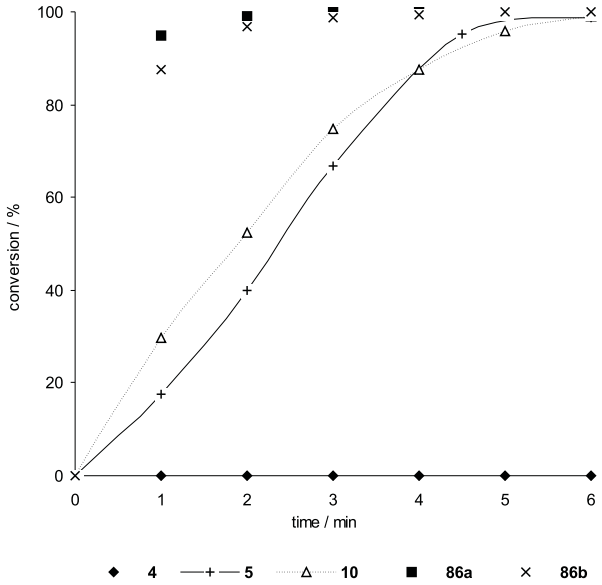

Figure 6.9: Monitoring ROMP of COD via ^{1}H NMR spectroscopy (20 °C), COD/catalyst = 3000, catalyst concentration = 0.452 mM, solvent = $CDCl_3$.

the bulky RCM substrate. A more demanding steric environment stems from the three-dimensional bulk of the aliphatic amino side groups compared with the only two-dimensional bulk of the flat aromatic side groups. This extra bulkiness is expected to cause a greater shielding of the metal center and explains the lower RCM activity of all new complexes compared with the benchmark catalysts **4**, **5** and **10**. These data are in agreement with earlier findings, which indicated that future NHC ligand design should focus on a rigorously selected steric environment, rather than on a tuning of electronic effects.[203,206,329]

Figure 6.11 illustrates the high stability of Hoveyda-Grubbs complexes. Using a temperature of 100 °C, and reaction times of several hours, most of the complexes decompose only with a few %. The robustness of these complexes, particularly in comparison to Grubbs-type complexes (Figure 5.11), results from the chelating character of the 2-isopropoxystyrene ligand, which dissociates reluctantly from the metal center.
The complexes **86a** and **86b** bearing aliphatic NHC ligands are somewhat less stable than the standard Hoveyda-Grubbs complexes **4** and **5**. A lower thermal stability of **80a** and **84a** can be attributed to failure of the small methyl amino group in the NHC ligand to sterically protect the metal center. The relatively low stability of complexes **80a** and **86a** explains the 'flattened' reaction curves

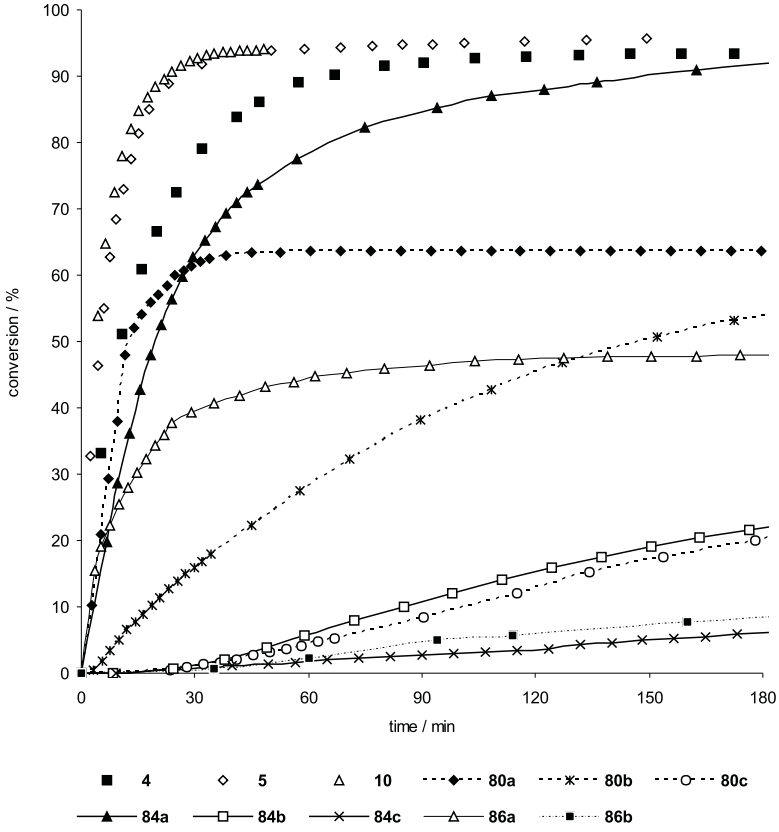

Figure 6.10: Monitoring RCM of diethyl diallylmalonate via ^{1}H NMR spectroscopy (20 °C) - diethyl diallylmalonate/catalyst = 200, catalyst concentration = 4.52 mM, solvent = CD_2Cl_2.

observed in the RCM experiments (Figure 6.10). On the other hand, the low RCM activity found for complexes **80b**, **80c**, **84b**, **84c**, and **86b** is not to be attributed to catalyst decomposition. For these stable complexes, the conversion of the RCM reaction keeps increasing, though at a slow rate, and high conversions are reached when reaction times of one to several days are used.
During the ring-closing reaction of terminal alkenes, a 14-elektron ruthenium methylidene species [$Cl_2LRu{=}CH_2$] is formed *in situ*. Methylidene species are generally very active and very unstable and can only exist in the reaction mixture for short time periods. It is important to note here that the amino side groups of the NHC ligands not only exert a certain influence on the RCM activity of the corresponding complex through steric interactions with the substrate molecule,

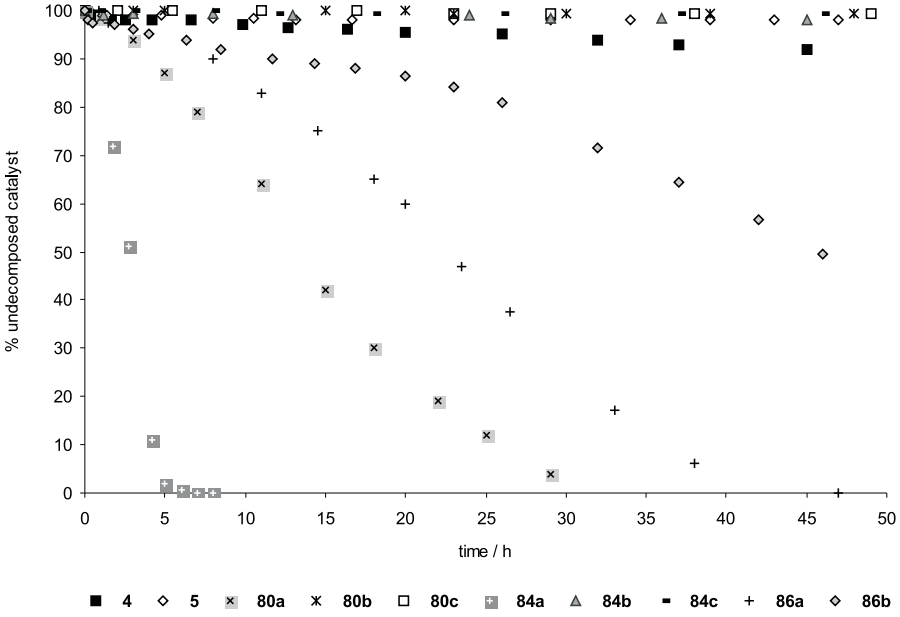

Figure 6.11: Decomposition at 100 °C in toluene-d_8 using coronene as an internal standard.

but possibly also have a substantial impact on the reactivity and stability of the *in situ* formed methylidene species.

The applicability in CM was examined for the challenging substrate acrylonitrile (Table 6.2). The catalytic activity was measured using two catalyst loadings (2.5 and 5 mol%) and compared with the results obtained for the conventional complexes **4**, **5** and **10**. Phosphine complex **4** demonstrates very poor activity; the NHC-bearing complexes show better results. Our modified complexes **80a-c**, **84a-c**, and **86a-b** display lower activity than the classic Hoveyda-Grubbs complexes **5** and **10**, and induce different E/Z selectivities. The complexes bearing symmetric NHC ligands (**5**, **10**, **86a-b**) show higher Z selectivity. For all but one (**80c**) of the complexes coordinated with an asymmetrical NHC, a remarkable E/Z selectivity reversal is observed.
These results demonstrate that changes in the NHC ligand sphere not only alter the catalytic activity of the corresponding complexes, but also induce significant changes in their catalytic selectivity. With this knowledge, it becomes possible to adapt the 2^{nd} generation catalysts for specific organic applications.

Catalyst	Loading(mol%)	Conversion(%)	E/Z ratio
4	5	<2	-
5	2.5	91	0.7/1
10	2.5	93	0.5/1
80a	2.5	20	1.9/1
80a	5	34	1.8/1
80b	2.5	33	1.5/1
80b	5	39	1/1
80c	2.5	43	0.6/1
80c	5	44	0.6/1
84a	2.5	15	2.5/1
84a	5	31	2.8/1
84b	2.5	12	3.2/1
84b	5	26	2.9/1
84c	2.5	21	2.2/1
84c	5	31	2.4/1
86a	2.5	5	0.8/1
86a	5	26	0.6/1
86b	2.5	7	0.5/1
86b	5	30	0.4/1

Table 6.2: CM of allylbenzene and acrylonitrile. 40 °C, 3h, solvent = CH_2Cl_2. Conversion and E/Z ratios determined by ^{1}H NMR. ($ArCH_2R$ protons allylbenzene: δ 3.36, Z-isomer: δ 3.73, E-isomer: δ 3.51.)

6.3 Conclusion

In summary, a comparison between the classical Hoveyda-Grubbs complexes **5**, **10** and complexes **80a-b** and **84a-b** demonstrates that the introduction of one aliphatic group into the NHC framework does not improve the catalytic activity in any of the tested metathesis reactions. The introduction of two aliphatic amino side groups (complexes **86a-b**) enhances the reactivity in the ROMP reaction while the increase of steric interactions lowers the RCM and CM activity. The lower activity of the *N*-alkyl-*N*'-(2,6-diisopropylphenyl) heterocyclic carbene complexes **84a-b** compared with the *N*-alkyl-*N*'-mesityl heterocyclic carbene complexes **80a-b**, may analogously be attributed to a more demanding steric environment. While small differences in donor capacities might cause a significantly different catalytic behavior, it is thus plausible that subtle steric differences exert a more determining influence on the activity of the catalysts. Furthermore, the obtained results confirm that the NHC's amino side groups play a pivotal role in determining the reactivity, selectivity as well as the stability of the corresponding catalysts.

6.4 Experimental Section

6.4.1 General remarks

All reactions and manipulations involving organometallic compounds were conducted in oven-dried glassware under an argon atmosphere using standard Schlenk techniques. Solvents were dried with appropriate drying agents and distilled prior to use. COD and allylbenzene were dried over CaH_2. Acrylonitrile, stabilised with 35-45 ppm hydrochinonmonomethylether, was distilled prior to use.
Complexes **5**[90], **10**[338,428] and **80a**[290] were prepared according to literature procedure. Synthetic procedures for the NHC ligands H_2IMeMes, H_2ICyMes, H_2I*i*PCampMes, H_2IMePr, H_2ICyPr, H_2ICy, and H_2I*i*PCamp were described in chapter 5.

6.4.2 Hoveyda precursor 4

Optimized methods to synthesize the 2-isopropoxystyrene ligand and the Hoveyda complex **4** are described below.

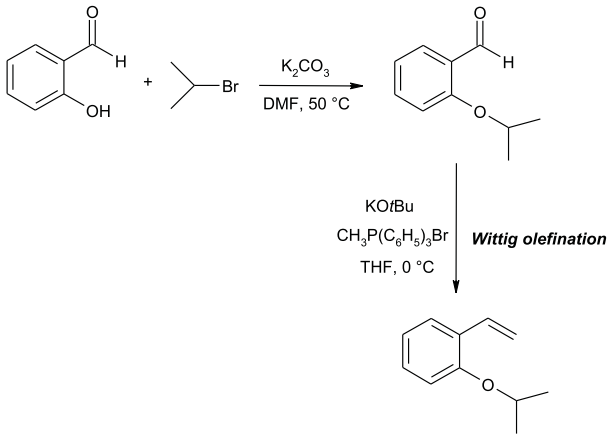

Figure 6.12: Synthesis of 2-isopropoxystyrene.

2-isopropoxybenzaldehyde (alkylation of salicylaldehyde)
To a suspension of salicylaldehyde (2.5 mL, 23.4 mmol), 2-bromopropane (11.1 mL, 117 mmol, 5 equiv) and potassiumcarbonate (6.6 g, 48 mmol, 2 equiv) was added DMF (25 mL). The resulting mixture was stirred at 50 °C during 30 h. Water (60 mL) was added and the reaction mixture was extracted three times with EtOAc. The combined organic extracts were washed with brine and dried over $MgSO_4$. After evaporation of solvents, a yellowish oil was obtained which was used in the next step without further purification. Yield: 61%.
^{1}H NMR ($CDCl_3$): δ 10.50 (s, 1H, O=C*H*), 7.83 (d, 1H, Ar-H), 7.52 (m, 1H,

Ar-H), 6.99 (m, 2H, Ar-H), 4.69 (sept, 1H, C*H*(CH_3)$_2$), 1.41 (d, 6H, CH(C*H*$_3$)$_2$). ^{13}C NMR ($CDCl_3$): δ 190.5 (*C*=O), 136.0 (Ar*C*-O), 128.5 (Ar*C*-CH=O), 120.6 (Ar-C), 114.2 (Ar-C), 71.3 (*C*H(CH_3)$_2$), 22.2 (CH(*C*H_3)$_2$).

2-isopropoxystyrene (Wittig olefination)
A dry flask was charged with KOtBu (2.165 g, 18.33 mmol) and methyltriphenylphosphonium bromide (6.55 g, 18.33 mmol) in dry THF (30 mL) at 0 °C. The resulting suspension was stirred at 0 °C during 15 min. Then a solution of 2-isopropoxybenzaldehyde (1.50 g, 9.16 mmol) in dry THF (10 mL) was added and the mixture was stirred for an additional 15 min at 0 °C. A saturated NH_4Cl solution was poured into the solution, followed by extraction with EtOAc. After evaporation of the solvent, the residue was purified by column chromatography using hexane/EtOAc 2/8 as the eluent. The desired product was obtained as a yellowish oil. Yield: 87%.
^{1}H NMR ($CDCl_3$): δ 7.49 (d, 1H, Ar-H), 7.20 (m, 1H, C*H*=CH_2), 7.06 (t, 1H, Ar-H), 6.89 (m, 2H, Ar-H), 5.73 (d, 1H, CH=C*H*$_2$ *E*), 5.23 (d, 1H, CH=C*H*$_2$ *Z*), 4.54 (sept, 1H, C*H*(CH_3)$_2$), 1.34 (d, 6H, CH(C*H*$_3$)$_2$). ^{13}C NMR ($CDCl_3$): δ 132.2 (Ar-C), 128.9 (Ar-C), 126.7 (Ar-C), 125.3 (*C*H=CH_2), 120.8 (Ar-C), 114.5 (Ar-C), 114.1 (CH=*C*H_2), 71.1 (*C*H(CH_3)$_2$), 22.4 (CH(*C*H_3)$_2$).

Hoveyda precursor 4
Complex **1** (1.31 g, 1.59 mmol), CuCl (0.16 g, 1.61 mmol) and 2-isopropoxystyrene (0.26 g, 1.61 mmol) were stirred in dry CH_2Cl_2 during 1h at 40 °C. The solution was filtered and the solvent removed by evaporation. The crude product was purified by column chromatography (hexane/CH_2Cl_2 : 1/1) and precipitated in pure hexane as a brown solid in good yield (84%). NMR data matched those reported in literature.[88]

6.4.3 1-(2,6-diisopropylphenyl)-3-isopinocampheyl-4,5-dihydroimidazolium chloride

***N*-(2,6-diisopropylphenyl)-*N*'-isopinocampheyl-oxalamide**
N-(2,6-diisopropylphenyl)-oxanilic acid ethyl ester (2.366 g, 8.57 mmol) and (1*R*, 2*R*,3*R*,5*S*)-(-)-isopinocampheylamine (1.51 mL, 1 equiv) were dissolved in toluene (50 mL). To this mixture was added triethylamine (1.27 mL, 1.05 equiv). The suspension was then heated to reflux overnight. EtOAc and 2M HCl were added, followed by extraction. The organic layer was washed with 2M HCl; the aqueous layer with EtOAc. The combined organic layers were dried over $MgSO_4$. The solvent was removed by evaporation, leaving a yellowish solid, which was washed with toluene and hexane. Yield: 73%

^{1}H NMR ($CDCl_3$): δ 8.83 (s, 1H, ArNH), 7.46 (d, 1H, *i*PCampN*H*), 7.34 (t, 1H, Ar-H), 7.21 (d, 2H, Ar-H), 4.31 (m, 1H, N-C*H*), 3.01 (sept, 2H, C*H*(CH_3)$_2$), 2.64 (m, 1H), 2.44 (m, 1H), 1.98 (m, 1H), 1.88 (m, 1H), 1.65 (m, 1H), 1.42 (t, 1H), 1.26

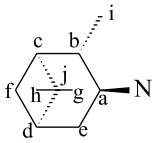

(s, 3H, H_h), 1.20 (d, 12H, $CH(CH_3)_2$), 1.17 (d, 3H, H_i), 1.09 (s, 3H, H_g), 0.94 (d, 1H). ^{13}C NMR ($CDCl_3$): δ 159.9 (NH*C*=O), 159.8 (NH*C*=O), 146.04 (Ar *i*-C), 129.9 (Ar *o*-C), 129.0 (Ar *m*-C), 123.9 (Ar *p*-C), 49.0 (C_a *i*PCamp), 47.9 - 45.8 - 41.6 (C_c, C_b and C_d), 38.6 (C_j), 36.7 (C_e), 35.3 (C_f), 29.1 (*C*H(CH_3)$_2$), 28.2 (C_h), 23.9 (CH(C*H*$_3$)$_2$), 23.7 (C_g), 21.1 (C_i).

1-(2,6-diisopropylphenyl)-3-isopinocampheyl-4,5-dihydroimidazolium chloride [H_2I*i*PCampPr]

To *N*-(2,6-diisopropylphenyl)-*N*'-isopinocampheyl-oxalamide (1.42 g, 3.69 mmol) was added BH_3.THF (1M in THF, 30 mL, 30 mmol, 8 equiv). The resulting solution was refluxed overnight. It was then cooled to room temperature and MeOH was added slowly till all bubbling ceased. Conc. HCl (12M, 1.5 mL) was added and the solvent was removed by evaporation. The resulting solid was redissolved in MeOH and the solvent was again evaporated to remove the boron as $B(OMe)_3$. MeOH was added and removed in this way twice more. The residue was thoroughly dried under vacuum. To the remaining white solid was added triethyl orthoformate (30 mL). The resulting suspension was heated at 120 °C overnight. Then the solvent was removed under reduced pressure. The residue was suspended in Et_2O and the product which precipitated overnight was filtered off and washed with hexane to leave an off-white sticky solid. Yield: 62 %.
^{1}H NMR ($CDCl_3$): δ 10.09 (s, 1H, NC*H*N), 7.42 (t, 1H, Ar-H), 7.24 (m, 2H, Ar-H), 5.37 (m, 1H, N-C_aH), 4.29-4.17 (m, 4H, -NCH_2CH_2N-), 2.97 (sept, 2H, C*H*(CH_3)$_2$), 2.76 (m, 1H), 2.49 (m, 1H), 2.18 (t, 1H), 2.07 (s, 1H), 1.94 (m, 1H), 1.83 (s, 1H), 1.32 (s, 3H, H_h), 1.29 (d, 6H, CH(C*H*$_3$)$_2$), 1.26 (d, 6H, CH(C*H*$_3$)$_2$), 1.22 (d, 3H, H_i), 1.14 (s, 3H, H_g), 0.87 (d, 1H). ^{13}C NMR ($CDCl_3$): δ 160.2 (N*C*HN), 146.4 (Ar i-C), 131.3 (Ar-C), 125.3 (Ar-C), 125.0 (Ar-C), 57.2 (C_a *i*PCamp), 53.2 (*C*H_2NMes), 47.4 (*i*PCamp N*C*H_2), 43.9, 41.5, 40.7 (C_c, C_b and C_d), 38.7 (C_j), 35.4 (C_e), 31.9 (C_f), 29.3 (*C*H(CH_3)$_2$), 29.1 (*C*H(CH_3)$_2$), 28.2 (C_h), 25.4 (CH(*C*H$_3$)$_2$), 25.2 (CH(*C*H$_3$)$_2$), 24.5 (CH(*C*H$_3$)$_2$), 24.2 (CH(*C*H$_3$)$_2$), 23.8 (C_g), 20.1 (C_i).

6.4.4 Complex synthesis

(H_2ICyMes)Cl_2Ru=CH-*o*-O*i*PrC_6H_4 (80b)

(H_2ICyMes)(PCy_3)Cl_2Ru=CHPh **77c** (0.114 g, 0.14 mmol) and CuCl (0.014 g, 0.14 mmol) were weighed into a dry Schlenk flask. 2-isopropoxystyrene (0.023 g, 0.14 mmol) in CH_2Cl_2 (10 mL) was added and the resulting solution was

stirred at 40 °C for 1h. The reaction mixture was filtered and concentrated in vacuo. The crude product was purified by column chromatography using hexane/CH_2Cl_2 (1/1) as an eluent. After concentration of the solvent, the desired complex precipitated as a bright green solid which was filtered and vacuum dried. Yield: 80%.
^{1}H NMR ($CDCl_3$): δ 16.32 (s, 1H, Ru=C*H*), 7.51 (t, 1H, Ar-H), 7.05 (s, 2H, Ar-H), 6.92 (m, 3H, Ar-H), 5.17 (sept, 1H, OC*H*$(CH_3)_2$), 5.06 (m, 1H, N-C*H*(Cy)), 3.94 (app. s., 4H, NCH_2CH_2N), 2.45 (s, 3H, *p*-CH_3), 2.23 (s, 6H, *o*-CH_3), 1.99 (m, 2H), 1.81 (s, 6H, CH_3), 1.56 (m, 6H), 1.26 (m, 2H). ^{13}C NMR ($CDCl_3$): δ 293.3 (Ru=*C*H), 206.8 (CyN*C*NAr), 152.6 (Ar-C), 144.5 (Ar-C), 138.8 (Ar-C), 138.6 (Ar-C), 138.0 (Ar-C), 129.7 (Ar-C), 122.9 (Ar-C), 122.7 (Ar-C), 113.1 (Ar-C), 74.9 (O*C*H(CH_3)2), 61.3 (N*C*H), 51.6 (N*C*H), 43.7 (N*C*H), 31.1 (C-2 Cy), 26.1 (C-3 Cy), 25.8 (C-4 Cy), 22.3 (CH(*C*$H_3)_2$), 21.4 (*p*-*C*H_3), 18.4 (*o*-*C*H_3).
Elemental analysis calcd (%) for $C_{28}H_{38}N_2Cl_2ORu$ (590.6): C 56.94, H 6.49, N 4.74; found C 56.68 H 6.65 N 4.79.

(H_2I*i*PCampMes)Cl_2Ru=CH-*o*-O*i*PrC_6H_4 (80c)
Analogously (H_2I*i*PCampMes)(PCy_3)Cl_2Ru=CHPh **77a** (0.122 g, 0.14 mmol), CuCl (0.014 g, 0.14 mmol) and 2-isopropoxystyrene (0.023 g, 0.14 mmol) afforded complex **80c**, which was purified by column chromatography using hexane/CH_2Cl_2 (1/1) as an eluent. Yield: 84%.
^{1}H NMR ($CDCl_3$): δ 16.39 (s, 1H, Ru=C*H*), 7.52 (t, 1H, Ar-H), 7.06 (s, 1H, Ar-H), 7.05 (s, 1H, Ar-H), 6.91 (m, 3H, Ar-H), 5.52 (m, 1H, N-C$_a$H), 5.12 (sept, 1H, OC*H*$(CH_3)_2$), 4.04-3.95 (m, 4H, NCH_2CH_2N), 3.16 (m, 1H), 2.50 (m, 2H), 2.45 (s, 3H), 2.23 (d, 6H), 2.10 (s, 1H), 1.98 (m, 2H), 1.74 (m, 6H), 1.54 (m, 3H), 1.29 (s, 3H), 1.22 (s, 3H), 0.94 (d, 1H). ^{13}C NMR ($CDCl_3$): δ 294.5 (Ru=*C*H), 209.3 (N*C*N), 152.3, 144.9, 138.8, 138.6, 138.5, 138.3, 129.8, 129.7, 123.0, 122.7, 113.2, 74.9 (O*C*H$(CH_3)_2$), 59.9 (N*C*H), 51.7 (N*C*H), 48.5 (N*C*H), 43.6, 42.0, 41.1, 38.8, 34.4, 34.1, 28.0, 23.8, 22.3, 21.8, 21.4, 18.4.
Elemental analysis calcd (%) for $C_{32}H_{44}N_2Cl_2ORu$ (644.7): C 59.62, H 6.88, N 4.35; found C 58.13 H 6.65 N 4.27.

(H_2IMePr)Cl_2Ru=CH-*o*-O*i*PrC_6H_4 (84a) - Figure 6.1, Route B
Bis(NHC) complex **79a** (0.152 g, 0.20 mmol) and 2-isopropoxystyrene (0.170 g, 1.05 mmol, 5.25 equiv) were weighed into a dry Schlenk flask and dissolved in toluene (5 mL). The solution was heated at 80 °C for 2 h. After evaporation of the solvent, the crude product was purified by column chromatography (hexane/CH_2Cl_2 = 2/3). The product was obtained as a light green solid, and washed with hexane. Yield: 75%.
^{1}H NMR ($CDCl_3$): δ 16.22 (s, 1H, Ru=C*H*), 7.60 (t, 1H, Ar-H), 7.48 (m, 1H, Ar-H), 7.38 (m, 2H, Ar-H), 6.94 (d, 1H, Ar-H), 6.85 (m, 2H, Ar-H), 5.17 (sept, 1H, OC*H*$(CH_3)_2$), 4.02-3.98 (m, 7H, CH_3N and NCH_2CH_2N), 3.14 (m, 2H, C*H*$(CH_3)_2$), 1.80 (d, 6H, OCH(C$H_3)_2$), 1.21 (d, 6H, CH(C$H_3)_2$), 0.86 (d, 6H, CH(C$H_3)_2$). ^{13}C NMR ($CDCl_3$): δ 290.3 (Ru=*C*H), 210.2 (MeN*C*NAr), 152.9,

148.8, 143.5, 137.5, 129.8, 129.6, 125.1, 122.5, 122.3, 113.1, 75.4 (O*C*H$(CH_3)_2$), 55.3 (N*C*H), 51.7 (N*C*H), 38.7 (N*C*H), 28.1 (*C*H$(CH_3)_2$), 25.8 (CH(*C*$H_3)_2$), 24.0 (CH(*C*$H_3)_2$), 22.4 (CH(*C*$H_3)_2$).
Elemental analysis calcd (%) for $C_{26}H_{36}N_2Cl_2ORu$ (564.57): C 55.32, H 6.43, N 4.96; found C 55.32, H 6.43, N 4.94.

(H_2ICyPr)Cl_2Ru=CH-*o*-O*i*PrC_6H_4 (84b) - Route B
Analogously, bis(NHC) complex **79b** (0.207 g, 0.23 mmol) and 2-isopropoxystyrene (0.187 g, 1.15 mmol, 5 equiv) were weighed into a dry Schlenk flask and dissolved in toluene (10 mL). The solution was stirred at 80 °C during 2 h. The reaction mixture was concentrated in vacuo. The dark green residue was purified by column chromatography using hexane/CH_2Cl_2 (1/1) as an eluent. The desired complex was obtained as a bright green solid, which was washed with hexane. Yield: 84%.
^{1}H NMR ($CDCl_3$): δ 16.30 (s, 1H, Ru=C*H*), 7.58 (t, 1H, Ar-H), 7.48 (m, 1H, Ar-H), 7.37 (d, 2H, Ar-H), 6.92 (d, 1H, Ar-H), 6.86 (m, 2H, Ar-H), 5.13 (m, 2H, OC*H*$(CH_3)_2$ and N-C*H*), 3.92 (app. s. 4H, NCH_2CH_2N), 3.11 (m, 2H, C*H*$(CH_3)_2$), 2.51 (m, 2H), 2.00 (m, 2H), 1.81 (d, 6H, OCH(C$H_3)_2$), 1.61 (m, 2H), 1.55 (m, 4H), 1.20 (d, 6H, CH(C$H_3)_2$), 0.87 (d, 6H, CH(C$H_3)_2$). ^{13}C NMR ($CDCl_3$): δ 290.5 (Ru=*C*H), 207.3 (CyN*C*NAr), 152.9, 149.0, 143.9, 137.7, 129.6, 129.4, 125.0, 122.6, 122.4, 113.2, 75.0 (O*C*H$(CH_3)_2$), 61.4 (N*C*H), 54.9 (N*C*H), 43.5 (N*C*H), 31.2, 29.9, 28.1, 26.2, 25.9, 25.8, 24.0, 22.5.
Elemental analysis calcd (%) for $C_{31}H_{44}N_2Cl_2ORu$ (632.69): C 58.85, H 7.01, N 4.43; found C 58.62, H 7.00, N 4.40.

Complexes 84a-c : Route C - General Procedure
Complex **4** (1 equiv) and 1.4 equiv of the appropriate NHC chloride salt were weighed into a dry Schlenk flask, and toluene was added. The resulting suspension was treated with LiHMDS (lithium hexamethyldisilazane, 1.0 M sol. in toluene, 1.4 equiv) and stirred at room temperature for 1 h. The mixture was then filtered to remove residual salts and concentrated in vacuo. The dark green residue was analyzed as a mixture of the phosphine bearing complex **83a/b/c** and the desired complex **84a/b/c**. To achieve full formation of the desired complex, the crude product was dissolved in chloroform and stirred during 1 h. The solution was then evaporated and the remainder was subjected to column chromatography (hexane/CH_2Cl_2 1/1) to obtain pure complexes **84a** (yield 76 %), **84b** (yield 72 %), or **84c** (yield 73 %).

(H_2I*i*PCampPr)Cl_2Ru=CH-*o*-O*i*PrC_6H_4 (84c)
^{1}H NMR ($CDCl_3$): δ 16.36 (s, 1H, Ru=C*H*), 7.59 (t, 1H, Ar-H), 7.48 (m, 1H, Ar-H), 7.38 (d, 2H, Ar-H), 6.91 (d, 1H, Ar-H), 6.85 (m, 2H, Ar-H), 5.57 (m, 1H, N-C_aH), 5.11 (sept, 1H, OC*H*$(CH_3)_2$), 4.02-3.92 (m, 4H, NCH_2CH_2N), 3.14 (m, 3H), 2.50 (m, 2H), 2.11 (s, 1H), 1.98 (m, 2H), 1.77 (d, 6H), 1.57 (m, 3H), 1.30 (s, 3H), 1.22 (m, 9H), 1.05 (m, 1H), 0.89 (d, 6H). ^{13}C NMR ($CDCl_3$): δ 291.2

(Ru=*C*H), 209.8 (N*C*N), 152.7, 148.9, 148.6, 144.2, 138.4, 129.6, 125.0, 122.5, 113.3, 75.1 (O*C*H(CH_3)$_2$), 60.0 (N*C*H), 54.9 (N*C*H), 48.6 (N*C*H), 43.3, 42.0, 41.1, 38.8, 34.5, 34.1, 28.1, 26.0, 25.8, 24.0, 23.8, 22.5, 21.9.
Elemental analysis calcd (%) for $C_{35}H_{50}N_2Cl_2ORu$ (686.78): C 61.21, H 7.34, N 4.08; found C 61.28 H 7.39 N 4.05.

(H_2ICy)Cl_2Ru=CH-*o*-O*i*PrC_6H_4 (86a)
[H_2ICy][BF_4] (0.201 g, 0.624 mmol, 1.4 equiv), complex **4** (0.268 g, 0.446 mmol, 1 equiv) and toluene (5 mL) were placed in a Schlenk flask. LiHMDS (0.624 mL, 0.624 mmol, 1.4 equiv) was added and the resulting suspension was stirred at room temperature for 1 h. The mixture was then filtered and the filtrate was concentrated in vacuo to afford a brownish residue, which was analyzed as the phosphine bearing complex **85a** (benzylidene α-proton: δ 20.82 ppm). Full formation of complex **86a** required stirring in chloroform (20 mL) for 8 h. Purification was achieved by column chromatography with gradient elution (CH_2Cl_2/hexane 3/1 to 100% CH_2Cl_2). The desired complex was obtained as an olive green solid in 58% yield.
^{1}H NMR ($CDCl_3$): δ 18.27 (s, 1H, Ru=C*H*), 7.67 (m, 2H, Ar-H), 7.07 (m, 2H, Ar-H), 5.24 (sept, 1H, OC*H*(CH_3)$_2$), 4.96 (m, 1H, N-C*H*), 4.72 (m, 1H, N-C*H*), 3.68 (m, 4H, NCH_2CH_2N), 2.20 (broad signal, 4H), 1.89 (m, 4H), 1.83 (d, 6H), 1.72 (m, 2H), 1.56 (m, 8H), 1.15 (m, 2H). ^{13}C NMR ($CDCl_3$): δ 287.9 (Ru=*C*H), 203.0 (N*C*N), 153.3, 145.1, 129.8, 123.1, 122.9, 113.6, 75.2 (O*C*H(CH_3)$_2$), 60.0 (broad signal, N*C*H), 57.7 (broad signal, N*C*H), 44.4 (N*C*H), 43.5 (N*C*H), 31.8, 26.0, 25.8, 22.4.
Elemental analysis calcd (%) for $C_{25}H_{38}N_2Cl_2ORu$ (554.57): C 54.15, H 6.91, N 5.05, found C 53.67 H 6.91 N 4.99.

(H_2I*i*PCamp)Cl_2Ru=CH-*o*-O*i*PrC_6H_4 (86b)
[H_2I*i*PCamp][Cl] **75a** (0.173 g, 0.456 mmol, 1.4 equiv) and **4** (0.196 g, 0.326 mmol) were weighed into a dry Schlenk flask and dry toluene (5 mL) was added. The resulting suspension was treated with LiHMDS (0.456 mL of a 1.0 M sol. in toluene, 1.4 equiv) and stirred at room temperature for 1 h. The reaction mixture was filtered to remove residual salts and evaporated. The brownish residue was analyzed as the phosphine bearing complex **85b** (benzylidene α-proton: δ 18.74 ppm). Chloroform (25 mL) was added and the solution was stirred for 1 h at room temperature. The so-formed complex was purified by column chromatography using hexane/CH_2Cl_2 (2/3) as the eluent. After evaporation of the chromatography solvent, the product was obtained as a bright green solid, which was filtered off, washed with hexane and thoroughly dried under vacuum. Yield: 81%.
^{1}H NMR ($CDCl_3$): δ 18.74 (s, 1H, Ru=C*H*), 7.67 (m, 2H, Ar-H), 7.05 (m, 2H, Ar-H), 5.42 (br s, 2H, NC$_a$H), 5.20 (sept, 1H, OC*H*(CH_3)$_2$), 3.84 (m, 4H, NCH_2CH_2N), 2.65 (broad signal, 2H), 2.36 (m, 2H), 2.31 (t, 2H), 1.99 (m, 2H), 1.91 (m, 2H), 1.83-1.78 (m, 12H), 1.47 (d, 6H), 1.23 (s, 6H), 1.02 (m, 2H), 0.94 (d,

2H). ^{13}C NMR ($CDCl_3$): δ 289.9 (Ru=*C*H), 206.3 (N*C*N), 153.3, 145.1, 129.8, 122.9, 121.8, 113.8, 75.4 (O*C*H(CH_3)$_2$), 59.7 (broad signal, N*C*H), 58.1 (broad signal, N*C*H), 48.5 (N*C*H), 43.3, 42.2, 40.4, 38.9, 34.6, 28.3, 23.5, 22.5, 22.2, 21.9. Elemental analysis calcd (%) for $C_{33}H_{49}N_2Cl_2ORu$ (661.75) C 59.90, H 7.46, N 4.23; found C 59.01 H 7.27 N 4.23.

Note:
CCDC-634495, CCDC-634496, CCDC-634497, CCDC-634498, and CCDC-634499 contain the supplementary crystallographic data for this chapter. These data can be obtained free of charge from The Cambridge Crystallographic Data Centre via www.ccdc.cam.ac.uk/data_request/cif.

6.4.5 Catalytic reactions

Monitoring ROMP of COD (Figures 6.8 - 6.9)

After charging an NMR tube with the appropriate amount of catalyst dissolved in $CDCl_3$, *cis*-cycloocta-1,5-diene (COD) was added. The polymerization reaction was monitored as a function of time at 20 °C by integrating olefinic ^{1}H signals of the formed polymer (5.38 - 4.44 ppm) and the consumed monomer (5.58 ppm).

Monitoring RCM of diethyl diallylmalonate (Figure 6.10)

An NMR tube was charged with 0.6 mL of a catalyst solution in CD_2Cl_2 (4.52 mM or 2.712 μmol catalyst per experiment). Next 200 equiv or 0.13 mL of diethyl diallylmalonate was added and the NMR tube was closed and wrapped with parafilm. The progress of the ring-closing reaction was monitored at 25 °C by integration of ^{1}H signals of allylic protons of the ring closed product (2.25 ppm) and of the substrate (2.64 ppm).

Typical procedure for the CM reaction

(Catalyst loading = 2.5 mol%)
A dry Schlenk flask equipped with a reflux condenser was charged with 0.0495 mmol of catalyst in 25 mL of dry CH_2Cl_2. Acrylonitrile (0.14 mL, 2.13 mmol, 43 equiv) and allylbenzene (0.26 mL, 1.96 mmol, 40 equiv) were added and the resulting reaction mixture was stirred at 40 °C during 3 hours. The reaction mixture was analyzed by ^{1}H NMR spectroscopy after evaporation of CH_2Cl_2.

Note: To allow full NMR characterization of the reaction products (*E* and *Z* isomers), the crude reaction mixture was subjected to column chromatography (pentane/Et_2O 9/1):
***Z* isomer** ^{1}H NMR ($CDCl_3$): δ 7.31-7.20 (5H, Ar-H), 6.57 (m, 1H, RC*H*=CHCN), 5.37 (d, 1H, RCH=C*H*CN), 3.73 (d, 2H, ArCH_2). ^{13}C NMR ($CDCl_3$): δ 153.0

(R*C*H=CHCN), 137.1 (Ar-C1), 129.1 (Ar-C3), 128.6 (Ar-C2), 127.3 (Ar-C4), 116.1 (RCH=CH*C*N), 100.2 (RCH=*C*HCN), 38.2 (Ar*C*H_2).
***E* isomer** ^{1}H NMR ($CDCl_3$): δ 7.31-7.18 (5H, Ar-H), 6.82 (m, 1H, RC*H*=CHCN), 5.25 (d, 1H, RCH=C*H*CN), 3.51 (d, 2H, ArCH_2). ^{13}C NMR ($CDCl_3$): δ 154.3 (R*C*H=CHCN), 136.3 (Ar-C1), 129.2 (Ar-C3), 129.0 (Ar-C2), 127.4 (Ar-C4), 117.5 (RCH=CH*C*N), 101.1 (RCH=*C*HCN), 39.6 (Ar*C*H_2).
Determination of the conversion and E/Z ratios during our experiments was then based on the ArCH_2 ^{1}H chemical shifts. (ArCH_2R allylbenzene: δ 3.36, *Z*-isomer: δ 3.73, *E*-isomer: δ 3.51.)

Decomposition experiment (Figure 6.11)

30 μmol of catalyst was weighed out in a dry NMR tube and 0.6 mL of toluene-d_8 along with coronene (^{1}H NMR: δ 8.39 ppm) as an internal standard was added. The NMR tube was then closed and placed in a 100 °C oil bath. Decomposition of the catalysts was measured at different time intervals using ^{1}H NMR spectroscopy. All decomposition reactions were repeated to establish their reproducibility.

Chapter 7

Conclusion

This section summarizes the conclusions and main contributions made throughout the dissertation, and gives a brief outlook for future developments in the field of olefin metathesis.

7.1 Summary

The research presented in this thesis addresses the development of *efficient* catalysts for olefin metathesis reactions. There are several properties such as the stability, reactivity, and selectivity, determining the efficiency of a catalyst (Figure 7.1). Even a minor change in the ligand sphere of the catalyst can significantly alter one of these three aspects, and thus enhance or reduce its efficiency. We focused on ruthenium alkylidene catalysts, which have drawn a lot of attention because they exhibit high reactivity for a variety of metathesis reactions under mild conditions and they are tolerant of many organic functional groups. The electron donating ability and size of the ligands on the Ru center were found to be key in optimizing the catalytic efficiency of these complexes.

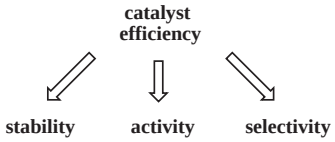

Figure 7.1: Catalyst efficiency

The experimental work done in this thesis was divided into three main parts. In a first part, the development of a phosphine free Schiff base catalyst is described. The chelating Schiff base ligand is responsible for a high stability of the

complex, which goes together with a catalytic inactivity at room temperature. Upon addition of a Brönsted (HCl) or Lewis acid, it was possible to chemically activate the catalyst. Decoordination of the Schiff base imine moiety is then stimulated, generating a catalytically active 14-electron species *in situ*. Such a switchable latent catalyst is beneficial for industrial reaction injection molding (RIM) technology, since it allows for storage of the 'sleeping' catalyst in the ROMP monomer. A cocatalyst (acid) is then brought into a second monomer feed. When both monomer feeds mix in the reaction mold, the polymerization is initiated. The *in situ* generated systems were found to be very active, allowing for the generation of large amounts of polymer using small catalyst loadings. By having such a latent catalyst available, the handling properties of monomer formulations during pot-life and mixing is on a very practical level, while upon deblocking of the catalyst a very fast reaction occurs.
A short ^{1}H NMR spectroscopy investigation gave some more insight in the actual mechanism of the acid activation reaction, and revealed which catalytic species were formed. The addition of HCl (as an Et_2O solution) to the latent catalyst induced decondensation of the Schiff base imine bond. This does imply the reaction with some H_2O present in the commercial HCl solution. Using rigorously dry conditions, a large excess of the acid $HSiCl_3$ was added to the Schiff base catalyst. Surprisingly, the corresponding ^{1}H NMR spectrum did not point to any reaction between acid and catalyst. Still, this mixture polymerized COD without any initiation period, indicating a fast reaction between catalyst and silane. Thereupon the activation was assigned to the reversible formation of an adduct between the Lewis acid and the two electrons on the nitrogen of the Schiff base. Our hypothesis found support in literature, were the reversible reaction between silanes and amines had been evidenced. The formation of a silane-amine complex is expected to prevent electron donation from the basic nitrogen towards the ruthenium center, with formation of a 14-electron catalytically active species. The activation with strong Lewis acids was found to be somewhat less efficient than the silane induced activation, which can be attributed to a faster decomposition of the catalyst. On the other hand, the $HSiCl_3$ activated system retains a high stability, which allows for RCM reactions over a time course of several hours. The coexisting high catalytic activity *and* high stability of this system is quite exceptional, as generally an increased initiation rate goes together with a faster decomposition reaction. The unique reversible formation of a silane-amine complex with a non-covalent intermolecular Si-*N* interaction is held responsible for this beneficial catalytic feature.

In a second part of this thesis was focused on the coordination of saturated NHC ligands to Ru dimer. Our goal was to contribute to the search for new synthetic routes, which circumvent the need for patented Grubbs intermediates. In this context, it was of particular interest to develop a cheaper alternative for the above described industrially relevant Schiff base benzylidene catalyst **36**.

Due to their high catalytic activity and stability, Grubbs benzylidene complexes have drawn large attention. However, their synthesis form a hazardous diazoalkane is of concern. Furthermore, their Ru precursor $RuCl_2(PPh_3)_3$ is air sensitive and necessitates rigorous inert reaction conditions. We were hoping to find a valid alternative for the Grubbs 2nd generation catalyst, which is synthesized through undemanding reactants and intermediates. The easy to handle Ru dimer $[(p\text{-cymene})RuCl_2]_2$ was chosen as a starting material, since it is easy to synthesize and air stable. As the coordination of the saturated NHC ligand H_2IMes was found to be unattainable, bidentate NHC analogues were synthesized instead. These are O-hydroxyaryl substituted NHC ligands, capable of binding with the metal center through the oxygen as well as through the carbene carbon. Their chelating properties improved the stability of the corresponding Ru complexes, allowing for a more successful isolation. These Ru arene complexes displayed negligible olefin metathesis activity in the ROMP of 2-norbornene. Attempts to *in situ* generate a *Ru=C* unit through the addition of TMSD or a terminal alkyne did not substantially improve catalytic activity. Therefore, the complexes were treated with hydrochloric acid to effectuate a breaking of the Ru-O bond. Loss of the chelate effect was expected to lower the extreme stability of our NHC arene complexes, and to increase their metathesis activity. However, the so formed complexes $[(p\text{-cymene})RuCl_2(L)]$, with L = monodentate imidazolinylidene, were found to be very unstable, limiting their utility as catalysts or catalyst precursors. The coordination of H_2IMes or a similar NHC ligand to Ru dimer was thus shown to be troublesome, while the resulting complexes lack stability. In order to come up with an acceptable alternative for the ruthenium benzylidene complexes, it was found necessary to elaborate other synthetic routes.

In an alternative synthetic approach, H_2IMes was succesfully coordinated to an allenylidene complex of type **40** and a vinylidene complex of type **46** respectively. The 2nd and 3rd generation allenylidene complexes afforded substantial olefin metathesis activity, but showed somewhat inferior to the Grubbs catalysts **1**, **2** and **3b**. The corresponding vinylidene complex displayed poor metathesis activity, and indubitably failed to compete with the Grubbs catalysts.

Upon coordination of a Schiff base ligand, the allenylidene analogue of the latent Schiff base benzylidene catalyst **36** (described in chapter 3) was obtained. Where only one isomer of complex **36** was formed, the formation of three isomers was observed for its allenylidene counterpart. The major isomer **61** was isolated, and tested in a few olefin metathesis reactions. The Schiff base allenylidene exhibited a lower latency compared with the benzylidene complex **36** at room temperature. At 40 °C, the complex even almost reached the catalytic activity of its 2nd generation analogue **58**. On the other hand, only low activity was measured in the RCM of diethyl diallylmalonate.

Acids such as HCl and $HSiCl_3$ were found to nourish the metathesis reaction initiated by the new Schiff base complex, but turnover numbers did not meet those obtained for complex **36**. ^{1}H NMR monitoring of the activation reaction revealed that Brönsted acids react directly with the allenylidene unit. This was

confirmed by an ORTEP plot of complex **71**, which resulted from the reaction of allenylidene Schiff base complex **61** and an excess of HCl. The molecular structure of **71** evidenced the protonation of the allenylidene C_β and loss of the Schiff base ligand. A neutral Ru carbyne complex coordinated with 3 chloride ligands was thus formed. This *in situ* formation of an alkylidyne explains an activity enhancement which is less impressive than the activity enhancement found for benzylidene complex **36**.
To avoid the formation of a carbyne species, the acid $HSiCl_3$ was replaced for $PhSiCl_3$. Using this Lewis acid higher turnover numbers (up to 30 000) were reached. One important drawback of this activated catalytic system is that rigorously dry reaction conditions have to be used. The acid can react with water to form HCl, which eventually leads to the generation of a Ru carbyne and lower metathesis activity.

In a third part of this dissertation, small modifications in the *N*-heterocyclic carbene framework were shown to allow fine tuning of Grubbs and Hoveyda-Grubbs catalysts.
Electronic and steric parameters characterizing the NHC ligand can rarely be separated unambiguously. To aim at a good combination of the electronic and steric factors, we thus found it necessary to synthesize a range of different ligands. Three types of new NHCs were synthesized, these are symmetrical *N,N*'-dialkyl carbenes, unsymmetrical *N*-alkyl-*N*'-mesityl carbenes and *N*-alkyl-*N*'-diisopropylphenyl carbenes. When the symmetric aliphatic ligands were reacted with the Grubbs precursor, coordination turned out to be difficult. On the other hand, coordination of the nonsymmetrical NHC ligands proceeded a lot smoother. ORTEP-plots unveiled that intramolecular π-π stacking between an aromatic NHC amino side group and the benzylidene moiety might constitute an important structural element in Grubbs 2nd generation analogues. The absence of such a π-π interaction when introducing *N,N*'-dialkyl carbenes, explains their burdensome coordination and a reduced catalyst stability. While for relatively small aliphatic NHCs such as H_2ICy, H_2I*i*PCamp and H_2I*n*oct some NHC coordination could be evidenced through ^{31}P NMR and ^{1}H NMR spectroscopy, the bulky ligand H_2I*t*Bu did not react at all with the Grubbs precursor **1**. This was rationalized by the higher steric demand of the *N*-*tert*-butyl substituents, causing steric obstruction. Variation of the aliphatic amino side group in *N*-alkyl-*N*'-mesityl carbene ligands was found to exert a critical influence on the olefin metathesis activity of the corresponding catalysts. In the ROMP of cycloocta-1,5-diene (COD), all complexes except for the ones endowed with a steric *N*-*t*butyl-*N*'-mesityl or *N*-adamantyl-*N*'-mesityl carbene showed increased activity relative to their parent complex **1**. The complexes **74** and **77b** are completely inactive at room temperature, and they are green in colour which contrasts with the pinkish colour of catalysts bearing less steric NHCs (**77a**, **77c-e**). This different characteristics were assigned to the three-dimensional bulk of the *tert*-butyl and adamantyl entities which inhibits the

NHC to orient its aliphatic amino group perpendicularly to the imidazoline plane in order to minimize steric interactions. For the more active catalysts **77a** and **77c-e**, a higher initiation rate in comparison to the classic Grubbs 2^{nd} generation catalyst **2** was found in $CDCl_3$ as a solvent. This effect was less pronounced in C_6D_6. Also in the RCM of diethyl diallylmalonate steric effects induced by the NHC amino side groups exert a highly determining influence, this is, more than electronic effects. Catalyst **77e** bearing a small methyl group surpassed the traditional Grubbs catalyst **2** in activity, and displayed a significantly faster initiation. On the other hand, complexes endowed with more crowded NHCs corresponded to lower RCM activity.
Next to the catalytic activity, also the complex stability was found to rely upon the NHC *N*-substituents. Half lifes between ≈10 min (**77a**) and 7 hours (**77b**) were measured at 80 °C.

Unlike the *N*-alkyl-*N*'-mesityl carbenes, *N*-alkyl-*N*'-diisopropylphenyl carbene ligands induced preferential bis-substitution; this is, both phosphine ligands on the Grubbs 1^{st} generation complex were exchanged for an *N*-heterocyclic carbene. The resulting bis(NHC) complexes showed substantial olefin metathesis activity at elevated temperature. One NHC ligand was expected to dissociate from the metal center for the catalyst to be activated. This NHC ligand lability was confirmed by the observation that both NHCs are exchangeable when the complexes are treated with an excess of PCy_3. Furthermore, the heating of a bis(NHC) complex in presence of an excess of phosphine allowed for the isolation of the corresponding mono(NHC) complex. Catalytic test reactions revealed that, resulting from the incorporation of a 2,6-diisopropylphenyl amino side group, this mono(NHC) complex exhibits an irregularly fast initiation, which was held responsible for its tendency to coordinate a second NHC.

The interesting and occasionally surprising features of these new NHC ligands stimulated us to investigate the effect of an additional catalyst modification. The benzylidene unit in the Grubbs complexes was replaced for an isopropoxystyrene ligand. The resulting Hoveyda-Grubbs complexes showed an enhanced stability, while their catalytic activity was again very dependent on the steric and electronic properties of the amino side groups. The coordination of *N*,*N*'-dialkyl carbenes to a Hoveyda-Grubbs precursor was found to be straightforward, which highly contrasts with the more cumbersome coordination described above for Grubbs complexes. The sterically less demanding geometry of Hoveyda-Grubbs complexes likely explains a more fruitful outcome. Two new 2^{nd} generation complexes **86a-b** were synthesized, fully characterized, and tested in different types of metathesis reactions. The catalysts were found inferior to the standard catalyst in the field (complex **5**) for the RCM of diethyl diallylmalonate and the CM of allylbenzene with acrylonitrile. In the ROMP of the low strain cycloocta-1,5-diene (COD), **86a-b** outperformed the classic Hoveyda-Grubbs complexes **4** and **5**. These results demonstrate that the tested metathesis catalysts are substrate specific,

and that none of them is superlative for all substrates.
In addition, we successfully synthesized several Hoveyda-Grubbs complexes bearing *N*-alkyl-*N*'-trimethylphenyl and *N*-alkyl-*N*'-diisopropylphenyl carbenes. Remarkably, these complexes all have their aromatic amino side group oriented towards the benzylidene unit. The formation of only one isomer is well precedented for Grubbs-type complexes, and was assigned to a π-π interaction between the two nearly coplanar aromatic groups. In the here described Hoveyda-Grubbs type complexes the two aromatic groups are arranged almost perpendicularly and the observed arrangement can thus not be ascribed to an intramolecular π-π stacking as stated above for Grubbs complexes. In the ROMP of COD, the complexes coordinated with an *N*-alkyl-*N*'-mesityl carbene displayed a higher activity than the ones substituted with an N-alkyl-N'-(2,6-diisopropylphenyl) carbene. In the RCM of diethyl diallylmalonate, the influence of the steric bulk of the NHC amino side groups was found to play an even more decisive role in determining the activity. As the steric bulk of the NHC ligand increased, a decrease in catalyst activity was found. In the CM of allylbenzene and acrylonitrile the new complexes displayed lower activity than the classic Hoveyda-Grubbs complex **5**, and all but one (**80c**) induced a remarkable E/Z selectivity reversal.

The experimental results as described in chapters 5 and 6 illustrate that the remodeling of the NHC amino side groups alters the reactivity, stability, and selectivity of the corresponding complexes. A better insight was obtained in the factors which determine these three catalyst properties. Steric effects appeared to have a major impact, and were found to be more decisive than electronic effects. Depending on the substrate and the reaction conditions applied, an appropriate choice of the NHC amino groups may thus eventually allow fine tuning. Our results were backed-up by a series of X-ray structures of non-symmetrical complexes that show the benzylidene carbene residing under the aromatic rather than the aliphatic *N*-substituent. This molecular feature was observed in both the Grubbs and Hoveyda-Grubbs type complexes. Furthermore, the observation of a preferential bis-substitution for *N*-alkyl-*N*'-diisopropylphenyl carbene ligands and decoordination of these NHCs at elevated temperature, rejects the generally accepted idea that saturated NHC ligands consistently afford mono(NHC) complexes with strong NHC to metal bonds.
This thesis part described some new results obtained with 'saturated' unsymmetrically substituted NHC ligands in ruthenium metathesis initiators. Our first publication[9] and an almost simultaneous publication by Blechert et al.[290] seems to have inspired other research groups to follow the same strategy (section 2.4.3).[342,356] Hopefully, more positive results will be obtained in this direction, as we are convinced that an improvement in catalyst activity or selectivity constitutes an interesting benefit for organic synthesis applications in particular.

In conclusion, we hope to have successfully contributed to the fascinating chemistry of ligand effects in olefin metathesis catalyst design. Over the last decade

and during the four years of this thesis, the area kept expanding, while more interesting research results are likely to come from various research groups in the near future.

7.2 Outlook

There is no doubt that, over the next years, olefin metathesis will further compete with the more established palladium catalyzed carbon-carbon bond formation reactions and grow as a powerful tool in the hands of many synthetic chemists. The easy handling of ruthenium complexes, also for chemists with minor catalysis experience, and the increasing number of commercially available catalysts will likely broaden the olefin metathesis application profile. While the importance of this reaction type for polymer chemistry has already been widely appreciated for many years, it has started to shape the landscape of synthetic organic chemistry only over the last 15 years.[100] Judging from a short but appealing history, the influence of olefin metathesis transformations in total synthesis is still bound to increase.

In pharmaceutical syntheses the olefin metathesis substrates contain much more functional groups in comparison to the simple molecules used in industrial-scale metathesis polymerizations. As a consequence, more of the catalyst is needed, and quantities often reach a few mole percent. Therefore efforts are being made to create catalysts with longer lifetimes and higher turnover numbers that can be used in parts-per-million amounts. Our group as well as many other academic research groups continue to improve the catalytic performance through a sterical and electronical tuning of the catalyst structures. New ligand design is also being directed by the improved understanding of the decomposition modes of the complexes. Higher turnover numbers resulting from increased catalyts life times are likely to open a number of new opportunities, especially for pharmaceutical companies.

The present metathesis catalyst portfolio contains several efficient Ru systems which are commercially available at reasonable cost. However, this interesting set of catalysts can still be expanded. New or improved synthetic routes with easy to handle starting materials, would circumvent the air sensitive and hazardous compounds that are often necessary in the existing reaction procedures.

The design of chiral NHCs for use in stereoselective catalytic transformations is destined to provide an additional dimension to the field. This area recently expanded dramatically with reports on chiral NHC catalysts providing significant enantioselectivity in hydrogenations, hydrosilylations, phenylations, alkylations and even ring-closing metathesis reactions.[127–131,143,246,429–436] The knowledge gathered on Pd, Rh, and Cu complexes bearing chiral NHCs, is being extended to ruthenium metathesis catalysts. Due to the strong metal-carbene bond, the chiral information is efficiently anchored to the metal center and does not suffer from 'dilution' by dissociation equilibria. The most recent reports by Grubbs et al.

and Collins et al. describe asymmetric ring-closing metathesis, asymmetric ring-opening cross metathesis, and asymmetric cross metathesis reactions with high enantioselectivities, which show great potential for organic synthesists.[83,312,356] Commercialization of these or other enantioselective metathesis intiators, would give an extra boost to the olefin metathesis transformations as synthetic tools in organic synthesis.

Currently, theory is not developed to the stage where it is possible to identify with confidence which ligand combination will afford an attractive metathesis catalyst. The large number of involved parameters challenges the predictive theoretical chemistry, and the discovery of new interesting catalysts is mainly an empirical endeavour. However, recent reports indicate that there exists a certain potential for computer-aided catalyst design.[203] Quantitative structure-property and structure-activity relationships (QSPR/QSAR) based on theoretically generated descriptors could allow for a more cost-efficient optimization of the existing olefin metathesis initiators.

In the context of green chemistry, there should be looked for the best compromise between the catalyst efficiency and the possibility of catalyst recycling. Recycling is becoming more important nowadays as environmental harms increase and as resources are becoming scarcer. Towards this goal, catalyst immobilization by using solid phases, polymers, tagging, and ionic liquids often facilitates recycling.[89,344,437–447] An additional advantage is that immobilized catalysts avoid the formation of ruthenium by-products in the reaction solution. Furthermore, new opportunities for olefin metathesis reactions in high-throughput and continuous-flow reactors are opened up.

Also aqueous olefin metathesis promises a greener approach to the metathesis chemistry and is attractive for biological applications. Aqueous conditions would be particularly useful for ring-closing reactions where highly dilute conditions are required. As the classical Grubbs and Hoveyda-Grubbs catalysts are insoluble in water, a modification of the ligand environment becomes necessary. Several examples already exist[345,346,372,448], and further improvement of their catalytic performances will likely encourage this research area.

With this gathering of examples, it is clear that olefin metathesis catalyst design did not end with the development of the commercially available Grubbs catalysts. New modifications will continue to adapt these catalysts for specific functions, and are bound to further stretch out the field of metathesis applications.

"Following the development of olefin metathesis from an interesting reaction that was only useful for unfunctionalized olefins, used ill-defined catalysts, and proceeded by a totally unknown mechanism to the present highly active, well-defined, functional group tolerant, and mechanistically well understood catalyst systems has been fun. A number of times along the way, I thought the journey was complete. However, the reaction keeps fooling me. It will be interesting to see where it leads next."

R. H. Grubbs
Tetrahedron, **2004**, *60*, 7117-7140

Chapter 8

Nederlandse Samenvatting

8.1 Inleiding

Deze thesis behandelt de ontwikkeling en optimalisatie van katalysatorsystemen voor de olefine metathese reactie. Olefine metathese is één van de belangrijkste reacties in de polymeer en organische chemie waarbij de uitwisseling van substituenten tussen twee olefines resulteert in nieuwe producten (Figure 8.1).

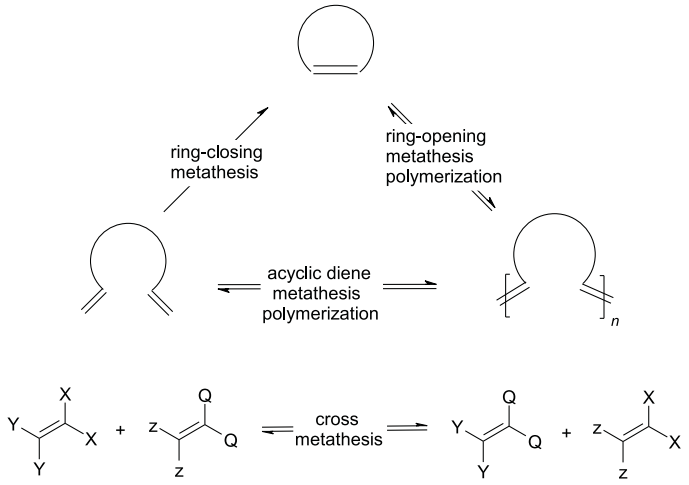

Figure 8.1: Olefine metathese transformaties.

Sinds hun beschrijving door Grubbs et al. hebben de drie generaties Grubbs katalysatoren **1**, **2** en **3** bewezen goede olefine metathese initiators te zijn.[63,65–70]

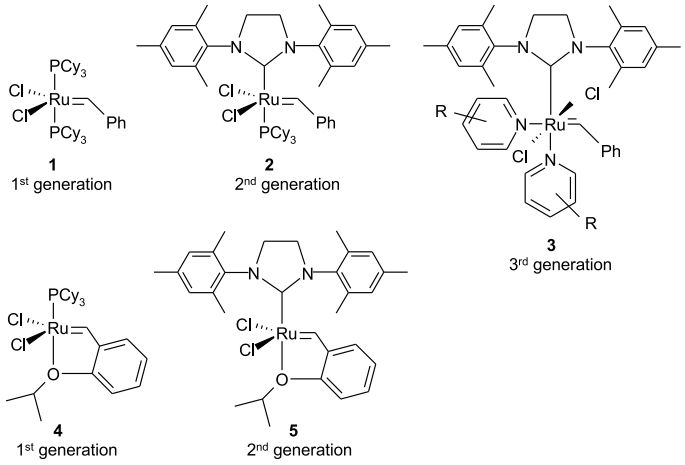

Figure 8.2: Grubbs and Hoveyda-Grubbs katalysatoren.

Deze ruthenium gebaseerde complexen wonnen vooral interesse dankzij hun hoge tolerantie t.o.v. functionele groepen, en hun lagere lucht- en vochtgevoeligheid i.vgl.m. molybdeen of wolfraam gebaseerde complexen.[37,59–61] Een succesvolle modificatie van de Grubbs katalysator bleek mogelijk door de uitwisseling van de benzylideen groep voor een isopropoxystyreen groep. Dit resulteerde in de Hoveyda-Grubbs complexen **4** en **5**, die een hogere robuustheid en recycleerbaarheid vertonen dan hun Grubbs precusoren.[88–91] Bovendien geeft de 2^{de} generatie katalystor **5** aanleiding to selectiviteiten in cross metathese en ring sluitende metathese die niet haalbaar zijn met het benzylideen analoog **2**. Dankzij de commerciële verkrijgbaarheid van de complexen **1**, **2**, **4** en **5** werd het gebruik van de olefine metathese transformatie sterk gestimuleerd. Olefine metathese geeft nu aanleiding tot een meer efficiënte en minder dure industriële productie van polymeren, fijnchemicaliën, pesticides, en farmaceutische intermediairen. De recente Nobel Prijs Chemie (2005) voor Y. Chauvin, R. R. Schrock en R. H. Grubbs als grondleggers van de hedendaagse olefine metathese populariteit, gaf de toenemende industriële interesse een extra boost.[2–4]

Ondanks een opmerkelijke recente progressie, blijft het zoeken naar een verhoogde efficiëntie van de katalytische systemen. Met het oog op commerciële applicaties, wordt elke toename in katalytische efficiëntie van groot belang. Er zijn verschillende eigenschappen zoals de stabiliteit, reactiviteit, en selectiviteit die de efficiëntie van een katalysator bepalen. Zelfs een minieme modificatie in de ligandsfeer van de katalysator kan één van deze drie aspecten significant veranderen, en dus de efficiëntie verhogen of verlagen. De hedendaagse katalysator systemen zijn goed gedefinieerd en het reactiemechanisme is gekend. Dit laat

de ontwikkeling van nieuwe katalysatoren of het verbeteren van bestaande katalytische systemen toe. Daar specifiek gemodelleerde liganden de sleutel zijn tot optimalisatie, werd onze aandacht dan ook vooral gericht op de effecten van ligandmodificaties.

De in dit doctoraat beschreven katalysatoren omvatten ruthenium gebaseerde complexen en zijn een variatie op de gekende Grubbs en Hoveyda-Grubbs 2de generatie katalysatoren. Door de introductie van gemodificeerde liganden was het mogelijk de reactiviteit van de traditionele katalysatoren drastisch te veranderen. Een eerste type ligand dat onze aandacht trok, was een bidentaat Schiffse base ligand. Schiffse basen verhogen sterk de stabiliteit van de corresponderende complexen d.m.v. het chelaat effect. Deze eigenschap werd benut in de ontwikkeling van een latente katalysator, die chemisch wordt geactiveerd door de additie van zuren. Een tweede type ligand dat een voorname rol speelt in het hier beschreven onderzoek zijn *N*-heterocyclische carbeen (NHC) liganden. NHCs werden in de organometaalchemie geïntroduceerd als fosfine mimics maar hebben deze laatste op vele vlakken overtroffen. Algemeen verbetert de incorporatie van een NHC ligand de lucht- en temperatuursgevoeligheid van de complexen en maakt ze meer resistent tegen oxidatie. NHCs zijn sterker gebonden dan fosfines en blijven veelal aan het metaalcentrum gebonden tijdens de katalytische cyclus. Door meerdere variaties in de amino zijgroepen van de NHC liganden aan te brengen, werd gestreefd naar katalysator tuning. Een reeks katalysatoren werd zodoende gesynthetiseerd, gekarakteriseerd met NMR spectroscopie, elementaire analyse en X-straal diffractie, en getest in olefine metathese reacties.
Bij het ontwikkelen van nieuwe systemen, dient men niet enkel te focussen op de katalysatorefficiëntie daar gesofisticeerde complexen veelal te duur zijn voor industriële applicaties. Andere aspecten die aandacht verdienen zijn de kost om de katalysator te maken, de beschikbaarheid van de startmaterialen, en de complexiteit van de synthetische routes. Bovendien is het vaak relevant op zoek te gaan naar patent-vrije syntheses. In deze context kadert een deel van deze thesis waarin een bijdrage in de zoektocht naar alternatieven voor de klassieke ruthenium benzylideen complexen staat beschreven. Het stabiele, eenvoudig aan te maken, Ru dimeer $[(p\text{-cymene})RuCl_2]_2$ werd hierbij als katalystor precursor verkozen.

8.2 Zuuractivatie van een ruthenium Schiffse base complex

In een eerste experimenteel deel van het proefschrift werd een fosfine vrije Schiffse base katalysator ontwikkeld (Figure 8.3). Dit complex vertoont zeer interessante eigenschappen als latente katalysator. Het chelaterend Schiffse base ligand zorgt voor een hoge stabiliteit van het complex, wat tegelijkertijd een katalytische

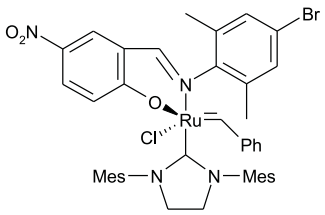

Figure 8.3: Schiffse base katalysator.

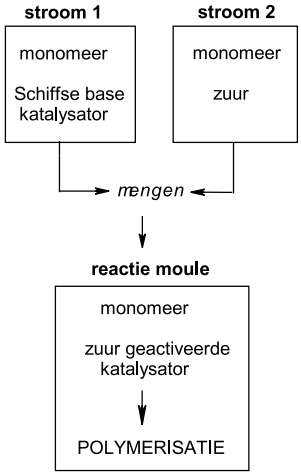

Figure 8.4: RIM proces.

inactiviteit bij kamertemperatuur met zich meebrengt. Door de additie van een Brönsted (HCl) of Lewiszuur (voornamelijk silanen bleken zeer efficiënt) kan het systeem chemisch worden geactiveerd. Decoördinatie van de Schiffse base imine groep wordt gestimuleerd, waarbij het katalytisch actief species *in situ* wordt vrijgesteld. Het gegenereerd systeem bleek zeer actief en liet bovendien het gebruik van lage katalysator loadings toe. Een dergelijk latent systeem is industrieel heel relevant aangezien het stockage van de 'slapende' katalysator in het monomeer toelaat. De co-katalysator (zuur) wordt in een tweede monomeerstroom gebracht. Wanneer beide monomeerstromen mengen in een moule, wordt de polymerisatie geïnitieerd (Figure 8.4). Elaboratie van een dergelijk RIM (Reaction Injection Molding) proces viel buiten de grenzen van dit doctoraatsonderzoek, maar de vermelde resultaten illustreren dat de *in situ* zuuractivatie interessante mogelijkheden met zich meebrengt.

8.3 Alternatieve synthesestrategieën

In een tweede deel van deze thesis werd gestreefd naar het coördineren van een verzadigd NHC ligand op Ru dimeer. Ons doel hierbij was bij te dragen tot de zoektocht naar nieuw synthetische routes, die gepatenteerde Grubbs intermediairen vermijden. Omwille van hun hoge katalytische activiteit en stabiliteit, genieten Grubbs benzylideen complexen aanzienlijke populariteit. Hun synthese via risicovolle diazoalkanen is echter een nadeel. Bovendien is de gebruikte Ru precursor $RuCl_2(PPh_3)_3$ sterk luchtgevoelig en zijn rigoureuze inerte reactie omstandigheden noodzakelijk. We hoopten een alternatief te vinden voor de Grubbs 2^{de} generatie katalysator, dat via weinig veeleisende reactanten en intermediairen kan worden gesynthetiseerd.
Het eenvoudig hanteerbare Ru dimeer (Figuur 8.5) werd als startmateriaal gekozen vermits het moeiteloos kan worden aangemaakt en stabiel is aan de lucht. Daar de coördinatie van het verzadigd NHC ligand bij uitstek, H_2IMes, niet mogelijk bleek, werden bidentate NHC analogen gesynthetiseerd. Dit zijn O-hydroxyaryl gesubstitueerde NHC liganden, die met het metaal centrum kunnen binden via de zuurstof, zowel als via het carbeen atoom (Figuur 8.6). Deze chelaterende eigenschappen verhoogden de stabiliteit van de corresponderende Ru complexen, wat een meer succesvolle isolatie toeliet. De resulterende Ru NHC arene complexen bleken weinig actief in de ROMP van 2-norborneen. Pogingen om *in situ* een *Ru=C* unit te genereren door de additie van TMSD (trimethylsilyl diazomethaan) of een terminaal alkyne, konden de katalytische activiteit niet veel opdrijven. Door behandeling met HCl kon de Ru-O binding worden gebroken. De zo gevormde [(*p*-cymene)$RuCl_2$(L)] complexen, met L = monodentaat imidazolinylideen, vertoonden lagere stabiliteit, wat verwacht werd gepaard te gaan met een verhoogde metathese activiteit. Helaas konden slechts beperkte activiteiten waargenomen worden en bleef het praktisch nut van deze Ru arene complexen als katalysatoren of katalysator precursoren dus beperkt.

Deze observaties toonden aan dat de coördinatie van H_2IMes of een gelijkaardig NHC ligand aan Ru dimeer niet evident is, en dat de resulterende complexen stabiliteit missen. Het werd duidelijk dat om tot een aanvaardbaar alternatief voor

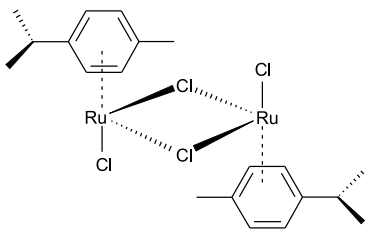

Figure 8.5: Ru dimeer.

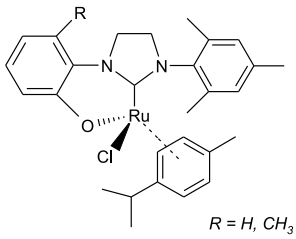

Figure 8.6: NHC arene complexen.

de Ru benzylideen complexen te komen, andere synthetische routes uitgewerkt dienden te worden.
Zodoende werd onze aandacht gericht op een synthetische strategie waarbij eerst een alkylideen eenheid wordt geïntroduceerd en pas daarna, in een tweede stap, de coördinatie van het NHC ligand wordt bewerkstelligd. Daar het 2de generatie vinylideen complex slechts gebrekkige metathese activiteit bleek te bezitten, werd vooral gefocust op allenylideen complexen. Ook deze laatste zijn minder actief dan de traditionele Grubbs benzylideen complexen, maar hun lage kost en meer praktische synthese kunnen hiervoor enigszins compenseren. Bij de coördinatie van een bidentaat Schiffse base ligand aan het allenylideen 3de generatie complex, werd vastgesteld dat drie isomeren werden gevormd. Dit contrasteert met het benzylideen Schiffse base complex eerder vermeld waarvoor slechts één isomeer werd gevonden. De drie isomeren die ons het meest plausibel lijken zijn voorgesteld in figuur 8.7.
D.m.v. kolomchromatografie kon het isomeer dat met het hoogste percentage werd gevormd, succesvol van de andere twee isomeren worden geïsoleerd. Het Schiffse base allenylideen complex werd vervolgens op z'n metathese activiteit getest. In de ROMP van COD bereikte het complex bij 40 °C een aanzienlijke activiteit. In de RCM van diethyl diallylmalonaat werd echter slechts beperkte activiteit gemeten. De additie van HCl of $HSiCl_3$ bleek de metathese reactie te stimuleren, maar turnover numbers (TONs) bleven een stuk lager dan voor het zuurgeactiveerde

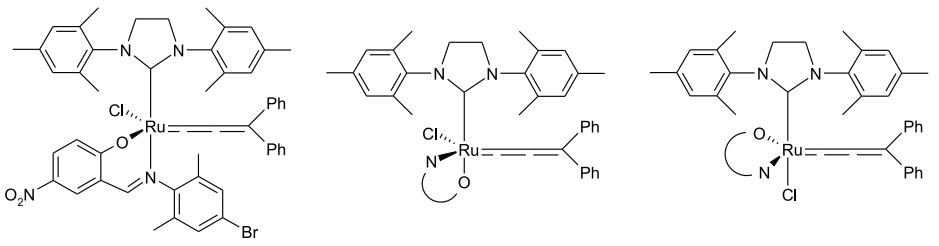

Figure 8.7: Schiffse base allenylideen isomeren.

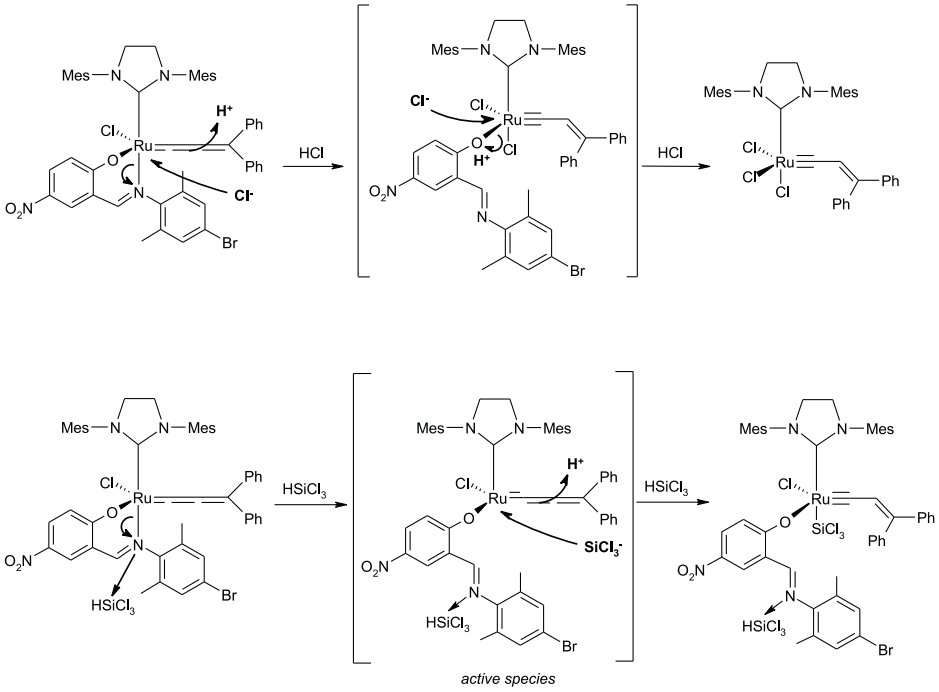

Figure 8.8: De vorming van een Ru carbyne complex.

Schiffse base benzylideen complex. Het volgen van de activatie reactie met behulp van ^{1}H NMR spectroscopie, gaf aan dat een Brönsted zuur met het allenylideen ligand reageert, eerder dan met het Schiffse base ligand (Figuur 8.8). Dit werd bevestigd a.d.h.v. een ORTEP plot van het product in de reactie tussen het Schiffse base allenylideen complex en een overmaat aan HCl. De complexstructuur wees op protonatie van de allenylideen C_β en op decoördinatie van het Schiffse base ligand. Een neutraal ruthenium carbyne complex gecoördineerd met 3 chloride liganden werd aldus gevormd. Deze *in situ* vorming van een alkylidyne verklaart de beperkte activiteitstoename van het Schiffse base allenylideen complex i.vgl.m. het benzylideen complex na toevoegen van een zure cokatalysator. Een meer succesvolle activatie door toevoeging van $HSiCl_3$ (t.o.v. HCl) kan dan worden toegeschreven aan de vorming van een intermediair actief species dat ontstaat door een intermoleculaire Si-N interactie met het Schiffse base ligand (Figuur 8.8). Om de *in situ* vorming van een carbyne species te vermijden, werd het zuur $HSiCl_3$ vervangen door $PhSiCl_3$. Gebruik makend van dit Lewis zuur konden hogere turnover numbers (tot 30 000) worden gehaald. Een belangrijk nadeel van dit zuurgeactiveerd katalytisch systeem is echter dat uiterst droge reactiecondities vereist zijn. Het zuur kan immers met water reageren wat leidt tot het vrijstellen

van HCl. Dit Brönsted zuur veroorzaakt de vorming van het Ru carbyne en geeft dus aanleiding tot lagere metathese activiteit.

8.4 NHCs in Grubbs katalysatoren

Een derde deel van het onderzoek was gericht op de introductie van nieuwe *N*-heterocyclische carbeen (NHC) liganden in Grubbs-type complexen. Drie series liganden werden aangemaakt: symmetrische *N*,*N*'-dialkyl carbenen, asymmetrische *N*-alkyl-*N*'-trimethylphenyl carbenen en *N*-alkyl-*N*'-diisopropylphenyl carbenen. Wanneer de symmetrische alifatische liganden met de Grubbs precursor werden gereageerd, bleek coördinatie zeer moeilijk. Coördinatie van de asymmetrische *N*-alkyl-*N*'-trimethylphenyl carbenen verliep daarentegen heel vlot (Figuur 8.9). Voor elk van de complexen, werd slechts één isomeer gevormd. X-straal analyse gaf te kennen dat het carbeen ligand zo coördineert dat de aromatische mesitylgroep gericht is naar de benzylideengroep. De twee aromatische ringen zijn nagenoeg coplanair wat intramoleculaire π,π-stacking toelaat. De observatie dat π,π-interactie een belangrijk structureel element kan vormen voor Grubbs 2de generatie analogen werd eerder vermeld door Fürstner et al. voor 'onverzadigde' NHCs.[332,334] Het ontbreken van een dergelijke π,π-interactie bij het inbrengen van *N*,*N*'-dialkyl carbenen verklaart de moeizame coördinatie en verlaagde katalysatorstabiliteit.
Bij variatie van de sterische bulk van de alifatische aminogroep in *N*-alkyl-*N*'-trimethylphenyl carbeen liganden, werd vastgesteld dat de activiteit in ROMP (ringopening metathese polymerisatie) en RCM (ringsluitende metathese) testreacties sterk werd beïnvloed. Voor elk van de complexen, behalve complex **b** (Figuur 8.9), werd een hogere ROMP activiteit gemeten t.o.v. het Grubbs startcomplex **1**. De minieme katalytische activiteit van complex **b** kan worden toegekend aan de hogere stericiteit van het NHC ligand. Dit complex is het enige in de serie waar het eerste koolstofatoom in de NHC amino zijgroep gebonden is aan drie andere koolstoffen. Terwijl dus elk ander NHC z'n zijgroep loodrecht op het imidazoline vlak kan richten om sterische interacties te minimaliseren,

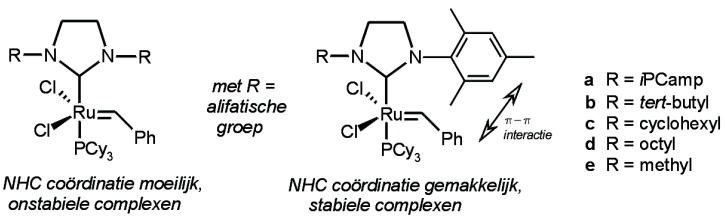

Figure 8.9: Gemodificeerde Grubbs katalysatoren.

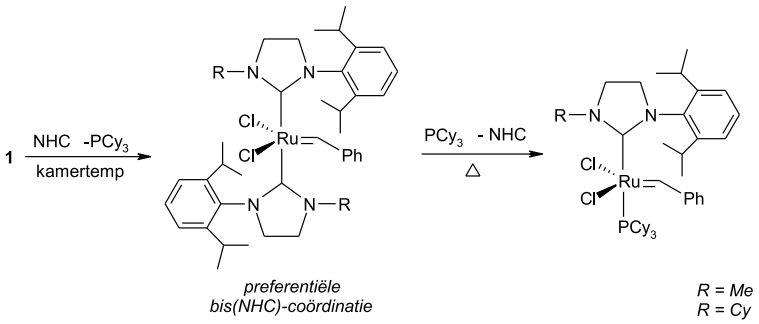

Figure 8.10: *N*-alkyl-*N*'-diisopropylphenyl carbenen in Grubbs katalysatoren.

is deze oriëntatie niet haalbaar voor de *tert*-butyl groep in complex **b**. In de RCM van diethyl diallylmalonaat bleek de activiteit nog meer afhankelijk van de sterische bulk van de NHC amino zijgroep. De meest sterische NHCs komen overeen met de laagste katalytische activiteit, terwijl die sterk toeneemt voor complexen met minder sterische carbeenliganden. De katalysator met een *N*-methyl-*N*'-trimethylphenyl carbeen overtreft hierbij de traditionele Grubbs 2de katalysator **2** in activiteit en vertoont een veel kleinere initiatietijd.
Het derde type ligand, *N*-alkyl-*N*'-diisopropylphenyl carbenen, gaf onverwacht aanleiding tot preferentiële bis-substitutie: Beide fosfine liganden in de Grubbs 1ste generatie precursor werden voor een *N*-heterocyclisch carbeen (NHC) ligand uitgewisseld. Door het bis(NHC) complex te verwarmen in aanwezigheid van een overmaat fosfine was het mogelijk het mono(NHC) complex te isoleren (Figuur 8.10). Katalytische testreacties gaven aan dat dit mono(NHC) complex een ongewoon snelle initiatie vertoont, wat de opmerkelijke neiging tot het coördineren van een tweede NHC ligand kan verklaren. De preferentiële bis-substitutie van *N*-alkyl-*N*'-diisopropylphenyl carbeen liganden en de observatie dat de NHC liganden kunnen decoördineren bij verhoogde temperatuur weerlegden de algemeen aanvaarde idee dat verzadigde NHC liganden mono(NHC) complexen met een moeilijk te breken metaal-NHC binding vormen.

8.5 NHCs in Hoveyda-Grubbs katalysatoren

De interessante en veelal verrassende eigenschappen van deze nieuwe NHC liganden in Grubbs-type complexen stimuleerden ons om het effect na te gaan van een bijkomende katalysatormodificatie: Het benzylidene gedeelte werd vervangen door een isopropoxystyrene ligand. De resulterende aryl-ether chelate complexen vertonen een opmerkelijke stabiliteit, zonder verlies van hun metathese activiteit. Het is opmerkelijk dat voor de complexen **a**-**f** (Figuur 8.11) telkens slechts 1 isomeer wordt gevormd, zijnde het isomeer waarbij de aromatische amino

zijgroep naar dezelfde kant als het isopropoxystyrene ligand is gericht. Deze geometrische schikking werd eerder geobserveerd voor Grubbs-type complexen en werd toegeschreven aan een π,π-interactie tussen de twee nagenoeg planaire aromatische groepen. In de hier beschreven Hoveyda-Grubbs katalysatoren staan de twee aromaten eerder loodrecht t.o.v. elkaar geplaatst, en kan dus de waargenomen oriëntatie van het NHC ligand niet worden toegekend aan een intramoleculaire π,π-stacking zoals eerder gesteld voor Grubbs complexen. Naast deze asymmetrische NHCs werden twee symmetrische alifatische NHC liganden met succes aan de Hoveyda-Grubbs precursor gecoördineerd. In tegenstelling tot de analoge Grubbs complexen die slechts lage stabiliteit vertoonden en daardoor niet geïsoleerd konden worden (vide supra), zijn de complexen **g**-**h** (Figuur 8.11) stabiel en verloopt de ligandsubstitutie vlot. De lagere stabiliteit van de Grubbs complexen kon worden toegeschreven aan een sterisch effect dat de NHC-metaal binding verzwakt, terwijl de sterisch minder veeleisende geometrie van Hoveyda-Grubbs complexen een meer succesvol resultaat verklaart.

Om het katalytisch potentieel van de nieuwe Hoveyda-Grubbs type complexen te exploreren, werden ze in een aantal klassieke olefine metathese reacties getest. De activiteit in de ring-opening metathese polymerisatie en ring-closing metathese werd ook hier sterk beïnvloed door de variatie in de amino zijgroepen van het NHC ligand. In de ROMP van COD vertoonden de complexen gecoördineerd met een *N*-alkyl-*N*-mesityl carbeen (**a**-**c**) een hogere activiteit dan de complexen met een *N*-alkyl-*N*'-diisopropylphenyl carbeen (**d**-**f**). De complexen **g** en **h** overtreffen duidelijk de klassieke Hoveyda-Grubbs katalysatoren **3** en **4**. In de RCM van diethyl diallylmalonaat daarentegen ligt de activiteit lager dan voor de standaard katalysatoren. De sterische bulk van de NHC amino groepen blijkt hier een nog meer beslissende invloed uit te oefenen dan in de ROMP reactie. Waar de bulk van het NHC ligand stijgt, wordt een dalende activiteit gevonden (**a**>**b**>**c** en **d**>**e**>**f**). In de cross metathese reactie van allylbenzeen en acrylonitrile vertonen alle complexen **a**-**h** een lagere activiteit dan complex **4**. Met uitzondering van complex **c**, induceren ze bovendien alle een significant gewijzigde E/Z ratio.

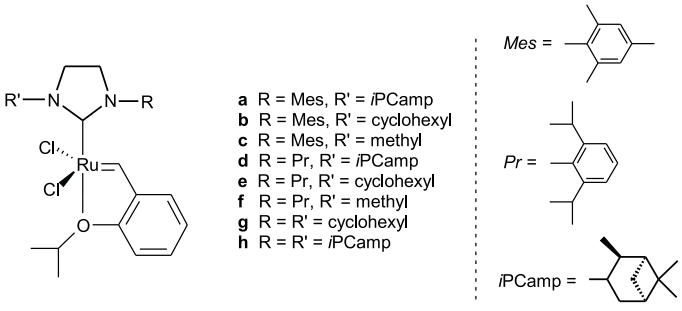

Figure 8.11: Gemodificeerde Hoveyda-Grubbs katalysatoren.

Deze resultaten laten zien dat de getested Hoveyda-Grubbs katalysatoren substraat specifiek zijn, en dat dus geen van hen superieur is voor *alle* metathese reacties. Daarnaast wordt geïllustreerd dat het modelleren van de NHC amino groepen de reactiviteit, stabiliteit en selecticiteit van de corresponderende complexen verandert. Op die manier werd een beter inzicht verkregen in de aard van de factoren die deze eigenschappen bepalen. Sterische effecten bleken hierbij van groot belang, meer dan elektronische effecten.

8.6 Besluit

De voorgestelde onderzoeksresultaten kenschetsen de fascinerende chemie van de olefine metathese reacties en de uitdagende zoektocht naar verbeterde katalysatorsystemen. Het is meer dan waarschijnlijk dat dit onderzoeksdomein z'n grenzen nóg verder zal verleggen met een groeiend aantal toepassingen in vele takken van de chemie. Vermoedelijk, of hopelijk, heeft het beschreven onderzoek hiertoe positief bijgedragen.

References

1. Truett, W. L.; Johnson, D. R.; Robinson, I. M.; Montague, B. A. *J. Am. Chem. Soc.* **1960,** *82,* 2337-2340.
2. Chauvin, Y. *Angew. Chem. Int. Ed.* **2006,** *45,* 3741-3747.
3. Grubbs, R. H. *Angew. Chem. Int. Ed.* **2006,** *45,* 3760-3765.
4. Schrock, R. R. *Angew. Chem. Int. Ed.* **2006,** *45,* 3748-3759.
5. Ledoux, N.; Allaert, B.; Schaubroeck, D.; Monsaert, S.; Drozdzak, R.; Van Der Voort, P.; Verpoort, F. *J. Organomet. Chem.* **2006,** *691,* 5482-5486.
6. Allaert, B.; Dieltiens, N.; Ledoux, N.; Vercaemst, C.; Van Der Voort, P.; Stevens, C. V.; Linden, A.; Verpoort, F. *J. Mol. Cat. A* **2006,** *260,* 221-226.
7. Ledoux, N.; Drozdzak, R.; Allaert, B.; Linden, A.; Van Der Voort, P.; Verpoort, F. *Dalton Trans.* **2007,** in press.
8. Ledoux, N.; Allaert, B.; Verpoort, F. *Eur. J. Inorg. Chem.* **2007,** in press.
9. Ledoux, N.; Allaert, B.; Pattyn, S.; Vander Mierde, H.; Vercaemst, C.; Verpoort, F. *Chem. Eur. J.* **2006,** *12,* 4654-4661.
10. Ledoux, N.; Allaert, B.; Linden, A.; Van Der Voort, P.; Verpoort, F. *Organometallics* **2007,** *26,* 1052-1056.
11. Ledoux, N.; Linden, A.; Allaert, B.; Vander Mierde, H.; Verpoort, F. *Adv. Synth. & Cat.* **2007,** *349,* 1692-1700.
12. Grubbs, R. H.; Chang, S. *Tetrahedron* **1998,** *54,* 4413-4450.
13. Grubbs, R. H. *Tetrahedron* **2004,** *60,* 7117-7140.
14. Fürstner, A. *Angew. Chem. Int. Ed.* **2000,** *39,* 3012-3043.
15. Schuster, M.; Blechert, S. *Angew. Chem. Int. Ed.* **1997,** *36,* 2036-2056.
16. Fürstner, A.; Seidel, G. *J. Organomet. Chem.* **2000,** *606,* 75-78.
17. Lacombe, F.; Radkowski, K.; Seidel, G.; Fürstner, A. *Tetrahedron* **2004,** *60,* 7315-7324.
18. Fürstner, A.; Grela, K. *Angew. Chem. Int. Ed.* **2000,** *39,* 1234-1236.
19. Bunz, U. H. F.; Kloppenburg, L. *Angew. Chem. Int. Ed.* **1999,** *38,* 478-481.
20. Steffen, W.; Köhler, B.; Altmann, M.; Scherf, U.; Stitzer, K.; zur Loye, H.-C.; Bunz, U. H. F. *Chem. Eur. J.* **2001,** *7,* 117-126.
21. Brizius, G.; Pschirer, N. G.; Steffen, W.; Stitzer, K.; zur Loye, H.-C.; Bunz, U. H. F. *J. Am. Chem. Soc.* **2000,** *122,* 12435-12440.
22. Diver, S. T.; Giessert, A. J. *Chem. Rev.* **2004,** *104,* 1317-1382.
23. Lippstreu, J. J.; Straub, B. F. *J. Am. Chem. Soc.* **2005,** *127,* 7444-7457.

24. Mori, M. *J. Mol. Cat. A* **2004,** *213,* 73-79.
25. Diver, S. T. *J. Mol. Cat.: A.* **2006,** *254,* 29-42.
26. Kitamura, T.; Kuzuba, Y.; Sato, Y.; Wakamatsu, H.; Fujita, R.; Mori, M. *Tetrahedron* **2004,** *60,* 7375-7389.
27. Kinoshita, A.; Mori, M. *J. Org. Chem.* **1996,** *61,* 8356-8357.
28. Mori, M.; Kitamura, T.; Sakakibara, N.; Sato, Y. *Org. Lett.* **2000,** *2,* 543-545.
29. Banti, D.; Groaz, E.; North, M. *Tetrahedron* **2004,** *60,* 8043-8052.
30. Boyer, F.-D.; Hanna, I. *Eur. J. Org. Chem.* **2006,** 471-482.
31. Rückert, A.; Eisele, D.; Blechert, S. *Tetrahedron Lett.* **2001,** *42,* 5245-5247.
32. Stragies, R.; Schuster, M.; Blechert, S. *Chem. Commun.* **1999,** 237-238.
33. Connon, S. J.; Blechert, S. *Angew. Chem. Int. Ed.* **2003,** *42,* 1900-1923.
34. Chatterjee, A. K.; Choi, T.-L.; Sanders, D. P.; Grubbs, R. H. *J. Am. Chem. Soc* **2003,** *125,* 11360-11370.
35. Grubbs, R. H.; Miller, S. J.; Fu, G. C. *Acc. Chem. Res.* **1995,** *28,* 446-452.
36. Tallarico, J. A.; Randall, M. L.; Snapper, M. L. *Tetrahedron* **1997,** *53,* 16511-16520.
37. Grubbs, R. H. *Handbook of Metathesis* **2003,** *Wiley-VCH,* volume 1-3.
38. Bielawski, C. W.; Grubbs, R. H. *Prog. Polym. Sci.* **2007,** *32,* 1-29.
39. Schwendeman, J. E.; Church, A. C.; Wagener, K. B. *Adv. Synth. & Cat.* **2002,** *344,* 597-613.
40. Calderon, N.; Chen, H. Y.; Scott, K. W. *Tetrahedron Lett.* **1967,** *34,* 3327-3329.
41. Calderon, N.; Ofstead, E. A.; Ward, J. P.; Judy, W. A.; Scott, K. W. *J. Am. Chem. Soc.* **1968,** 4133-4140.
42. Calderon, N. *Acc. Chem. Res.* **1972,** *5,* 127-132.
43. Grubbs, R. H.; Brunck, T. K. *J. Am. Chem. Soc.* **1972,** *94,* 2538-2540.
44. Grubbs, R. H.; Burk, P. L.; Carr, D. D. *J. Am. Chem. Soc.* **1975,** *97,* 3265-3267.
45. Grubbs, R. H.; Carr, D. D.; Hoppin, C.; Burk, P. L. *J. Am. Chem. Soc.* **1976,** *98,* 3478-3483.
46. Hérisson, J. L.; Chauvin, Y. *Makromol. Chem.* **1971,** *141,* 161-176.
47. Katz, T. J.; McGinnis, J. *J. Am. Chem. Soc.* **1975,** *97,* 1592-1594.
48. Katz, T. J.; Rothchild, R. *J. Am. Chem. Soc.* **1976,** *98,* 2519-2526.
49. Katz, T. J.; McGinnis, J. *J. Am. Chem. Soc.* **1977,** *99,* 1903-1911.
50. Schrock, R. R. *J. Am. Chem. Soc.* **1974,** *96,* 6796-6797.
51. Schrock, R. R.; Rocklage, S.; Wengrovius, J. H.; Rupprecht, G.; Fellmann, J. *J. Mol. Catal.* **1980,** *8,* 73-83.
52. Wengrovius, J. H.; Sancho, J.; Schrock, R. R. *J. Am. Chem. Soc.* **1981,** *103,* 3932-3934.
53. Schrock, R. R.; DePue, R. T.; Feldman, J.; Schaverien, C. J.; Dewan, J. C.; Liu, A. H. *J. Am. Chem. Soc.* **1988,** *110,* 1423-1435.
54. Schrock, R. R. *Acc. Chem. Res.* **1990,** *23,* 158-165.
55. Schrock, R. R. *Tetrahedron* **1999,** *55,* 8141-8153.

56. Schrock, R. R. *J. Mol. Cat. A.* **2004,** *213,* 21-30.
57. Schrock, R. R.; Hoveyda, A. H. *Angew. Chem. Int. Ed.* **2003,** *42,* 4592-4633.
58. Schrock, R. R.; Murdzek, J. S.; Bazan, G. C.; Robbins, J.; DiMare, M.; O'Regan, M. *J. Am. Chem. Soc.* **1990,** *112,* 3875-3886.
59. Kirkland, T. A.; Lynn, D. M.; Grubbs, R. H. *J. Org. Chem.* **1998,** *63,* 9904-9909.
60. Trnka, T. M.; Grubbs, R. H. *Acc. Chem. Res.* **2001,** *34,* 18-29.
61. Chatterjee, A. K.; Morgan, J. P.; Scholl, M.; Grubbs, R. H. *J. Am. Chem. Soc.* **2000,** *122,* 3783-3784.
62. Nguyen, S. T.; Johnson, L. K.; Grubbs, R. H.; Ziller, J. W. *J. Am. Chem. Soc.* **1992,** *114,* 3974-3975.
63. Schwab, P.; Grubbs, R. H.; Ziller, J. W. *J. Am. Chem. Soc.* **1996,** *118,* 100-110.
64. Weskamp, T.; Schattenmann, W. C.; Spiegler, M.; Herrmann, W. A. *Angew. Chem. Int. Ed.* **1998,** *37,* 2490-2493.
65. Scholl, M.; Trnka, T. M.; Morgan, J. P.; Grubbs, R. H. *Tetrahedron Lett.* **1999,** *40,* 2247-2250.
66. Huang, J.; Stevens, E. D.; Nolan, S. P.; Peterson, J. L. *J. Am. Chem. Soc.* **1999,** *121,* 2674-2678.
67. Scholl, M.; Ding, S.; Lee, C. W.; Grubbs, R. H. *Org. Lett.* **1999,** *1,* 953-956.
68. Sanford, M. S.; Love, J. A.; Grubbs, R. H. *Organometallics* **2001,** *20,* 5314-5318.
69. Love, J. A.; Morgan, J. P.; Trnka, T. M.; Grubbs, R. H. *Angew. Chem. Int. Ed.* **2002,** *41,* 4035-4037.
70. Choi, T.-L.; Grubbs, R. H. *Angew. Chem. Int. Ed.* **2003,** *42,* 1743-1746.
71. Seiders, T. J.; Ward, D. W.; Grubbs, R. H. *Org. Lett.* **2001,** *3,* 3225-3228.
72. Romero, P. E.; Piers, W. E.; McDonald, R. *Angew. Chem. Int. Ed.* **2004,** *43,* 6161-6165.
73. Dubberley, S. R.; Romero, P. E.; Piers, W. E.; McDonald, R.; Parvez, M. *Inorg. Chim. Acta* **2006,** *359,* 2658-2664.
74. van der Schaaf, P. A.; Kolly, R.; Kirner, H.-J.; Rime, F.; Mühlebach, A.; Hafner, A. *J. Organomet. Chem.* **2000,** *606,* 65-74.
75. Conrad, J. C.; Amoroso, D.; Czechura, P.; Yap, G. P. A.; Fogg, D. E. *Organometallics* **2003,** *22,* 3634-3636.
76. Conrad, J. C.; Parnas, H. H.; Snelgrove, J. L.; Fogg, D. E. *J. Am. Chem. Soc.* **2005,** *127,* 11882-11883.
77. Slugovc, C.; Perner, B.; Stelzer, F.; Mereiter, K. *J. Am. Chem. Soc.* **2004,** *23,* 3622-3626.
78. Jafarpour, L.; Schanz, H.-J.; Stevens, E. D.; Nolan, S. P. *Organometallics* **1999,** *18,* 5416-5419.
79. Fürstner, A.; Guth, O.; Düffels, A.; Seidel, G.; Liebl, M.; Gabor, B.; Mynott, R. *Chem. Eur. J.* **2001,** *7,* 4811-4820.
80. Hansen, S. M.; Rominger, F.; Metz, M.; Hofmann, P. *Chem. Eur. J.* **1999,** *5,* 557-566.

81. Wolf, J.; Stüer, W.; Grünwald, C.; Werner, H.; Schwab, P.; Schulz, M. *Angew. Chem. Int. Ed* **1998,** *37,* 1124-1126.
82. Stüer, W.; Wolf, J.; Werner, H.; Schwab, P.; Schulz, M. *Angew. Chem. Int. Ed* **1998,** *37,* 3421-3423.
83. Funk, T. W.; Berlin, J. M.; Grubbs, R. H. *J. Am. Chem. Soc.* **2006,** *128,* 1840-1846.
84. Forman, G. S.; McConell, A. E.; Hanton, M. J.; Slawin, A. M. Z.; Tooze, R. P.; Janse van Rensburg, W.; Meyer, W. H.; Dwyer, C.; Kirk, M. M.; Serfontein, D. W. *Organometallics* **2004,** *23,* 4824-4827.
85. Barbasiewicz, M.; Szadkowska, A.; Bujok, R.; Grela, K. *Organometallics* **2006,** *25,* 3599-3604.
86. Harrity, J. P. A.; Visser, M. S.; Gleason, J. D.; Hoveyda, A. H. *J. Am. Chem. Soc.* **1997,** *119,* 1488-1489.
87. Harrity, J. P. A.; La, D. S.; Cefalo, D. R.; Visser, M. S.; Hoveyda, A. H. *J. Am. Chem. Soc.* **1998,** *120,* 2343-2351.
88. Kingsbury, J. S.; Harrity, J. P. A.; Bonitatebus, P. J.; Hoveyda, A. H. *J. Am. Chem. Soc.* **1999,** *121,* 791-799.
89. Kingsbury, J. S.; Hoveyda, A. H. *J. Am. Chem. Soc.* **2005,** *127,* 4510-4517.
90. Garber, S. B.; Kingsbury, J. S.; Gray, L. B.; Hoveyda, A. H. *J. Am. Chem. Soc.* **2000,** *122,* 8168-8179.
91. Gessler, S.; Randl, S.; Blechert, S. *Tetrahedron Lett.* **2000,** *41,* 9973-9976.
92. Wakamatsu, H.; Blechert, S. *Angew. Chem. Int. Ed.* **2002,** *41,* 794-796.
93. Wakamatsu, H.; Blechert, S. *Angew. Chem. Int. Ed.* **2002,** *41,* 2403-2405.
94. Dunne, A. M.; Mix, S.; Blechert, S. *Tetrahedron Lett.* **2003,** *44,* 2733-2736.
95. Grela, K.; Harutyunyan, S.; Michrowska, A. *Angew. Chem. Int. Ed.* **2002,** *41,* 4038-4040.
96. Michrowska, A.; Bujok, R.; Harutyunyan, S.; Sashuk, V.; Dolgonos, G.; Grela, K. *J. Am. Chem. Soc.* **2004,** *126,* 9318-9325.
97. Gulajski, L.; Michrowska, A.; Bujok, R.; Grela, K. *J. Mol. Cat. A.* **2006,** *254,* 118-123.
98. Bieniek, M.; Michrowska, A.; Gulajski, L.; Grela, K. *Organometallics* **2007,** *26,* 1096-1099.
99. Zaja, M.; Connon, S. J.; Dunne, A. M.; Rivard, M.; Buschmann, N.; Jiricek, J.; Blechert, S. *Tetrahedron* **2003,** *59,* 6545-6558.
100. Nicolaou, K. C.; Bulger, P. G.; Sarlah, D. *Angew. Chem. Int. Ed.* **2005,** *44,* 4490-4527.
101. Mol, J. C. *J. Mol. Cat. A* **2004,** *213,* 39-45.
102. Frenzel, U.; Nuyken, O. *J. Polym. Sci. Part A: Polym. Chem.* **2002,** *40,* 2895-2916.
103. Hafner, A.; Mühlebach, A.; van der Schaaf, P. A. *Angew. Chem. Int. Ed.* **1997,** *360,* 2121-2124.
104. Fürstner, A.; Leitner, A. *Angew. Chem. Int. Ed.* **2003,** *42,* 308-311.
105. Fürstner, A.; Jeanjean, F.; Razon, P.; Wirtz, C.; Mynott, R. *Chem. Eur. J.* **2003,** *9,* 307-319.

106. Fürstner, A.; Jeanjean, F.; Razon, P. *Angew. Chem. Int. Ed.* **2002,** *41,* 2097-2101.
107. Fürstner, A.; Jeanjean, F.; Razon, P.; Wirtz, C.; Mynott, R. *Chem. Eur. J.* **2003,** *9,* 320-326.
108. Andreana, P. R.; McLellan, J. S.; Chen, Y.; Wang, P. G. *Org. Lett.* **2002,** *4,* 3875-3878.
109. Felpin, F. X.; Lebreton, J. *Eur. J. Org. Chem.* **2003,** 3693-3712.
110. Mohapatra, D. K.; Ramesh, D. K.; Giardello, M. A.; Chorghade, M. S.; Gurjar, M. K.; Grubbs, R. H. *Tetrahedron Lett.* **2007,** *48,* 2621-2625.
111. *EP993465, US6407190, WO9900396* .
112. Katayama, H.; Nagao, M.; Ozawa, F. *Organometallics* **2003,** *22,* 586-593.
113. *CN2005100803792, PCT patent application for WO and USA in process* .
114. *WO9951344* .
115. Kadyrov, R.; Almena, J.; Monsees, A.; Riermeier, T. *Chemistry Today* **2006,** *24/5,* 14-15.
116. Briel, O. *Chemistry Today* **2006,** *24/5,* 18-19.
117. Clavier, H.; Nolan, S. P. *Chem. Eur. J.* **2007,** in press.
118. Tsantrizos, Y. S.; Ferland, J.-M.; McClory, A.; Poirier, M.; Farina, V.; Yee, N. K.; Wang, X.-J.; Haddad, N.; Wei, X.; Xu, J.; Zhang, L. *J. Organomet. Chem.* **2006,** *691,* 5163-5171.
119. Herrmann, W. A. *Angew. Chem. Int. Ed.* **2002,** *41,* 1290-1309.
120. Markó, I. E.; Stérin, S.; Buisine, O.; Mignani, G.; Branlard, P.; Tinant, B.; Declerq, J.-P. *Science* **2002,** *298,* 204-206.
121. Hillier, A. C.; Lee, H. M.; Stevens, E. D.; Nolan, S. P. *Organometallics* **2001,** *20,* 4246-4252.
122. Lee, H. M.; Jiang, T.; Stevens, E. D.; P., N. S. *Organometallics* **2001,** *20,* 1255-1258.
123. Vasquez-Serrano, L. D.; Owens, B. T.; Buriak, J. M. *Chem. Commun.* **2002,** 2518-2519.
124. Grasa, G.; Viciu, M. S.; Huang, J.; Nolan, S. P. *J. Org. Chem.* **2001,** *66,* 7729-7737.
125. Grasa, G.; Viciu, M. S.; Huang, J.; Zhang, C.; Trudell, M. L.; Nolan, S. P. *Organometallics* **2002,** *21,* 2866-2873.
126. Navarro, O.; Kelly III, R.; Nolan, S. P. *J. Am. Chem. Soc.* **2003,** *125,* 16194-16195.
127. César, V.; Bellemin-Laponnaz, S.; Gade, L. *Chem. Soc. Rev.* **2004,** *33,* 619-636.
128. Enders, D.; Balensiefer, T. *Acc. Chem. Res.* **2004,** *37,* 534-541.
129. Perry, M. C.; Burgess, K. *Tetrahedron: Asymm.* **2003,** *14,* 951-961.
130. Lee, S.; Hartwig, J. F. *J. Org. Chem.* **2001,** *66,* 3402-3415.
131. Herrmann, W. A.; Baskakov, D.; Herdtweck, E.; Hoffmann, S. D.; Bunlaksananusorn, T.; Rampf, F.; Rodefeld, L. *Organometallics* **2006,** *25,* 2449-2456.
132. Huang, J.; Schanz, H.-J.; Stevens, E. D.; Nolan, S. P. *Organometallics*

1999, *18,* 2370-2375.
133. Jafarpour, L.; Nolan, S. P. *Adv. Organomet. Chem.* **2001,** *46,* 181-222.
134. Dorta, R.; Stevens, E. D.; Scott, N. M.; Costabile, C.; Cavallo, L.; Hoff, C. D.; Nolan, S. P. *J. Am. Chem. Soc.* **2005,** *127,* 2485-2495.
135. Díez-González, S.; Nolan, S. *Coord. Chem. Rev.* **2006,** *251,* 874-883.
136. Herrmann, W. A.; Köcher, C. *Angew. Chem. Int. Ed.* **1997,** *36,* 2162-2187.
137. Arduengo, A. J. *Acc. Chem. Res.* **1999,** *32,* 913-921.
138. Bourissou, D.; Guerret, O.; Gabbaï, F. P.; Bertrand, G. *Chem. Rev.* **2000,** *100,* 39-91.
139. Denk, M. K.; Rodezno, J. M.; Gupta, S.; Lough, A. J. *J. Organomet. Chem.* **2001,** *617-618,* 242-253.
140. Arduengo III, A. J.; Dias, H. V. R.; Harlow, R. L.; Kline, M. *J. Am. Chem. Soc.* **1992,** *114,* 5530-5534.
141. Arduengo III, A. J.; Goerlich, J. G.; Marshall, W. *J. Am. Chem. Soc.* **1991,** *113,* 361-363.
142. Enders, D.; Breuer, K.; Raabe, G.; Runsink, J.; Teles, J. H.; Melder, J.-P.; Ebel, K.; Brode, S. *Angew. Chem. Int. Ed.* **1995,** *34,* 1021-1023.
143. Enders, D.; Gielen, H. *J. Organomet. Chem.* **2001,** *617-618,* 70-80.
144. Altenhoff, G.; Goddard, R.; Lehmann, C. W.; Glorius, F. *Angew. Chem. Int. Ed.* **2003,** *42,* 3690-3693.
145. Altenhoff, G.; Goddard, R.; Lehmann, C. W.; Glorius, F. *J. Am. Chem. Soc.* **2004,** *126,* 15195-15201.
146. Alcarazo, M.; Roseblade, S. J.; Cowley, A. R.; Fernández, R.; Brown, J. M.; Lassaletta, J. M. *J. Am. Chem. Soc.* **2005,** *127,* 3290-3291.
147. Herrmann, W. A.; Goossen, L. J.; Artus, G. R. J.; Köcher, C. *Organometallics* **1997,** *16,* 2472-2477.
148. Herrmann, W. A.; Goossen, L. J.; Spiegler, M. *Organometallics* **1998,** *17,* 2162-2168.
149. Fürstner, A.; Alcarazo, M.; César, V.; Lehmann, C. W. *Chem. Commun.* **2006,** 2176-2178.
150. Magill, A. M.; Cavell, K. J.; Yates, B. F. *J. Am. Chem. Soc.* **2004,** *126,* 8717-8724.
151. Taton, T. A.; Chen, P. *Angew. Chem. Int. Ed.* **1996,** *35,* 1011-1013.
152. Alder, R. W.; Blake, M. E.; Chaker, L.; Harvey, J. N.; Paolini, F.; Schütz, J. *Angew. Chem. Int. Ed.* **2004,** *43,* 5896-5911.
153. Denk, M. K.; Thadani, A.; Hatano, K.; Lough, A. J. *Angew. Chem. Int. Ed.* **1997,** *36,* 2607-2608.
154. Çetinkaya, E.; Hitchcock, P. B.; Jasim, H. A.; Lappert, M. F.; Spyropoulos, K. J. *J. Chem. Soc. Perkin Trans. 1* **1992,** 561-567.
155. Hahn, F. E.; Paas, M.; Le Van, D.; Fröhlich, R. *Chem. Eur. J.* **2005,** *11,* 5080-5085.
156. Denk, M. K.; Hezarkhani, A.; Zheng, F.-L. *Eur. J. Inorg. Chem.* **2007,** 3527-3534.
157. Hahn, F. E. *Angew. Chem. Int. Ed.* **2006,** *45,* 1348-1352.

158. Despagnet-Ayoub, E.; Grubbs, R. H. *J. Am. Chem. Soc.* **2004,** *126,* 10198-10199.
159. Despagnet-Ayoub, E.; Grubbs, R. H. *Organometallics* **2005,** *24,* 338-340.
160. Bazinet, P.; Yap, G. P. A.; Richeson, D. S. *J. Am. Chem. Soc.* **2003,** *125,* 13314-13315.
161. Alder, R. W.; Blake, M. E.; Bortolotti, C.; Bufali, S.; Butts, C. P.; Linehan, E.; Oliva, J. M.; Orpen, A. G.; Quale, M. J. *Chem. Commun.* **1999,** 241-242.
162. Yun, J.; Marinez, E. R.; Grubbs, R. H. *Organometallics* **2004,** *23,* 4172-4173.
163. Özdemir, I.; Demir, S.; Çetinkaya, B.; Çetinkaya, E. *J. Organomet. Chem.* **2005,** *690,* 5849-5855.
164. Mayr, M.; Wurst, K.; Ongania, K. H.; Buchmeiser, M. R. *Chem. Eur. J.* **2004,** *10,* 1256-1266.
165. Herrmann, W. A.; Schneider, S. K.; Öfele, K.; Sakamoto, M.; Herdtweck, E. *J. Organomet. Chem.* **2004,** *689,* 2441-2449.
166. Zhang, Y.; Wang, D.; Wurst, K.; Buchmeiser, M. R. *J. Organomet. Chem.* **2005,** *690,* 5728-5735.
167. Schneider, S. K.; Herrmann, W. A.; Herdtweck, E. *J. Mol. Catal. A: Chem.* **2006,** *245,* 248-254.
168. Scarborough, C. C.; Grrady, M. J. W.; Guzei, I. A.; Gandhi, B. A.; Bunel, E. E.; Stahl, S. S. *Angew. Chem. Int. Ed.* **2005,** *44,* 5269-5272.
169. Scarborough, C. C.; Popp, B. V.; Guzei, I. A.; Stahl, S. S. *J. Organomet. Chem.* **2005,** *690,* 6143-6155.
170. Alder, R. W.; Allen, P. R.; Murray, M.; Orpe, A. G. *Angew. Chem. Int. Ed.* **1996,** *35,* 1121-1122.
171. Denk, K.; Sirsch, P.; Herrmann, W. A. *J. Organomet. Chem.* **2002,** *649,* 219-224.
172. Frey, G. D.; Herdtweck, E.; Herrmann, W. A. *J. Organomet. Chem.* **2006,** *691,* 2465-2478.
173. Herrmann, W. A.; Schütz, J.; Frey, G. D.; Herdtweck, E. *Organometallics* **2006,** *25,* 2437-2448.
174. Alcarazo, M.; Roseblade, S. J.; Alonso, E.; Fernández, R.; Alvarez, E.; Lahoz, F. J.; Lassaletta, J. M. *J. Am. Chem. Soc.* **2004,** *126,* 13424-13243.
175. Cattoën, X.; Miqueu, K.; Gornitzka, H.; Bourissou, D.; Bertrand, G. *J. Am. Chem. Soc.* **2005,** *127,* 3292-3293.
176. Cattoën, X.; Gornitzka, H.; Tham, F. S.; Miqueu, K.; Bourissou, D.; Bertrand, G. *Eur. J. Org. Chem.* **2007,** 912-917.
177. Krahulic, K. E.; Enright, G. D.; Parvez, M.; Roesler, R. *J. Am. Chem. Soc.* **2005,** *127,* 4142-4143.
178. Arduengo, A. J.; Bock, H.; Chen, H.; Denk, M.; Dixon, D. A.; Green, J. C.; Herrmann, W. A.; Jones, N. L.; Wagner, M.; West, R. *J. Am. Chem. Soc.* **1994,** *116,* 6641-6649.
179. Gehrhus, B.; Lappert, M. F. *J. Organomet. Chem.* **2001,** *617-618,* 209-223.

180. Haaf, M.; Schmiedl, A.; Schmedake, T. A.; Powell, R. A.; Millevolte, A. J.; Denk, M.; West, R. *J. Am. Chem. Soc.* **1998,** *120,* 12714-12719.
181. Urquhart, S.; Hitchcock, A. P.; Denk, M. K. *Organometallics* **1998,** *17,* 2352-2360.
182. Denk, M.; Lennon, R.; Hayashi, R.; West, R.; Haaland, A.; Belyakov, A. V.; Verne, H. P.; Wagner, M.; Metzler, N. *J. Am. Chem. Soc.* **1994,** *116,* 2691-2692.
183. Denk, M.; Hayashi, R. K.; R., W. *J. Am. Chem. Soc.* **1994,** *116,* 10813-10814.
184. Zeller, A.; Bielert, F.; Haerter, P.; Herrmann, W. A.; Strassner, T. *J. Organomet. Chem.* **2005,** *690,* 3292-3299.
185. Herrmann, W. A.; Denk, M.; Behm, J.; Scherer, W.; Klingan, F.-R.; Bock, H.; Solouki, B.; Wagner, M. *Angew. Chem. Int. Ed.* **1992,** *31,* 1485-1488.
186. Denk, M. K.; Gupta, S.; Ramachandran, R. *Eur. J. Inorg. Chem.* **1999,** 41-49.
187. Denk, M. K.; Gupta, S.; Ramachandran, R. *Tetrahedron Lett.* **1996,** *37,* 9025-9028.
188. Couture, P.; Terlouw, J. K.; Warkentin, J. *J. Am. Chem. Soc.* **1996,** *118,* 4214-4215.
189. Alder, R. W.; Butts, C. P.; Orpen, A. G. *J. Am. Chem. Soc.* **1998,** *120,* 11526-11527.
190. Wolf, J.; Böhlmann, W.; Findeisen, M.; Gelbrich, T.; Hofmann, H.-J.; Schulze, B. *Angew. Chem. Int. Ed.* **2007,** *46,* 1-5.
191. Cattoën, X.; Gornitzka, H.; Bourissou, D.; Bertrand, G. *J. Am. Chem. Soc.* **2004,** *126,* 1342-1343.
192. Lavallo, V.; Mafhouz, J.; Canac, Y.; Donnadieu, B.; Schoeller, W. W.; Bertrand, G. *J. Am. Chem. Soc.* **2004,** *126,* 8670-8671.
193. Lavallo, V.; Canac, Y.; Präsang, C.; Donnadieu, B.; Bertrand, G. *Angew. Chem. Int. Ed.* **2005,** *44,* 2-6.
194. Jazzar, R.; Liang, H.; Donnadieu, B.; Bertrand, G. *J. Organomet. Chem.* **2006,** *691,* 3201-3205.
195. Merceron-Saffon, N.; Baceiredo, A.; Gornitzka, H.; Bertrand, G. *Science* **2003,** *301,* 1223-1225.
196. Merceron-Saffon, N.; Gornitzka, H.; Baceiredo, A.; Bertrand, G. *J. Organomet. Chem.* **2004,** *689,* 1431-1435.
197. Teuma, E.; Lyon-Saunier, C.; Gornitzka, H.; Mignani, G.; Baceiredo, A.; Bertrand, G. *J. Organomet. Chem.* **2005,** *690,* 5541-5545.
198. Canac, Y.; Conejero, S.; Soleilhavoup, M.; Donnadieu, B.; Bertrand, G. *J. Am. Chem. Soc.* **2006,** *128,* 459-464.
199. Lai, C.-L.; Guo, W.-H.; Lee, M.-T.; Hu, C.-H. *J. Organomet. Chem.* **2005,** *690,* 5867-5875.
200. Martin, D.; Baceiredo, A.; Gornitzka, H.; Schoeller, W. W.; Bertrand, G. *Angew. Chem. Int. Ed.* **2005,** *44,* 1700-1703.

201. Masuda, J. D.; Martin, D.; Lyon-Saunier, C.; Baceiredo, A.; Gornitzka, H.; Donnadieu, B.; Bertrand, G. *Chem. Asian J.* **2006,** *2,* 178-187.
202. Schoeller, W. W.; Schroeder, D.; Rozhenko, A. B. *J. Organomet. Chem.* **2005,** *690,* 6079-6088.
203. Occhipinti, G.; Bjorsvik, H.-R.; Jensen, V. R. *J. Am. Chem. Soc.* **2006,** *128,* 6952-6964.
204. Heinemann, C.; M¨uller, T.; Apeloig, Y.; Schwarz, H. *J. Am. Chem. Soc.* **1996,** *118,* 2023-2038.
205. Boehme, C.; Frenking, G. *J. Am. Chem. Soc.* **1996,** *118,* 2039-2046.
206. Cavallo, L.; Correa, A.; Costabile, C.; Jacobsen, H. *J. Organomet. Chem.* **2005,** *690,* 5407-5413.
207. Hu, X.; Tang, Y.; Gantzel, P.; Meyer, K. *Organometallics* **2003,** *22,* 612-614.
208. Hu, X.; Castro-Rodriguez, I.; Olsen, K.; Meyer, K. *Organometallics* **2004,** *23,* 755-764.
209. Nemcsok, D.; Wichmann, K.; Frenking, G. *Organometallics* **2004,** *23,* 3640-3646.
210. Scott, N. M.; Dorta, R.; Stevens, E. D.; Correa, A.; Cavallo, L.; Nolan, S. P. *J. Am. Chem. Soc.* **2005,** *127,* 3516-3526.
211. Jacobsen, H.; Correa, A.; Costabile, C.; Cavallo, L. *J. Organomet. Chem* **2006,** *691,* 4350-4358.
212. Tafipolsky, M.; Scherer, W.; Ofele, K.; Artus, G.; Pedersen, B.; Herrmann, W. A.; McGrady, G. S. *J. Am. Chem. Soc* **2002,** *124,* 5865-5880.
213. Frison, G.; Sevin, A. *J. Organomet. Chem.* **2002,** *643-644,* 105-111.
214. Frison, G.; Sevin, A. *J. Chem. Soc., Perkin Trans 2* **2002,** 1692-1697.
215. Boehme, C.; Frenkin, G. *Organometallics* **1998,** *17,* 5801-5809.
216. Deubel, D. V. *Organometallics* **2002,** *21,* 4303-4305.
217. Baba, E.; Cundari, T. R.; Firkin, I. *Inorg. Chim. Acta* **2005,** *358,* 2867-2875.
218. Abernethy, C. D.; Codd, G. M.; Spicer, M. D.; Taylor, M. K. *J. Am. Chem. Soc.* **2003,** *125,* 1128-1129.
219. Termaten, A. T.; Schakel, M.; Ehlers, A. W.; Lutz, M.; Spek, A. L.; Lammertsma, K. *Chem. Eur. J.* **2003,** *9,* 3577-3582.
220. Garrison, J. C.; Simons, R. S.; Kofron, W. G.; Tessier, C. A.; Youngs, W. J. *Chem. Commun.* **2001,** 1780-1781.
221. Tulloch, A. A. D.; Danapoulos, A. A.; Kleinhenz, S.; Light, M. A.; Hursthouse, M. B.; Eastham, G. *Organometallics* **2001,** *20,* 2027-2031.
222. Mercs, L.; Labat, G.; Neels, A.; Ehlers, A.; Albrecht, M. *Organometallics* **2006,** *25,* 5648-5656.
223. Weskamp, T.; Böhm, V. P. W.; Herrmann, W. A. *J. Organomet. Chem.* **2000,** *600,* 12-22.
224. Raubenheimer, H. H.; Cronje, S. *J. Organomet. Chem.* **2001,** *617-618,* 170-181.

225. Lappert, M. F.; Pye, P. L. *J. Chem. Soc. Dalton Trans.* **1977,** 2172-2180.
226. Hitchcock, P. B.; Lappert, M. F.; Pye, P. L. *J. Chem. Soc. Dalton Trans.* **1978,** 826-836.
227. Lappert, M. F. *J. Organomet. Chem.* **1988,** *358,* 185-214.
228. J., A. A.; Calabrese, J. C.; Davidson, F.; Dias, H. V. R.; Goerlich, J. R.; Krafczyk, R.; Marshall, W. J.; Tamm, M.; Schmutzler, R. *Helv. Chim. Acta* **1999,** *82,* 2348-2363.
229. Çetinkaya, B.; Çetinkaya, E.; Chamizo, J. A.; Hitchcock, P. B.; Jasim, H. A.; Küçükbay, H.; Lappert, M. F. *J. Chem. Soc. Perkin Trans 1* **1998,** 2047-2054.
230. Trnka, T. M.; Morgan, J. P.; Sanford, M. S.; Wilhelm, T. E.; Scholl, M.; Choi, T.-L.; Ding, S.; Day, M. W.; Grubbs, R. H. *J. Am. Chem. Soc.* **2003,** *125,* 2546-2558.
231. Türkmen, H.; Çetinkaya, B. *J. Organomet. Chem.* **2006,** *691,* 3749-3759.
232. Teles, J. H.; Melder, J. P.; Ebel, K.; Schneider, R.; Gehrer, E.; Harder, W.; Brode, S.. Enders, D.; Breuer, K.; Raabe, G. *Helv. Chim. Acta* **1996,** *79,* 61-83.
233. Nyce, G. W.; Csihony, S.; Waymouth, R. M.; Hedrick, J. L. *Chem. Eur. J.* **2004,** *10,* 4073-4079.
234. Blum, A. P.; Ritter, T.; Grubbs, R. H. *Organometallics* **2007,** *28,* 2122-2124.
235. Jafarpour, L.; Hillier, A. C.; Nolan, S. P. *Organometallics* **2002,** *21,* 442-444.
236. Voutchkova, A. M.; Appelhans, L. N.; Chianese, A. R.; Crabtree, R. H. *J. Am. Chem. Soc.* **2005,** *127,* 17624-17625.
237. Tudose, A.; Demonceau, A.; Delaude, L. *J. Organomet. Chem.* **2006,** *691,* 5356-5365.
238. Duong, H. A.; Tekavec, T. N.; Arif, A. M.; Louie, J. *Chem. Commun.* **2004,** 112-113.
239. Kuhn, N.; Kratz, T. *Synthesis* **1993,** 561-562.
240. Hahn, F. E.; Wittenbecher, L.; Boese, R.; Bläzer, D. *Chem. Eur. J.* **1996,** *5,* 1931-1935.
241. Hahn, F. E.; Paas, M.; Le Van, D.; Lügger, T. *Angew. Chem. Int. Ed.* **2003,** *42,* 5243-5246.
242. Garrison, J. C.; Youngs, W. J. *Chem. Rev.* **2005,** *105,* 3978-4008.
243. Wang, H. M. J.; Lin, I. J. B. *Organometallics* **1998,** *17,* 972-975.
244. Nielsen, D. J.; Cavell, K. J.; Skelton, B. W.; White, A. H. *Inorg. Chim. Acta* **2002,** *327,* 116-125.
245. Chiu, P. L.; Lee, H. M. *Organometallics* **2005,** *24,* 1692-1702.
246. Roland, S.; Audouin, M.; Mangeney, P. *Organometallics* **2004,** *23,* 3075-3078.
247. Csabai, P.; Joó, F. *Organometallics* **2004,** *23,* 5640-5643.
248. Geldbach, T. J.; Laurenczy, G.; Scopelliti, R.; Dyson, P. J. *Organometallics* **2006,** *25,* 733-742.

249. Poyatos, M.; Maisse-François, A.; Bellemin-Laponnaz, S. *J. Organomet. Chem.* **2006,** *691,* 2713-2720.
250. Ritter, T.; Day, M. W.; Grubbs, R. H. *J. Am. Chem. Soc.* **2006,** *128,* 11768-11769.
251. Yamaguchi, Y.; Kashiwabara, T.; Ogata, K.; Miura, Y.; Nakamura, Y.; Kobayashi, K.; Ito, T. *Chem. Comm.* **2004,** 2160-2161.
252. Ogata, K.; Yamaguchi, Y.; Kashiwabara, T.; Ito, T. *J. Organomet. Chem.* **2005,** *690,* 5701-5709.
253. McGuinness, D. S.; Cavell, K. J.; Yates, B. F. *Chem. Comm.* **2001,** 355-356.
254. McGuinness, D. S.; Cavell, K. J.; Yates, B. F.; Skelton, B. W.; White, A. H. *J. Am. Chem. Soc.* **2001,** *123,* 8317-8328.
255. Fürstner, A.; Seidel, G.; Kremzow, D.; Lehman, C. W. *Organometallics* **2003,** *22,* 907-909.
256. Baker, M. V.; Brown, D. H.; Hesler, V. J.; Skelton, B. W.; White, A. H. *Organometallics* **2007,** *26,* 250-252.
257. Clement, N. D.; Cavell, K. J. *Angew. Chem. Int. Ed.* **2004,** *43,* 3845-3847.
258. Crudden, C. M.; Allen, D. P. *Coord. Chem. Rev.* **2004,** *248,* 2247-2273.
259. Scott, N. M.; Nolan, S. P. *Eur. J. Inorg. Chem.* **2005,** 1815-1828.
260. McGuinness, D. S.; Cavell, K. J.; Skelton, B. W.; White, A. H. *Organometallics* **1999,** *18,* 1596-1605.
261. McGuinness, D. S.; Saendig, N.; Yates, B. F.; Cavell, K. J. *J. Am. Chem. Soc.* **2001,** *123,* 4029-4040.
262. McGuinness, D. S.; Green, M. J.; Cavell, K. J.; Skelton, B. W.; White, A. H. *J. Organomet. Chem.* **1998,** *565,* 165-178.
263. Hitchcock, P. B.; Lappert, M. F.; Terrenos, P. *J. Organomet. Chem.* **1982,** *239,* C26-30.
264. Prinz, M.; Grosche, M.; Herdtweck, E.; Herrmann, W. A. *Organometallics* **2000,** *19,* 1692-1694.
265. Hitchcock, P. B.; Lappert, M. F.; Pye, P. L.; Thomas, S. *J. Chem. Soc., Dalton. Trans.* **1979,** 1929-1942.
266. Huang, J.; Stevens, E. D.; Nolan, S. P. *Organometallics* **2000,** *19,* 1194-1197.
267. Dorta, R.; Stevens, E. D.; Nolan, S. P. *J. Am. Chem. Soc.* **2004,** *126,* 5054-5055.
268. Jazzar, R. F. R.; Macgregor, S. A.; Mahon, M. F.; Richards, S. P.; Whittlesey, M. K. *J. Am. Chem. Soc.* **2002,** *124,* 4944-4945.
269. Caddick, S.; Cloke, F. G. N.; Hitchcock, P. B.; Lewis, A. K. d. K. *Angew. Chem. Int. Ed.* **2004,** *43,* 5824-5827.
270. Burling, S.; Mahon, M. F.; Paine, B. M.; Whittlesey, M. K.; Williams, J. M. J. *Organometallics* **2004,** *25,* 4537-4539.
271. Cabeza, J. A.; del Rio, I.; Miguel, D.; Sánchez-Vega, M. G. *Chem. Commun.* **2005,** 3956-3958.
272. Hanasaka, F.; Tanabe, Y.; Fujita, K.-I.; Yamaguchi, R. *Organometallics* **2006,** *25,* 826-831.

273. Burling, S.; Paine, B. M.; Nama, D.; Brown, V. S.; Mahon, M. F.; Prior, T. J.; Pregosin, P. S.; Whittlesey, M. K.; Williams, J. M. J. *J. Am. Chem. Soc.* **2007,** *129,* 1987-1995.
274. Hong, S. H.; Chlenov, A.; Day, M. W.; Grubbs, R. H. *Angew. Chem. Int. Ed.* **2007,** *46,* 5148-5151.
275. Allen, D. P.; Crudden, C. M.; Calhoun, L. A.; Wang, R. *J. Organomet. Chem.* **2004,** *689,* 3203-3209.
276. Dorta, R.; Stevens, E. D.; Hoff, C. D.; Nolan, S. P. *J. Am. Chem. Soc.* **2003,** *125,* 10490-10491.
277. Weskamp, T.; Köhl, F. J.; Herrmann, W. A. *J. Organomet. Chem.* **1999,** *582,* 362-365.
278. Becker, E.; Stingl, V.; Dazinger, G.; Puchberger, M.; Mereiter, K.; Kirchner, K. *J. Am. Chem. Soc.* **2006,** *128,* 6572-6573.
279. Danopoulos, A. A.; Tsoureas, N.; Green, J. C.; Hursthouse, M. B. *Chem. Commun.* **2003,** 756-757.
280. McGuinness, D. S.; Cavell, K. J. *Organometallics* **2000,** *19,* 4918-4920.
281. Hong, S. H.; Day, M. W.; Grubbs, R. H. *J. Am. Chem. Soc.* **2004,** *126,* 7414-7415.
282. Waltman, A. W.; Ritter, T.; Grubbs, R. H. *Organometallics* **2006,** *25,* 4238-4239.
283. Galan, B. R.; Gembicky, M.; Dominiak, P. M.; Keister, J. B.; Diver, S. T. *J. Am. Chem. Soc.* **2005,** *127,* 15702-15703.
284. Shmidt, B. *Eur. J. Org. Chem.* **2004,** *9,* 1865-1880.
285. Lehman, S. E.; Schwendeman, J. E.; O'Donnell, P. M.; Wagener, K. B. *Inorg. Chim. Acta* **2003,** *345,* 190-198.
286. Courchay, F. C.; Sworen, J. C.; Wagener, K. B. *Proceedings of the* 16$^{\text{th}}$ *International Symposium on Olefin Metathesis and Related Reactions, Poznán, Poland* **2005,** *August 7-12,* P9.
287. Courchay, F. C.; Sworen, J. C.; Ghiviriga, I.; Abboud, K. A.; Wagener, K. B. *Organometallics* **2006,** *25,* 6074-6086.
288. Simms, R. W.; Drewitt, M. J.; Baird, M. C. *Organometallics* **2002,** *21,* 2958-2963.
289. Titcomb, L. R.; Caddick, S.; Cloke, F. G. N.; Wilson, D. J.; McKerrecher, D. *Chem. Commun.* **2001,** 1388-1389.
290. Vehlow, K.; Maechling, S.; Blechert, S. *Organometallics* **2006,** *25,* 25-28.
291. Dinger, M. B.; Mol, J. C. *Adv. Synth. & Cat.* **2002,** *344,* 671-677.
292. Dinger, M. B.; Nieczypor, P.; Mol, J. C. *Organometallics* **2003,** *22,* 5291-5296.
293. Dias, E. L.; Nguyen, S. T.; Grubbs, R. H. *J. Am. Chem. Soc.* **1997,** *119,* 3887-3897.
294. Vyboishchikov, S. F.; Bühl, M.; Thiel, W. *Chem. Eur. J.* **2002,** *8,* 3962-3975.
295. Fomine, S.; Vargas, S. M.; Tlenkopatchev, M. A. *Organometallics* **2003,** *22,* 93-99.

296. Bernardi, F.; Bottoni, A.; Miscione, G. P. *Organometallics* **2003,** *22,* 940-947.
297. van Rensburg, W. J.; Steynberg, P. J.; Meyer, W. H.; Kirk, M. M.; S., F. G. *J. Am. Chem. Soc.* **2004,** *126,* 14332-14333.
298. Adlhart, C.; Chen, P. *J. Am. Chem. Soc.* **2004,** *126,* 3496-3510.
299. Jordaan, M.; van Helden, P.; Sittert, C. G. C. E.; Vosloo, H. C. M. *J. Mol. Cat. A* **2006,** *254,* 145-154.
300. Cavallo, L. *J. Am. Chem. Soc.* **2002,** *124,* 8965-8973.
301. Aagaard, O. M.; Meier, R.; Buda, F. *J. Am. Chem. Soc.* **1998,** *120,* 7174-7182.
302. Ulman, M.; Grubbs, R. H. *Organometallics* **1998,** *17,* 2484-2489.
303. Sanford, M. S.; Love, J.; Grubbs, R. H. *J. Am. Chem. Soc.* **2001,** *123,* 6543-6554.
304. Sanford, M. S.; Ulman, M.; Grubbs, R. H. *J. Am. Chem. Soc.* **2001,** *123,* 749-750.
305. Hinderling, C.; Adlhart, C.; Chen, P. *Angew. Chem. Int. Ed.* **1998,** *37,* 2685-2689.
306. Volland, M. A. O.; Adlhart, C.; Kiener, C. A.; Chen, P.; Hofmann, P. *Chem. Eur. J.* **2001,** *7,* 4621-4632.
307. Romero, P. E.; Piers, W. E. *J. Am. Chem. Soc.* **2005,** *127,* 5032-5033.
308. Adlhart, C.; Hinderling, C.; Baumann, H.; Chen, P. *J. Am. Chem. Soc.* **2000,** *122,* 8204-8214.
309. Trnka, T. M.; Day, M. W.; Grubbs, R. H. *Organometallics* **2001,** *20,* 3845-3847.
310. Anderson, D. R.; Hickstein, D. D.; O'Leary, D. J.; Grubbs, R. H. *J. Am. Chem. Soc.* **2006,** *128,* 8386-8387.
311. Tallarico, J. A.; Bonitatebus, J. P. J.; Snapper, M. L. *J. Am. Chem. Soc.* **1997,** *119,* 7157-7158.
312. Berlin, J. M.; Goldberg, S. D.; Grubbs, R. H. *Angew. Chem. Int. Ed.* **2006,** *45,* 7591-7595.
313. Costabile, C.; Cavallo, L. *J. Am. Chem. Soc.* **2004,** *126,* 9592-9600.
314. Wenzel, A. G.; Grubbs, R. H. *J. Am. Chem. Soc.* **2006,** *128,* 16048-16049.
315. Correa, A.; Cavallo, L. *J. Am. Chem. Soc.* **2006,** *128,* 13352-13353.
316. Benitez, D.; Goddard, W. A. I. *J. Am. Chem. Soc.* **2005,** *127,* 12218-12219.
317. Romero, P. E.; Piers, W. E. *J. Am. Chem. Soc.* **2007,** *129(6),* 1698-1704.
318. Adlhart, C.; Chen, P. *Angew. Chem. Int. Ed.* **2002,** *41,* 4484-4487.
319. Adlhart, C.; Chen, P. *Helv. Chim. Acta* **2003,** *86,* 941-949.
320. Sabbagh, I. T.; Kaye, P. T. *J. Mol. Struct.: THEOCHEM* **2006,** *763,* 37-42.
321. Lord, R. L.; Wang, H.; Vieweger, M.; Baik, M.-H. *J. Organomet. Chem.* **2006,** *691,* 5505-5512.
322. Tsipis, A. C.; Orpen, A. G.; Harvey, J. N. *J. Chem. Soc.: Dalton Trans.* **2005,** 2849-2858.
323. Straub, B. F. *Angew. Chem. Int. Ed.* **2005,** *44,* 5974-5978.
324. Eisenstein, O.; Hoffmann, R.; Rossi, A. R. *J. Am. Chem. Soc.* **1981,** *103,*

5582-5584.
325. Suresh, C. H.; Koga, N. *Organometallics* **2004,** *23,* 76-80.
326. Straub, B. *Adv. Synth. & Cat.* **2007,** *349,* 204-214.
327. Hillier, A. C.; Sommer, W. J.; Yong, B. S.; Petersen, J. L.; Cavallo, L.; Nolan, S. P. *Organometallics* **2003,** *22,* 4322-4326.
328. Chianese, A. R.; Li, X.; Janzen, M. C.; Faller, J. W.; Crabtree, R. H. *Organometallics* **2003,** *22,* 1663-1667.
329. Marion, N.; Navarro, O.; Mei, J.; Stevens, E. D.; Scott, N. M.; Nolan, S. P. *J. Am. Chem. Soc.* **2006,** *128,* 4101-4111.
330. Randl, S.; Gessler, S.; Wakamatsu, H.; Blechert, S. *Synlett* **2001,** 430-432.
331. Ackermann, L.; Fürstner, A.; Weskamp, T.; Kohl, F. J.; Herrmann, W. A. *Tetrahedron Lett.* **1999,** *40,* 4787-4790.
332. Fürstner, A.; Ackermann, L.; Gabor, B.; Goddard, R.; Lehmann, C. W.; Mynott, R.; Stelzer, F.; Thiel, O. R. *Chem. Eur. J.* **2001,** *7,* 3236-3253.
333. Fürstner, A.; Krause, H.; Ackermann, L.; Lehmann, C. W. *Chem. Commun.* **2001,** 2240-2241.
334. Prühs, S.; Lehmann, C. W.; Fürstner, A. *Organometallics* **2004,** *23,* 280-287.
335. Bielawski, C. W.; Benitez, D.; Grubbs, R. H. *Science* **2002,** *297,* 2041-2044.
336. Bielawski, C. W.; Benitez, D.; Grubbs, R. H. *J. Am. Chem. Soc.* **2003,** *125,* 8424-8425.
337. Bielawski, C. W.; Grubbs, R. H. *Angew. Chem. Int. Ed.* **2000,** *39,* 2903-2905.
338. Courchay, F. C.; Sworen, J. C.; Coronado, A.; Wagener, K. B. *J. Mol. Cat. A.* **2006,** *254,* 111-117.
339. Zhang, W.; Bai, C.; Lu, X.; He, R. *J. Organomet. Chem.* **2007,** *692,* 3563-3567.
340. Stewart, I. C.; Ung, T.; Pletnev, A. A.; Berlin, J. M.; Grubbs, R. H.; Schrodi, Y. *Org. Lett.* **2007,** *9,* 1589-1592.
341. Berlin, J. M.; Campbell, K.; Ritter, T.; Funk, T. W.; Chlenov, A.; Grubbs, R. H. *Org. Lett.* **2007,** *9,* 1339-1342.
342. Vougioukalakis, G. C.; Grubbs, R. H. *Organometallics* **2007,** *26,* 2469-2472.
343. Schürer, S. C.; Gessler, S.; Buschmann, N.; Blechert, S. *Angew. Chem. Int. Ed.* **2000,** *40,* 3898-3901.
344. Randl, S.; Buschmann, N.; Connon, S. J.; S., B. *Synlett* **2001,** 1547-1550.
345. Hong, S. H.; Grubbs, R. H. *J. Am. Chem. Soc.* **2006,** *128,* 3508-3509.
346. Jordan, J. P.; Grubbs, R. H. *Angew. Chem. Int. Ed.* **2007,** *46,* 5152-5155.
347. Hong, S. H.; Grubbs, R. H. *Org. Lett.* **2007,** *9,* 1955-1975.
348. Süβner, M. S.; Plenio, H. *Angew. Chem. Int. Ed.* **2005,** *44,* 6885-6888.
349. Weigl, K.; Köcher, K.; Dechert, S.; Meyer, F. *Organometallics* **2005,** *24,* 4049-4056.
350. Blum, A. P.; Ritter, T.; H., G. R. *Organometallics* **2007,** *26,* 2122-2124.
351. Anderson, D. R.; Lavallo, V.; O'Leary, D. J.; Bertrand, G.; Grubbs, R. H. *Angew. Chem. Int. Ed.* **2007,** in press.

352. Lavallo, V.; Canac, Y.; DeHope, A.; Donnadieu, B.; Bertrand, G. *Angew. Chem. Int. Ed.* **2005,** *46,* 7236-7239.
353. Van Veldhuizen, J. J.; Garber, S. B.; Kingsbury, J. S.; Hoveyda, A. H. *J. Am. Chem. Soc.* **2002,** *124,* 4954-4955.
354. Gillingham, D. G.; Kataoka, O.; Garber, S. B.; Hoveyda, A. H. *J. Am. Chem. Soc.* **2004,** *126,* 12288-12290.
355. Van Veldhuizen, J. J.; Campbell, J. E.; Giudici, R. E.; Hoveyda, A. H. *J. Am. Chem. Soc.* **2005,** *127,* 6877-6882.
356. Fournier, P.-A.; Collins, S. K. *Organometallics* **2007,** *26,* 2945-2949.
357. Fürstner, A.; Thiel, O. R.; Lehmann, C. W. *Organometallics* **2002,** *21,* 331-335.
358. Hahn, F. E.; Paas, M.; Fröhlich, R. *J. Organomet. Chem.* **2005,** *690,* 5816-5821.
359. Ung, T.; Hejl, A.; Grubbs, R. H.; Schrodi, Y. *Organometallics* **2004,** *23,* 5399-5401.
360. Hejl, A.; Day, M. W.; Grubbs, R. H. *Organometallics* **2006,** *25(26),* 6149-6154.
361. Chang, S.; Jones II, L.; Wang, C.; Henling, L. M.; Grubbs, R. H. *Organometallics* **1998,** *17,* 3460-3465.
362. Slugovc, C.; Burtscher, D.; Stelzer, F.; Mereiter, K. *Organometallics* **2005,** *24,* 2255-2258.
363. Denk, K.; Fridgen, J.; Herrmann, W. A. *Adv. Synth. & Cat.* **2002,** *344,* 666-670.
364. Drozdzak, R.; Ledoux, N.; Allaert, B.; Dragutan, I.; Dragutan, V.; Verpoort, F. *Central Eur. J. Chem.* **2005,** *3,* 404-416.
365. Drozdzak, R.; Allaert, B.; Ledoux, N.; Dragutan, I.; Dragutan, V.; Verpoort, F. *Coord. Chem. Rev.* **2005,** *249,* 3055-3074.
366. Drozdzak, R.; Allaert, B.; Ledoux, N.; Dragutan, I.; Dragutan, V.; Verpoort, F. *Adv. Synth. & Cat.* **2005,** *347,* 1721-1743.
367. De Clercq, B.; Verpoort, F. *Tetrahedron Lett.* **2002,** *43,* 9101-9104.
368. De Clercq, B.; Verpoort, F. *Adv. Synth. & Cat.* **2002,** *344,* 1-11.
369. De Clercq, B.; Lefebvre, F.; Verpoort, F. *Applied Cat. A* **2002,** *247,* 345-364.
370. Opstal, T.; Verpoort, F. *J. Mol. Cat. A.* **2003,** *200,* 49-61.
371. Allaert, B. *Ph D dissertation* **2007,** Ghent University, in progress.
372. Binder, J. B.; Guzei, I. A.; Raines, R. T. *Adv. Synth. & Cat.* **2007,** *349,* 359-404.
373. Lynn, D. M.; Dias, E. L.; Grubbs, R. H.; Mohr, B. **2002,** US 2002/0055598A1.
374. Katayama, H.; Yoshida, T.; Ozawa, F. *J. Organomet. Chem.* **1998,** *562,* 203-206.
375. Sanford, M.; Henling, L. M.; Day, M. W.; Grubbs, R. H. *Angew. Chem. Int. Ed.* **2000,** *39,* 3451-3453.
376. Lynn, D. M.; Mohr, B.; Grubbs, R. H. *J. Am. Chem. Soc.* **1998,** *120,*

1627-1628.
377. Huang, J.; Schanz, H.-J.; Stevens, E. D.; Nolan, S. P. *Organometallics* **1999,** *18,* 5375-5380.
378. Meyer, W. H.; McConnell, A. E.; Forman, G. S.; Dwyer, C. L.; Kirk, M. M.; Ngidi, E. L.; Blignaut, A.; Saku, D.; Slawin, A. M. Z. *Inorganica Chim. Acta* **2006,** *359,* 2910-2917.
379. Sanford, M. S.; Henling, L. M.; Grubbs, R. H. *Organometallics* **1998,** *17,* 5384-5389.
380. *EP01577282, WO05082819* .
381. De Clercq, B.; Verpoort, F. *J. Organomet. Chem.* **2003,** *672,* 11-16.
382. Bielawski, C. W.; Benitez, D.; Morita, T.; Grubbs, R. H. *Macromolecules* **2001,** *34,* 8610-8618.
383. Morgan, J. P.; Grubbs, R. H. *Org. Lett.* **2000,** *2,* 3153-3155.
384. Burgio, J.; Yardy, N. M.; Petersen, J. L.; Lemke, F. R. *Organometallics* **2003,** *22,* 4928-4932.
385. Osipov, A. L.; Gerdov, S. M.; Kuzmina, L. G.; Howard, J. A. K.; Nikonov, G. I. *Organometallics* **2005,** *24,* 587-602.
386. Dias, E. L.; Grubbs, R. H. *Organometallics* **1998,** *17,* 2758-2767.
387. Rivard, M.; Blechert, S. *Eur. J. Org. Chem.* **2003,** 2225-2228.
388. Nakash, M.; Goldvaser, M. *J. Am. Chem. Soc.* **2004,** *126,* 3436-3437.
389. Nakash, M.; Gut, D.; Goldvaser, M. *Inorg. Chem.* **2005,** *44,* 1023-1030.
390. Arduengo III, A. J.; Krafczyk, R.; Schmutzler, R.; Craig, H. A.; Goerlich, J. R.; Marshall, W. J.; Unverzagt, M. *Tetrahedron* **1999,** *55,* 14523-14534.
391. Harlow, K. J.; Hill, A. F.; Wilton-Eley, J. D. E. T. *J. Chem. Soc., Dalton Trans.* **1999,** 285-291.
392. Fürstner, A.; Picquet, M.; Bruneau, C.; Dixneuf, P. *Chem. Commun.* **1998,** 1315-1316.
393. Fürstner, A.; Liebl, M.; Lehmann, C.; Picquet, M.; Kunz, R.; Bruneau, C.; Touchard, D.; Dixneuf, P. H. *Chem. Eur. J.* **2000,** *6,* 1847-1857.
394. Rigaut, S.; D. Touchard, D.; Dixneuf, P. H. *Coord. Chem. Rev.* **2004,** *248,* 1585-1601.
395. Winter, R.; Zalis, S. *Coord. Chem. Rev.* **2004,** *248,* 1565-1583.
396. Picquet, M.; Touchard, D.; Bruneau, C.; Dixneuf, P. H. *New J. Chem.* **1999,** *23,* 141-143.
397. Bruneau, C.; Dixneuf, P. H. *Angew. Chem. Int. Ed.* **2006,** *45,* 2176-2203.
398. Schanz, H.-J.; Jafarpour, L.; Stevens, E. D.; Nolan, S. P. *Organometallics* **1999,** *18,* 5187-5190.
399. Jafarpour, L.; Huang, J.; Stevens, E. D.; Nolan, S. P. *Organometallics* **1999,** *18,* 3760-3763.
400. Jafarpour, L.; Nolan, S. P. *J. Organomet. Chem.* **2001,** *617-618,* 17-27.
401. Katayama, H.; Ozawa, F. *Coord. Chem. Rev.* **2004,** *248,* 1703-1715.
402. Katayama, H.; Ozawa, F. *Organometallics* **1998,** *17,* 5190-5196.
403. Katayama, H.; Ozawa, F. *Chem. Lett.* **1998,** 67-68.

404. Louie, J.; Grubbs, R. H. *Angew. Chem. Int. Ed.* **2001,** *40,* 247-249.
405. Castarlenas, R.; Eckert, M.; Dixneuf, P. H. *Angew. Chem. Int. Ed.* **2005,** *44,* 2576-2579.
406. Castarlenas, R.; Dixneuf, P. H. *Angew. Chem. Int. Ed.* **2003,** *42,* 4524-4527.
407. Castarlenas, R.; Vovard, C.; Fischmeister, C.; Dixneuf, P. H. *J. Am. Chem. Soc.* **2006,** *128,* 4079-4089.
408. Delaude, L.; Demonceau, A.; Noels, A. F. *Chem. Commun.* **2001,** 986-987.
409. Delaude, L.; Szypa, M.; Demonceau, A.; Noels, A. F. *Adv. Synth. & Cat.* **2002,** *344,* 749-756.
410. Waltman, A. W.; Grubbs, R. H. *Organometallics* **2004,** *23,* 3105-3107.
411. Demonceau, A.; Stumpf, A. W.; Saive, E.; Noels, A. F. *Macromolecules* **1997,** *30,* 3127-3136.
412. Karlen, T.; Ludi, A.; Mühlebach, A.; Bernhard, P.; Pharisa, C. *J. Polym. Sci. Part A: Polym. Chem.* **1995,** *33,* 1665-1674.
413. Fürstner, A.; Ackermann, L. *Chem. Comm.* **1999,** 95-96.
414. Castarlenas, R.; Sémeril, D.; Noels, A. F.; Demonceau, A.; Dixneuf, P. H. *J. Organomet. Chem.* **2002,** *663,* 235-238.
415. Bennett, M. A.; Huang, T. N.; Matheson, T. W.; Smith, A. K. *Inorg. Synth.* **1985,** *21,* 75.
416. Melis, K.; De Vos, D.; Jacobs, P.; Verpoort, F. *J. Organomet. Chem.* **2003,** *671,* 131-136.
417. Melis, K.; Verpoort, F. *J. Mol. Cat. A* **2003,** *201,* 33-41.
418. Melis, K.; Verpoort, F. *J. Mol. Cat. A* **2003,** *194,* 39-47.
419. Huang, J.; Jafarpour, L.; Hillier, A. C.; Stevens, E. D.; Nolan, S. P. *Organometallics* **2001,** *20,* 2878-2882.
420. Viciu, M. S.; Navarro, O.; Germananeau, R. F.; Kelly III, R. A.; Sommer, W.; Marion, N.; Stevens, E. D.; Cavallo, L.; Nolan, S. P. *Organometallics* **2004,** *23,* 1629-1635.
421. Paas, M.; Wibbeling, B.; Fröhlich, R.; Hahn, F. E. *Eur. J. Inorg. Chem.* **2006,** 158-162.
422. Clavier, H.; Coutable, L.; Guillemin, J.-C.; Mauduit, M. *Tetrahedron: Asymm.* **2005,** *16,* 921-914.
423. Love, J. A.; Sanford, M. S.; Day, M. W.; Grubbs, R. H. *J. Am. Chem. Soc.* **2003,** *125,* 10103-10109.
424. Jordaan, M.; van Helden, P.; Sittert, C. G. C. E.; Vosloo, H. C. M. *J. Mol. Cat. A* **2006,** *254,* 145-154.
425. Süβner, M. S.; Plenio, H. *Chem. Comm.* **2005,** 5417-5419.
426. Hoveyda, A. H.; Gillingham, D. G.; Van Veldhuizen, J. J.; Kataoka, O.; Garber, S. B.; Kingsbury, J. S.; Harrity, J. P. A. *Org. Biomol. Chem.* **2004,** *2,* 1-16.
427. Gulajski, L.; Michrowska, A.; Bujok, R.; Grela, K. *J. Mol. Cat. A.* **2006,** *254,* 118-123.
428. Courchay, F. C.; Sworen, J. C.; Wagener, K. B. *Macromolecules* **2003,** *36,* 8231-8239.

429. Douthwaite, R. E. *Coord. Chem. Rev* **2007,** *251,* 702-717.
430. Duan, W.-L.; Shi, M.; Rong, G.-B. *Chem. Commun* **2003,** 2916-2917.
431. Bonnet, L. G.; Douthwaite, R. E.; Kariuki, B. M. *Organometallics* **2003,** *22,* 4187-4189.
432. Gade, L. H.; César, V.; Bellemin-Laponnaz, S. *Angew. Chem. Int. Ed.* **2004,** *43,* 1014-1017.
433. Song, C.; Ma, C.; Ma, Y.; Feng, W.; Ma, S.; Chai, Q.; Andrus, M. B. *Tetrahedron Lett.* **2005,** *46,* 3241-3244.
434. Marshall, C.; Ward, M. F.; Harrison, W. T. A. *J. Organomet. Chem.* **2005,** *690,* 3970-3975.
435. Arao, T.; Kondo, K.; Aoyama, T. *Tetrahedron Lett.* **2006,** *47,* 1417-1420.
436. Winn, C. L.; Guillen, F.; Pytkowicz, J.; Roland, S.; Mangeney, P.; Alexakis, A. *J. Organomet. Chem.* **2005,** *690,* 5672-5695.
437. Connon, S. J.; Blechert, S. *Biorganic & Medicinal Chem. Lett.* **2002,** *12,* 1873-1876.
438. Fischer, D.; Blechert, S. *Adv. Synt. & Cat.* **2005,** *347,* 1329-1332.
439. Mennecke, K.; Grela, K.; Kunz, U.; Kirschning, A. *Synlett* **2005,** 2948-2952.
440. Michrowska, A.; Mennecke, K.; Kunz, U.; Kirschning, A.; Grela, K. *J. Am. Chem. Soc.* **2006,** *128,* 13261-13267.
441. Buchmeiser, M. R. *New J. Chem.* **2004,** *28,* 549-557.
442. Yang, L.; Mayer, M.; Wurst, K.; Buchmeiser, M. R. *Chem. Eur. J.* **2004,** *10,* 5761-5770.
443. Audic, N.; Clavier, H.; Mauduit, M.; Guillemin, J.-C. *J. Am. Chem. Soc.* **2003,** *125,* 9248-9249.
444. Clavier, H.; Audic, N.; Mauduit, M.; Guillemin, J.-C. *Chem. Commun* **2003,** 2282-2283.
445. Clavier, H.; Audic, N.; Guillemin, J.-C.; Mauduit, M. *J. Organomet. Chem.* **2005,** *690,* 3583-3599.
446. Rix, D.; Clavier, H.; Coutard, Y.; Gulajski, L.; Grela, K.; Mauduit, M. *J. Organomet. Chem.* **2006,** *691,* 5397-5405.
447. Copéret, C.; Basset, J. M. *Adv. Synt. & Cat.* **2007,** *349,* 78-92.
448. Gallivan, J. P.; Jordan, J. P.; Grubbs, R. H. *Tetrahedron Lett.* **2005,** *46,* 2577-2580.